Spring 2015

Novel computational methods for stochastic design optimization of high-dimensional complex systems

Xuchun Ren
University of Iowa

NOVEL COMPUTATIONAL METHODS FOR STOCHASTIC DESIGN OPTIMIZATION OF HIGH-DIMENSIONAL COMPLEX SYSTEMS

by

Xuchun Ren

A thesis submitted in partial fulfillment of the
requirements for the Doctor of Philosophy
degree in Mechanical Engineering
in the Graduate College of
The University of Iowa

May 2015

Thesis Supervisor: Professor Sharif Rahman

Graduate College
The University of Iowa
Iowa City, Iowa

CERTIFICATE OF APPROVAL

_____

PH.D. THESIS

_____

This is to certify that the Ph.D. thesis of

Xuchun Ren

has been approved by the Examining Committee for the
thesis requirement for the Doctor of Philosophy degree
in Mechanical Engineering at the May 2015 graduation.

Thesis Committee: _____
                  Sharif Rahman, Thesis Supervisor

                  _____
                  Kyung K. Choi

                  _____
                  Jia Lu

                  _____
                  Shaoping Xiao

                  _____
                  Aixin Tan

To Xin, Hutchinson, and Rebecca

ACKNOWLEDGEMENTS

ABSTRACT

The primary objective of this study is to develop new computational methods for robust design optimization (RDO) and reliability-based design optimization (RBDO) of high-dimensional, complex engineering systems. Four major research directions, all anchored in polynomial dimensional decomposition (PDD), have been defined to meet the objective. They involve: (1) development of new sensitivity analysis methods for RDO and RBDO; (2) development of novel optimization methods for solving RDO problems; (3) development of novel optimization methods for solving RBDO problems; and (4) development of a novel scheme and formulation to solve stochastic design optimization problems with both distributional and structural design parameters.

The major achievements are as follows. Firstly, three new computational methods were developed for calculating design sensitivities of statistical moments and reliability of high-dimensional complex systems subject to random inputs. The first method represents a novel integration of PDD of a multivariate stochastic response function and score functions, leading to analytical expressions of design sensitivities of the first two moments. The second and third methods, relevant to probability distribution or reliability analysis, exploit two distinct combinations built on PDD: the PDD-SPA method, entailing the saddlepoint approximation (SPA) and score functions; and the PDD-MCS method, utilizing the embedded Monte Carlo simulation (MCS) of the PDD approximation and score functions. For all three methods devel-

oped, both the statistical moments or failure probabilities and their design sensitivities are both determined concurrently from a single stochastic analysis or simulation. Secondly, four new methods were developed for RDO of complex engineering systems. The methods involve PDD of a high-dimensional stochastic response for statistical moment analysis, a novel integration of PDD and score functions for calculating the second-moment sensitivities with respect to the design variables, and standard gradient-based optimization algorithms. The methods, depending on how statistical moment and sensitivity analyses are dovetailed with an optimization algorithm, encompass direct, single-step, sequential, and multi-point single-step design processes. Thirdly, two new methods were developed for RBDO of complex engineering systems. The methods involve an adaptive-sparse polynomial dimensional decomposition (AS-PDD) of a high-dimensional stochastic response for reliability analysis, a novel integration of AS-PDD and score functions for calculating the sensitivities of the failure probability with respect to design variables, and standard gradient-based optimization algorithms, resulting in a multi-point, single-step design process. The two methods, depending on how the failure probability and its design sensitivities are evaluated, exploit two distinct combinations built on AS-PDD: the AS-PDD-SPA method, entailing SPA and score functions; and the AS-PDD-MCS method, utilizing the embedded MCS of the AS-PDD approximation and score functions. In addition, a new method, named as the augmented PDD method, was developed for RDO and RBDO subject to mixed design variables, comprising both distributional and structural design variables. The method comprises a new augmented PDD of a high-

dimensional stochastic response for statistical moment and reliability analyses; an integration of the augmented PDD, score functions, and finite-difference approximation for calculating the sensitivities of the first two moments and the failure probability with respect to distributional and structural design variables; and standard gradient-based optimization algorithms, leading to a multi-point, single-step design process. The innovative formulations of statistical moment and reliability analysis, design sensitivity analysis, and optimization algorithms have achieved not only highly accurate but also computationally efficient design solutions. Therefore, these new methods are capable of performing industrial-scale design optimization with numerous design variables.

PUBLIC ABSTRACT

A great many complex systems and engineering structures are innately plagued by extant uncertainties found in manufacturing processes and operating environments. Under this Ph.D. study, design optimization of complex systems in the presence of uncertainty was conducted; in other words, developing methods to achieve the best possible design solution in which the nature of the system behavior is uncertain. The research involved new fundamental developments and integration of novel computational methods to study two principal classes of design optimization: (1) robust design optimization, which improves product quality by reducing the sensitivity of an optimal design; and (2) reliability-based design optimization, which concentrates on attaining an optimal design by ensuring sufficiently low risk of failure. Depending on the objective set forth by a designer, uncertainty is effectively mitigated by these design optimization methods. The innovative formulations of statistical moment and reliability analyses, design sensitivity analysis, and optimization algorithms - the necessary ingredients of the computer models developed - have achieved not only highly accurate, but also computationally efficient design solutions. Therefore, these new models are capable of performing industrial-scale design optimization with numerous design variables. Potential engineering applications comprise ground vehicle design for improved durability and crashworthiness, fatigue- and fracture-resistant design for civil and aerospace applications, and reliable design of microelectronic packaging under harsh environments, to name a few.

TABLE OF CONTENTS

xiii

LIST OF TABLES

LIST OF FIGURES

xvii

xviii

CHAPTER 1
INTRODUCTION

1.1   Background and Motivation

A great many complex systems and engineering structures are innately plagued by extant uncertainties found in manufacturing processes and operating environments. Conventional design procedures, which rely on heuristically derived safety factors, cannot account for the quantitative nature of the statistical variation of a system response. Consequently, the resultant designs are either unnecessarily conservative in overcompensating for uncertainties or unknowingly risky due to the inherent uncertainties.

Given the existence of uncertainties, the assessment of stochastic responses must be addressed during the design process of complex systems. To this end, three distinct theories that rely on the information available—fuzzy set theory, information theory, and probability theory—can be employed to characterize uncertainties and assess stochastic responses. The probability theory, owing to its rigorousness, has been mostly viewed as the most competitive way to model output uncertainties as long as the knowledge of probability distributions of input uncertainties is provided. When employing the probability theory to characterize uncertainties, depending on the objective of the optimization, two major types of design problems, referred to as robust design optimization (RDO) and reliability-based design optimization (RBDO), have been increasingly employed by engineers and studied by researchers.

Robust design optimization constitutes a mathematical framework for solving design problems in the presence of uncertainty, manifested by statistical descriptions of the objective and/or constraint functions [1–6]. Aimed at improving product quality, it minimizes the propagation of input uncertainty to output responses of interest, leading to an insensitive design. Pioneered by Taguchi *et al.* [1], RDO is increasingly viewed as an enabling technology for the design of aerospace, civil, and automotive structures subject to uncertainty [2–6]. The objective or constraint functions in RDO often involve second-moment properties, such as means and standard deviations, of stochastic responses, describing the objective robustness or feasibility robustness of a given design [3]. The main target of RDO is to reduce the variability of the system performance, which is characterized most often by its standard deviations [7].

Compared with RDO, which concentrates on the optimal designs that make the performance less sensitive to uncertainties, RBDO aims to find the optimal designs with low probabilities of failure corresponding to some critical failure mechanisms. In constraints of RBDO, known as probabilistic constraints or reliability constraints, particular attention is paid to the issue of structural safety in extreme events. Therefore, a limit state function is required to define the failure of the structural system. In a traditional RBDO problem, the objective function is always defined in the mean (or deterministic) sense. In a generalized RBDO problem, the objective function depends on the mean and standard deviation of certain response, which leads to reliability-based robust design optimization [3, 8, 9], an integrated framework that blends the design objective robustness and probabilistic constraints. Therefore, an

RBDO problem using probability theory typically requires complete statistical information on the responses. For the same reason, the implementation of RBDO is known for computationally expensive reliability analysis.

Solving a practical RDO or RBDO problem draws in uncertainty quantification of random responses and its coupling with gradient-based optimization algorithms, consequently demanding a greater computational effort. Unfortunately, existing methods for solving RDO and RBDO problems are usually restricted or even prohibitive, owing to the following limitations: (1) the efficiency or accuracy of inherent stochastic analysis for moments or reliabilities drops when the dimensionality of the problem is high; (2) for many of the existing methods, stochastic sensitivity analysis requires additional stochastic analyses, thus increasing the computational cost; (3) existing methods for solving RDO problems permit the objective and constraint functions and their sensitivities to be calculated only at a fixed design, requiring new statistical moment and sensitivity analyses at every design iteration until convergence is attained; and (4) existing methods have not been adequately developed for high-dimensional RBDO problems due to the loss of accuracy or efficiency in stochastic analysis, stochastic sensitivity analysis, and optimization algorithms. The major motivation for this work is to develop methods of solving RDO and RBDO with greater accuracy and/or better efficiency than traditional methods by addressing the four aforementioned limitations of existing methods.

1.2   Objective of the Study

The primary objective of this study is to develop new computational methods for RDO and RBDO of high-dimensional, complex engineering systems. Four major research directions, all anchored in polynomial dimensional decomposition (PDD), have been defined to meet the objective. They involve: (1) development of new sensitivity analysis methods for RDO and RBDO; (2) development of novel optimization methods for solving RDO problems; (3) development of novel optimization methods for solving RBDO problems; and (4) development of a novel scheme and formulation to solve stochastic design optimization problems with both distributional and structural design parameters. Figure 1.1 presents the integration of the four research directions, including their coverage in Chapters 3 through 6.

1.3   Outline of the Thesis

The thesis is organized as follows. Chapter 2 presents the preliminaries of probability theory. This chapter also furnishes the state-of-the-art review of existing methods for design under uncertainty. Finally, the needs for fundamental research are outlined.

Chapter 3 presents three new computational methods for calculating design sensitivities of statistical moments and reliability of high-dimensional complex systems subject to random input. The first method represents a novel integration of polynomial dimensional decomposition (PDD) of a multivariate stochastic response function and score functions. The second and third methods, relevant to probability

distribution or reliability analysis, exploit two distinct combinations built on PDD: the PDD-SPA method, which entails the saddlepoint approximation (SPA) and score functions, and the PDD-MCS method, which utilizes the embedded Monte Carlo simulation (MCS) of the PDD approximation and score functions. Five numerical examples are solved with the proposed methods, and the results are compared with at least one of two crude MCS-based approaches or the exact solution.

Chapter 4 introduces four new PDD-based methods for RDO of complex engineering systems. The methods depend on how statistical moment and sensitivity analyses are dovetailed with an optimization algorithm, encompassing direct, single-step, sequential, and multi-point single-step design processes. Four numerical examples entailing mathematical functions and solid-mechanics problems, including an industrial-scale lever-arm design, illustrate the accuracy, convergence properties, and computational efficiency of the proposed methods.

Chapter 5 puts forward two new methods for reliability-based design optimization (RBDO) of complex engineering systems. The methods involve an adaptive-sparse polynomial dimensional decomposition (AS-PDD) of a high-dimensional stochastic response for reliability analysis, a novel integration of AS-PDD and score functions for calculating the sensitivities of the failure probability with respect to design variables, and standard gradient-based optimization algorithms, encompassing a multi-point, single-step design process. The two methods, depending on how the failure probability and its design sensitivities are evaluated, exploit two distinct combinations built on AS-PDD: the AS-PDD-SPA method, entailing the saddlepoint approximation

(SPA) and score functions; and the AS-PDD-MCS method, utilizing the embedded Monte Carlo simulation (MCS) of the AS-PDD approximation and score functions. Four numerical results stemming from mathematical functions or engineering problems, including the shape design of a 79-dimensional jet engine bracket, demonstrate the power of the methods developed to tackle practical RBDO problems.

Chapter 6 presents a new method, named as the augmented PDD method, for robust design optimization and reliability-based design optimization subject to mixed design variables accounting for both distributional and structural design variables. The method comprises a new augmented PDD of a high-dimensional stochastic response for statistical moment and reliability analyses; an integration of the augmented PDD, score functions, and finite-difference approximation for calculating the sensitivities of the first two moments and the failure probability with respect to distributional and structural design variables; and standard gradient-based optimization algorithms, encompassing a multi-point, single-step design process. Four numerical examples, involving mathematical functions and solid-mechanics problems, contrast the accuracy and computational efficiency of the proposed methods for sensitivity analysis and RDO/RBDO, all entailing mixed design variables.

Finally, conclusions are drawn and future research directions are suggested in Chapter 7.
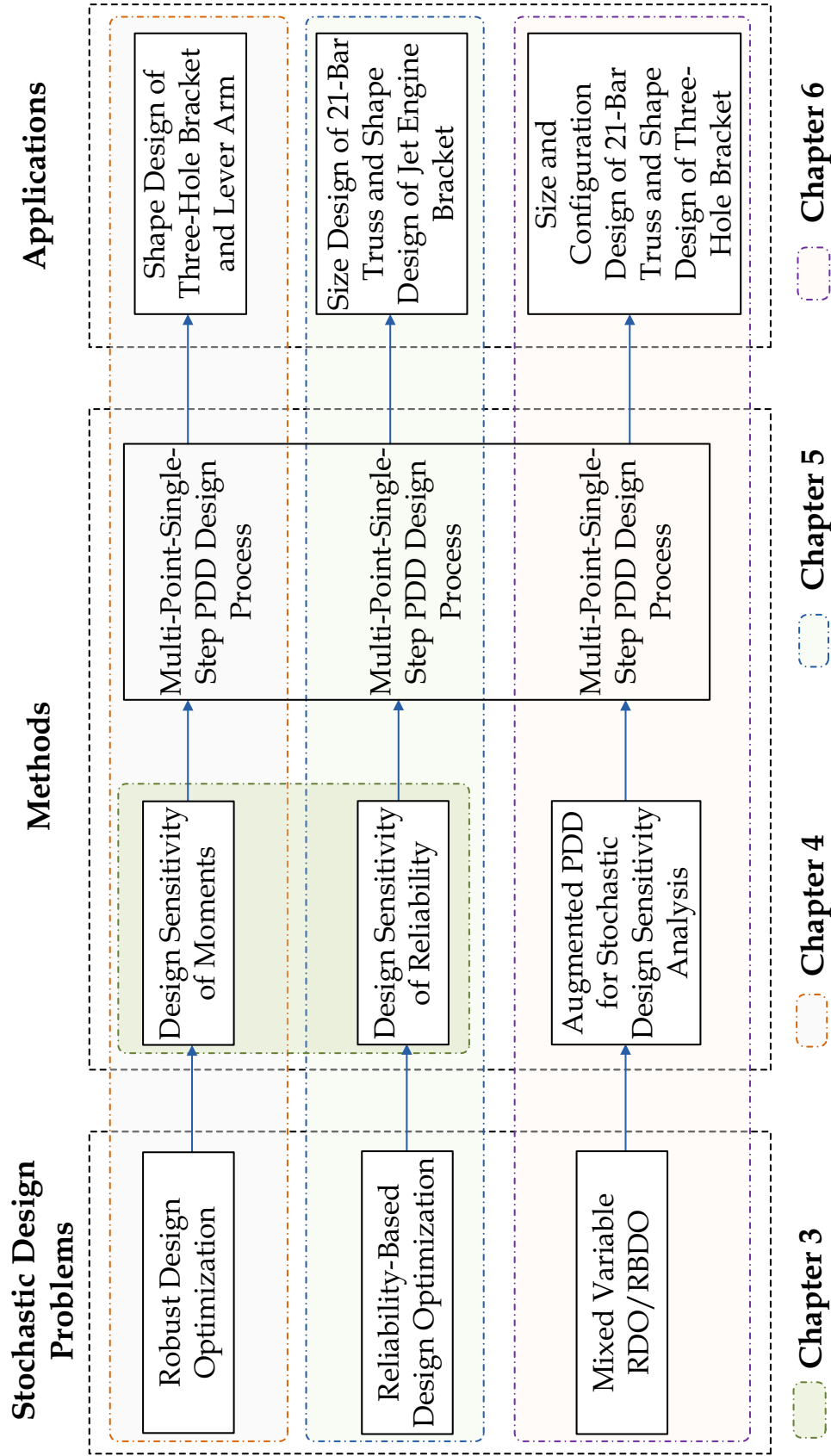
Figure 1.1: The integration of the four research directions

CHAPTER 2
STATE-OF-THE-ART REVIEW

This chapter presents mathematical generalities and existing methods and algorithms, reviewing those widely employed for solving RDO and RBDO problems, and then discusses the need for fundamental research. Section 2.1 elucidates the preliminaries of probability theory. The mathematical formulations of RDO and RBDO are defined in Section 2.2. Section 2.3 briefly reviews the existing methods for statistical moments analysis and reliability analysis. Section 2.4 contains existing methods for stochastic design sensitivity analysis. The state-of-the-art reviews of the prevailing methods for solving RDO and RBDO are rendered in Sections 2.5 and 2.6, respectively. Finally, the needs for fundamental research are outlined in Section 2.7.

2.1 Mathematical Preliminaries

The prevailing model for uncertainties in engineering is based on probability theory. This section represents some essential definitions and notations in probability theory that will be required here and throughout the forthcoming chapters.

2.1.1 Probability space

The probability space is a triple $(\Omega, \mathcal{F}, P)$, where the sample space Ω of a random experiment is a collection of all possible outcomes of the random experiment. The σ-field or σ-algebra $\mathcal{F}$ is a non-empty collection of subsets of Ω that satisfies the following:

1. The empty set $\varnothing \in \mathcal{F}$.

2. If any event $A \in \mathcal{F}$, then $A^C \in \mathcal{F}$.

3. If $A_i \in \mathcal{F}$ is a countable sequence of sets, then $\cup_i A_i \in \mathcal{F}$.

The probability measure $P : \mathcal{F} \to [0,1]$ is a function defined on $\mathcal{F}$ that has the following properties:

1. For any event A in $\mathcal{F}$, $0 \leq P(A) \leq 1$.

2. If $A_i \in \mathcal{F}$ is a countable sequence of disjoint sets, then $P(\cup_i A_i) = \sum_i P(A_i)$.

3. $P(\Omega) = 1$, and $P(\phi) = 0$, where ϕ denotes the empty set.

In short, a probability space is a measure space such that the measure of the whole space is equal to *one* [10].

2.1.2   Random variable

Consider a probability space $(\Omega, \mathcal{F}, P)$ and denote by $\mathbb{R}$ the set of real numbers; then, a random variable, denoted by $X(\omega)$, is a function mapping every elementary event $\omega \in \Omega$ to an associated real number. A random variable X induces a probability measure on $\mathbb{R}$ called its distribution, usually described by giving its cumulative distribution function (CDF), $F_X(x) := P(X \leq x)$. For a continuous random variable X, the probability density function (PDF), denoted by $f_X(x)$, is $f_X(x) := dF_X(x)/dx$, if it exists. The PDF is non-negative everywhere, and its integral over the entire space is equal to *one*. The rth statistical moment of a random variable X is defined as

$$m^{(r)} = \mathbb{E}[X^r] = \int_{\mathbb{R}} x^r \, f_X(x) \, dx, \tag{2.1}$$

where $\mathbb{E}$ is the expectation operator with respect to the probability measure $f_X(x)dx$ of X. The first moment $m^{(1)}$ of a random variable X is called its mean $\mu_X := \mathbb{E}[X] := \int_{\mathbb{R}} x\, f_X(x)\, dx$. A central moment is a moment of a random variable about its mean. For instance, the variance of X, denoted by σ_X^2, is its second central moment and is defined as $\sigma_X^2 := \mathbb{E}\left[(X - \mu_X)^2\right] := \int_{\mathbb{R}} (x - \mu_X)^2\, f_X(x)\, dx$; here, σ_X is called the standard deviation of X. The third and fourth central moments are called skewness and kurtosis of X, respectively. This research involves systems with random input parameters following a variety of probability distributions like Beta, exponential, Gaussian, Gumbel, Lognormal, Weibull etc., details of which can be found in the literature [11].

2.1.3   Random vector

A collection of N random variables, where $N < \infty$, forms a column vector $\mathbf{X} = (X_1, \ldots, X_N)^{\mathrm{T}}$, called a random vector, whose components $X_1, \ldots, X_N$ are scalar-valued random variables and often correlated with each other. The joint CDF, denoted by $F_{\mathbf{X}}(\mathbf{x})$, of $\mathbf{X}$ is defined by the mapping $\mathbf{X} : \Omega \to \mathbb{R}^N$ and the probability measure P, i.e., $F_{\mathbf{X}}(\mathbf{x}) := P\left(\cap_{i=1}^N \{X_i \le x_i\}\right)$. If $F_{\mathbf{X}}(\mathbf{x})$ is such that $f_{\mathbf{X}}(\mathbf{x}) = \partial^N F_{\mathbf{X}}(\mathbf{x})/\partial x_1 \cdots \partial x_N$ exists, then $f_{\mathbf{X}}$ is called the joint PDF of $\mathbf{X}$. If the components of a random vector are independent, then the joint PDF $f_{\mathbf{X}}(\mathbf{x})$ is a product of their marginal PDFs, i.e., $f_{\mathbf{X}}(\mathbf{x}) = \prod_{i=1}^N f_{X_i}(x_i)$. The mean $\boldsymbol{\mu}_{\mathbf{X}}$ of a random vector $\mathbf{X}$ is a fixed vector $\mathbb{E}(\mathbf{X})$ whose elements are the expected values of the respective random variables.

The covariance matrix, $\mathbf{\Sigma_X} := \mathbb{E}[(\mathbf{X}-\boldsymbol{\mu_X})(\mathbf{X}-\boldsymbol{\mu_X})^{\mathrm{T}}]$, of a random vector is an $N \times N$ matrix whose i, j element is the covariance $\mathrm{Cov}(X_i, X_j) := \mathbb{E}[(X_i-\mu_i)(X_j-\mu_j)]$ between the ith and the jth random variables. The variance of X_i is the ith diagonal element of $\mathbf{\Sigma_X}$. The correlation coefficient, $\rho_{ij} := \Sigma_{ij}/(\sigma_i\sigma_j)$, is defined only if both of the standard deviations are finite and both of them are nonzero. When X_i and X_j are independent, then X_i and X_j are uncorrelated, i.e., $\rho_{ij} = 0$. But if X_i and X_j are uncorrelated, then X_i and X_j are not necessarily independent.

2.1.4 Hilbert space

A vector space with an inner product defined on it is called inner product space. A Hilbert space is a complete inner product space. In fact, Hilbert spaces are probably the most natural generalization of Euclidean space, and their theory is richer and retains many features of Euclidean space, a central concept being orthogonality. A particular type of Hilbert space is the $\mathcal{L}_2$-space, which is defined as the set of all functions $f : \mathbb{R}^N \to \mathbb{R}$ such that the integral of the square of the absolute value of the function is finite, i.e., $\int_\Omega |f(\mathbf{x})|^2 \, d\mathbf{x} < \infty$, induced by the inner product $\langle f, g \rangle := \int_\Omega f(\mathbf{x})g(\mathbf{x})d\mathbf{x}$, which also exists and is finite. Therefore, denoted by $\mathcal{L}_2(\Omega, \mathcal{F}, P)$ the $\mathcal{L}_2$-space associated with the probability triple $(\Omega, \mathcal{F}, P)$, the real random variables $\mathbf{X} \in \mathcal{L}_2(\Omega, \mathcal{F}, P)$ exist with a finite second moment, i.e., $\mathbb{E}[X_i^2] < \infty$, $i = 1, \ldots, N$, and $\mathbb{E}[X_iX_j] < \infty$, $i, j = 1, \ldots, N$.

2.2   Design under Uncertainty

Let $\mathbb{N}$, $\mathbb{N}_0$, $\mathbb{R}$, and $\mathbb{R}_0^+$ represent the sets of positive integer (natural), non-negative integer, real, and non-negative real numbers, respectively. For $k \in \mathbb{N}$, denote by $\mathbb{R}^k$ the k-dimensional Euclidean space and by $\mathbb{N}_0^k$ the k-dimensional multi-index space. These standard notations will be used throughout the forthcoming sections.

Consider a measurable space $(\Omega_{\mathbf{d}}, \mathcal{F}_{\mathbf{d}})$, where $\Omega_{\mathbf{d}}$ is a sample space and $\mathcal{F}_{\mathbf{d}}$ is a σ-field on $\Omega_{\mathbf{d}}$. For $M \in \mathbb{N}$ and $N \in \mathbb{N}$, let $\mathbf{d}_T = (\mathbf{d}, \mathbf{s}) = (d_1, \cdots, d_{M_d}, s_1, \cdots, s_{M_s})^T \in \mathcal{D}$ be an $\mathbb{R}^M$-valued design vector with non-empty closed set $\mathcal{D} \subseteq \mathbb{R}^M$, where $M_d, M_s \in \mathbb{N}$ and $M_d + M_s = M$, and let $\mathbf{X} := (X_1, \cdots, X_N)^T : (\Omega_{\mathbf{d}}, \mathcal{F}_{\mathbf{d}}) \to (\mathbb{R}^N, \mathcal{B}^N)$ be an $\mathbb{R}^N$-valued input random vector with $\mathcal{B}^N$ representing the Borel σ-field on $\mathbb{R}^N$, describing the statistical uncertainties in loads, material properties, and geometry of a complex mechanical system. The design variables are grouped into two major classes: (1) distributional design vector $\mathbf{d}$ with dimensionality M_d, and (2) structural design vector $\mathbf{s}$ with dimensionality M_s. A distributional design variable d_k, $k = 1, \cdots, M_d$, can be any distribution parameter or a statistic—for instance, the mean and standard deviation—of one or more random variables. A structural design variable s_p, $p = 1, \cdots, M_s$, can be any deterministic parameter of a performance function. Defined over $(\Omega_{\mathbf{d}}, \mathcal{F}_{\mathbf{d}})$, let $\{P_{\mathbf{d}} : \mathcal{F} \to [0,1]\}$ be a family of probability measures. The probability law of $\mathbf{X}$ is completely defined by a family of the joint probability density functions (PDF) $\{f_{\mathbf{X}}(\mathbf{x}; \mathbf{d}), \ \mathbf{x} \in \mathbb{R}^N, \ \mathbf{d} \in \mathcal{D}\}$ that are associated with corresponding probability measures $\left\{P_{\mathbf{d}}, \mathbf{d} \in \mathbb{R}^{M_d}\right\}$, so that the probability triple $(\Omega_{\mathbf{d}}, \mathcal{F}_{\mathbf{d}}, P_{\mathbf{d}})$ of $\mathbf{X}$ depends on $\mathbf{d}$.

Let $y_l(\mathbf{X}; \mathbf{d}, \mathbf{s})$, $l = 0, 1, 2, \cdots, K$, be a collection of $K + 1$ real-valued, square-integrable, measurable transformations on $(\Omega_{\mathbf{d}}, \mathcal{F}_{\mathbf{d}})$, describing relevant geometry (*e.g.*, length, area, volume, mass) and performance functions of a complex system. The function $y_l : (\mathbb{R}^N, \mathcal{B}^N) \to (\mathbb{R}, \mathcal{B})$ in general is not only an explicit function of distributional and structural design variables $\mathbf{d}$ and $\mathbf{s}$, but also implicitly depends on distributional design variables $\mathbf{d}$ via the probability law of $\mathbf{X}$.

2.2.1 RDO

The mathematical formulation of a general RDO problem involving an objective function $c_0 : \mathbb{R}^M \to \mathbb{R}$ and constraint functions $c_l : \mathbb{R}^M \to \mathbb{R}$, where $l = 1, \cdots, K$ and $1 \leq K < \infty$, requires one to

$$\min_{(\mathbf{d},\mathbf{s}) \in \mathcal{D} \subseteq \mathbb{R}^M} c_0(\mathbf{d}, \mathbf{s}) := g_0 \left(\mathbb{E}_{\mathbf{d}} \left[y_0(\mathbf{X}; \mathbf{d}, \mathbf{s}) \right], \operatorname{var}_{\mathbf{d}} \left[y_0(\mathbf{X}; \mathbf{d}, \mathbf{s}) \right], \mathbf{d}, \mathbf{s} \right),$$

$$\text{subject to} \quad c_l(\mathbf{d}, \mathbf{s}) := g_l \left(\mathbb{E}_{\mathbf{d}} \left[y_l(\mathbf{X}; \mathbf{d}, \mathbf{s}) \right], \operatorname{var}_{\mathbf{d}} \left[y_l(\mathbf{X}; \mathbf{d}, \mathbf{s}) \right], \mathbf{d}, \mathbf{s} \right) \leq 0, \ l = 1, \cdots, K,$$

$$d_{k,L} \leq d_k \leq d_{k,U}, \ k = 1, \cdots, M_d,$$

$$s_{p,L} \leq s_p \leq s_{p,U}, \ p = 1, \cdots, M_s,$$

$$(2.2)$$

where $\mathbb{E}_{\mathbf{d}}[y_l(\mathbf{X}; \mathbf{d}, \mathbf{s})] := \int_{\mathbb{R}^N} y_l(\mathbf{x}; \mathbf{d}, \mathbf{s}) f_{\mathbf{X}}(\mathbf{x}; \mathbf{d}) d\mathbf{x}$ is the mean of $y_l(\mathbf{X}; \mathbf{d}, \mathbf{s})$ with $\mathbb{E}$ denoting the expectation operator with respect to the probability measure $f_{\mathbf{X}}(\mathbf{x}; \mathbf{d}) d\mathbf{x}$ of $\mathbf{X}$, $\operatorname{var}_{\mathbf{d}}[y_l(\mathbf{X}; \mathbf{d}, \mathbf{s})] := \mathbb{E}_{\mathbf{d}}[\{y_l(\mathbf{X}; \mathbf{d}, \mathbf{s}) - \mathbb{E}_{\mathbf{d}}[y_l(\mathbf{X}; \mathbf{d}, \mathbf{s})]\}^2]$ is the variance of $y_l(\mathbf{X}; \mathbf{d}, \mathbf{s})$, g_l, $l = 0, 1, \cdots, K$, are arbitrary functions of $\mathbb{E}_{\mathbf{d}}[y_l(\mathbf{X}; \mathbf{d}, \mathbf{s})]$ and $\operatorname{var}_{\mathbf{d}}[y_l(\mathbf{X}; \mathbf{d}, \mathbf{s})]$, $d_{k,L}$ and $d_{k,U}$ are the lower and upper bounds, respectively, of d_k, and $s_{p,L}$ and $s_{p,U}$ are the lower and upper bounds, respectively, of s_p. However, a special case of Equa-

tion (2.2), commonly adopted in the RDO society [9, 12–14], involves the following assumptions: (1) the design variables comprise solely distributional parameters, that is, $\mathbf{d}_T = \mathbf{d}$; (2) g_l, $l = 0, \cdots, K$, are not explicit functions of $\mathbf{d}$ and $\mathbf{s}$ and are linear transformations of the mean and standard deviation of y_l; and (3) the responses y_l, $l = 0, \cdots, K$, do not explicitly depend on $\mathbf{d}$ and $\mathbf{s}$, although y_l implicitly depends on $\mathbf{d}$ via the probability law of $\mathbf{X}$, leading one to

$$\min_{\mathbf{d} \in \mathcal{D} \subseteq \mathbb{R}^M} \quad c_0(\mathbf{d}) := w_1 \frac{\mathbb{E}_{\mathbf{d}}\left[y_0(\mathbf{X})\right]}{\mu_0^*} + w_2 \frac{\sqrt{\operatorname{var}_{\mathbf{d}}\left[y_0(\mathbf{X})\right]}}{\sigma_0^*},$$

$$\text{subject to} \quad c_l(\mathbf{d}) := \alpha_l \sqrt{\operatorname{var}_{\mathbf{d}}\left[y_l(\mathbf{X})\right]} - \mathbb{E}_{\mathbf{d}}\left[y_l(\mathbf{X})\right] \le 0, \; l = 1, \cdots, K, \quad (2.3)$$

$$d_{k,L} \le d_k \le d_{k,U}, \; k = 1, \cdots, M,$$

where $w_1 \in \mathbb{R}_0^+$ and $w_2 \in \mathbb{R}_0^+$ are two non-negative, real-valued weights, satisfying $w_1 + w_2 = 1$; $\mu_0^* \in \mathbb{R} \setminus \{0\}$ and $\sigma_0^* \in \mathbb{R}_0^+ \setminus \{0\}$ are two non-zero, real-valued scaling factors; and $\alpha_l \in \mathbb{R}_0^+$, $l = 0, 1, \cdots, K$, are non-negative, real-valued constants associated with the probabilities of constraint satisfaction.

In Equation (2.3), $c_0(\mathbf{d})$ describes the objective robustness, and $c_l(\mathbf{d})$, $l = 1, \cdots, K$, describe the feasibility robustness of a given design. Evaluations of both objective robustness and feasibility robustness, involving the first two moments of various responses, are required for solving RDO problems, consequently demanding statistical moment analysis. Coupling with gradient-based optimization algorithms mandates that the gradients of $c_l(\mathbf{d})$ be formulated, thus requiring design sensitivity analysis of the first two moments. Existing approaches for statistical moment analysis and design sensitivity of moments are elucidated in the forthcoming sections.

2.2.2   RBDO

The mathematical formulation of a general RBDO problem involving an objective function $c_0 : \mathbb{R}^M \to \mathbb{R}$ and constraint functions $c_l : \mathbb{R}^M \to \mathbb{R}$, where $l = 1, \cdots, K$ and $1 \leq K < \infty$, requires one to

$$\min_{(\mathbf{d}, \mathbf{s}) \in \mathcal{D} \subseteq \mathbb{R}^M} \quad c_0(\mathbf{d}, \mathbf{s}) := g_0 \left(\mathbb{E}_{\mathbf{d}} \left[y_0(\mathbf{X}; \mathbf{d}, \mathbf{s}) \right], \mathrm{var}_{\mathbf{d}} \left[y_0(\mathbf{X}; \mathbf{d}, \mathbf{s}) \right], \mathbf{d}, \mathbf{s} \right),$$

$$\text{subject to} \quad c_l(\mathbf{d}, \mathbf{s}) := P_{\mathbf{d}} \left[\mathbf{X} \in \Omega_{F,l}(\mathbf{d}, \mathbf{s}) \right] - p_l \leq 0, \ l = 1, \cdots, K,$$

$$d_{k,L} \leq d_k \leq d_{k,U}, \ k = 1, \cdots, M_d,$$

$$s_{p,L} \leq s_p \leq s_{p,U}, \ p = 1, \cdots, M_s,$$

$$(2.4)$$

where $\Omega_{F,l}(\mathbf{d}, \mathbf{s}) \subseteq \Omega$ is the lth failure set that, in general, may depend on $\mathbf{d}$ and $\mathbf{s}$, and $0 \leq p_l \leq 1, \ l = 1, \cdots, K$, are target failure probabilities. However, in most engineering applications, RBDO is commonly formulated to

$$\min_{\mathbf{d} \in \mathcal{D} \subseteq \mathbb{R}^M} \quad c_0(\mathbf{d}),$$

$$\text{subject to} \quad c_l(\mathbf{d}) := P_{\mathbf{d}} \left[\mathbf{X} \in \Omega_{F,l}(\mathbf{d}) \right] - p_l \leq 0, \ l = 1, \cdots, K,$$

$$d_{k,L} \leq d_k \leq d_{k,U}, \ k = 1, \cdots, M,$$

$$(2.5)$$

where the distributional parameters solely describe the design variables, that is, $\mathbf{d}_T = \mathbf{d}$, c_0 is a prescribed deterministic function of $\mathbf{d}$, and $y_l(\mathbf{X}), \ l = 1, \cdots, K$, are not explicit functions of $\mathbf{d}$, although y_l implicitly depends on $\mathbf{d}$ via the probability law of $\mathbf{X}$. Relying on the nature of the failure domain $\Omega_{F,l}$, a component or a system failure probability can be envisioned. For component failure probability, the failure domain is often adequately described by a single performance function $y(\mathbf{X})$, for instance, $\Omega_{F,l} := \{\mathbf{x} \ : \ y_l(\mathbf{x}) < 0\}$. In contrast, multiple, interdependent performance

functions $y_{l,i}(\mathbf{x})$, $i = 1, 2, \cdots$, are required for system reliability analysis, leading, for example, to $\Omega_{F,l} := \{\mathbf{x} : \cup_i y_{l,i}(\mathbf{x}) < 0\}$ and $\Omega_{F,l} := \{\mathbf{x} : \cap_i y_{l,i}(\mathbf{x}) < 0\}$ for series and parallel systems, respectively.

Generally, the objective function c_0 in Equation (2.5) is an explicit function of $\mathbf{d}$ in default of any assessment of stochastic responses. It can also be a function of the mean and standard deviation of a certain response function, defining the objective robustness as in Equation (2.3), leading to reliability-based robust design optimization [3, 8, 9].

In Equation (2.5), evaluation of the reliability constraints $c_l(\mathbf{d})$, $l = 1, \cdots, K$, requires calculating the component or system probability of failure defined by the performance functions. Coupling with gradient-based optimization algorithms mandates that the gradients of $c_l(\mathbf{d})$ be formulated, thus requiring design sensitivity analysis of failure probability. A brief review of existing methods for reliability analysis and design sensitivity of failure probability is provided in the forthcoming sections.

2.3 Stochastic Analysis

2.3.1 Methods of statistical moment analysis

The fundamental problem rooted in statistical moment analysis entails calculation of a high-dimensional integral with respect to the probability measure $f_{\mathbf{X}}(\mathbf{x}; \mathbf{d})d\mathbf{x}$ of $\mathbf{X}$ over $\mathbb{R}^N$, where N is the number of random variables. In general, such an integral cannot be evaluated analytically. Direct numerical integration can be performed, but it is not economically feasible when N exceeds three or four. Existing approximate

methods for statistical moment analysis include the point estimate method (PEM) [15, 16], Taylor series expansion or perturbation method [17, 18], tensor product quadrature (TPQ) [19], Neumann expansion method [20], polynomial chaos expansion (PCE) [20], statistically equivalent solution [21], dimension-reduction method [22, 23], and others [24]. A few of these methods are further discussed as follows.

The point estimate method, originally proposed by Rosenblueth [15, 25] for calculating the moments of a random response function of one or several random variables, has been employed in several engineering applications [16, 26]. Let X be an input random variable and $y(X)$ be a response function of interest. The two-point PEM evaluates statistical moments of $y(X)$ by using two specified points x_- and x_+, and associated weights, which are determined by matching the first three moments of X. When y is a function of N random variables, the two-point PEM requires 2^N points, causing exponentially increased computational efforts. Harr [27] extended Roseblueth's PEM to accommodate large numbers of random variables by employing a rotational transformation to transform a correlated system into an uncorrelated system, leading to a scheme requiring only $2N$ points for the two-point PEM scheme. However, Harr's PEM does not utilize the moments higher than the second order and may result in loss of accuracy when the skewness of X, for example, is not *zero*. In fact, Rosenblueth's PEM is a special case of the Gauss quadrature rule [28]. When input random variables follow well-known probability distributions, such as normal, exponential, and uniform distribution, the PEM generates points and weights as the points and weights of the well-known Gauss-Hermite, Gauss-Laguerre, and Gauss-Legendre

quadratures. However, for arbitrary distributed input variables, transformations from an arbitrary random variable to a well-known random variable are required, bringing nonlinearity into the response function, and thus may cause a degradation of accuracy. Furthermore, when confronted with a large number of random variables, the PEM is usually restrictive or even prohibitive due to exponentially scaled computational demand.

The Taylor series expansion methods, introduced in the early 1980s in the context of the stochastic finite element method, have been successfully employed for random eigenvalue problems [29, 30], geotechnical problems [31, 32], and dynamic problems [33]. As the name implies, the Taylor series expansion methods, requiring that the performance function $y(\mathbf{X})$ be differentiable, employ Taylor series approximation of $y(\mathbf{X})$ at the mean values of input random vector $\mathbf{X}$. It can be used advantageously in cases where the input uncertainties and output nonlinearity are small, such that terms of a certain order and higher are negligible. When the first- or second-order Taylor series expansion is applied, the first two moments of $y(\mathbf{X})$ are evaluated from the knowledge of second-moment properties of $\mathbf{X}$ and gradients of the function $y(\mathbf{X})$. For an N-dimensional random input $\mathbf{X}$, if the gradients of $y(\mathbf{X})$ are computed with the forward or backward finite difference technique, the total numbers of function evaluations are $N + 1$ and $\frac{1}{2}N(N + 1) + 1$ for the first- and second-order Taylor series expansions, respectively. Consequently, the second-order Taylor series expansion is more computationally expensive than the first-order one, although it is generally more accurate than the latter. As mentioned earlier, the two major lim-

itations of these methods are that both the uncertainty of random inputs and the nonlinearity of performance functions must be small enough so that the contribution from high-order terms can be ignored.

Recently, the tensor product quadrature method [19] has been employed for statistical moment analysis. It should be noted that the TPQ method has close relations with the aforementioned PEM [14, 16, 28]. The nodes and weights of the TPQ method, satisfying the moment matching condition that is employed in the PEM, are obtained through rigorous approaches such as the Stieltjes procedure or the modified Chebyshev algorithm. For an arbitrary probability distribution, those nodes and weights can be easily obtained, unlike the PEM, in which an additional transformation is required and may lead to loss of accuracy. Similar to the PEM, the TPQ method may also be restrictive or prohibitive for high-dimensional problems due to exponentially increased computational burden.

2.3.2   Methods of reliability analysis

In 1969, Cornell [34] employed the first-order Taylor series expansion to estimate reliability, referred to as the mean-value first-order second moment (FOSM) method. The mean-value FOSM is inaccurate and sensitive to the mathematical formulation of the performance function, as the mean value point is usually not found on the failure surface [35]. Hasofer and Lind [36] proposed the H-L reliability index, laying the groundwork for the first- and second-order reliability method (FORM and SORM) [37–43]. The FORM is based on the linear approximation of the failure surface

at the most probable point (MPP), not the mean value point, and therefore is considered accurate as long as the curvature of the failure function in the standard Gaussian image $\mathbf{u}$ of the original random variable space $\mathbf{x}$ is not too large at the MPP [35]. As a natural extension to FORM, the SORM employs the quadratic approximation of the failure surface. There are two ways to construct the quadratic approximation. The first is called curvature fitting by Breitung *et al.* [39] and involves using the second-order derivative of the performance function at the MPP. The second is referred to as point fitting by Der Kiureghian *et al.* [40] and entails semi-paraboloids to interpolate the performance function around the MPP. The determination of the MPP involves nonlinear constrained optimizations, which can be formulated by the reliability index approach (RIA) to find the point on the performance surface to minimize the distance to the origin of the $\mathbf{u}$ space. The minimized distance is the H-L reliability index β_{HL}. The probability of failure by FORM is approximated by $\Phi(-\beta_{HL})$, where $\Phi(\cdot)$ is the CDF of a standard Gaussian random variable [35]. For SORM, various asymptotic formulae [39, 44] and non-asymptotic formulae [45, 46] exist. In most applications, FORM is chosen because of its relatively low computational cost. However, it encounters difficulties when dealing with strongly nonlinear performance functions and is criticized for its inherent error in approximating the failure surface as linear. The error can be reduced by SORM, which requires some curvatures to be calculated, resulting in aggravated computational burden. Moreover, both methods may yield considerable error due to the multiple MPPs resulting from a multimodal performance function.

Simulation methods are widely used to estimate probability of failure. Crude Monte Carlo simulation (MCS) [47], relying on independent random sampling and repeated deterministic trials, is insensitive to the number of input random variables. Denoting by L the sample size, the convergence rate of direct MCS is $O(L^{-1/2})$. Therefore, to achieve high accuracy, crude MCS requires a large sample size and hence many numerical analyses and thus is computationally intensive. In this regard, several variance-reduction techniques, such as importance sampling [48, 49], stratified sampling [50, 51], and directional simulation [52, 53], have been proposed. The basic idea behind importance sampling and stratified sampling is that certain points of the random variable space, which have more impact on the parameter being estimated than others, should be emphasized by sampling more frequently. On the other hand, the directional simulation method, as an efficient version of MCS, utilizes the χ^2-distribution and conditional expectation to reduce variance. The subset simulation, cooperating with a modified Metropolis algorithm [54], has been applied recently for estimation of failure probability [55]. It formulates the calculation of a small failure probability as a product of a sequence of relatively large probabilities by conditioning on various subsets. The major limitation of subset simulation is that the proposed PDFs for the Metropolis algorithm, which heavily impact the convergence of the algorithm, have to be chosen based on experience. Nonetheless, the simulation methods mentioned above mainly deal with the reliability analysis of simple mechanical systems. For complex mechanical systems requiring time-consuming finite element analysis (FEA), they become impractical or prohibitive.

In the context of reliability analysis, many other methods can be found in the literature. Using inverse Fourier transformation, exponential power series expansion, and Hermite polynomial approximation, Daniels [56] developed the saddlepoint approximation (SPA), providing an asymptotic formula for PDF of mean of n independent identically distributed random variables. The SPA, as a tool for estimating the densities and distribution function, was introduced to the area of structural reliability analysis by Du *et al.* [57, 58]. As extensions of FORM and SORM, the advanced mean value method (AMV) [41] and two-point nonlinear approximation (TANA) [59] have also been developed to treat nonlinear performance functions. However, these methods may result in significant errors in the case of multimodal performance functions, as demonstrated by Bichon *et al.* [60].

2.3.3 Dimensional decomposition methods

The dimensional decomposition is a finite, hierarchical, and convergent expansion of a multivariate output function in terms of its input variables with increasing dimensions [61–64]. The decomposition ameliorates the curse of dimensionality [65] to some extent by developing an input-output behavior of complex systems with low effective dimensions [66], wherein the degrees of interactions between input variables attenuate rapidly or vanish altogether. There exist two important variants of dimensional decomposition, described as follows, in the context of distributional design parameters only.

2.3.3.1 ANOVA dimensional decomposition

Let $y(\mathbf{X})$ be a real-valued, square-integrable, measurable transformation on $(\Omega, \mathcal{F})$, describing the relevant performance function of a complex system. It is assumed that $y : (\mathbb{R}^N, \mathcal{B}^N) \rightarrow (\mathbb{R}, \mathcal{B})$ is not an explicit function of $\mathbf{d}$, although y implicitly depends on $\mathbf{d}$ via the probability law of $\mathbf{X}$. Assuming independent coordinates of $\mathbf{X}$, its joint PDF is expressed by a product, $f_{\mathbf{X}}(\mathbf{x}; \mathbf{d}) = \prod_{i=1}^{i=N} f_{X_i}(x_i; \mathbf{d})$, of marginal PDF $f_{X_i} : \mathbb{R} \rightarrow \mathbb{R}_0^+$ of X_i, $i = 1, \cdots, N$, defined on its probability triple $(\Omega_i, \mathcal{F}_i, P_{i,\mathbf{d}})$ with a bounded or an unbounded support on $\mathbb{R}$. Then, for a given subset $u \subseteq \{1, \cdots, N\}$, $f_{\mathbf{X}_{-u}}(\mathbf{x}_{-u}; \mathbf{d}) := \prod_{i=1, i \notin u}^{N} f_{X_i}(x_i; \mathbf{d})$ defines the marginal density function of $\mathbf{X}_{-u} := \mathbf{X}_{\{1, \cdots, N\} \setminus u}$. The analysis-of-variance (ANOVA) dimensional decomposition (ADD), expressed by the recursive form [62–64]

$$y(\mathbf{X}) = \sum_{u \subseteq \{1, \cdots, N\}} y_u(\mathbf{X}_u; \mathbf{d}), \tag{2.6}$$

$$y_\emptyset(\mathbf{d}) = \int_{\mathbb{R}^N} y(\mathbf{x}) f_{\mathbf{X}}(\mathbf{x}; \mathbf{d}) d\mathbf{x}, \tag{2.7}$$

$$y_u(\mathbf{X}_u; \mathbf{d}) = \int_{\mathbb{R}^{N-|u|}} y(\mathbf{X}_u, \mathbf{x}_{-u}) f_{\mathbf{X}_{-u}}(\mathbf{x}_{-u}; \mathbf{d}) d\mathbf{x}_{-u} - \sum_{v \subset u} y_v(\mathbf{X}_v; \mathbf{d}), \tag{2.8}$$

is a finite, hierarchical expansion of y in terms of its input variables with increasing dimensions, where $u \subseteq \{1, \cdots, N\}$ is a subset with the complementary set $-u = \{1, \cdots, N\} \setminus u$ and cardinality $0 \leq |u| \leq N$, and y_u is a $|u|$-variate component function describing a constant or the interactive effect of $\mathbf{X}_u = (X_{i_1}, \cdots, X_{i_{|u|}})^T$, $1 \leq i_1 < \cdots < i_{|u|} \leq N$, a subvector of $\mathbf{X}$, on y when $|u| = 0$ or $|u| > 0$. The summation in Equation (2.6) comprises 2^N terms, with each term depending on a group of variables indexed by a particular subset of $\{1, \cdots, N\}$, including the empty set $\emptyset$. In Equation

(2.8), $(\mathbf{X}_u, \mathbf{x}_{-u})$ denotes an N-dimensional vector whose ith component is X_i if $i \in u$ and x_i if $i \notin u$. When $u = \emptyset$, the sum in Equation (2.8) vanishes, resulting in the expression of the constant function $y_\emptyset$ in Equation (2.7). When $u = \{1, \cdots, N\}$, the integration in Equation (2.8) is on the empty set, reproducing Equation (2.6) and hence finding the last function $y_{\{1, \cdots, N\}}$. Indeed, all component functions of y can be obtained by interpreting literally Equation (2.8).

The ANOVA component functions y_u, $\emptyset \neq u \subseteq \{1, \cdots, N\}$, are uniquely determined from the annihilating conditions [63, 64],

$$\int_\mathbb{R} y_u(\mathbf{x}_u; \mathbf{d}) f_{X_i}(x_i; \mathbf{d}) dx_i = 0 \text{ for } i \in u, \tag{2.9}$$

resulting in two remarkable properties: (1) the component functions, y_u, $\emptyset \neq u \subseteq \{1, \cdots, N\}$, have zero means; and (2) any two distinct component functions y_u and y_v, where $u \subseteq \{1, \cdots, N\}$, $v \subseteq \{1, \cdots, N\}$, and $u \neq v$, are orthogonal [64]. However, the ADD component functions are difficult to obtain because they require calculation of high-dimensional integrals.

Remark 2.1. The coefficient $y_\emptyset = \mathbb{E}_\mathbf{d}[y(\mathbf{X})]$ in Equation (2.7) is a function of the design vector $\mathbf{d}$, which describes the probability distribution of the random vector $\mathbf{X}$. Therefore, the adjective "constant" used to describe $y_\emptyset$ should be interpreted with respect to $\mathbf{X}$, not $\mathbf{d}$. A similar condition applies for the non-constant component functions y_u, $\emptyset \neq u \subseteq \{1, \cdots, N\}$, which also depend on $\mathbf{d}$.

2.3.3.2   Referential Dimensional Decomposition

Consider a reference point $\mathbf{c}(\mathbf{d}) = (c_1(\mathbf{d}), \cdots, c_N(\mathbf{d}))^T \in \mathbb{R}^N$ that generally depends on the design vector $\mathbf{d}$ and the associated Dirac measure $\prod_{i=1}^{N} \delta(x_i - c_i) dx_i$. The referential dimensional decomposition (RDD) is created when $\prod_{i=1}^{N} \delta(x_i - c_i) dx_i$ replaces the probability measure in Equations (2.6)-(2.8), leading to the recursive form [64]

$$y(\mathbf{X}) = \sum_{u \subseteq \{1, \cdots, N\}} w_u(\mathbf{X}_u; \mathbf{c}(\mathbf{d})), \qquad (2.10)$$

$$w_\emptyset(\mathbf{d}) = y(\mathbf{c}(\mathbf{d})), \qquad (2.11)$$

$$w_u(\mathbf{X}_u; \mathbf{c}(\mathbf{d})) = y(\mathbf{X}_u, \mathbf{c}_{-u}(\mathbf{d})) - \sum_{v \subset u} w_v(\mathbf{X}_v; \mathbf{c}(\mathbf{d})), \qquad (2.12)$$

also known as cut-HDMR [67], anchored decomposition [68–70], and anchored-ANOVA decomposition [71], with the latter two referring to the reference point as the anchor. Xu and Rahman introduced Equations (2.10)-(2.12) with the aid of Taylor series expansion, calling them dimension-reduction [22] and decomposition [23] methods for statistical moment and reliability analyses, respectively, of mechanical systems. Compared with ADD, RDD lacks orthogonal features, but its component functions are easier to obtain as they only involve function evaluations at a chosen reference point.

Remark 2.2. The constant $w_\emptyset$ in Equation (2.11) is a function $\mathbf{c}$, which is generally selected as the mean of the random vector $\mathbf{X}$ with the probability measure that depends on $\mathbf{d}$. Therefore, the adjective "constant" used to describe $w_\emptyset$ should be interpreted with respect to $\mathbf{X}$, not $\mathbf{d}$. Similar conditions prevail for the non-constant component functions w_u, $\emptyset \neq u \subseteq \{1, \cdots, N\}$, which also depend on $\mathbf{d}$ via $\mathbf{c}$.

2.3.3.3   Truncated ADD and RDD

Both ADD and RDD decompositions are grounded on a fundamental conjecture known to be true in many real-world applications: given a high-dimensional function y, its $|u|$-variate component functions decay rapidly with respect to $|u|$, leading to accurate lower-variate approximations of y. Indeed, given an integer $0 \leq S < N$, for all $1 \leq |u| \leq S$, the truncated dimensional decompositions

$$\tilde{y}_S(\mathbf{X}) = \sum_{\substack{u \subseteq \{1,\cdots,N\} \\ 0 \leq |u| \leq S}} y_u(\mathbf{X}_u; \mathbf{d}), \tag{2.13}$$

$$\hat{y}_S(\mathbf{X}; \mathbf{c}) = \sum_{\substack{u \subseteq \{1,\cdots,N\} \\ 0 \leq |u| \leq S}} w_u(\mathbf{X}_u; \mathbf{c}(\mathbf{d})), \tag{2.14}$$

respectively, describe S-variate ADD and RDD approximations, which for $S > 0$ includes interactive effects of at most S input variables $X_{i_1}, \cdots, X_{i_S}$, $1 \leq i_1 < \cdots < i_S \leq N$, on y. It is elementary to show that when $S \to N$, $\tilde{y}_S$ and $\hat{y}_S$ both converge to y in the mean-square sense, generating a hierarchical and convergent sequence of approximation of y from each decomposition.

For error analysis, a suitable direct form of Equation (2.14) is desirable. Theorem 2.3 supplies such a form, which was originally obtained by Xu and Rahman [22] using the Taylor series expansion.

Let $\mathbf{j}_k = (j_1, \cdots, j_k) \in \mathbb{N}_0^k$, $1 \leq k \leq S$, be a k-dimensional multi-index with each component representing a non-negative integer. The multi-index, used in Theorem 2.3, obeys the following standard notations: (1) $|\mathbf{j}_k| = \sum_{p=1}^{p=k} j_p$; (2) $\mathbf{j}_k! = \prod_{p=1}^{p=k} j_p!$; (3) $\partial^{\mathbf{j}_k} y(\mathbf{c}) = \partial^{j_1 + \cdots + j_k} y(\mathbf{c}) / \partial X_{i_1}^{j_1} \cdots \partial X_{i_k}^{j_k}$; (4) $(\mathbf{X}_u - \mathbf{c}_u)^{\mathbf{j}_k} = \prod_{p=1}^{p=k} (X_{i_p} - c_{i_p})^{j_p}$, $1 \leq i_1 < \cdots < i_k \leq N$.

Theorem 2.3. *For a differentiable multivariate function $y : \mathbb{R}^N \to \mathbb{R}$ and $0 \leq S < N$, if*

$$\hat{y}_S(\mathbf{X}; \mathbf{c}) = \sum_{k=0}^{S} (-1)^k \binom{N - S + k - 1}{k} \sum_{\substack{u \subseteq \{1, \cdots, N\} \\ |u| = S - k}} y(\mathbf{X}_u, \mathbf{c}_{-u}) \qquad (2.15)$$

represents an S-variate RDD approximation of $y(\mathbf{X})$, then $\hat{y}_S(\mathbf{X}; \mathbf{c})$ consists of all terms of the Taylor series expansion of $y(\mathbf{X})$ at $\mathbf{c}$ that have less than or equal to S variables, i.e.,

$$\hat{y}_{S,R}(\mathbf{X}; \mathbf{c}) = \sum_{k=0}^{S} t_k,$$

where

$$t_0 = y(\mathbf{c}),$$

$$t_k = \sum_{\substack{\mathbf{j}_k \in \mathbb{N}_0^k \\ j_1, \cdots, j_k \neq 0}} \frac{1}{\mathbf{j}_k!} \sum_{\substack{\emptyset \neq u \subseteq \{1, \cdots, N\} \\ |u| = k}} \partial^{\mathbf{j}_k} y(\mathbf{c}) \left(\mathbf{X}_u - \mathbf{c}_u \right)^{\mathbf{j}_k} ; \ 1 \leq k \leq S.$$

Proof. Xu and Rahman [22] proved this theorem in pages 1996-2000 of their paper when $\mathbf{c} = \mathbf{0}$ without loss of generality.

The stochastic method associated with the RDD approximation was simply called the "decomposition method" [23]. Theorem 2.3 implies that the RDD approximation $\hat{y}_S(\mathbf{X}; \mathbf{c})$ in Equation (2.15), when compared with the Taylor series expansion of $y(\mathbf{X})$, yields residual error that includes only terms of dimensions $S + 1$ and higher. All higher-order S- and lower-variate terms of $y(\mathbf{X})$ are included in Equation (2.15), which should therefore generally provide a higher-order approximation of a multivariate function than the equation derived from an S-order Taylor expansion.

For ADD or RDD to be useful, what are the approximation errors committed by $\tilde{y}_S(\mathbf{X})$ and $\hat{y}_S(\mathbf{X}; \mathbf{c})$ in Equations (2.13) and (2.14)? More importantly, for a given

$0 \leq S < N$, which approximation between ADD and RDD is better? A recently obtained theoretical result, Theorem 2.4, provides the answer.

Theorem 2.4. *Let $\mathbf{c} = (c_1, \cdots, c_N)^T \in \mathbb{R}^N$ be a random vector with the joint probability density function of the form $f_{\mathbf{X}}(\mathbf{c}; \mathbf{d}) = \prod_{j=1}^{j=N} f_j(c_j; \mathbf{d})$, where f_j is the marginal probability density function of its jth coordinate of $\mathbf{X} = (X_1, \cdots, X_N)^T$. Define two second-moment errors*

$$e_{S,A} := \mathbb{E}\left[(y(\mathbf{X}) - \tilde{y}_S(\mathbf{X}))^2\right] := \int_{\mathbb{R}^N} [y(\mathbf{x}) - \tilde{y}_S(\mathbf{x})]^2 f_{\mathbf{X}}(\mathbf{x}; \mathbf{d}) d\mathbf{x} \qquad (2.16)$$

and

$$e_{S,R}(\mathbf{c}) := \mathbb{E}\left[(y(\mathbf{X}) - \hat{y}_S(\mathbf{X}; \mathbf{c}))^2\right] := \int_{\mathbb{R}^N} [y(\mathbf{x}) - \hat{y}_S(\mathbf{x}; \mathbf{c})]^2 f_{\mathbf{X}}(\mathbf{x}; \mathbf{d}) d\mathbf{x}, \qquad (2.17)$$

committed by the S-variate ADD and RDD approximations, respectively, of $y(\mathbf{X})$. Then the lower and upper bounds of the expected error $\mathbb{E}[e_{S,R}] := \int_{\mathbb{R}^N} e_{S,R}(\mathbf{c}) f_{\mathbf{X}}(\mathbf{c}; \mathbf{d}) d\mathbf{c}$ from the S-variate RDD approximation, expressed in terms of the error $e_{S,A}$ from the S-variate ADD approximation, are

$$2^{S+1} e_{S,A} \leq \mathbb{E}[e_{S,R}] \leq \left[1 + \sum_{k=0}^{S} \binom{N-S+k-1}{k}^2 \binom{N}{S-k}\right] e_{S,A}. \qquad (2.18)$$

where $0 \leq S < N$, $S + 1 \leq N < \infty$.

Proof. See Theorem 4.12 and Corollary 4.13 provided by Rahman [64]. ∎

Remark 2.5. Theorem 2.4 reveals that the expected error from the univariate ($S = 1$) RDD approximation is at least four times larger than the error from the univariate ADD approximation. In contrast, the expected error from the bivariate ($S = 2$) RDD

approximation can be eight times larger or more than the error from the bivariate ADD approximation. Given an arbitrary truncation, an ADD approximation is superior to an RDD approximation. In addition, RDD approximations may perpetrate very large errors at upper bounds when there exist a large number of variables and appropriate conditions. Therefore, existing stochastic methods anchored in RDD approximations should be used with caveat. Furthermore, Rahman [64] has shown that for a given $1 \leq S < N$, the S-variate ADD approximation is optimal, whereas the S-variate RDD approximation is sub-optimal regardless of how the reference point is selected.

More recently, a polynomial version of ADD approximation, referred to as the polynomial dimensional decomposition (PDD) method, has been developed for uncertainty quantification of high-dimensional complex systems. The PDD, which inherits all desirable properties of ADD, also alleviates the curse of dimensionality to some extent by splitting a high-dimensional output function into a finite sum of simpler component functions that are arranged with respect to the degree of interaction among input random variables. In addition, the PDD exploits the smoothness properties of a stochastic response, whenever possible, by expanding its component functions in terms of measure-consistent orthogonal polynomials, leading to closed-form expressions of the second-moment characteristics of a stochastic solution. Although the same polynomials are extant in PCE, a recent study found that when the degrees of interaction become progressively weaker or vanish altogether, the PDD approximation commits smaller error than does the polynomial chaos approximation

for identical expansion orders [64].

2.4 Stochastic Design Sensitivity Analysis

Denote by $\mathcal{L}_r(\Omega, \mathcal{F}, P_{\mathbf{d}})$ a collection of real-valued random variables including $y(\mathbf{X})$, which is defined on $(\Omega, \mathcal{F}, P_{\mathbf{d}})$ such that $\mathbb{E}_{\mathbf{d}}[y^r(\mathbf{X})] < \infty$, where $r \geq 1$ is an integer and $\mathbb{E}_{\mathbf{d}}$ represents the expectation operator with respect to the probability measure $P_{\mathbf{d}}$. The rth moment of $y(\mathbf{X})$ is defined by the integral

$$m^{(r)}(\mathbf{d}) := \mathbb{E}_{\mathbf{d}}[y^r(\mathbf{X})] := \int_{\mathbb{R}^N} y^r(\mathbf{x}) f_{\mathbf{X}}(\mathbf{x}; \mathbf{d}) \mathrm{d}\mathbf{x}; \qquad r = 1, 2, \cdots. \tag{2.19}$$

Similarly, the failure probability, entailed in reliability analysis, is defined by the integral

$$P_{\mathbf{d}}[\mathbf{X} \in \Omega_F] := \int_{\mathbb{R}^N} I_{\Omega_F}(\mathbf{x}) f_{\mathbf{X}}(\mathbf{x}; \mathbf{d}) \mathrm{d}\mathbf{x} := \mathbb{E}_{\mathbf{d}}[I_{\Omega_F}(\mathbf{X})], \tag{2.20}$$

where Ω_F is the failure set described by $y(\mathbf{x})$ and

$$I_{\Omega_F}(\mathbf{x}) := \begin{cases} 1 & \text{if } \mathbf{x} \in \Omega_F, \\ 0 & \text{otherwise}, \end{cases} \tag{2.21}$$

is an indicator function. Therefore, the expressions of moments and the failure probability in Equations (2.19) and (2.20) can be consolidated into a generic probabilistic response

$$h(\mathbf{d}) = \mathbb{E}_{\mathbf{d}}[g(\mathbf{X})] := \int_{\mathbb{R}^N} g(\mathbf{x}) f_{\mathbf{X}}(\mathbf{x}; \mathbf{d}) \mathrm{d}\mathbf{x}, \tag{2.22}$$

where $h(\mathbf{d})$ is the statistical moment if $g(\mathbf{x}) = y^r(\mathbf{x})$, or failure probability if $g(\mathbf{x}) = I_{\Omega_F}(\mathbf{x})$. Based on these notations, the methods for stochastic sensitivity analysis are elucidated as follows.

2.4.1 Finite difference method

Because of its simple implementation, the finite difference method [72, 73] is commonly employed to estimate design sensitivities. All variants of the finite difference formulae, including the forward difference, central difference, and backward difference, can be derived by truncating a Taylor series expanded about a given point. A common estimate for the design sensitivity of the generic probabilistic response $h(\mathbf{d})$ defined in Equation (2.22) is the forward difference

$$\frac{\partial h(\mathbf{d})}{\partial d_k} \cong \frac{\int_{\mathbb{R}^N} g(\mathbf{x}) f_{\mathbf{X}}(\mathbf{x}; \mathbf{d} + \Delta d_k \cdot \mathbf{e}_k) \mathrm{d}\mathbf{x} - \int_{\mathbb{R}^N} g(\mathbf{x}) f_{\mathbf{X}}(\mathbf{x}; \mathbf{d}) \mathrm{d}\mathbf{x}}{\Delta d_k}, \ k = 1, \cdots, M,$$

(2.23)

where $\mathbf{e}_k$ is the M-dimensional basis vector in the design space, in which the kth component is *one* and other components are *zeros*; and Δd_k represents a small perturbation in the design variable d_k.

The finite difference method is probably the easiest method to implement for design sensitivities. However, it suffers from computational inefficiency and possible inaccuracy. First, one stochastic sensitivity analysis costs $M + 1$ times stochastic analysis for the forward or backward difference method, or $2M$ times stochastic analysis for the central difference method. Second, the size of perturbation Δd_k greatly affects the accuracy of the estimate. For a highly nonlinear $h(\mathbf{d})$, a large perturbation leads to inaccurate results. Theoretically, accurate results by Equation (2.23) can be expected when Δd_k approaches *zero*. However, numerical noises become dominant if too small a perturbation is used, thus ruining the results.

2.4.2 Score function method

The score function method [74, 75] has been mostly viewed as a competitive method, where both a stochastic response and its sensitivities can be obtained from a single stochastic simulation. To calculate the sensitivities of the generic probabilistic response $h(\mathbf{d})$ defined in Equation (2.22), the score function method requires the differential operator and the integral operator to commute; thus the following four regularity conditions must be held.

1. The PDF $f_{\mathbf{X}}(\mathbf{x}; \mathbf{d})$ is continuous.

2. The design variable $d_k \in \Theta_k \subset \mathbb{R}, \ k = 1, \cdots, M$, where Θ_k is an open interval on $\mathbb{R}$.

3. The partial derivative $\partial f_{\mathbf{X}}(\mathbf{x}; \mathbf{d})/\partial d_k$ exists and is finite for all $\mathbf{x}$ and $d_k \in \Theta_k$. In addition, $h(\mathbf{d})$ is differentiable with respect to $\mathbf{d}$.

4. $g(\mathbf{x})\partial f_{\mathbf{X}}(\mathbf{x}; \mathbf{d})/\partial d_k$ is dominated by some Lebesgue integrable function $z(\mathbf{x})$ in the sense that

$$\left| g(\mathbf{x}) \frac{\partial f_{\mathbf{X}}(\mathbf{x}; \mathbf{d})}{\partial d_k} \right| < z(\mathbf{x}). \tag{2.24}$$

With the above regularity conditions, applying the Lebesgue dominated convergence theorem [76] to $\partial h(\mathbf{d})/\partial d_k$ leads to

$$
\begin{aligned}
\frac{\partial h(\mathbf{d})}{\partial d_k} &= \frac{\partial}{\partial d_k} \int_{\mathbb{R}^N} g(\mathbf{x}) f_{\mathbf{X}}(\mathbf{x}; \mathbf{d}) d\mathbf{x} \\
&= \int_{\mathbb{R}^N} g(\mathbf{x}) \frac{\partial \ln f_{\mathbf{X}}(\mathbf{x}; \mathbf{d})}{\partial d_k} f_{\mathbf{X}}(\mathbf{x}; \mathbf{d}) d\mathbf{x} \\
&=: \mathbb{E}_{\mathbf{d}} \left[g(\mathbf{X}) s_{d_k}^{(1)}(\mathbf{X}; \mathbf{d}) \right].
\end{aligned}
\tag{2.25}
$$

In last line of Equation (2.25), $s_{d_k}^{(1)}(\mathbf{X}; \mathbf{d}) := \partial \ln f_{\mathbf{X}}(\mathbf{X}; \mathbf{d})/\partial d_k$ is known as the first-order score function for the design variable d_k [74, 75]. In general, the sensitivities

are not available analytically since the probabilistic responses $h(\mathbf{d})$ are not either. Nonetheless, the responses and their sensitivities have both been formulated as expectations of stochastic quantities with respect to the same probability measure, facilitating their concurrent evaluations in a single stochastic simulation or analysis.

2.4.3   Other methods

As explained in Subsection 2.3.2, the probability of failure can be approximated from the knowledge of the reliability index β_{HL}. When applying FORM or SORM to solve RBDO problems, it is therefore of interest to study the sensitivity of β_{HL} with respect to design variables d_k [35, 77]. When d_k is a structural design variable, the sensitivity of β_{HL} simply involves the gradients of the performance function with respect to d_k and random variables. When d_k is a distributional design variable, the Rosenblatt transformation [78], required to convert the input random variables into standard Gaussian variables, is a function of d_k. Consequently, the sensitivity of β_{HL} in this case demands the partial derivative of the Rosenblatt transformation with respect to d_k. Nonetheless, the sensitivity analysis of β_{HL}, rooted in the linear or quadratic approximation of the failure surface by FORM or SORM, inherits the limitations of FORM or SORM. Therefore, when applied to highly nonlinear or multimodal performance functions, it may yield inaccurate or inadequate estimates of design sensitivities.

Recently, the kernel function method has been applied to estimate stochastic sensitivity [79]. This method is very similar to the score function method. Further

details of this method are available elsewhere [80].

2.5   Robust Design Optimization

The key component of RDO is the assessment of the first two moments of stochastic response functions and their sensitivities. There are various methods or approaches to estimate these quantities: point estimate methods [12], Taylor series expansion [12], PCE [13], dimension-reduction methods [9, 14, 22, 23, 75], and TPQ [14], to name a few. There exist three principal concerns or shortcomings when conducting RDO with existing approaches or techniques.

First, commonly used stochastic methods, including the Taylor series or perturbation expansions, PEM, PCE, TPQ rule, and dimension-reduction methods may not be adequate or applicable for uncertainty quantification of many large-scale practical problems. For instance, the Taylor series expansion and PEMs, although simple and inexpensive, begin to break down when the input-output mapping is highly nonlinear or the input uncertainty is arbitrarily large. Furthermore, truly high-dimensional problems are all but impossible to solve using the PCE and TPQ rule due to the curse of dimensionality. The dimension-reduction methods, developed by Xu and Rahman [22, 81], including a modification [82], alleviate the curse of dimensionality to some extent, but they are rooted in the referential dimensional decomposition, resulting in sub-optimal approximations of a multivariate function [64, 83].

Second, many of the aforementioned methods invoke finite-difference techniques to calculate design sensitivities of the statistical moments. They demand re-

peated stochastic analyses for nominal and perturbed values of design parameters and are, therefore, expensive and unwieldy. Although some methods, such as Taylor series expansions, also provide the design sensitivities economically, the sensitivities are either inaccurate or unreliable because they inherit errors from the affiliated second-moment analysis. Therefore, alternative stochastic methods should be explored for calculating the statistical moments and design sensitivities as accurately as possible and simultaneously, but without the computational burden of crude MCS.

Third, existing methods for solving RDO problems permit the objective and constraint functions and their sensitivities to be calculated only at a fixed design, requiring new statistical moment and sensitivity analyses at every design iteration until convergence is attained. Consequently, the current RDO methods, entailing expensive FEA or similar numerical calculations, are computationally intensive, if not prohibitive, when confronted with a large number of design or random variables. New or significantly improved design paradigms, possibly requiring a single or a few stochastic simulations, are needed for solving the entire RDO problem. Further complications may arise when an RDO problem is formulated in conjunction with a multi-point approximation [84] − a setting frequently encountered when tackling a practical optimization problem with a large design space. In that case, one must integrate stochastic analysis, design sensitivity analysis, and optimization algorithms on a local subregion of the entire design space.

2.6 Reliability-Based Design Optimization

2.6.1 FORM/SORM-based methods

Methods based on FORM and SORM for solving RBDO can be classified, according to how reliability analysis and optimization iteration are integrated, into three categories: the double-loop approach [85–87], the single-loop approach [88, 89], and the sequential approach [90, 91]. The double-loop approach consists of an outer optimization loop that is used to obtain an optimum reliability-based design and an inner optimization loop to conduct reliability analysis every time the design variables are changed. As explained in Subsection 2.3.2, the inner optimization problem can be formulated by RIA to find the point on the performance surface to minimize the distance to the origin of the $\mathbf{u}$ space. Instead of the RIA, Tu *et al.* [86] proposed the performance measure approach (PMA), in which inverse reliability analysis is formulated to search for a point with the lowest performance function value on a hyper-surface determined by the target reliability index. The PMA was reported to be computationally more efficient than the RIA owing to its spherical equality constraint [87]. However, regardless of how the inner optimization problem is solved, the double-loop approach is expensive because, for each design (outer) iteration, a set of reliability (inner) iterations involving costly function evaluations has to be generated for locating the MPP. To overcome the high computational expense, Liang *et al.* [88, 89] proposed a single-loop approach in which the inner-loop calculations are replaced with an approximated solution obtained by the Karush-Kuhn-Tucker (KKT) optimality condition. Consequently, the double-loop optimization problem is converted into an

equivalent single-loop problem, which has been reported to have efficiency almost equivalent to deterministic optimization and accuracy comparable to the double-loop approach [89]. To avoid a nested loop, Du and Chen [91] also proposed a sequential optimization and reliability assessment (SORA) approach, which formulates serial "equivalent" deterministic optimization problems to achieve a progressive and rapid convergence. The reliability assessments are conducted only after solving deterministic optimization to verify probabilistic constraints. Therefore, shifting boundaries of the violated constraints to the feasible domain, based on the reliability information obtained in the previous iteration, is required. Nonetheless, given that double-loop, single-loop, and sequential approaches are based on FORM/SORM, there are four major concerns for these three methods. First, the linear or quadratic may not be adequate or applicable for highly nonlinear practical problems. Furthermore, it was noted that SORA confronts a convergence difficulty when the objective and/or constraint functions are highly nonlinear or non-smooth [91]. Second, the three methods inherit the possible inaccuracy of sensitivity analysis resulting from FORM/SORM as summarized in Subsection 2.4.3. Therefore, alternative stochastic methods are desired for accurate and efficient sensitivity analysis of reliability. Indeed, recent results from Zou and Mahadevan [92] and Rahman and Wei [93] reveal that a FORM-based RBDO process may produce infeasible or inaccurate design. Third, it should be noted that no formal proof of convergence exists for either single-loop or sequential algorithms [90]. Fourth, these methods demand evaluations of objective and/or constraint and sensitivity analyses at every design iteration, so new or significantly improved

design paradigms are needed for solving the RBDO problem as efficiently as possible, simultaneously, and without degrading the accuracy.

2.6.2 RDD-based methods

Rahman and Wei [93] proposed the univariate RDD method for reliability sensitivity analysis and RBDO. Their method renders a univariate approximation of a general multivariate function in the rotated Gaussian space for reliability analysis and analytical expressions for sensitivity of failure probability with respect to design variables. Computational effort for both failure probabilities and their sensitivities has been reduced owing to performing multiple one-dimensional integrations. In their recent work [94], a new multi-point univariate decomposition method was developed for structural reliability analysis involving multiple MPPs. The method provided a novel function decomposition at all MPPs, facilitating multiple local univariate approximations of a performance function. More applications of RDD in RBDO can be found in the literature [9, 14]. With the aid of RDD, these methods alleviate the curse of dimensionality to some extent. However, a recent error analysis [64] reveals the sub-optimality of RDD approximations, meaning that an RDD approximation, regardless of how the reference point is chosen, cannot be better than an ANOVA approximation for identical degrees of interaction.

2.6.3 Simulation-based methods

Simulation-based methods [95, 96] are recommended or used when tackling highly nonlinear or non-smooth performance functions. Royset and Polak [95] pro-

posed a simulation formulation to estimate the sensitivity of failure probability, in which either crude MCS or Monte Carlo with importance sampling can be employed. Another approach, referred to as stochastic subset optimization [96], directly integrates the subset simulation technique with RBDO and permits the simultaneous evaluation of structural reliability and identification of optimum of RBDO. With this approach, it is also possible to identify a subset of the design variables that are significant to objective or constraint functions. When an RBDO problem involves highly nonlinear or noisy performance function, the FORM/SORM and other surrogate methods can be significantly deteriorated, whereas the simulation-based methods still have the merit of accuracy. However, simulation-based methods are often computationally prohibitive, particularly when an RBDO mandates FEA of complex mechanical systems.

2.7   Need for Fundamental Research

In summary, a new computational thinking challenging existing methods or approaches should be pursued for advancing the frontiers of RDO and RBDO. Not only novel computational methods are needed for calculating probabilistic characteristics of responses or their design sensitivities, but also new or significantly improved design paradigms, possibly requiring a single or a few stochastic simulations for solving an entire design optimization problem, should be created. To meet this objective, four research directions, all anchored in PDD, are proposed, as follows.

2.7.1 PDD methods for stochastic sensitivity analysis

Existing methods for stochastic sensitivity analysis, including the finite difference, score function, and FORM- or SORM-based methods, have been extensively employed to solve RDO or RBDO problems of mechanical systems. However, when confronted with a highly nonlinear and high-dimensional complex system, these methods often deteriorate in terms of accuracy or become prohibitive due to the loss of efficiency. The RDD method ameliorates the curse of dimensionality to some extent by developing an input-output behavior of complex systems with low effective dimensions. Unfortunately, it cannot be better than the ANOVA approximation for identical degrees of interaction. The PDD, which inherits all desirable properties of the ANOVA dimensional decomposition, has not been systematically studied for stochastic sensitivity analysis. Therefore, it is of interest to extend PDD, aimed at both high accuracy and/or high efficiency, from the following three aspects: (1) exploiting the orthonormal property of polynomial bases to develop analytical expressions of the sensitivities of the moments of stochastic responses; (2) coupling the PDD, SPA, and score function for sensitivities of reliability; and (3) integrating the PDD, MCS, and score function for sensitivities of reliability.

2.7.2 PDD methods for RDO

Current design paradigms for solving RDO problems demand new statistical moment and sensitivity analyses at every design iteration to evaluate objective and/or constraint functions and their sensitivities. When dealing with a large number of de-

sign or random variables or industrial-scale problems that entail expensive FEA or similar numerical calculations, the current RDO methods are computationally intensive, if not prohibitive. For this reason, it is necessary to develop a new or significantly improved design paradigm in which only a single or a few stochastic simulations are needed for solving the entire RDO problem. The new design paradigms should seamlessly integrate the PDD method into stochastic analysis, design sensitivity analysis, and optimization algorithms.

2.7.3 PDD methods for RBDO

When applied to practical design problems involving highly nonlinear or high-dimensional performance functions, existing RBDO methods, such as FORM/SORM-based, RDD-based, and simulation-based methods, may not work due to degradation of solution accuracy or prohibitively high computational cost. They all point to a qualitative as well as quantitative difference between what has been studied and what is required. To this end, a new PDD-based RBDO method is desirable to fulfill the following requirements: accurate evaluations of both failure probabilities and their design sensitivities, fast convergence of RBDO iterations, and satisfactory numerical stability.

2.7.4 PDD methods for mixed design variables

Two major classes of design variables, distributional design variables and structural design variables, are involved in design optimization under uncertainty. However, much of the existing research, whether in conjunction with RDO or RBDO,

focus on only one of the two classes of design variables. Indeed, there is a lack of integrated frameworks for tackling stochastic design optimization problems in the presence of both classes of design variables, referred to as mixed design variable problems. Therefore, the last topic of this research delves into developing a PDD-based framework for solving RDO and RBDO problems involving mixed design variables by conducting accurate and efficient stochastic sensitivity analyses with respect to both distributional and structural design variables.

CHAPTER 3
STOCHASTIC SENSITIVITY ANALYSIS

3.1   Introduction

This chapter presents three new computational methods for calculating design sensitivities of statistical moments and reliability of high-dimensional complex systems subject to random input. The first method represents a novel integration of PDD of a multivariate stochastic response function and Fourier-polynomial expansions of score functions associated with the probability measure of the random input. Applied to the statistical moments, the method provides analytical expressions of design sensitivities of the first two moments of a stochastic response. The second and third methods, relevant to probability distribution or reliability analysis, exploit two distinct combinations grounded in PDD: the PDD-SPA method, entailing SPA and score functions; and the PDD-MCS method, utilizing the embedded MCS of PDD approximation and score functions. Section 3.2 formally defines RDO and RBDO problems, including their concomitant mathematical statements. Section 3.3 describes the PDD approximation of a multivariate function, resulting in explicit formulae for the first two moments, and the PDD-SPA and PDD-MCS methods for reliability analysis. Section 3.4 defines score functions and unveils new closed-form formulae or numerical procedures for design sensitivities of moments. The convergence of the sensitivities of moments by the proposed method is also proved in this section. Section 3.5 describes the PDD-SPA and PDD-MCS methods for sensitivity

analysis and explains how the effort required to calculate the failure probability also delivers its design sensitivities, sustaining no additional cost. The calculation of PDD expansion coefficients, required in sensitivity analyses of both moments and failure probability, is discussed in Section 3.6. In Section 3.7, five numerical examples are presented to probe the convergence properties, accuracy, and computational efficiency of the proposed methods. Finally, conclusions are drawn in Section 3.8.

3.2 Design under Uncertainty

Consider a measurable space $(\Omega_{\mathbf{d}}, \mathcal{F}_{\mathbf{d}})$, where $\Omega_{\mathbf{d}}$ is a sample space and $\mathcal{F}_{\mathbf{d}}$ is a σ-field on $\Omega_{\mathbf{d}}$. Defined over $(\Omega_{\mathbf{d}}, \mathcal{F}_{\mathbf{d}})$, let $\{P_{\mathbf{d}} : \mathcal{F} \to [0,1]\}$ be a family of probability measures, where for $M \in \mathbb{N}$ and $N \in \mathbb{N}$, $\mathbf{d} = (d_1, \cdots, d_M)^T \in \mathcal{D}$ is an $\mathbb{R}^M$-valued design vector with non-empty closed set $\mathcal{D} \subseteq \mathbb{R}^M$, and let $\mathbf{X} := (X_1, \cdots, X_N)^T : (\Omega_{\mathbf{d}}, \mathcal{F}_{\mathbf{d}}) \to (\mathbb{R}^N, \mathcal{B}^N)$ be an $\mathbb{R}^N$-valued input random vector with $\mathcal{B}^N$ representing the Borel σ-field on $\mathbb{R}^N$, describing the statistical uncertainties in the loads, material properties, and geometry of a complex mechanical system. The probability law of $\mathbf{X}$ is completely defined by a family of the joint probability density functions (PDF) $\{f_{\mathbf{X}}(\mathbf{x}; \mathbf{d}), \mathbf{x} \in \mathbb{R}^N, \mathbf{d} \in \mathcal{D}\}$ that are associated with probability measures $\{P_{\mathbf{d}}, \mathbf{d} \in \mathcal{D}\}$, so that the probability triple $(\Omega_{\mathbf{d}}, \mathcal{F}_{\mathbf{d}}, P_{\mathbf{d}})$ of $\mathbf{X}$ depends on $\mathbf{d}$. A design variable d_k can be any distribution parameter or a statistic — for instance, the mean or standard deviation — of X_i.

Let $y_l(\mathbf{X})$, $l = 1, 2, \cdots, K$, be a collection of $K + 1$ real-valued, square-integrable, measurable transformations on $(\Omega_{\mathbf{d}}, \mathcal{F}_{\mathbf{d}})$, describing performance functions

of a complex system. It is assumed that $y_l : (\mathbb{R}^N, \mathcal{B}^N) \to (\mathbb{R}, \mathcal{B})$ is not an explicit

function of $\mathbf{d}$, although y_l implicitly depends on $\mathbf{d}$ via the probability law of $\mathbf{X}$.

3.2.1   RDO

A common mathematical formulation for RDO problems involving an objective

function $c_0 : \mathbb{R}^M \to \mathbb{R}$ and constraint functions $c_l : \mathbb{R}^M \to \mathbb{R}$, where $l = 1, \cdots, K$ and

$1 \leq K < \infty$, requires one to

$$\min_{\mathbf{d} \in \mathcal{D} \subseteq \mathbb{R}^M} \quad c_0(\mathbf{d}) := w_1 \frac{\mathbb{E}_{\mathbf{d}}\left[y_0(\mathbf{X})\right]}{\mu_0^*} + w_2 \frac{\sqrt{\operatorname{var}_{\mathbf{d}}\left[y_0(\mathbf{X})\right]}}{\sigma_0^*},$$

$$\text{subject to} \quad c_l(\mathbf{d}) := \alpha_l \sqrt{\operatorname{var}_{\mathbf{d}}\left[y_l(\mathbf{X})\right]} - \mathbb{E}_{\mathbf{d}}\left[y_l(\mathbf{X})\right] \leq 0, \ l = 1, \cdots, K, \quad (3.1)$$

$$d_{k,L} \leq d_k \leq d_{k,U}, \ k = 1, \cdots, M,$$

where $\mathbb{E}_{\mathbf{d}}[y_l(\mathbf{X}; \mathbf{d})] := \int_{\mathbb{R}^N} y_l(\mathbf{x}; \mathbf{d}) f_{\mathbf{X}}(\mathbf{x}; \mathbf{d}) d\mathbf{x}$ is the mean of $y_l(\mathbf{X}; \mathbf{d})$ with $\mathbb{E}$ denoting

the expectation operator with respect to the probability measure $f_{\mathbf{X}}(\mathbf{x}; \mathbf{d}) d\mathbf{x}$ of $\mathbf{X}$;

$\operatorname{var}_{\mathbf{d}}[y_l(\mathbf{X}; \mathbf{d})] := \mathbb{E}_{\mathbf{d}}[\{y_l(\mathbf{X}; \mathbf{d}) - \mathbb{E}_{\mathbf{d}}[y_l(\mathbf{X}; \mathbf{d})]\}^2]$ is the variance of $y_l(\mathbf{X}; \mathbf{d})$; g_l, $l =$

$0, 1, \cdots, K$, are arbitrary functions of $\mathbb{E}_{\mathbf{d}}[y_l(\mathbf{X}; \mathbf{d})]$ and $\operatorname{var}_{\mathbf{d}}[y_l(\mathbf{X}; \mathbf{d})]$; $d_{k,L}$ and $d_{k,U}$

are the lower and upper bounds, respectively, of d_k; $w_1 \in \mathbb{R}_0^+$ and $w_2 \in \mathbb{R}_0^+$ are two

non-negative, real-valued weights, satisfying $w_1 + w_2 = 1$; $\mu_0^* \in \mathbb{R} \setminus \{0\}$ and $\sigma_0^* \in$

$\mathbb{R}_0^+ \setminus \{0\}$ are two non-zero, real-valued scaling factors; and $\alpha_l \in \mathbb{R}_0^+$, $l = 0, 1, \cdots, K$,

are non-negative, real-valued constants associated with the probabilities of constraint

satisfaction.

In Equation (3.1), evaluations of both objective robustness and feasibility ro-

bustness, involving the first two moments of various responses, are required for solving

RDO problems, consequently demanding statistical moment analysis. Coupling with

gradient-based optimization algorithms mandates that the gradients of $c_l(\mathbf{d})$ be formulated, thus requiring design sensitivity analysis of the first two moments.

3.2.2   RBDO

A well-known mathematical formulation for RBDO problems involving an objective function $c_0 : \mathbb{R}^M \to \mathbb{R}$ and constraint functions $c_l : \mathbb{R}^M \to \mathbb{R}$, where $l = 1, \cdots, K$ and $1 \leq K < \infty$, requires one to

$$\min_{\mathbf{d} \in \mathcal{D} \subseteq \mathbb{R}^M} \; c_0(\mathbf{d}),$$

$$\text{subject to} \quad c_l(\mathbf{d}) := P_{\mathbf{d}}\left[\mathbf{X} \in \Omega_{F,l}(\mathbf{d})\right] - p_l \leq 0, \; l = 1, \cdots, K, \tag{3.2}$$

$$d_{k,L} \leq d_k \leq d_{k,U}, \; k = 1, \cdots, M,$$

where $\Omega_{F,l}(\mathbf{d}) \subseteq \Omega$ is the lth failure set that, in general, may depend on $\mathbf{d}$; $0 \leq p_l \leq 1$, $l = 1, \cdots, K$, are target failure probabilities; the distributional parameters solely describe the design variables, that is $\mathbf{d}_T = \mathbf{d}$, c_0 is a prescribed deterministic function of $\mathbf{d}$; and $y_l(\mathbf{X})$, $l = 1, \cdots, K$, are not explicit functions of $\mathbf{d}$, although y_l implicitly depends on $\mathbf{d}$ via the probability law of $\mathbf{X}$.

In Equation (3.2), evaluation of the reliability constraints $c_l(\mathbf{d})$, $l = 1, \cdots, K$, requires calculating the component or system probability of failure defined by the performance functions. Coupling with gradient-based optimization algorithms mandates that the gradients of $c_l(\mathbf{d})$ be formulated, thus requiring design sensitivity analysis of failure probability.

3.3 Stochastic Analyses

3.3.1 Polynomial Dimensional Decomposition

Let $y(\mathbf{X})$ be a real-valued, square-integrable, measurable transformation on $(\Omega, \mathcal{F})$, describing the relevant performance function of a complex system. It is assumed that $y : (\mathbb{R}^N, \mathcal{B}^N) \to (\mathbb{R}, \mathcal{B})$ is not an explicit function of $\mathbf{d}$, although y implicitly depends on $\mathbf{d}$ via the probability law of $\mathbf{X}$. Assuming independent coordinates of $\mathbf{X}$, its joint PDF is expressed by a product, $f_{\mathbf{X}}(\mathbf{x}; \mathbf{d}) = \prod_{i=1}^{i=N} f_{X_i}(x_i; \mathbf{d})$, of marginal PDF $f_{X_i} : \mathbb{R} \to \mathbb{R}_0^+$ of X_i, $i = 1, \cdots, N$, defined on its probability triple $(\Omega_i, \mathcal{F}_i, P_{i,\mathbf{d}})$ with a bounded or an unbounded support on $\mathbb{R}$. Then, for a given subset $u \subseteq \{1, \cdots, N\}$, $f_{\mathbf{X}_{-u}}(\mathbf{x}_{-u}; \mathbf{d}) := \prod_{i=1, i \notin u}^{N} f_{X_i}(x_i; \mathbf{d})$ defines the marginal density function of $\mathbf{X}_{-u} := \mathbf{X}_{\{1, \cdots, N\} \setminus u}$.

3.3.1.1 Orthonormal Polynomials and Stochastic Expansions

Let $\{\psi_{ij}(x_i; \mathbf{d}); \ j = 0, 1, \cdots\}$ be a set of univariate, orthonormal polynomial basis functions in the Hilbert space $\mathcal{L}_2(\Omega_i, \mathcal{F}_i, P_{i,\mathbf{d}})$ that is consistent with the probability measure $P_{i,\mathbf{d}}$ or $f_{X_i}(x_i; \mathbf{d})dx_i$ of X_i for a given design $\mathbf{d}$. For $\emptyset \neq u = \{i_1, \cdots, i_{|u|}\} \subseteq \{1, \cdots, N\}$, where $1 \leq |u| \leq N$ and $1 \leq i_1 < \cdots < i_{|u|} \leq N$, let $(\times_{p=1}^{p=|u|}\Omega_{i_p}, \times_{p=1}^{p=|u|}\mathcal{F}_{i_p}, \times_{p=1}^{p=|u|}P_{i_p,\mathbf{d}})$ be the product probability triple of $\mathbf{X}_u = (X_{i_1}, \cdots, X_{i_{|u|}})$. Denote the associated space of the $|u|$-variate component functions of y by

$$\mathcal{L}_2\left(\times_{p=1}^{p=|u|}\Omega_{i_p}, \times_{p=1}^{p=|u|}\mathcal{F}_{i_p}, \times_{p=1}^{p=|u|}P_{i_p,\mathbf{d}}\right) := \left\{y_u : \int_{\mathbb{R}^{|u|}} y_u^2(\mathbf{x}_u; \mathbf{d})f_{\mathbf{X}_u}(\mathbf{x}_u; \mathbf{d})d\mathbf{x}_u < \infty\right\},$$

(3.3)

which is a Hilbert space. Since the joint density of $\mathbf{X}_u$ is separable (independence of x_i, $i \in u$), that is, $f_{\mathbf{X}_u}(\mathbf{x}_u; \mathbf{d}) = \prod_{p=1}^{|u|} f_{X_{i_p}}(x_{i_p}; \mathbf{d}) dx_{i_p}$, the product $\psi_{u\mathbf{j}_{|u|}}(\mathbf{X}_u; \mathbf{d}) := \prod_{p=1}^{|u|} \psi_{i_p j_p}(X_{i_p}; \mathbf{d})$, where $\mathbf{j}_{|u|} = (j_1, \cdots, j_{|u|}) \in \mathbb{N}_0^{|u|}$, a $|u|$-dimensional multi-index with ∞-norm $||\mathbf{j}_{|u|}||_\infty = \max(j_1, \cdots, j_{|u|})$, constitutes a multivariate orthonormal polynomial basis in $\mathcal{L}_2(\times_{p=1}^{p=|u|} \Omega_{i_p}, \times_{p=1}^{p=|u|} \mathcal{F}_{i_p}, \times_{p=1}^{p=|u|} P_{i_p,\mathbf{d}})$. Two important properties of these product polynomials from tensor products of Hilbert spaces are as follows.

Proposition 3.1. *The product polynomials* $\psi_{u\mathbf{j}_{|u|}}(\mathbf{X}_u; \mathbf{d})$, $\emptyset \neq u \subseteq \{1, \cdots, N\}$, $j_1, \cdots, j_{|u|} \neq 0$, $\mathbf{d} \in \mathcal{D}$, *have zero means, i.e.,*

$$\mathbb{E}_{\mathbf{d}} \left[\psi_{u\mathbf{j}_{|u|}}(\mathbf{X}_u; \mathbf{d}) \right] = 0. \tag{3.4}$$

Proposition 3.2. *Any two distinct product polynomials* $\psi_{u\mathbf{j}_{|u|}}(\mathbf{X}_u; \mathbf{d})$ *and* $\psi_{v\mathbf{k}_{|v|}}(\mathbf{X}_v; \mathbf{d})$ *for* $\mathbf{d} \in \mathcal{D}$, *where* $\emptyset \neq u \subseteq \{1, \cdots, N\}$, $\emptyset \neq v \subseteq \{1, \cdots, N\}$, $j_1, \cdots, j_{|u|} \neq 0$, $k_1, \cdots, k_{|v|} \neq 0$, *are uncorrelated and each has unit variance, i.e.,*

$$\mathbb{E}_{\mathbf{d}} \left[\psi_{u\mathbf{j}_{|u|}}(\mathbf{X}_u; \mathbf{d}) \psi_{v\mathbf{k}_{|v|}}(\mathbf{X}_v; \mathbf{d}) \right] = \begin{cases} 1 & \text{if } u = v; \mathbf{j}_{|u|} = \mathbf{k}_{|v|}, \\ 0 & \text{otherwise.} \end{cases} \tag{3.5}$$

Proof. The results of Propositions 3.1 and 3.2 follow by recognizing independent coordinates of $\mathbf{X}$ and using the second-moment properties of univariate orthonormal polynomials: (1) $\mathbb{E}_{\mathbf{d}}[\psi_{ij}(X_i; \mathbf{d})] = 1$ when $j = 0$ and *zero* when $j \geq 1$; and (2) $\mathbb{E}_{\mathbf{d}}[\psi_{ij_1}(X_i; \mathbf{d})\psi_{ij_2}(X_i; \mathbf{d})] = 1$ when $j_1 = j_2$ and *zero* when $j_1 \neq j_2$ for an arbitrary random variable X_i.

Remark 3.3. Given a probability measure $P_{i,\mathbf{d}}$ of any random variable X_i, the well-known three-term recurrence relation is commonly used to construct the associated

orthogonal polynomials [97, 98]. For $m \in \mathbb{N}$, the first m recursion coefficient pairs are uniquely determined by the first $2m$ moments of X_i that must exist. When these moments are exactly calculated, they lead to exact recursion coefficients, some of which belong to classical orthogonal polynomials. For an arbitrary probability measure, approximate methods, such as the Stieltjes procedure, can be employed to obtain the recursion coefficients [97, 98].

The orthogonal polynomial expansion of a non-constant $|u|$-variate ANOVA component function in Equation (2.8) becomes [97, 99]

$$y_u(\mathbf{X}_u; \mathbf{d}) = \sum_{\substack{\mathbf{j}_{|u|} \in \mathbb{N}_0^{|u|} \\ j_1, \cdots, j_{|u|} \neq 0}} C_{u\mathbf{j}_{|u|}}(\mathbf{d}) \psi_{u\mathbf{j}_{|u|}}(\mathbf{X}_u; \mathbf{d}) \qquad (3.6)$$

for any $\emptyset \neq u \subseteq \{1, \cdots, N\}$ with

$$C_{u\mathbf{j}_{|u|}}(\mathbf{d}) := \int_{\mathbb{R}^N} y(\mathbf{x}) \psi_{u\mathbf{j}_{|u|}}(\mathbf{x}_u; \mathbf{d}) f_{\mathbf{X}}(\mathbf{x}; \mathbf{d}) d\mathbf{x} \qquad (3.7)$$

representing the corresponding expansion coefficient. Similar to $y_\emptyset$, the coefficient $C_{u\mathbf{j}_{|u|}}$ also depends on the design vector $\mathbf{d}$. When $u = \{i\}$, $i = 1, \cdots, N$, the univariate component functions and expansion coefficients are

$$y_{\{i\}}(X_i; \mathbf{d}) = \sum_{j=1}^{\infty} C_{ij}(\mathbf{d}) \psi_{ij}(X_i; \mathbf{d}) \qquad (3.8)$$

and $C_{ij}(\mathbf{d}) := C_{\{i\}(j)}(\mathbf{d})$, respectively. When $u = \{i_1, i_2\}$, $i_1 = 1, \cdots, N-1$, $i_2 = i_1 + 1, \cdots, N$, the bivariate component functions and expansion coefficients are

$$y_{\{i_1, i_2\}}(X_{i_1}, X_{i_2}; \mathbf{d}) = \sum_{j_1=1}^{\infty} \sum_{j_2=1}^{\infty} C_{i_1 i_2 j_1 j_2}(\mathbf{d}) \psi_{i_1 j_1}(X_{i_1}; \mathbf{d}) \psi_{i_2 j_2}(X_{i_2}; \mathbf{d}) \qquad (3.9)$$

and $C_{i_1 i_2 j_1 j_2}(\mathbf{d}) := C_{\{i_1, i_2\}(j_1, j_2)}(\mathbf{d})$, respectively, and so on. Using Propositions 3.1 and 3.2, all component functions y_u, $\emptyset \neq u \subseteq \{1, \cdots, N\}$, are found to satisfy the annihilating conditions of the ANOVA dimensional decomposition. The end result of combining Equations (2.6)-(2.8) and (3.6) is the PDD [97, 99],

$$y(\mathbf{X}) = y_\emptyset(\mathbf{d}) + \sum_{\emptyset \neq u \subseteq \{1, \cdots, N\}} \sum_{\substack{\mathbf{j}_{|u|} \in \mathbb{N}_0^{|u|} \\ j_1, \cdots, j_{|u|} \neq 0}} C_{u\mathbf{j}_{|u|}}(\mathbf{d}) \psi_{u\mathbf{j}_{|u|}}(\mathbf{X}_u; \mathbf{d}), \tag{3.10}$$

providing an exact, hierarchical expansion of y in terms of an infinite number of coefficients or orthonormal polynomials. In practice, the number of coefficients or polynomials must be finite, say, by retaining at most mth-order polynomials in each variable. Furthermore, in many applications, the function y can be approximated by a sum of at most S-variate component functions, where $S \in \mathbb{N}; 1 \leq S \leq N$, resulting in the S-variate, mth-order PDD approximation

$$\tilde{y}_{S,m}(\mathbf{X}) = y_\emptyset(\mathbf{d}) + \sum_{\substack{\emptyset \neq u \subseteq \{1, \cdots, N\} \\ 1 \leq |u| \leq S}} \sum_{\substack{\mathbf{j}_{|u|} \in \mathbb{N}_0^{|u|}, ||\mathbf{j}_{|u|}||_\infty \leq m \\ j_1, \cdots, j_{|u|} \neq 0}} C_{u\mathbf{j}_{|u|}}(\mathbf{d}) \psi_{u\mathbf{j}_{|u|}}(\mathbf{X}_u; \mathbf{d}), \tag{3.11}$$

containing $\sum_{k=0}^{S} \binom{N}{k} m^k$ number of PDD coefficients and corresponding orthonormal polynomials. Due to its additive structure, the approximation in Equation (3.11) includes degrees of interaction among at most S input variables $X_{i_1}, \cdots, X_{i_S}$, $1 \leq i_1 \leq \cdots \leq i_S \leq N$. For instance, by selecting $S = 1$ and 2, the functions

$$\tilde{y}_{1,m}(\mathbf{X}) = y_\emptyset + \sum_{i=1}^{N} \sum_{j=1}^{m} C_{ij}(\mathbf{d}) \psi_{ij}(X_i; \mathbf{d}) \tag{3.12}$$

and

$$
\begin{aligned}
\tilde{y}_{2,m}(\mathbf{X}) &= y_\emptyset(\mathbf{d}) + \sum_{i=1}^{N}\sum_{j=1}^{m} C_{ij}(\mathbf{d})\psi_{ij}(X_i; \mathbf{d}) + \\
&\sum_{i_1=1}^{N-1}\sum_{i_2=i_1+1}^{N}\sum_{j_1=1}^{m}\sum_{j_2=1}^{m} C_{i_1 i_2 j_1 j_2}(\mathbf{d}) \times \psi_{i_1 j_1}(X_{i_1}; \mathbf{d})\psi_{i_2 j_2}(X_{i_2}; \mathbf{d}),
\end{aligned}
\tag{3.13}
$$

respectively, provide univariate and bivariate mth-order PDD approximations, contain contributions from all input variables, and should not be viewed as first- and second-order approximations, nor as limiting the nonlinearity of y. Depending on how the component functions are constructed, arbitrarily high-order univariate and bivariate terms of y could be lurking inside $\tilde{y}_{1,m}$ and $\tilde{y}_{2,m}$. When $S \to N$ and $m \to \infty$, $\tilde{y}_{S,m}$ converges to y in the mean-square sense, permitting Equation (3.11) to generate a hierarchical and convergent sequence of approximations of y. Further details of PDD can be found elsewhere [97, 99].

3.3.2   Statistical Moment Analysis

Let $m^{(r)}(\mathbf{d}) := \mathbb{E}_{\mathbf{d}}[y^r(\mathbf{X})]$, if it exists, define the raw moment of y of order r, where $r \in \mathbb{N}$. Given an S-variate, mth-order PDD approximation $\tilde{y}_{S,m}(\mathbf{X})$ of $y(\mathbf{X})$, let $\tilde{m}_{S,m}^{(r)}(\mathbf{d}) := \mathbb{E}_{\mathbf{d}}[\tilde{y}_{S,m}^r(\mathbf{X})]$ define the raw moment of $\tilde{y}_{S,m}$ of order r. The following subsections describe the explicit formulae or analytical expressions for calculating the moments by PDD approximations.

3.3.2.1 First- and Second-Order Moments

Applying the expectation operator on $\tilde{y}_{S,m}(\mathbf{X})$ and $\tilde{y}_{S,m}^2(\mathbf{X})$, and recognizing Propositions 3.1 and 3.2, the first moment or mean [100]

$$\tilde{m}_{S,m}^{(1)}(\mathbf{d}) := \mathbb{E}_{\mathbf{d}}\left[\tilde{y}_{S,m}(\mathbf{X})\right] = y_\emptyset(\mathbf{d}) = \mathbb{E}_{\mathbf{d}}\left[y(\mathbf{X})\right] =: m^{(1)}(\mathbf{d}) \qquad (3.14)$$

of the S-variate, mth-order PDD approximation matches the exact mean of y, regardless of S or m, whereas the second moment [100]

$$\tilde{m}_{S,m}^{(2)}(\mathbf{d}) := \mathbb{E}_{\mathbf{d}}\left[\tilde{y}_{S,m}^2(\mathbf{X})\right] = y_\emptyset^2(\mathbf{d}) + \sum_{\substack{\emptyset \neq u \subseteq \{1,\cdots,N\} \\ 1 \leq |u| \leq S}} \sum_{\substack{\mathbf{j}_{|u|} \in \mathbb{N}_0^{|u|}, ||\mathbf{j}_{|u|}||_\infty \leq m \\ j_1,\cdots,j_{|u|} \neq 0}} C_{u\mathbf{j}_{|u|}}^2(\mathbf{d}) \qquad (3.15)$$

is calculated as the sum of squares of all expansion coefficients of $\tilde{y}_{S,m}(\mathbf{X})$. Clearly, the approximate second moment in Equation (3.15) approaches the exact second moment

$$m^{(2)}(\mathbf{d}) := \mathbb{E}_{\mathbf{d}}\left[y^2(\mathbf{X})\right] = y_\emptyset^2(\mathbf{d}) + \sum_{\emptyset \neq u \subseteq \{1,\cdots,N\}} \sum_{\substack{\mathbf{j}_{|u|} \in \mathbb{N}_0^{|u|} \\ j_1,\cdots,j_{|u|} \neq 0}} C_{u\mathbf{j}_{|u|}}^2(\mathbf{d}) \qquad (3.16)$$

of y when $S \to N$ and $m \to \infty$. The mean-square convergence of $\tilde{y}_{S,m}$ is guaranteed as y, and its component functions are all members of the associated Hilbert spaces. In addition, the variance of $\tilde{y}_{S,m}(\mathbf{X})$ is also mean-square convergent.

For the two special cases, $S = 1$ and $S = 2$, the univariate and bivariate PDD approximations yield the same exact mean value $y_\emptyset(\mathbf{d})$, as noted in Equation (3.14). However, the respective second-moment approximations,

$$\tilde{m}_{1,m}^{(2)}(\mathbf{d}) = y_\emptyset^2(\mathbf{d}) + \sum_{i=1}^{N}\sum_{j=1}^{m} C_{ij}^2(\mathbf{d}) \qquad (3.17)$$

and

$$\tilde{m}_{2,m}^{(2)}(\mathbf{d}) = y_\emptyset^2(\mathbf{d}) + \sum_{i=1}^{N}\sum_{j=1}^{m} C_{ij}^2(\mathbf{d}) + \sum_{i_1=1}^{N-1}\sum_{i_2=i_1+1}^{N}\sum_{j_2=1}^{m}\sum_{j_1=1}^{m} C_{i_1 i_2 j_1 j_2}^2(\mathbf{d}), \qquad (3.18)$$

differ, depend on m, and progressively improve as S becomes larger. Recent works on error analysis indicate that the second-moment properties obtained from the ANOVA dimensional decomposition, which leads to PDD approximations, are superior to those derived from dimension-reduction methods that are grounded in RDD [64, 83].

3.3.2.2 Higher-Order Moments

When calculating higher-order ($2 < r < \infty$) moments by the PDD approximation, no explicit formulae exist for a general function y or the probability distribution of $\mathbf{X}$. In which instance, two options are proposed to estimate the higher-order moments.

Option I entails expanding the rth power of the PDD approximation of y by

$$\tilde{y}_{S,m}^r(\mathbf{X}) = g_\emptyset(\mathbf{d}) + \sum_{\substack{\emptyset \neq u \subseteq \{1,\cdots,N\} \\ 1 \leq |u| \leq \min(rS,N)}} g_u(\mathbf{X}_u; \mathbf{d}) \tag{3.19}$$

in terms of a constant $g_\emptyset(\mathbf{d})$ and at most $\min(rS, N)$-variate polynomial functions $g_u(\mathbf{X}_u; \mathbf{d})$ and then calculating the moment

$$
\begin{aligned}
\tilde{m}_{S,m}^{(r)}(\mathbf{d}) &= \int_{\mathbb{R}^N} \tilde{y}_{S,m}^r(\mathbf{x}) f_{\mathbf{X}}(\mathbf{x}; \mathbf{d}) d\mathbf{x} \\
&= g_\emptyset(\mathbf{d}) + \sum_{\substack{\emptyset \neq u \subseteq \{1,\cdots,N\} \\ 1 \leq |u| \leq \min(rS,N)}} \int_{\mathbb{R}^{|u|}} g_u(\mathbf{x}_u; \mathbf{d}) f_{\mathbf{X}_u}(\mathbf{x}_u; \mathbf{d}) d\mathbf{x}_u
\end{aligned} \tag{3.20}
$$

by integration, if it exists. For well-behaved functions, including many encountered in practical applications, $\tilde{m}_{S,m}^{(r)}(\mathbf{d})$ should render an accurate approximation of $m^{(r)}(\mathbf{d})$, the rth-order moment of $y(\mathbf{X})$, although there is no rigorous mathematical proof of convergence when $r > 2$. Note that Equation (3.20) involves integrations of elementary polynomial functions and does not require any expensive evaluation of the original function y. Nonetheless, since $\tilde{y}_{S,m}(\mathbf{X})$ is a superposition of at most S-variate

component functions of independent variables, the largest dimension of the integrals in Equation (3.20) is $\min(rS, N)$. Therefore, Option I mandates high-dimensional integrations if $\min(rS, N)$ is large. In addition, if $rS \geq N$ and N is large, then the resulting N-dimensional integration is infeasible.

As an alternative, Option II, relevant to large N, creates an additional $\bar{S}$-variate, $\bar{m}$th-order PDD approximation

$$\tilde{z}_{\bar{S},\bar{m}}(\mathbf{X}) = z_{\emptyset}(\mathbf{d}) + \sum_{\substack{\emptyset \neq u \subseteq \{1,\cdots,N\} \\ 1 \leq |u| \leq \bar{S}}} \sum_{\substack{\mathbf{j}_{|u|} \in \mathbb{N}_0^{|u|}, ||\mathbf{j}_{|u|}||_\infty \leq \bar{m} \\ j_1,\cdots,j_{|u|} \neq 0}} \bar{C}_{u\mathbf{j}_{|u|}}(\mathbf{d})\psi_{u\mathbf{j}_{|u|}}(\mathbf{X}_u; \mathbf{d}) \qquad (3.21)$$

of $\tilde{y}_{S,m}^r(\mathbf{X})$, where $\bar{S}$ and $\bar{m}$, potentially distinct from S and m, are accompanying truncation parameters, $z_{\emptyset}(\mathbf{d}) := \int_{\mathbb{R}^N} \tilde{y}_{S,m}^r(\mathbf{x})f_{\mathbf{X}}(\mathbf{x}; \mathbf{d})d\mathbf{x}$, and $\bar{C}_{u\mathbf{j}_{|u|}}(\mathbf{d}) := \int_{\mathbb{R}^N} \tilde{y}_{S,m}^r(\mathbf{x})$ $\psi_{u\mathbf{j}_{|u|}}(\mathbf{x}_u; \mathbf{d})f_{\mathbf{X}}(\mathbf{x}; \mathbf{d})d\mathbf{x}$ are the associated PDD expansion coefficients of $\tilde{z}_{\bar{S},\bar{m}}(\mathbf{X})$. Replacing $\tilde{y}_{S,m}^r(\mathbf{x})$ with $\tilde{z}_{\bar{S},\bar{m}}(\mathbf{x})$, the first line of Equation (3.20) produces

$$\tilde{m}_{S,m}^{(r)}(\mathbf{d}) = \int_{\mathbb{R}^N} \tilde{z}_{\bar{S},\bar{m}}(\mathbf{x})f_{\mathbf{X}}(\mathbf{x}; \mathbf{d})d\mathbf{x} =: z_{\emptyset}(\mathbf{d}). \qquad (3.22)$$

Then the evaluation of $z_{\emptyset}(\mathbf{d})$ from the definition, which also requires N-dimensional integration, leads Equation (3.22) back to Equation (3.20), raising the question of why Option II is introduced. Indeed, the distinction between the two options forms when the constant $z_{\emptyset}(\mathbf{d})$ is approximately calculated by dimension-reduction integration, to be explained in Section 3.6, entailing at most $\bar{S}$-dimensional integrations. Nonetheless, if $\bar{S} \ll rS < N$, then a significant dimension reduction is possible in Option II for estimating higher-order moments. In other words, Option II, which is an approximate version of Option I, may provide efficient solutions to high-dimensional problems, provided that a loss of accuracy in Option II, if any, is insignificant. The

higher-order moments are useful for approximating the probability distribution of a stochastic response or reliability analysis, including their sensitivity analyses, and will be revisited in the next subsection.

3.3.3   Reliability Analysis

A fundamental problem in reliability analysis entails calculation of the failure probability

$$P_F(\mathbf{d}) := P_{\mathbf{d}}\left[\mathbf{X} \in \Omega_F\right] = \int_{\mathbb{R}^N} I_{\Omega_F}(\mathbf{x}) f_{\mathbf{X}}(\mathbf{x}; \mathbf{d}) d\mathbf{x} =: \mathbb{E}_{\mathbf{d}}\left[I_{\Omega_F}(\mathbf{X})\right], \qquad (3.23)$$

where Ω_F is the failure set and $I_{\Omega_F}(\mathbf{x})$ is the associated indicator function, which is equal to *one* when $\mathbf{x} \in \Omega_F$ and *zero* otherwise. Depending on the nature of the failure domain Ω_F, a component or a system reliability analysis can be envisioned. For component reliability analysis, the failure domain is often adequately described by a single performance function $y(\mathbf{x})$, for instance, $\Omega_F := \{\mathbf{x} : y(\mathbf{x}) < 0\}$. In contrast, multiple, interdependent performance functions $y_i(\mathbf{x})$, $i = 1, 2, \cdots$, are required for system reliability analysis, leading, for example, to $\Omega_F := \{\mathbf{x} : \cup_i y_i(\mathbf{x}) < 0\}$ and $\Omega_F := \{\mathbf{x} : \cap_i y_i(\mathbf{x}) < 0\}$ for series and parallel systems, respectively. In this subsection, two methods are presented for estimating the failure probability. The PDD-SPA method, which blends the PDD approximation with SPA, is described first. Then the PDD-MCS method, which exploits the PDD approximation for MCS, is elucidated.

3.3.3.1   The PDD-SPA Method

Let $F_y(\xi) := P_{\mathbf{d}}[y \leq \xi]$ be the cumulative distribution function (CDF) of $y(\mathbf{X})$. Assume that the PDF $f_y(\xi) := dF_y(\xi)/d\xi$ exists and suppose that the cumulant generating function (CGF)

$$K_y(t) := \ln \left\{ \int_{-\infty}^{+\infty} \exp(t\xi) f_y(\xi) d\xi \right\} \tag{3.24}$$

of y converges for $t \in \mathbb{R}$ in some non-vanishing interval containing the origin. Using inverse Fourier transformation, exponential power series expansion, and Hermite polynomial approximation, Daniels [56] developed an SPA formula to approximately evaluate $f_y(\xi)$. However, the success of such formula is predicated on how accurately the CGF and its derivatives, if they exist, are calculated. In fact, determining $K_y(t)$ is immensely difficult because it is equivalent to knowing all higher-order moments of y. To mitigate this problem, consider the Taylor series expansion of

$$K_y(t) = \sum_{r \in \mathbb{N}} \frac{\kappa^{(r)} t^r}{r!} \tag{3.25}$$

at $t = 0$, where $\kappa^{(r)} := d^r K_y(0)/dt^r$, $r \in \mathbb{N}$, is known as the rth-order cumulant of $y(\mathbf{X})$. If some of these cumulants are effectively estimated, then a truncated Taylor series provides a useful means to approximate $K_y(t)$. For instance, assume that, given a positive integer $Q < \infty$, the raw moments $\tilde{m}_{S,m}^{(r)}(\mathbf{d})$ of order at most Q have been calculated with sufficient accuracy using an S-variate, mth-order PDD approximation $\tilde{y}_{S,m}(\mathbf{X})$ of $y(\mathbf{X})$, as described in the preceding subsection. Then the corresponding approximate cumulants are easily obtained from the well-known cumulant-moment

relationship,

$$
\tilde{\kappa}_{S,m}^{(r)}(\mathbf{d}) = \begin{cases} \tilde{m}_{S,m}^{(1)}(\mathbf{d}) & : \quad r = 1, \\ \tilde{m}_{S,m}^{(r)}(\mathbf{d}) - \sum\limits_{p=1}^{r-1} \binom{r-1}{p-1} \tilde{\kappa}_{S,m}^{(p)}(\mathbf{d}) \tilde{m}_{S,m}^{(r-p)}(\mathbf{d}) & : \quad 2 \leq r \leq Q, \end{cases} \tag{3.26}
$$

where the functional argument $\mathbf{d}$ serves as a reminder that the moments and cumulants all depend on the design vector $\mathbf{d}$. Setting $\kappa^{(r)} = \tilde{\kappa}_{S,m}^{(r)}$ for $r = 1, \cdots, Q$, and *zero* otherwise in Equation (3.25), the result is an S-variate, mth-order PDD approximation

$$
\tilde{K}_{y,Q,S,m}(t;\mathbf{d}) = \sum_{r=1}^{Q} \frac{\tilde{\kappa}_{S,m}^{(r)}(\mathbf{d}) t^r}{r!} \tag{3.27}
$$

of the Qth-order Taylor series expansion of $K_y(t)$. It is elementary to show that $\tilde{K}_{y,Q,S,m}(t;\mathbf{d}) \to K_y(t)$ when $S \to N$, $m \to \infty$, and $Q \to \infty$.

Using the CGF approximation in Equation (3.27), Daniels' SPA leads to the explicit formula [56],

$$
\tilde{f}_{y,PS}(\xi;\mathbf{d}) = \left[2\pi \tilde{K}''_{y,Q,S,m}(t_s;\mathbf{d}) \right]^{-\frac{1}{2}} \exp \left[\tilde{K}_{y,Q,S,m}(t_s;\mathbf{d}) - t_s \xi \right], \tag{3.28}
$$

for the approximate PDF of y, where t_s is the saddlepoint that is obtained from solving

$$
\tilde{K}'_{y,Q,S,m}(t_s;\mathbf{d}) = \xi \tag{3.29}
$$

with $\tilde{K}'_{y,Q,S,m}(t;\mathbf{d}) := d\tilde{K}_{y,Q,S,m}(t;\mathbf{d})/dt$ and $\tilde{K}''_{y,Q,S,m}(t;\mathbf{d}) := d^2\tilde{K}_{y,Q,S,m}(t;\mathbf{d})/dt^2$ defining the first- and second-order derivatives, respectively, of the approximate CGF of y with respect to t. Furthermore, based on a related work of Lugannani and Rice [101], the approximate CDF of y becomes

$$
\tilde{F}_{y,PS}(\xi;\mathbf{d}) = \Phi(w) + \phi(w)\left(\frac{1}{w} - \frac{1}{v}\right),
$$
$$
w = \operatorname{sgn}(t_s)\left\{ 2\left[t_s\xi - \tilde{K}_{y,Q,S,m}(t_s;\mathbf{d}) \right] \right\}^{\frac{1}{2}}, \quad v = t_s \left[\tilde{K}''_{y,Q,S,m}(t_s;\mathbf{d}) \right]^{\frac{1}{2}}, \tag{3.30}
$$

where $\Phi(\cdot)$ and $\phi(\cdot)$ are the CDF and PDF, respectively, of the standard Gaussian variable and $\text{sgn}(t_s) = +1, -1,$ or 0, depending on whether t_s is positive, negative, or zero. According to Equation (3.30), the CDF of y at a point ξ is obtained using solely the corresponding saddlepoint t_s, that is, without the need to integrate Equation (3.28) from $-\infty$ to ξ.

Finally, using Lugannani and Rice's formula, the PDD-SPA estimate $\tilde{P}_{F,PS}(\mathbf{d})$ of the component failure probability $P_F(\mathbf{d}) := P[y(\mathbf{X}) < 0]$ is obtained as

$$\tilde{P}_{F,PS}(\mathbf{d}) = \tilde{F}_{y,PS}(0; \mathbf{d}), \tag{3.31}$$

the PDD-SPA generated CDF of y at $\xi = 0$. It is important to recognize that no similar SPA-based formulae are available for the joint PDF or joint CDF of dependent stochastic responses. Therefore, the PDD-SPA method in the current form cannot be applied to general system reliability analysis.

The PDD-SPA method contains several truncation parameters that should be carefully selected. For instance, if Q is too small, then the truncated CGF from Equation (3.27) may spoil the method, regardless of how large are the S and m chosen in the PDD approximation. On the other hand, if Q is overly large, then many higher-order moments involved may not be accurately calculated by the PDD approximation. More significantly, a finite-order truncation of CGF may cause loss of convexity of the actual CGF, meaning that the one-to-one relationship between ξ and t_s in Equation (3.29) is not ensured for every threshold ξ. Furthermore, the important property $\tilde{K}''_{y,Q,S,m}(t_s; \mathbf{d}) > 0$ may not be maintained. To resolve this quandary, Yuen et al. [102] presented for $Q = 4$ several distinct cases of the cumulants, de-

scribing the interval (t_l, t_u), where $-\infty \leq t_l \leq 0$ and $0 \leq t_u \leq \infty$, such that $t_l \leq t_s \leq t_u$ and $\tilde{K}''_{y,Q,S,m}(t_s; \mathbf{d}) > 0$, ruling out any complex values of the square root in Equation (3.28) or (3.30). Table 3.1 summarizes these cases, which were employed in the PDD-SPA method described in this chapter. If the specified threshold $\xi \in (\tilde{K}'_{y,Q,S,m}(t_l; \mathbf{d}), \tilde{K}'_{y,Q,S,m}(t_u; \mathbf{d}))$, then the saddlepoint t_s is uniquely determined from Equation (3.29), leading to the CDF or reliability in Equation (3.30) or (3.31). Otherwise, the PDD-SPA method will fail to provide a solution. It is important to note that developing similar cases for $Q > 4$, assuring a unique solution of the saddlepoint, is not trivial, and was not considered in this work.

Table 3.1: Intervals of the saddlepoint for $Q = 4^{\text{(a)}}$

Case	Condition	t_l	t_u
1	$\tilde{\kappa}_{S,m}^{(4)} > 0,\ \Delta > 0,$ $\tilde{\kappa}_{S,m}^{(3)} > 0$	$\dfrac{-\tilde{\kappa}_{S,m}^{(3)} + \sqrt{\Delta}}{\tilde{\kappa}_{S,m}^{(4)}}$	$+\infty$
2	$\tilde{\kappa}_{S,m}^{(4)} > 0,\ \Delta > 0,$ $\tilde{\kappa}_{S,m}^{(3)} < 0$	$-\infty$	$\dfrac{-\tilde{\kappa}_{S,m}^{(3)} - \sqrt{\Delta}}{\tilde{\kappa}_{S,m}^{(4)}}$
3	$\tilde{\kappa}_{S,m}^{(4)} > 0,\ \Delta = 0$	$-\infty^{\text{(b)}}$	$+\infty^{\text{(b)}}$
4	$\tilde{\kappa}_{S,m}^{(4)} > 0,\ \Delta < 0$	$-\infty$	$+\infty$
5	$\tilde{\kappa}_{S,m}^{(4)} = 0,\ \tilde{\kappa}_{S,m}^{(3)} > 0$	$-\dfrac{\tilde{\kappa}_{S,m}^{(2)}}{\tilde{\kappa}_{S,m}^{(3)}}$	$+\infty$
6	$\tilde{\kappa}_{S,m}^{(4)} = 0,\ \tilde{\kappa}_{S,m}^{(3)} = 0$	$-\infty$	$+\infty$
7	$\tilde{\kappa}_{S,m}^{(4)} = 0,\ \tilde{\kappa}_{S,m}^{(3)} < 0$	$-\infty$	$-\dfrac{\tilde{\kappa}_{S,m}^{(2)}}{\tilde{\kappa}_{S,m}^{(3)}}$
8	$\tilde{\kappa}_{S,m}^{(4)} < 0$	$\dfrac{-\tilde{\kappa}_{S,m}^{(3)} + \sqrt{\Delta}}{\tilde{\kappa}_{S,m}^{(4)}}$	$\dfrac{-\tilde{\kappa}_{S,m}^{(3)} - \sqrt{\Delta}}{\tilde{\kappa}_{S,m}^{(4)}}$

(a) For $\tilde{K}_{y,4,S,m}(t;\mathbf{d}) = \tilde{\kappa}_{S,m}^{(1)}(\mathbf{d})t + \frac{1}{2!}\tilde{\kappa}_{S,m}^{(2)}(\mathbf{d})t^2 + \frac{1}{3!}\tilde{\kappa}_{S,m}^{(3)}(\mathbf{d})t^3 + \frac{1}{4!}\tilde{\kappa}_{S,m}^{(4)}(\mathbf{d})t^4$, the discriminant of $\tilde{K}'_{y,4,S,m}(t;\mathbf{d})$ is $\Delta := \tilde{\kappa}_{S,m}^{(3)^2} - 2\tilde{\kappa}_{S,m}^{(2)}\tilde{\kappa}_{S,m}^{(4)}$.

(b) The point $-\tilde{\kappa}_{S,m}^{(3)}/(2\tilde{\kappa}_{S,m}^{(2)})$ should not be an element of (t_l, t_u), i.e., $(t_l, t_u) = (-\infty, \infty) \setminus \{-\tilde{\kappa}_{S,m}^{(3)}/(2\tilde{\kappa}_{S,m}^{(2)})\}$.

3.3.3.2 The PDD-MCS Method

Depending on component or system reliability analysis, let $\tilde{\Omega}_{F,S,m} := \{\mathbf{x} : \tilde{y}_{S,m}(\mathbf{x}) < 0\}$ or $\tilde{\Omega}_{F,S,m} := \{\mathbf{x} : \cup_i \tilde{y}_{i,S,m}(\mathbf{x}) < 0\}$ or $\tilde{\Omega}_{F,S,m} := \{\mathbf{x} : \cap_i \tilde{y}_{i,S,m}(\mathbf{x}) < 0\}$ be an approximate failure set as a result of S-variate, mth-order PDD approximations $\tilde{y}_{S,m}(\mathbf{X})$ of $y(\mathbf{X})$ or $\tilde{y}_{i,S,m}(\mathbf{X})$ of $y_i(\mathbf{X})$. Then the PDD-MCS estimate of the failure probability $P_F(\mathbf{d})$ is

$$\tilde{P}_{F,PM}(\mathbf{d}) = \mathbb{E}_\mathbf{d}\left[I_{\tilde{\Omega}_{F,S,m}}(\mathbf{X})\right] = \lim_{L\to\infty}\frac{1}{L}\sum_{l=1}^{L} I_{\tilde{\Omega}_{F,S,m}}(\mathbf{x}^{(l)}), \qquad (3.32)$$

where L is the sample size, $\mathbf{x}^{(l)}$ is the lth realization of $\mathbf{X}$, and $I_{\tilde{\Omega}_{F,S,m}}(\mathbf{x})$ is another indicator function, which is equal to *one* when $\mathbf{x} \in \tilde{\Omega}_{F,S,m}$ and *zero* otherwise.

Note that the simulation of the PDD approximation in Equation (3.32) should not be confused with crude MCS commonly used for producing benchmark results. The crude MCS, which requires numerical calculations of $y(\mathbf{x}^{(l)})$ or $y_i(\mathbf{x}^{(l)})$ for input samples $\mathbf{x}^{(l)}, l = 1, \cdots, L$, can be expensive or even prohibitive, particularly when the sample size L needs to be very large for estimating small failure probabilities. In contrast, the MCS embedded in PDD requires evaluations of simple analytical functions that stem from an S-variate, mth-order approximation $\tilde{y}_{S,m}(\mathbf{x}^{(l)})$ or $\tilde{y}_{i,S,m}(\mathbf{x}^{(l)})$. Therefore, an arbitrarily large sample size can be accommodated in the PDD-MCS method. In which case, the PDD-MCS method also furnishes the approximate CDF $\tilde{F}_{y,PM}(\xi; \mathbf{d}) := P_{\mathbf{d}}[\tilde{y}_{S,m}(\mathbf{X}) \le \xi]$ of $y(\mathbf{X})$ or even the joint CDF of dependent stochastic responses, if desired.

Although the PDD-SPA and PDD-MCS methods are both rooted in the same PDD approximation, the former requires additional layers of approximations to calculate the CGF and saddlepoint. Therefore, the PDD-SPA method, when it works, is expected to be less accurate than the PDD-MCS method at comparable computational efforts. However, the PDD-SPA method facilitates an analytical means to estimate the probability distribution and reliability − a convenient process not supported by the PDD-MCS method. The respective properties of both methods extend to sensitivity analysis, presented in the following two sections.

3.4   Design Sensitivity Analysis of Moments

When solving RDO problems using gradient-based optimization algorithms, at least first-order derivatives of the first and second moments of a stochastic response with respect to each design variable are required. In this section, a new method, developed by blending PDD with score functions, for design sensitivity analysis of moments of an arbitrary order, is presented.

3.4.1   Score functions

Suppose that the first-order derivative of a moment $m^{(r)}(\mathbf{d})$, where $r \in \mathbb{N}$, of a generic stochastic response $y(\mathbf{X})$ with respect to a design variable d_k, $1 \leq k \leq M$, is sought. Taking a partial derivative of the moment with respect to d_k and then applying the Lebesgue dominated convergence theorem [76], which permits the differential and integral operators to be interchanged, yields the sensitivity

$$
\begin{aligned}
\frac{\partial m^{(r)}(\mathbf{d})}{\partial d_k} &:= \frac{\partial \mathbb{E}_{\mathbf{d}}\left[y^r(\mathbf{X})\right]}{\partial d_k} \\
&= \frac{\partial}{\partial d_k} \int_{\mathbb{R}^N} y^r(\mathbf{x}) f_{\mathbf{X}}(\mathbf{x}; \mathbf{d}) d\mathbf{x}, \\
&= \int_{\mathbb{R}^N} y^r(\mathbf{x}) \frac{\partial \ln f_{\mathbf{X}}(\mathbf{x}; \mathbf{d})}{\partial d_k} f_{\mathbf{X}}(\mathbf{x}; \mathbf{d}) d\mathbf{x}, \\
&=: \mathbb{E}_{\mathbf{d}}\left[y^r(\mathbf{X}) s_{d_k}^{(1)}(\mathbf{X}; \mathbf{d})\right]
\end{aligned}
\tag{3.33}
$$

provided that $f_{\mathbf{X}}(\mathbf{x}; \mathbf{d}) > 0$ and the derivative $\partial \ln f_{\mathbf{X}}(\mathbf{x}; \mathbf{d}) / \partial d_k$ exists. In the last line of Equation (3.33), $s_{d_k}^{(1)}(\mathbf{X}; \mathbf{d}) := \partial \ln f_{\mathbf{X}}(\mathbf{X}; \mathbf{d}) / \partial d_k$ is known as the first-order score function for the design variable d_k [74, 75]. In general, the sensitivities are not available analytically since the moments are not either. Nonetheless, the moments and their sensitivities have both been formulated as expectations of stochastic quantities with respect to the same probability measure, facilitating their concurrent evaluations

in a single stochastic simulation or analysis.

Remark 3.4. The evaluation of score functions, $s_{d_k}^{(1)}(\mathbf{X}; \mathbf{d})$, $k = 1, \cdots, M$, requires differentiating only the PDF of $\mathbf{X}$. Therefore, the resulting score functions can be determined easily and, in many cases, analytically − for instance, when $\mathbf{X}$ follows classical probability distributions [75]. If the density function of $\mathbf{X}$ is arbitrarily prescribed, the score functions can be calculated numerically, yet inexpensively, since no evaluation of the performance function is involved.

When $\mathbf{X}$ comprises independent variables, as assumed here, $\ln f_{\mathbf{X}}(\mathbf{X}; \mathbf{d}) = \sum_{i=1}^{i=N} \ln f_{X_i}(x_i; \mathbf{d})$ is a sum of N univariate log-density (marginal) functions of random variables. Hence, in general, the score function for the kth design variable, expressed by

$$s_{d_k}^{(1)}(\mathbf{X}; \mathbf{d}) = \sum_{i=1}^{N} \frac{\partial \ln f_{X_i}(X_i; \mathbf{d})}{\partial d_k} = \sum_{i=1}^{N} s_{ki}(X_i; \mathbf{d}), \qquad (3.34)$$

is also a sum of univariate functions $s_{ki}(X_i; \mathbf{d}) := \partial \ln f_{X_i}(X_i; \mathbf{d}) / \partial d_k, i = 1, \cdots, N$, which are the derivatives of log-density (marginal) functions. If d_k is a distribution parameter of a single random variable X_{i_k}, then the score function reduces to $s_{d_k}^{(1)}(\mathbf{X}; \mathbf{d}) = \partial \ln f_{X_{i_k}}(X_{i_k}; \mathbf{d}) / \partial d_k =: s_{ki_k}(X_{i_k}; \mathbf{d})$, the derivative of the log-density (marginal) function of X_{i_k}, which remains a univariate function. Nonetheless, combining Equations (3.33) and (3.34), the sensitivity is obtained from

$$\frac{\partial m^{(r)}(\mathbf{d})}{\partial d_k} = \sum_{i=1}^{N} \mathbb{E}_{\mathbf{d}} \left[y^r(\mathbf{X}) s_{ki}(X_i; \mathbf{d}) \right], \qquad (3.35)$$

the sum of expectations of products comprising stochastic response and log-density derivative functions with respect to the probability measure $P_{\mathbf{d}}, \mathbf{d} \in \mathcal{D}$.

3.4.2 Sensitivities of first- and second-order moments

For independent coordinates of $\mathbf{X}$, consider the Fourier-polynomial expansion of the kth log-density derivative function

$$s_{ki}(X_i; \mathbf{d}) = s_{ki,\emptyset}(\mathbf{d}) + \sum_{j=1}^{\infty} D_{k,ij}(\mathbf{d})\psi_{ij}(X_i; \mathbf{d}), \tag{3.36}$$

consisting of its own expansion coefficients

$$s_{ki,\emptyset}(\mathbf{d}) := \int_{\mathbb{R}} s_{ki}(x_i; \mathbf{d}) f_{X_i}(x_i; \mathbf{d}) dx_i \tag{3.37}$$

and

$$D_{k,ij}(\mathbf{d}) := \int_{\mathbb{R}} s_{ki}(x_i; \mathbf{d})\psi_{ij}(x_i; \mathbf{d}) f_{X_i}(x_i; \mathbf{d}) dx_i. \tag{3.38}$$

The expansion is valid if s_{ki} is square integrable with respect to the probability measure of X_i. When blended with the PDD approximation, the score function leads to analytical or closed-form expressions of the exact or approximate sensitivities as follows.

3.4.2.1 Exact Sensitivities

Employing Equations (3.10) and (3.36), the product appearing on the right side of Equation (3.35) expands to

$$y^r(\mathbf{X})s_{ki}(X_i; \mathbf{d}) = \left(y_\emptyset(\mathbf{d}) + \sum_{\emptyset \neq u \subseteq \{1,\cdots,N\}} \sum_{\substack{\mathbf{j}_{|u|} \in \mathbb{N}_0^{|u|} \\ j_1,\cdots,j_{|u|} \neq 0}} C_{u\mathbf{j}_{|u|}}(\mathbf{d})\psi_{u\mathbf{j}_{|u|}}(\mathbf{X}_u; \mathbf{d}) \right)^r \times$$
$$\left(s_{ki,\emptyset}(\mathbf{d}) + \sum_{j=1}^{\infty} D_{k,ij}(\mathbf{d})\psi_{ij}(X_i; \mathbf{d}) \right), \tag{3.39}$$

encountering the same orthonormal polynomial bases that are consistent with the probability measure $f_{\mathbf{X}}(\mathbf{x}; \mathbf{d})d\mathbf{x}$. The expectations of Equation (3.39) for $r = 1$ and 2, aided by Propositions 3.1 and 3.2, lead Equation (3.35) to

$$\frac{\partial m^{(1)}(\mathbf{d})}{\partial d_k} = \sum_{i=1}^{N} \left[y_\emptyset(\mathbf{d})s_{ki,\emptyset}(\mathbf{d}) + \sum_{j=1}^{\infty} C_{ij}(\mathbf{d})D_{k,ij}(\mathbf{d}) \right] \qquad (3.40)$$

and

$$\frac{\partial m^{(2)}(\mathbf{d})}{\partial d_k} = \sum_{i=1}^{N} \left[m^{(2)}(\mathbf{d})s_{ki,\emptyset}(\mathbf{d}) + 2y_\emptyset(\mathbf{d})\sum_{j=1}^{\infty} C_{ij}(\mathbf{d})D_{k,ij}(\mathbf{d}) + T_{ki} \right], \qquad (3.41)$$

representing closed-form expressions of the sensitivities in terms of the PDD or Fourier-polynomial expansion coefficients of the response or log-density derivative functions. The last term on the right side of Equation (3.41) is

$$\begin{aligned}
T_{ki} &= \sum_{i_1=1}^{N}\sum_{i_2=1}^{N}\sum_{j_1=1}^{\infty}\sum_{j_2=1}^{\infty}\sum_{j_3=1}^{\infty} C_{i_1 j_1}(\mathbf{d})C_{i_2 j_2}(\mathbf{d})D_{k,ij_3}(\mathbf{d}) \times \\
&\quad \mathbb{E}_{\mathbf{d}}\left[\psi_{i_1 j_1}(X_{i_1}; \mathbf{d})\psi_{i_2 j_2}(X_{i_2}; \mathbf{d})\psi_{ij_3}(X_i; \mathbf{d})\right],
\end{aligned} \qquad (3.42)$$

which requires expectations of various products of three random orthonormal polynomials and is further discussed in Subsection 3.2.4. Note that these sensitivity equations are exact because PDD and Fourier-polynomial expansions are exact representations of square-integrable functions.

3.4.2.2 Approximate Sensitivities

When $y(\mathbf{X})$ and $s_{ki}(X_i; \mathbf{d})$ are replaced with their S-variate, mth-order PDD and m'th-order Fourier-polynomial approximations, respectively, the resultant sensitivity equations, expressed by

$$\frac{\partial \tilde{m}_{S,m}^{(1)}(\mathbf{d})}{\partial d_k} := \frac{\partial \mathbb{E}_{\mathbf{d}}\left[\tilde{y}_{S,m}(\mathbf{X})\right]}{\partial d_k} = \sum_{i=1}^{N} \left[y_\emptyset(\mathbf{d})s_{ki,\emptyset}(\mathbf{d}) + \sum_{j=1}^{m_{\min}} C_{ij}(\mathbf{d})D_{k,ij}(\mathbf{d}) \right] \qquad (3.43)$$

and

$$
\begin{aligned}
\frac{\partial \tilde{m}_{S,m}^{(2)}(\mathbf{d})}{\partial d_k} &:= \frac{\partial \mathbb{E}_{\mathbf{d}}\big[\tilde{y}_{S,m}^2(\mathbf{X})\big]}{\partial d_k} \\
&= \sum_{i=1}^{N}\left[\tilde{m}_{S,m}^{(2)}(\mathbf{d})s_{ki,\emptyset}(\mathbf{d}) + 2y_\emptyset(\mathbf{d})\sum_{j=1}^{m_{\min}}C_{ij}(\mathbf{d})D_{k,ij}(\mathbf{d}) + \tilde{T}_{ki,m,m'}\right],
\end{aligned}
\tag{3.44}
$$

where $m_{\min} := \min(m, m')$ and

$$
\begin{aligned}
\tilde{T}_{ki,m,m'} &= \sum_{i_1=1}^{N}\sum_{i_2=1}^{N}\sum_{j_1=1}^{m}\sum_{j_2=1}^{m}\sum_{j_3=1}^{m'}C_{i_1j_1}(\mathbf{d})C_{i_2j_2}(\mathbf{d})D_{k,ij_3}(\mathbf{d})\times \\
&\quad \mathbb{E}_{\mathbf{d}}\left[\psi_{i_1j_1}(X_{i_1};\mathbf{d})\psi_{i_2j_2}(X_{i_2};\mathbf{d})\psi_{ij_3}(X_i;\mathbf{d})\right],
\end{aligned}
\tag{3.45}
$$

become approximate, relying on the truncation parameters S, m, and m' in general. At appropriate limits, the approximate sensitivities of the moments converge to exactness as described by Proposition 3.5.

Proposition 3.5. *Let $\tilde{y}_{S,m}(\mathbf{X})$ be an S-variate, mth-order PDD approximation of a square-integrable function $y(\mathbf{X})$, where $\mathbf{X} = (X_1, \cdots, X_N)^T \in \mathbb{R}^N$ comprises independent random variables with marginal probability distributions $f_{X_i}(x_i;\mathbf{d})$, $i = 1, \cdots, N$, and $\mathbf{d} = (d_1, \cdots, d_M)^T \in \mathcal{D}$ is a design vector with non-empty closed set $\mathcal{D} \subseteq \mathbb{R}^M$. Given the distribution parameter d_k, let the kth log-density derivative function $s_{ki}(X_i;\mathbf{d})$ of the ith random variable X_i be square integrable. Then for $k = 1, \cdots M$,*

$$
\lim_{S\to N,\, m,m'\to\infty}\frac{\partial \tilde{m}_{S,m}^{(1)}(\mathbf{d})}{\partial d_k} = \frac{\partial m^{(1)}(\mathbf{d})}{\partial d_k}
\tag{3.46}
$$

and

$$
\lim_{S\to N,\, m,m'\to\infty}\frac{\partial \tilde{m}_{S,m}^{(2)}(\mathbf{d})}{\partial d_k} = \frac{\partial m^{(2)}(\mathbf{d})}{\partial d_k}.
\tag{3.47}
$$

Proof. Taking the limits $S \to N$, $m \to \infty$, and $m' \to \infty$ on Equations (3.43) and (3.44) and recognizing $\tilde{m}_{S,m}^{(2)}(\mathbf{d}) \to m^{(2)}(\mathbf{d})$ and $\tilde{T}_{ki,m,m'} \to T_{ki}$,

$$
\begin{aligned}
\lim_{S\to N,\; m,m'\to\infty} \frac{\partial \tilde{m}_{S,m}^{(1)}(\mathbf{d})}{\partial d_k} &= \lim_{S\to N,\; m,m'\to\infty} \sum_{i=1}^{N}\left[y_\emptyset(\mathbf{d})s_{ki,\emptyset}(\mathbf{d}) + \sum_{j=1}^{m_{\min}} C_{ij}(\mathbf{d})D_{k,ij}(\mathbf{d}) \right] \\
&= \sum_{i=1}^{N}\left[y_\emptyset(\mathbf{d})s_{ki,\emptyset}(\mathbf{d}) + \sum_{j=1}^{\infty} C_{ij}(\mathbf{d})D_{k,ij}(\mathbf{d}) \right] \qquad (3.48) \\
&= \frac{\partial m^{(1)}(\mathbf{d})}{\partial d_k}
\end{aligned}
$$

and

$$
\begin{aligned}
&\lim_{s\to N,\; m,m'\to\infty} \frac{\partial \tilde{m}_{S,m}^{(2)}(\mathbf{d})}{\partial d_k} \\
&= \lim_{S\to N,\; m,m'\to\infty} \sum_{i=1}^{N}\left[\tilde{m}_{S,m}^{(2)2}(\mathbf{d})s_{ki,\emptyset}(\mathbf{d}) + 2y_\emptyset(\mathbf{d})\sum_{j=1}^{m_{\min}} C_{ij}(\mathbf{d})D_{k,ij}(\mathbf{d}) + \tilde{T}_{ki,m,m'} \right] \\
&= \sum_{i=1}^{N}\left[m^{(2)2}(\mathbf{d})s_{ki,\emptyset}(\mathbf{d}) + 2y_\emptyset(\mathbf{d})\sum_{j=1}^{\infty} C_{ij}(\mathbf{d})D_{k,ij}(\mathbf{d}) + T_{ki} \right] \qquad (3.49) \\
&= \frac{\partial m^{(2)}(\mathbf{d})}{\partial d_k},
\end{aligned}
$$

where the last lines follow from Equations (3.40) and (3.41).

Of the two sensitivities, $\partial \tilde{m}_{S,m}^{(1)}(\mathbf{d})/\partial d_k$ does not depend on S, meaning that both the univariate ($S = 1$) and bivariate ($S = 2$) approximations, given the same $m_{\min} < \infty$, form the same result, as displayed in Equation (3.43). However, the sensitivity equations of $\partial \tilde{m}_{S,m}^{(2)}(\mathbf{d})/\partial d_k$ for the univariate and bivariate approximations vary with respect to S, m, and m'. For instance, the univariate approximation results in

$$
\frac{\partial \tilde{m}_{1,m}^{(2)}(\mathbf{d})}{\partial d_k} = \sum_{i=1}^{N}\left[\tilde{m}_{1,m}^{(2)}(\mathbf{d})s_{ki,\emptyset}(\mathbf{d}) + 2y_\emptyset(\mathbf{d})\sum_{j=1}^{m_{\min}} C_{ij}(\mathbf{d})D_{k,ij}(\mathbf{d}) + \tilde{T}_{ki,m,m'} \right], \quad (3.50)
$$

whereas the bivariate approximation yields

$$\frac{\partial \tilde{m}_{2,m}^{(2)}(\mathbf{d})}{\partial d_k} = \sum_{i=1}^{N} \left[\tilde{m}_{2,m}^{(2)}(\mathbf{d}) s_{ki,\emptyset}(\mathbf{d}) + 2y_{\emptyset}(\mathbf{d}) \sum_{j=1}^{m_{\min}} C_{ij}(\mathbf{d}) D_{k,ij}(\mathbf{d}) + \tilde{T}_{ki,m,m'} \right]. \quad (3.51)$$

Analogous to the moments, the univariate and bivariate approximations of the sensitivities of the moments involve only univariate and at most bivariate expansion coefficients of y, respectively. Since the expansion coefficients of log-density derivative functions do not involve the response function, no additional cost is incurred from response analysis. In other words, the effort required to obtain the statistical moments of a response also furnishes the sensitivities of moments, a highly desirable trait for efficiently solving RDO problems.

Remark 3.6. Since the derivatives of log-density functions are univariate functions, their expansion coefficients require only univariate integration for their evaluations. When X_i follows classical distributions − for instance, the Gaussian distribution − then the coefficients can be calculated exactly or analytically. Otherwise, numerical quadrature is required. Nonetheless, there is no need to employ dimension-reduction integration for calculating the expansion coefficients of the derivatives of log-density functions.

3.4.2.3   Special Cases

There exist two special cases when the preceding expressions of the sensitivities of moments simplify slightly. They are contingent on how a distribution parameter affects the probability distributions of random variables.

First, when $\mathbf{X}$ comprises independent variables such that d_k is a distribution

parameter of a single random variable, say, X_{i_k}, $1 \leq i_k \leq N$, then $s_{k i_k}(X_{i_k}; \mathbf{d})$ — the kth log-density derivative function of X_{i_k} — is the only relevant function of interest. Consequently, the expansion coefficients $s_{ki,\emptyset}(\mathbf{d}) = s_{k i_k,\emptyset}(\mathbf{d})$ (say) and $D_{k,ij}(\mathbf{d}) = D_{k,i_k j}(\mathbf{d})$ (say), if $i = i_k$ and *zero* otherwise. Moreover, the outer sums of Equations (3.43) and (3.44) vanish, yielding

$$\frac{\partial \tilde{m}_{S,m}^{(1)}(\mathbf{d})}{\partial d_k} = y_\emptyset(\mathbf{d}) s_{k i_k,\emptyset}(\mathbf{d}) + \sum_{j=1}^{m_{\min}} C_{i_k j}(\mathbf{d}) D_{k,i_k j}(\mathbf{d}) \tag{3.52}$$

and

$$\frac{\partial \tilde{m}_{S,m}^{(2)}(\mathbf{d})}{\partial d_k} = \tilde{m}_{S,m}^{(2)}(\mathbf{d}) s_{k i_k,\emptyset}(\mathbf{d}) + 2 y_\emptyset(\mathbf{d}) \sum_{j=1}^{m_{\min}} C_{i_k j}(\mathbf{d}) D_{k,i_k j}(\mathbf{d}) + \tilde{T}_{k i_k,m,m'}. \tag{3.53}$$

Second, when $\mathbf{X}$ consists of independent and identical variables, then $s_{ki}(X_i; \mathbf{d}) = s_k(X_i; \mathbf{d})$ (say), that is, the kth log-density derivative functions of all random variables are alike. Accordingly, the expansion coefficients $s_{ki,\emptyset}(\mathbf{d}) = s_{k,\emptyset}(\mathbf{d})$ (say) and $D_{k,ij}(\mathbf{d}) = D_{k,j}(\mathbf{d})$ (say) for all $i = 1, \cdots, N$, producing

$$\frac{\partial \tilde{m}_{S,m}^{(1)}(\mathbf{d})}{\partial d_k} = \sum_{i=1}^{N} \left[y_\emptyset(\mathbf{d}) s_{k,\emptyset}(\mathbf{d}) + \sum_{j=1}^{m_{\min}} C_{ij}(\mathbf{d}) D_{k,j}(\mathbf{d}) \right] \tag{3.54}$$

and

$$\frac{\partial \tilde{m}_{S,m}^{(2)}(\mathbf{d})}{\partial d_k} = \sum_{i=1}^{N} \left[\tilde{m}_{S,m}^{(2)}(\mathbf{d}) s_{k,\emptyset}(\mathbf{d}) + 2 y_\emptyset(\mathbf{d}) \sum_{j=1}^{m_{\min}} C_{ij}(\mathbf{d}) D_{k,j}(\mathbf{d}) + \tilde{T}_{ki,m,m'} \right]. \tag{3.55}$$

The results of sensitivity equations from these two special cases will be discussed in the Numerical Examples section.

3.4.2.4 Evaluation of $\tilde{T}_{ki,m,m'}$

The evaluation of $\tilde{T}_{ki,m,m'}$ in Equation (3.45) requires expectations of various products of three random orthonormal polynomials. The expectations vanish when

$i_1 \neq i_2 \neq i_3$, regardless of the probability measures of random variables. For classical polynomials, such as Hermite, Laguerre, and Legendre polynomials, there exist formulae for calculating the expectations when $i_1 = i_2 = i_3 = i$ (say).

When X_i follows the standard Gaussian distribution, the expectations are determined from the properties of univariate Hermite polynomials, yielding [103]

$$\mathbb{E}_{\mathbf{d}}\left[\psi_{ij_1}(X_i;\mathbf{d})\psi_{ij_2}(X_i;\mathbf{d})\psi_{ij_3}(X_i;\mathbf{d})\right] = \frac{\sqrt{j_1!j_2!j_3!}}{(q-j_1)!(q-j_2)!(q-j_3)!}, \quad (3.56)$$

if $q \in \mathbb{N}$, $2q = j_1 + j_2 + j_3$, and $j_1, j_2, j_3 \leq q$, and *zero* otherwise. When X_i follows the exponential distribution with unit mean, the expectations are attained from the properties of univariate Laguerre polynomials, producing [104]

$$\begin{aligned}
&\mathbb{E}_{\mathbf{d}}\left[\psi_{ij_1}(X_i;\mathbf{d})\psi_{ij_2}(X_i;\mathbf{d})\psi_{ij_3}(X_i;\mathbf{d})\right] \\
&= (-1)^{j_1+j_2+j_3} \sum_{v=v_{\min}}^{v_{\max}} \frac{(j_1+j_2-v)!2^{j_3-j_1-j_2+2v}}{v!(j_1-v)!(j_2-v)!}\binom{v}{j_3-j_1-j_2+2v},
\end{aligned} \quad (3.57)$$

if $|j_1 - j_2| \leq j_3 \leq j_1 + j_2$, and *zero* otherwise, where $v_{\min} = \frac{1}{2}(j_1 + j_2 + 1 - j_3)$, $v_{\max} = \min(j_1, j_2, j_1 + j_2 - j_3)$. When X_i follows the uniform distribution on the interval $[-1, 1]$, the expectations are obtained from the properties of univariate Legendre polynomials, forming [104]

$$\begin{aligned}
&\mathbb{E}_{\mathbf{d}}\left[\psi_{ij_1}(X_i;\mathbf{d})\psi_{ij_2}(X_i;\mathbf{d})\psi_{ij_3}(X_i;\mathbf{d})\right] \\
&= \frac{1}{2}\sqrt{2(2j_1+1)(2j_2+1)(2j_3+1)} \times \\
&\quad \frac{(j_1+j_2-j_3-1)!!(j_2+j_3-j_1-1)!!(j_1+j_2+j_3)!!(j_1+j_3-j_2-1)!!}{(j_1+j_2-j_3)!!(j_2+j_3-j_1)!!(j_1+j_2+j_3+1)!!(j_1+j_3-j_2)!!},
\end{aligned} \quad (3.58)$$

if $q \in \mathbb{N}$, $2q = j_1 + j_2 + j_3$, and $|j_1 - j_2| \leq j_3 \leq j_1 + j_2$, and *zero* otherwise. The symbol !! in Equation (3.58) denotes the double factorial. However, deriving a master formula for arbitrary probability distributions of X_i is impossible. In which case, the

non-trivial solution of the expectation can be obtained by numerical integration of elementary functions.

3.4.3 Sensitivities of higher-order moments

No closed-form or analytical expressions are possible for calculating sensitivities of higher-order ($2 < r < \infty$) moments by the PDD approximation. Two options, consistent with statistical moment analysis in Subsection 2.2, are proposed for sensitivity analysis.

In Option I, the sensitivity is obtained by replacing y with $\tilde{y}_{S,m}$ in Equation (3.33) and utilizing Equations (3.19) and (3.34), resulting in

$$
\begin{aligned}
\frac{\partial \tilde{m}_{S,m}^{(r)}(\mathbf{d})}{\partial d_k} &= \int_{\mathbb{R}^N} \tilde{y}_{S,m}^r(\mathbf{x}) s_{d_k}^{(1)}(\mathbf{x}; \mathbf{d}) f_{\mathbf{X}}(\mathbf{x}; \mathbf{d}) d\mathbf{x} \\
&= g_\emptyset(\mathbf{d}) \sum_{i=1}^{N} \int_{\mathbb{R}} s_{ki}(x_i; \mathbf{d}) f_{X_i}(x_i; \mathbf{d}) dx_i + \\
&\quad \sum_{i=1}^{N} \sum_{\substack{\emptyset \neq u \subseteq \{1, \cdots, N\}, i \in u \\ 1 \leq |u| \leq \min(rS, N)}} \int_{\mathbb{R}^{|u|}} g_u(\mathbf{x}_u; \mathbf{d}) s_{ki}(x_i; \mathbf{d}) f_{\mathbf{X}_u}(\mathbf{x}_u; \mathbf{d}) d\mathbf{x}_u + \\
&\quad \sum_{i=1}^{N} \sum_{\substack{\emptyset \neq u \subseteq \{1, \cdots, N\}, i \notin u \\ 1 \leq |u| \leq \min(rS, N)}} \int_{\mathbb{R}^{|u|}} g_u(\mathbf{x}_u; \mathbf{d}) f_{\mathbf{X}_u}(\mathbf{x}_u; \mathbf{d}) d\mathbf{x}_u \times \\
&\quad \int_{\mathbb{R}} s_{ki}(x_i; \mathbf{d}) f_{X_i}(x_i; \mathbf{d}) dx_i,
\end{aligned} \tag{3.59}
$$

which involves at most $\min(rS, N)$-dimensional integrations. Similar to statistical moment analysis, this option becomes impractical when $\min(rS, N)$ is large or numerous $\min(rS, N)$-dimensional integrations are required.

In contrast, the sensitivity in Option II is attained by replacing $\tilde{y}_{S,m}^r$ with $\tilde{z}_{\bar{S}, \bar{m}}$

in the first line of Equation (3.59), yielding

$$
\begin{aligned}
\frac{\partial \tilde{m}_{S,m}^{(r)}(\mathbf{d})}{\partial d_k} \\
\cong \ & \int_{\mathbb{R}^N} \tilde{z}_{\bar{S},\bar{m}}(\mathbf{x}) s_{d_k}^{(1)}(\mathbf{x};\mathbf{d}) f_{\mathbf{X}}(\mathbf{x};\mathbf{d}) d\mathbf{x} \\
= \ & z_\emptyset(\mathbf{d}) \sum_{i=1}^{N} \int_{\mathbb{R}} s_{ki}(x_i;\mathbf{d}) f_{X_i}(x_i;\mathbf{d}) dx_i + \\
& \sum_{i=1}^{N} \sum_{\substack{\emptyset \neq u \subseteq \{1,\cdots,N\} \\ 1 \leq |u| \leq \bar{S}, \, i \in u}} \sum_{\substack{\mathbf{j}_{|u|} \in \mathbb{N}_0^{|u|}, ||\mathbf{j}_{|u|}||_\infty \leq \bar{m} \\ j_1,\cdots,j_{|u|} \neq 0}} \bar{C}_{u\mathbf{j}_{|u|}}(\mathbf{d}) \int_{\mathbb{R}^{|u|}} \psi_{u\mathbf{j}_{|u|}}(\mathbf{x}_u;\mathbf{d}) s_{ki}(x_i;\mathbf{d}) f_{\mathbf{X}_u}(\mathbf{x}_u;\mathbf{d}) d\mathbf{x}_u,
\end{aligned}
$$

$$(3.60)$$

requiring at most $\bar{S}$-dimensional integrations of at most $\bar{m}$th-order polynomials, where the terms related to $i \notin u$ vanish as per Proposition 3.1. Therefore, a significant gain in efficiency is possible in Option II for sensitivity analysis as well. The sensitivity equations further simplify for special cases, as explained in Section 3.2. Nonetheless, numerical integrations are necessary for calculating the sensitivities by either option.

3.5 Design Sensitivity Analysis of Reliability

When solving RBDO problems using gradient-based optimization algorithms, at least first-order derivatives of the failure probability with respect to each design variable are required. Two methods for the sensitivity analysis of the failure probability, named the PDD-SPA and PDD-MCS methods, are presented.

3.5.1 The PDD-SPA method

Suppose that the first-order derivative $\partial \tilde{F}_{y,PS}(\xi;\mathbf{d})/\partial d_k$ of the CDF $\tilde{F}_{y,PS}(\xi;\mathbf{d})$ of $\tilde{y}_{S,m}(\mathbf{X})$, obtained by the PDD-SPA method, with respect to a design variable d_k,

is desired. Applying the chain rule on the derivative of Equation (3.30),

$$\frac{\partial \tilde{F}_{y,PS}(\xi; \mathbf{d})}{\partial d_k} = \sum_{r=1}^{Q} \left(\frac{\partial \tilde{F}_{y,PS}}{\partial w} \frac{\partial w}{\partial \tilde{\kappa}_{S,m}^{(r)}} + \frac{\partial \tilde{F}_{y,PS}}{\partial v} \frac{\partial v}{\partial \tilde{\kappa}_{S,m}^{(r)}} \right) \frac{\partial \tilde{\kappa}_{S,m}^{(r)}}{\partial d_k} \qquad (3.61)$$

is obtained via the partial derivatives

$$\frac{\partial \tilde{F}_{y,PS}}{\partial w} = \phi(w) \left(\frac{w}{v} - \frac{1}{w^2} \right), \quad \frac{\partial \tilde{F}_{y,PS}}{\partial v} = \frac{\phi(w)}{v^2}, \qquad (3.62)$$

$$\frac{\partial \tilde{\kappa}_{S,m}^{(r)}}{\partial d_k} = \begin{cases} \dfrac{\partial \tilde{m}_{S,m}^{(1)}(\mathbf{d})}{\partial d_k} & : \quad r = 1, \\ \dfrac{\partial \tilde{m}_{S,m}^{(r)}(\mathbf{d})}{\partial d_k} - \displaystyle\sum_{p=1}^{r-1} \binom{r-1}{p-1} \left(\dfrac{\partial \tilde{\kappa}_{S,m}^{(r)}}{\partial d_k} \tilde{m}_{S,m}^{(r-p)}(\mathbf{d}) + \tilde{\kappa}_{S,m}^{(p)} \dfrac{\partial \tilde{m}_{S,m}^{(r-p)}}{\partial d_k} \right) & : \quad 2 \leq r \leq Q, \end{cases}$$

$$\qquad (3.63)$$

where the derivatives of moments, that is, $\partial \tilde{m}_{S,m}^{(r)}/\partial d_k$, $r = 1, \cdots, Q$, required to calculate the derivatives of cumulants, are obtained using score functions, as described in Section 3.4. The remaining two partial derivatives are expressed by

$$\frac{\partial w}{\partial \tilde{\kappa}_{S,m}^{(r)}} = \frac{\partial w}{\partial t_s} \frac{\partial t_s}{\partial \tilde{\kappa}_{S,m}^{(r)}} + \frac{\partial w}{\partial \tilde{K}_{y,Q,S,m}} \left[\frac{\partial \tilde{K}_{y,Q,S,m}}{\partial \tilde{\kappa}_{S,m}^{(r)}} + \frac{\partial \tilde{K}_{y,Q,S,m}}{\partial t_s} \frac{\partial t_s}{\partial \tilde{\kappa}_{S,m}^{(r)}} \right], \qquad (3.64)$$

and

$$\frac{\partial v}{\partial \tilde{\kappa}_{S,m}^{(r)}} = \frac{\partial v}{\partial t_s} \frac{\partial t_s}{\partial \tilde{\kappa}_{S,m}^{(r)}} + \frac{\partial v}{\partial \tilde{K}''_{y,Q,S,m}} \left[\frac{\partial \tilde{K}''_{y,Q,S,m}}{\partial \tilde{\kappa}_{S,m}^{(r)}} + \frac{\partial \tilde{K}''_{y,Q,S,m}}{\partial t_s} \frac{\partial t_s}{\partial \tilde{\kappa}_{S,m}^{(r)}} \right], \qquad (3.65)$$

where

$$\frac{\partial w}{\partial t_s} = \frac{\xi}{w}, \quad \frac{\partial w}{\partial \tilde{K}_{y,Q,S,m}} = -\frac{1}{w}, \quad \frac{\partial \tilde{K}_{y,Q,S,m}}{\partial t_s} = \xi, \quad \frac{\partial v}{\partial t_s} = \left[\tilde{K}''_{y,Q,S,m} \right]^{\frac{1}{2}}, \qquad (3.66)$$

$$\frac{\partial v}{\partial \tilde{K}''_{y,Q,S,m}} = \frac{t_s}{2\sqrt{\tilde{K}''_{y,Q,S,m}}}, \quad \frac{\partial t_s}{\partial \tilde{\kappa}_{S,m}^{(r)}} = -\frac{\dfrac{\partial \tilde{K}'_{y,Q,S,m}}{\partial \tilde{\kappa}_{S,m}^{(r)}}}{\dfrac{\partial \tilde{K}'_{y,Q,S,m}}{\partial t_s}}. \qquad (3.67)$$

The expressions of the partial derivatives $\partial \tilde{K}_{y,Q,S,m}/\partial \tilde{\kappa}_{S,m}^{(r)}$, $\partial \tilde{K}'_{y,Q,S,m}/\partial \tilde{\kappa}_{S,m}^{(r)}$, and $\partial \tilde{K}''_{y,Q,S,m}/\partial \tilde{\kappa}_{S,m}^{(r)}$, not explicitly presented here, can be easily derived from Equation

(3.27) once the cumulants $\tilde{\kappa}_{S,m}^{(r)}$, $r = 1, \cdots, Q$, and the saddlepoint t_s are obtained. Similar sensitivity equations were reported by Huang and Zhang [79]. However, Equation (3.61) is built on the PDD approximation of a stochastic response, as opposed to the RDD approximation used by Huang and Zhang. Furthermore, no transformations of random variables are necessary in the proposed PDD-SPA method.

Henceforth, the first-order derivative of the failure probability estimate by the PDD-SPA method is easily determined from

$$\frac{\partial \tilde{P}_{F,PS}(\mathbf{d})}{\partial d_k} = \frac{\partial \tilde{F}_{y,PS}(0; \mathbf{d})}{\partial d_k}, \tag{3.68}$$

the sensitivity of the probability distribution evaluated at $\xi = 0$. Algorithm 1 describes the procedure of the PDD-SPA method for calculating the reliability and its design sensitivity of a general stochastic problem.

Algorithm 3.1 Numerical implementation of the PDD-SPA method for CDF $\tilde{F}_{y,PS}(\xi; \mathbf{d})$ and its sensitivity $\partial \tilde{F}_{y,PS}(\xi; \mathbf{d})/\partial d_k$

Define ξ and $\mathbf{d}$
Specify S, $\bar{S}$, m, $\bar{m}$, and Q
Obtain the PDD approximation $\tilde{y}_{S,m}(\mathbf{X})$ ▷ [from Equation (3.11)]
for $r \leftarrow 1$ to Q **do**
    Calculate $\tilde{m}_{S,m}^{(r)}(\mathbf{d})$ ▷ [from Equation (3.20) for Option I, or Equation (3.22) for Option II;
                             if $r = 1$ and 2, then Equations (3.14) and (3.15) can be used]
    Calculate $\partial \tilde{m}_{S,m}^{(r)}(\mathbf{d})/\partial d_k$ ▷ [from Equation (3.59) for Option I, or Equation (3.60) for Option II;
                             if $r = 1$ and 2, then Equations (3.43) and (3.44) can be used]
end for
for $r \leftarrow 1$ to Q **do**
    Calculate $\tilde{\kappa}_{S,m}^{(r)}(\mathbf{d})$ ▷ [from Equation (3.26)]
    Calculate $\partial \tilde{\kappa}_{S,m}^{(r)}(\mathbf{d})/\partial d_k$ ▷ [from Equation (3.63)]
end for
Obtain interval (t_l, t_u) for the saddlepoint   ▷ [from Table 3.1 if $Q = 4$]
Calculate $\tilde{K}'_{y,Q,S,m}(t_l; \mathbf{d})$ and $\tilde{K}'_{y,Q,S,m}(t_u; \mathbf{d})$ ▷ [from Equation (3.27)]
if $\xi \in (\tilde{K}'_{y,Q,S,m}(t_l; \mathbf{d}), \tilde{K}'_{y,Q,S,m}(t_u; \mathbf{d}))$ **then**
    Calculate saddlepoint t_s ▷ [from Equations (3.27) and (3.29)]
    Calculate $\tilde{F}_{y,PS}(\xi; \mathbf{d})$ ▷ [from Equation (3.30)]
    Calculate $\partial \tilde{F}_{y,PS}(\xi; \mathbf{d})/\partial d_k$ ▷ [from Equations (3.61)-(3.67)]
else
    Stop   ▷ [the PDD-SPA method fails]
end if

3.5.2 The PDD-MCS method

Taking a partial derivative of the PDD-MCS estimate of the failure probability in Equation (3.32) with respect to d_k and then following the same arguments in deriving Equation (3.33) produces

$$
\begin{aligned}
\frac{\partial \tilde{P}_{F,PM}(\mathbf{d})}{\partial d_k} &:= \frac{\partial \mathbb{E}_{\mathbf{d}}\left[I_{\tilde{\Omega}_{F,S,m}}(\mathbf{X})\right]}{\partial d_k} \\
&= \mathbb{E}_{\mathbf{d}}\left[I_{\tilde{\Omega}_{F,S,m}}(\mathbf{X}) s_{d_k}^{(1)}(\mathbf{X};\mathbf{d})\right] \\
&= \lim_{L\to\infty} \frac{1}{L} \sum_{l=1}^{L} \left[I_{\tilde{\Omega}_{F,S,m}}(\mathbf{x}^{(l)}) s_{d_k}^{(1)}(\mathbf{x}^{(l)};\mathbf{d})\right],
\end{aligned}
\tag{3.69}
$$

where L is the sample size, $\mathbf{x}^{(l)}$ is the lth realization of $\mathbf{X}$, and $I_{\tilde{\Omega}_{F,S,m}}(\mathbf{x})$ is the PDD-generated indicator function, which is equal to *one* when $\mathbf{x} \in \tilde{\Omega}_{F,S,m}$ and *zero* otherwise. Again, they are easily and inexpensively determined by sampling analytical functions that describe $\tilde{y}_{S,m}$ and $s_{d_k}^{(1)}$. A similar sampling procedure can be employed to calculate the sensitivity of the PDD-MCS generated CDF $\tilde{F}_{y,PM}(\xi;\mathbf{d}) := P_{\mathbf{d}}[\tilde{y}_{S,m}(\mathbf{X}) \leq \xi]$. It is important to note that the effort required to calculate the failure probability or CDF also delivers their sensitivities, incurring no additional cost. Setting $S = 1$ or 2 in Equations (3.32) and (3.69), the univariate or bivariate approximation of the failure probability and its sensitivities are determined.

Remark 3.7. It is important to recognize that no Fourier-polynomial expansions of the derivatives of log-density functions are required or invoked in the PDD-MCS method for sensitivity analysis of failure probability. This is in contrast to the sensitivity analysis of the first two moments, where such Fourier-polynomial expansions aid in generating analytical expressions of the sensitivities. No analytical expressions are possible in the PDD-MCS method for sensitivity analysis of reliability or

probability distribution of a general stochastic response.

Remark 3.8. The score function method has the nice property that it requires differentiating only the underlying PDF $f_{\mathbf{X}}(\mathbf{x}; \mathbf{d})$. The resulting score functions can be easily and, in most cases, analytically determined. If the performance function is not differentiable or discontinuous − for example, the indicator function that comes from reliability analysis − the proposed method still allows evaluation of the sensitivity if the density function is differentiable. In reality, the density function is often smoother than the performance function, and therefore the proposed sensitivity methods will be able to calculate sensitivities for a wide variety of complex mechanical systems.

3.6   Expansion Coefficients

The determination of PDD expansion coefficients $y_{\emptyset}(\mathbf{d})$ and $C_{u\mathbf{j}_{|u|}}(\mathbf{d})$, where $\emptyset \neq u \subseteq \{1, \cdots, N\}$ and $\mathbf{j}_{|u|} \in \mathbb{N}_0^{|u|}|; |\mathbf{j}_{|u|}||_{\infty} \leq m; j_1, \cdots, j_{|u|} \neq 0$, is vitally important for evaluating the statistical moments and probabilistic characteristics, including their design sensitivities, of stochastic responses. The coefficients, defined in Equations (2.7) and (3.7), involve various N-dimensional integrals over $\mathbb{R}^N$. For large N, a full numerical integration employing an N-dimensional tensor product of a univariate quadrature formula is computationally prohibitive and is, therefore, ruled out. The author proposes that the dimension-reduction integration scheme, developed by Xu and Rahman [22], followed by numerical quadrature, be used to estimate the coefficients accurately and efficiently.

3.6.1 Dimension-Reduction integration

Let $\mathbf{c} = (c_1, \cdots, c_N)^T \in \mathbb{R}^N$, which is commonly adopted as the mean of $\mathbf{X}$, be a reference point, and $y(\mathbf{x}_v, \mathbf{c}_{-v})$ represent an $|v|$-variate RDD component function of $y(\mathbf{x})$, where $v \subseteq \{1, \cdots, N\}$ [64, 83]. Given a positive integer $S \leq R \leq N$, when $y(\mathbf{x})$ in Equations (2.7) and (3.7) is replaced with its R-variate RDD approximation, the coefficients $y_\emptyset(\mathbf{d})$ and $C_{u\mathbf{j}_{|u|}}(\mathbf{d})$ are estimated from [22]

$$y_\emptyset(\mathbf{d}) \cong \sum_{i=0}^{R} (-1)^i \binom{N-R+i-1}{i} \sum_{\substack{v \subseteq \{1,\cdots,N\} \\ |v|=R-i}} \int_{\mathbb{R}^{|v|}} y(\mathbf{x}_v, \mathbf{c}_{-v}) f_{\mathbf{X}_v}(\mathbf{x}_v; \mathbf{d}) d\mathbf{x}_v \quad (3.70)$$

and

$$C_{u\mathbf{j}_{|u|}}(\mathbf{d}) \cong \sum_{i=0}^{R} (-1)^i \binom{N-R+i-1}{i} \sum_{\substack{v \subseteq \{1,\cdots,N\} \\ |v|=R-i, u \subseteq v}} \int_{\mathbb{R}^{|v|}} y(\mathbf{x}_v, \mathbf{c}_{-v}) \psi_{u\mathbf{j}_{|u|}}(\mathbf{x}_u) f_{\mathbf{X}_v}(\mathbf{x}_v; \mathbf{d}) d\mathbf{x}_v,$$
$$(3.71)$$

respectively, requiring evaluation of at most R-dimensional integrals. The reduced integration facilitates calculation of the coefficients approaching their exact values as $R \to N$, and is significantly more efficient than performing one N-dimensional integration, particularly when $R \ll N$. Hence, the computational effort is significantly lowered using the dimension-reduction integration. For instance, when $R = 1$ or 2, Equations (3.70) and (3.71) involve one-, or at most, two-dimensional integrations, respectively.

For a general function y, numerical integrations are still required for performing various $|v|$-dimensional integrals over $\mathbb{R}^{|v|}$, $0 \leq |v| \leq R$, in Equations (3.70) and (3.71). When $R > 1$, multivariate numerical integrations are conducted by constructing a tensor product of underlying univariate quadrature rules. For a given $v \subseteq \{1, \cdots, N\}$,

$1 < |v| \leq R$, let $v = \{i_1, \cdots i_{|v|}\}$, where $1 \leq i_1 < \cdots < i_{|v|} \leq N$. Denote by $\{x_{i_p}^{(1)}, \cdots, x_{i_p}^{(n)}\} \subset \mathbb{R}$ a set of integration points of x_{i_p} and by $\{w_{i_p}^{(1)}, \cdots, w_{i_p}^{(n)}\}$ the associated weights generated from a chosen univariate quadrature rule and a positive integer $n \in \mathbb{N}$. Denote by $P^{(n)} = \times_{p=1}^{p=|v|}\{x_{i_p}^{(1)}, \cdots, x_{i_p}^{(n)}\}$ a rectangular grid consisting of all integration points generated by the variables indexed by the elements of v. Then the coefficients using dimension-reduction integration and numerical quadrature are approximated by

$$y_\emptyset(\mathbf{d}) \cong \sum_{i=0}^{R}(-1)^i \binom{N-R+i-1}{i} \sum_{\substack{v \subseteq \{1,\cdots,N\} \\ |v|=R-i}} \sum_{\mathbf{k}_{|v|} \in P^{(n)}} w^{(\mathbf{k}_{|v|})} y(\mathbf{x}_v^{(\mathbf{k}_{|v|})}, \mathbf{c}_{-v}) \quad (3.72)$$

and

$$C_{u\mathbf{j}_{|u|}}(\mathbf{d}) \cong \sum_{i=0}^{R}(-1)^i \binom{N-R+i-1}{i} \sum_{\substack{v \subseteq \{1,\cdots,N\} \\ |v|=R-i, u \subseteq v}} \sum_{\mathbf{k}_{|v|} \in P^{(n)}} w^{(\mathbf{k}_{|v|})} y(\mathbf{x}_v^{(\mathbf{k}_{|v|})}, \mathbf{c}_{-v}) \psi_{u\mathbf{j}_{|u|}}(\mathbf{x}_u^{(\mathbf{k}_{|u|})}),$$
$$(3.73)$$

where $\mathbf{x}_v^{(\mathbf{k}_{|v|})} = \{x_{i_1}^{(k_1)}, \cdots, x_{i_{|v|}}^{(k_{|v|})}\}$ and $w^{(\mathbf{k}_{|v|})} = \prod_{p=1}^{p=|v|} w_{i_p}^{(k_p)}$ is the product of integration weights generated by the variables indexed by the elements of v. Similarly, the coefficients $z_\emptyset(\mathbf{d})$ and $\bar{C}_{u\mathbf{j}_{|u|}}(\mathbf{d})$ of an $\bar{S}$-variate, $\bar{m}$th-order PDD approximation of $\tilde{y}_{S,m}^r(\mathbf{X})$, required in Option II for obtaining higher-order moments and their sensitivities, can also be estimated from the dimension-reduction integration. For independent coordinates of $\mathbf{X}$, as assumed here, a univariate Gauss quadrature rule is commonly used, where the integration points and associated weights depend on the probability distribution of X_i. They are readily available, for example, the Gauss-Hermite or Gauss-Legendre quadrature rule, when X_i follows Gaussian or uniform distribution. For an arbitrary probability distribution of X_i, the Stieltjes procedure can be em-

ployed to generate the measure-consistent Gauss quadrature formulae [97, 98]. An n-point Gauss quadrature rule exactly integrates a polynomial with a total degree of at most $2n - 1$.

3.6.2 Computational expense

The S-variate, mth-order PDD approximation requires evaluations of $\sum_{k=0}^{k=S} \binom{N}{k} m^k$ expansion coefficients, including $y_{\emptyset}(\mathbf{d})$. If these coefficients are estimated by dimension-reduction integration with $R = S < N$ and, therefore, involve at most an S-dimensional tensor product of an n-point univariate quadrature rule depending on m, then the total cost for the S-variate, mth-order approximation entails a maximum of $\sum_{k=0}^{k=S} \binom{N}{k} n^k(m)$ function evaluations. If the integration points include a common point in each coordinate $-$ a special case of symmetric input probability density functions and odd values of n $-$ the number of function evaluations reduces to $\sum_{k=0}^{k=S} \binom{N}{k}(n(m)-1)^k$. Nonetheless, the computational complexity of the S-variate PDD approximation is an Sth-order polynomial with respect to the number of random variables or integration points. Therefore, PDD with dimension-reduction integration of the expansion coefficients alleviates the curse of dimensionality to an extent determined by S.

3.7 Numerical Examples

Five numerical examples, comprising various mathematical functions and solid-mechanics problems, are illustrated to examine the accuracy, efficiency, and convergence properties of the PDD methods developed for calculating the first-order sen-

sitivities of statistical moments, probability distributions, and reliability. The PDD expansion coefficients were estimated by dimension-reduction integration with the mean input as the reference point, $R = S$, and $n = m + 1$, where S and m vary depending on the problem. In all examples, orthonormal polynomials and associated Gauss quadrature rules consistent with the probability distributions of input variables, including classical forms, if they exist, were employed. The first three examples entail independent and identical random variables, where d_k is a distribution parameter of all random variables, whereas the last three examples contain merely independent random variables, where d_k is a distribution parameter of a single random variable. The sample size for the embedded simulation of the PDD-MCS method is 10^6 in Examples 2 and 3, and 10^7 in Example 5. Whenever possible, the exact sensitivities were applied to verify the proposed methods, as in Examples 1 and 3. However, in Examples 2, 4, and 5, which do not support exact solutions, the benchmark results were generated from at least one of two crude MCS-based approaches: (1) crude MCS in conjunction with score functions (crude MCS/SF), which requires sampling of both the original function y and the score function $s_{d_k}^{(1)}$; and (2) crude MCS in tandem with one-percent perturbation of finite-difference analysis (crude MCS/FD), which entails sampling of the original function y only. The sample size for either version of the crude MCS is 10^6 in Examples 2, 3, and 4, and 10^7 in Example 5. The derivatives of log-density functions associated with the five types of random variables used in all examples are described in Table 3.2.

Table 3.2: Derivatives of log-density functions for various probability distributions

Distribution	$\mathbf{d}$	$f_X(x;\mathbf{d})$	$\frac{\partial \ln f_X(x;\mathbf{d})}{\partial d_1}$	$\frac{\partial \ln f_X(x;\mathbf{d})}{\partial d_2}$
Exponential	$\{\lambda\}^T$	$\lambda \exp(-\lambda x);$ $0 \le x \le +\infty$	$\frac{1}{\lambda} - x$	-
Gaussian	$\{\mu,\sigma\}^T$	$\frac{1}{\sqrt{2\pi}\sigma}\exp\left[-\frac{1}{2}\left(\frac{x-\mu}{\sigma}\right)^2\right];$ $-\infty \le x \le +\infty$	$\frac{1}{\sigma}\left(\frac{x-\mu}{\sigma}\right)$	$\frac{1}{\sigma}\left[\left(\frac{x-\mu}{\sigma}\right)^2 - 1\right]$
Lognormal[(a)]	$\{\mu,\sigma\}^T$	$\frac{1}{\sqrt{2\pi}x\tilde{\sigma}}\exp\left[-\frac{1}{2}\left(\frac{\ln x - \tilde{\mu}}{\tilde{\sigma}}\right)^2\right];$ $0 < x \le +\infty$	$-\frac{1}{\tilde{\sigma}}\frac{\partial\tilde{\sigma}}{\partial\mu} + \frac{1}{\tilde{\sigma}^2}\left(\frac{\ln x - \tilde{\mu}}{\tilde{\sigma}}\right)\times$ $\left[\tilde{\sigma}\frac{\partial\tilde{\mu}}{\partial\mu} + (\ln x - \tilde{\mu})\frac{\partial\tilde{\sigma}}{\partial\mu}\right]$	$-\frac{1}{\tilde{\sigma}}\frac{\partial\tilde{\sigma}}{\partial\sigma} + \frac{1}{\tilde{\sigma}^2}\left(\frac{\ln x - \tilde{\mu}}{\tilde{\sigma}}\right)\times$ $\left[\tilde{\sigma}\frac{\partial\tilde{\mu}}{\partial\sigma} + (\ln x - \tilde{\mu})\frac{\partial\tilde{\sigma}}{\partial\sigma}\right]$
Truncated[(b)] Gaussian	$\{\mu,\sigma\}^T$	$\frac{1}{\Phi(D)-\Phi(-D)}\frac{1}{\sqrt{2\pi}\sigma}\times$ $\exp\left[-\frac{1}{2}\left(\frac{x-\mu}{\sigma}\right)^2\right];$ $\mu - D \le x \le \mu + D$	$\frac{1}{\Phi(D)-\Phi(-D)}\frac{1}{\sigma}\left(\frac{x-\mu}{\sigma}\right)$	$\frac{1}{\Phi(D)-\Phi(-D)}\frac{1}{\sigma}\left[\left(\frac{x-\mu}{\sigma}\right)^2 - 1\right]$
Weibull	$\{\lambda,k\}^T$	$\frac{k}{\lambda}\left(\frac{x}{\lambda}\right)^{k-1}\exp\left[-\left(\frac{x}{\lambda}\right)^k\right];$ $0 \le x \le +\infty$	$\frac{k}{\lambda}\left[\left(\frac{x}{\lambda}\right)^k - 1\right]$	$\frac{1}{k} + (\ln x - \ln\lambda)\times$ $\left[1 - \left(\frac{x}{\lambda}\right)^k\right]$

[(a)] $\tilde{\sigma}^2 = \ln\left(1 + \sigma^2/\mu^2\right)$ and $\tilde{\mu} = \ln\mu - \tilde{\sigma}^2/2$. The partial derivatives of $\tilde{\mu}$ and $\tilde{\sigma}$ with respect to μ or σ can be easily obtained, so they are not reported here.
[(b)] $\Phi(\cdot)$ is the cumulative distribution function of a standard Gaussian variable; $D > 0$ is a constant.

3.7.1   Example 1: a trigonometric-polynomial function

Consider the function

$$y(\mathbf{X}) = \mathbf{a}_1^T\mathbf{X} + \mathbf{a}_2^T\sin\mathbf{X} + \mathbf{a}_3^T\cos\mathbf{X} + \mathbf{X}^T\mathbf{M}\mathbf{X}, \tag{3.74}$$

introduced by Oakley and O'Hagan [105], where $\mathbf{X} = (X_1,\cdots,X_{15})^T \in \mathbb{R}^{15}$ is a 15-dimensional Gaussian input vector with mean vector $\mathbb{E}[\mathbf{X}] = (\mu,\cdots,\mu)^T \in \mathbb{R}^{15}$ and covariance matrix $\mathbb{E}[\mathbf{X}\mathbf{X}^T] = \sigma^2\text{diag}[1,\cdots,1] =: \sigma^2\mathbf{I} \in \mathbb{R}^{15\times15}$; $\mathbf{d} = (\mu,\sigma)^T$; $\sin\mathbf{X} := (\sin X_1,\cdots,\sin X_{15})^T \in \mathbb{R}^{15}$ and $\cos\mathbf{X} := (\cos X_1,\cdots,\cos X_{15})^T \in \mathbb{R}^{15}$ are compact notations for 15-dimensional vectors of sine and cosine functions, respectively; and $\mathbf{a}_i \in \mathbb{R}^{15}$, $i = 1,2,3$, and $\mathbf{M} \in \mathbb{R}^{15\times15}$ are coefficient vectors and matrix, respectively,

obtained from Oakley and O'Hagan's paper [105]. The objective of this example is to evaluate the accuracy of the proposed PDD approximation in calculating the sensitivities of the first two moments, $m^{(1)}(\mathbf{d}) := \mathbb{E}_{\mathbf{d}}[y(\mathbf{X})]$ and $m^{(2)}(\mathbf{d}) := \mathbb{E}_{\mathbf{d}}[y^2(\mathbf{X})]$, with respect to the mean μ and standard deviation σ of X_i at $\mathbf{d}_0 = (0, 1)^T$.

Figures 3.1(a) through 3.1(d) present the plots of the relative errors in the approximate sensitivities, $\partial \tilde{m}_{S,m}^{(1)}(\mathbf{d}_0)/\partial \mu$, $\partial \tilde{m}_{S,m}^{(1)}(\mathbf{d}_0)/\partial \sigma$, $\partial \tilde{m}_{S,m}^{(2)}(\mathbf{d}_0)/\partial \mu$, and $\partial \tilde{m}_{S,m}^{(2)}(\mathbf{d}_0)/\partial \sigma$, obtained by the proposed univariate and bivariate PDD methods (Equations (3.54) and (3.55)) for increasing orders of orthonormal polynomials, that is, when the PDD truncation parameters $S = 1$ and 2, $1 \le m \le 8$, and $m' = 2$. The measure-consistent Hermite polynomials and associated Gauss-Hermite quadrature rule were used. The relative error is defined as the ratio of the absolute difference between the exact and approximate sensitivities, divided by the exact sensitivity, where the exact sensitivity can be easily calculated, as shown in the appendix, for the function y in Equation (3.74). Although y is a bivariate function of $\mathbf{X}$, the sensitivities of the first moment by the univariate and bivariate PDD approximations are identical for any m. This is because the expectations of $\tilde{y}_{1,m}(\mathbf{X})$ and $\tilde{y}_{2,m}(\mathbf{X})$, when $\mathbf{X}$ comprises independent variables, are the same function of $\mathbf{d}$. In this case, the errors committed by both PDD approximations drop at the same rate, as depicted in Figures 3.1(a) and 3.1(b), resulting in rapid convergence of the sensitivities of the first moment. However, the same condition does not hold true for the sensitivities of the second moment because the univariate and bivariate PDD approximations yield distinct sets of results. Furthermore, the errors in the sensitivities of the second moment by the

univariate PDD approximation do not decay strictly monotonically, leveling off when m crosses a threshold, as displayed in Figures 3.1(c) and 3.1(d). In contrast, the errors in the sensitivities of the second moment by the bivariate PDD approximation attenuate continuously with respect to m, demonstrating rapid convergence of the proposed solutions. The numerical results presented are consistent with the mean-square convergence of the sensitivities described by Proposition 3.5.
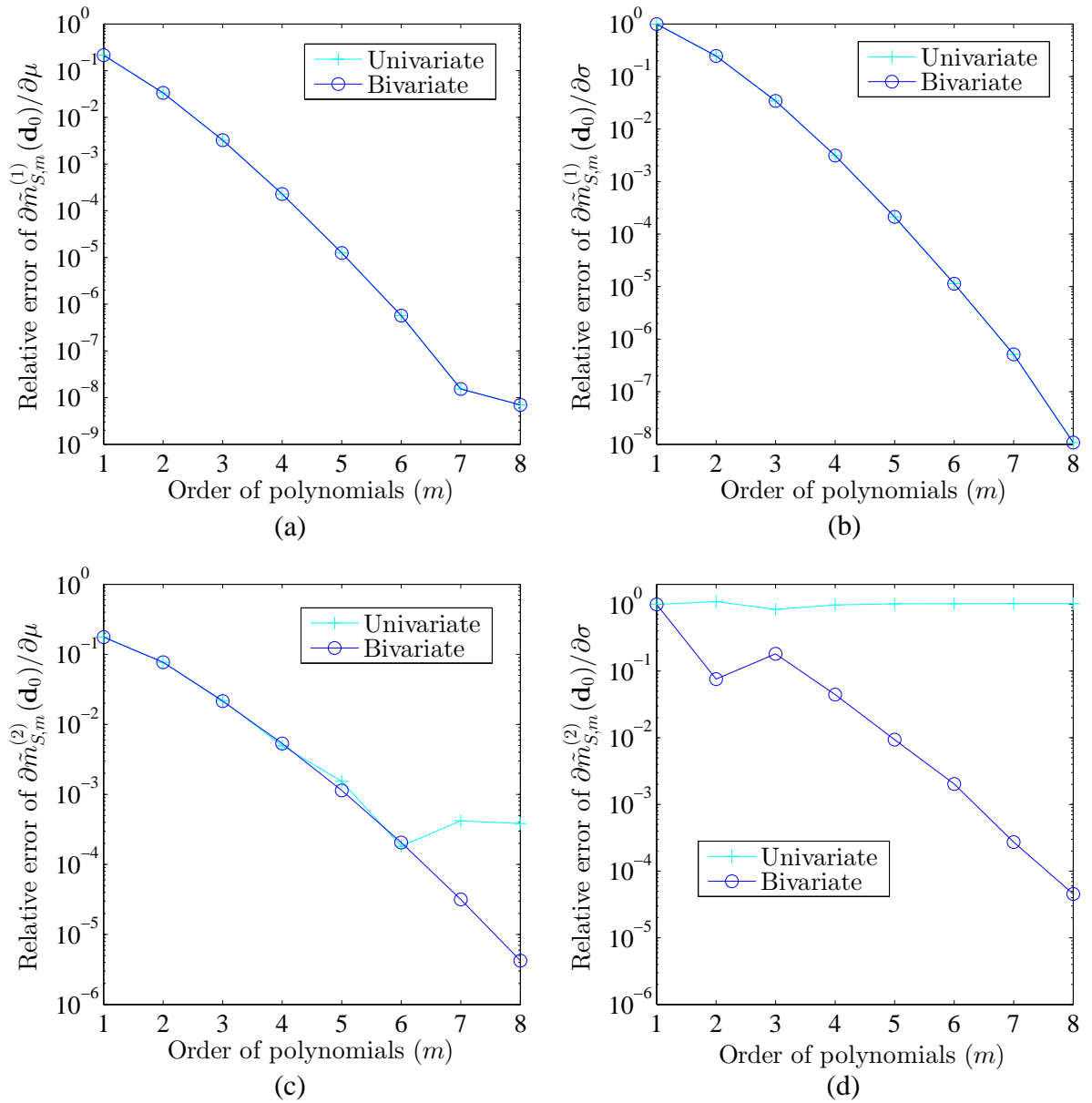
Figure 3.1: Relative errors in calculating the sensitivities of the first two moments of y due to various PDD truncations; (a) $\partial \tilde{m}_{S,m}^{(1)}(\mathbf{d}_0)/\partial \mu$; (b)$\partial \tilde{m}_{S,m}^{(1)}(\mathbf{d}_0)/\partial \sigma$; (c) $\partial \tilde{m}_{S,m}^{(2)}(\mathbf{d}_0)/\partial \mu$; (d) $\partial \tilde{m}_{S,m}^{(2)}(\mathbf{d}_0)/\partial \sigma$ (Example 1)

3.7.2 Example 2: a cubic polynomial function

The second example is concerned with calculating the sensitivities of the probability distribution of

$$y(\mathbf{X}) = 500 - (X_1 + X_2)^3 + X_1 - X_2 - X_3 + X_1 X_2 X_3 - X_4, \qquad (3.75)$$

where X_i, $i = 1, 2, 3, 4$, are four independent and identically distributed random variables. The sensitivities were calculated by the proposed PDD-MCS method using two approaches: (1) a direct approach employing measure-consistent orthonormal polynomials as bases and corresponding Gauss type quadrature rules for calculating the PDD expansion coefficients, and (2) an indirect approach transforming original random variables into Gaussian random variables, followed by Hermite orthonormal polynomials as bases and the Gauss-Hermite quadrature rule for calculating the expansion coefficients. Since Equation (3.75) represents a third-order polynomial, the measure-consistent orthonormal polynomials with the largest order $m = 3$ should exactly reproduce y. In which case, the highest order of integrands for calculating the PDD expansion coefficients is six; therefore, a four-point ($n = 4$) measure-consistent Gauss quadrature should provide exact values of the coefficients. In the direct approach, univariate ($S = 1$), bivariate ($S = 2$), and trivariate ($S = 3$) PDD approximations were applied, where the expansion coefficients were calculated using $R = S$, $m = 3$, and $n = 4$ in Equations (3.72) and (3.73). Therefore, the only source of error in a truncated PDD is the selection of S. In the indirect approach, the transformation of y, if the input variables follow non-Gaussian probability distributions, leads to non-polynomials in the space of Gaussian variables; therefore, approximation in a

truncated PDD occurs not only due to S, but also due to m. Hence several values of $3 \leq m \leq 6$ were employed for mappings into Gaussian variables. The coefficients in the indirect approach were calculated by the n-point Gauss-Hermite quadrature rule, where $n = m + 1$.

A principal objective of this example is to gain insights on the choice of orthonormal polynomials for solving this problem by PDD approximations. Two distinct cases, depending on the probability distribution of input variables, were studied.

3.7.2.1 Case 1: Exponential Distributions

For exponential distributions of input random variables, the PDF

$$f_{X_i}(x_i; \lambda) = \begin{cases} \lambda \exp(-\lambda x_i) & : \quad x_i \geq 0, \\ 0 & : \quad x_i < 0, \end{cases} \qquad (3.76)$$

where $\lambda > 0$ is the sole distribution parameter, $\mathbf{d} = \lambda \in \mathbb{R}$, and $\mathbf{d}_0 = 1$.

Figure 3.2(a) presents the sensitivities of the probability distribution of $y(\mathbf{X})$ with respect to λ calculated at $\mathbf{d}_0$ for different values of ξ by the direct approach. It contains four plots: one obtained from crude MCS/SF (10^6 samples) and the remaining three generated from univariate ($S = 1$), bivariate ($S = 2$), and trivariate ($S = 3$) PDD-MCS methods. For the PDD-MCS methods, the measure-consistent Laguerre polynomials and associated Gauss-Laguerre quadrature rule were used. The sensitivity of distributions, all obtained for $m = 3$, converge rapidly with respect to S. Compared with crude MCS/SF, the univariate PDD-MCS method is less accurate than others. This is due to the absence of the cooperative effects of random variables in the univariate approximation. The bivariate PDD-MCS solution, which captures

cooperative effects of any two variables, is remarkably close to the crude Monte Carlo results. The results from the trivariate decomposition and crude MCS/SF are coincident, as $\tilde{y}_{3,3}(\mathbf{X})$ is identical to $y(\mathbf{X})$, which itself is a trivariate function.

Using the indirect approach, Figures 3.2(b), 3.2(c), and 3.2(d) depict the sensitivities of the distribution of $y(\mathbf{X})$ by the univariate, bivariate, and trivariate PDD-MCS methods for several values of m, calculated when the original variables are transformed into standard Gaussian variables. The sensitivities obtained by all three decomposition methods from the indirect approach converge to the respective solutions from the direct approach when m and n increase. However, the lowest order of Hermite polynomials required to converge in the indirect approach is six, a number twice that employed in the direct approach employing Laguerre polynomials. This is due to higher nonlinearity of the mapped y induced by the transformation from exponential to Gaussian variables. Clearly, the direct approach employing Laguerre polynomials and the Gauss-Laguerre quadrature rule is the preferred choice for calculating sensitivities of the probability distribution by the PDD-MCS method.
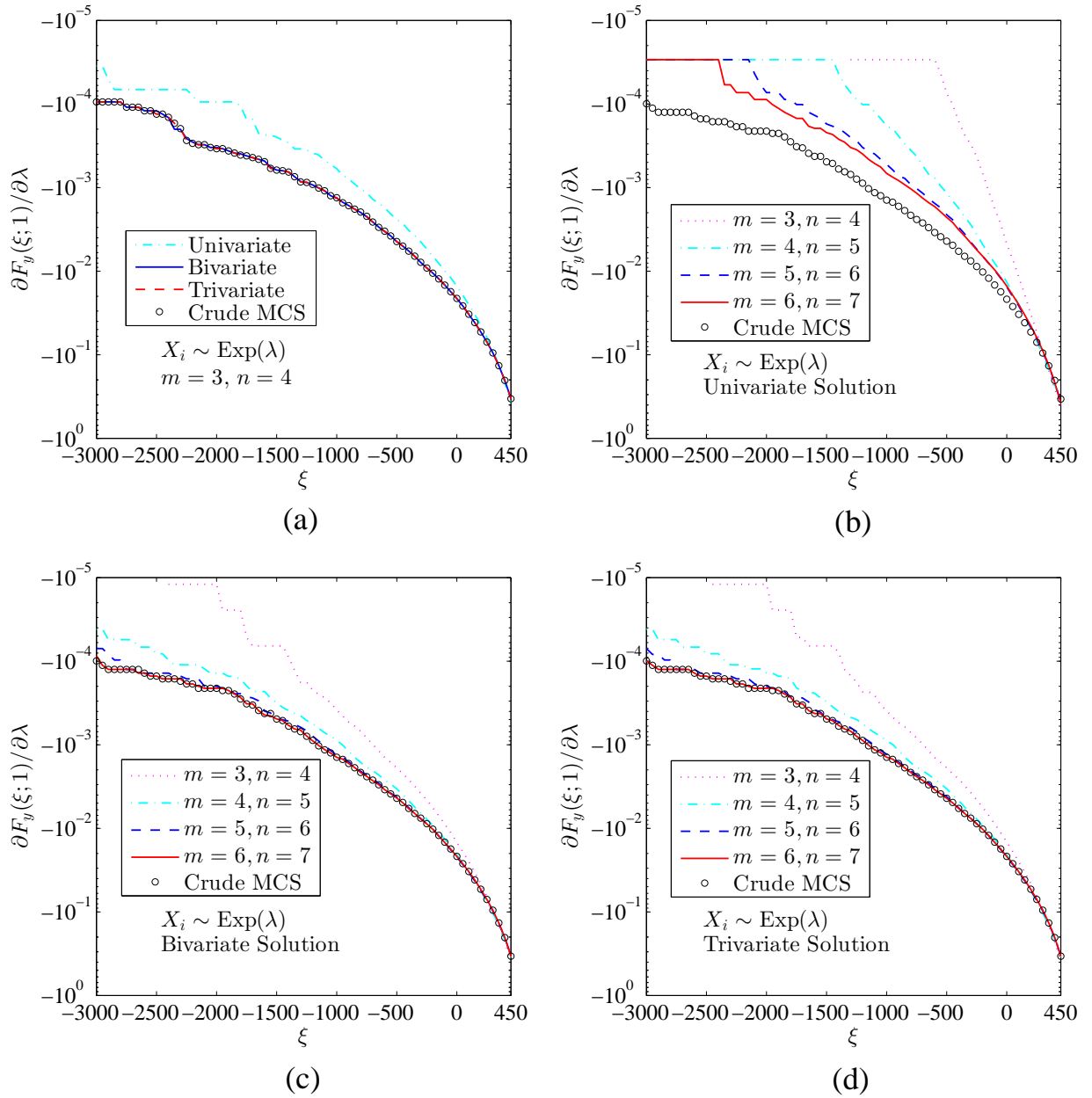
Figure 3.2: Sensitivities of the probability distribution of y with respect to λ for exponential distributions of input variables; (a) direct approach; (b) indirect approach-univariate; (c) indirect approach-bivariate; (d) indirect approach-trivariate (Example 2)

3.7.2.2 Case 2: Weibull Distributions

For Weibull distributions of input random variables, the PDF

$$f_{X_i}(x_i; \lambda, k) = \begin{cases} \dfrac{k}{\lambda}\left(\dfrac{x_i}{\lambda}\right)^{k-1} \exp\left[-\left(\dfrac{x_i}{\lambda}\right)^k\right] & : \quad x_i \geq 0, \\ 0 & : \quad x_i < 0, \end{cases} \quad (3.77)$$

where $\lambda > 0$ and $k > 0$ are scale and shape distribution parameters, respectively, $\mathbf{d} = (\lambda, k)^T \in \mathbb{R}^2$, and $\mathbf{d}_0 = (1, 0.5)^T$.

The sensitivities of the probability distribution of $y(\mathbf{X})$ with respect to λ and k, calculated by the direct approach, at $\mathbf{d}_0$ is exhibited in Figures 3.3(a) and 3.4(a), respectively. Again, four plots, comprising the solutions from crude MCS/SF (10^6 samples) and three PDD-MCS methods using the direct approach, are illustrated. Since classical orthonormal polynomials do not exist for Weibull probability measures, the Stieltjes procedure was employed to numerically determine the measure-consistent orthonormal polynomials and corresponding Gauss quadrature formula [97]. Similar to Case 1, both sensitivities of the distribution by the PDD-MCS method in Figures 3.3(a) and 3.4(a), all obtained for $m = 3$, converge rapidly to crude MCS solutions with respect to S. However, the sensitivities of the distribution by all three PDD-MCS approximations, when calculated using the indirect approach and shown in Figures 3.3(b) through 3.3(d) and Figures 3.4(b) through 3.4(d), fail to get closer even when the order of Hermite polynomials is twice that employed in the direct approach. The lack of convergence is attributed to a significantly higher nonlinearity of the transformation from Weibull to Gaussian variables than that from exponential to Gaussian variables. Therefore, a direct approach entailing measure-consistent orthogonal polynomials and associated Gauss quadrature rule, even in the absence of

classical polynomials, is desirable for generating both accurate and efficient solutions by the PDD-MCS method.
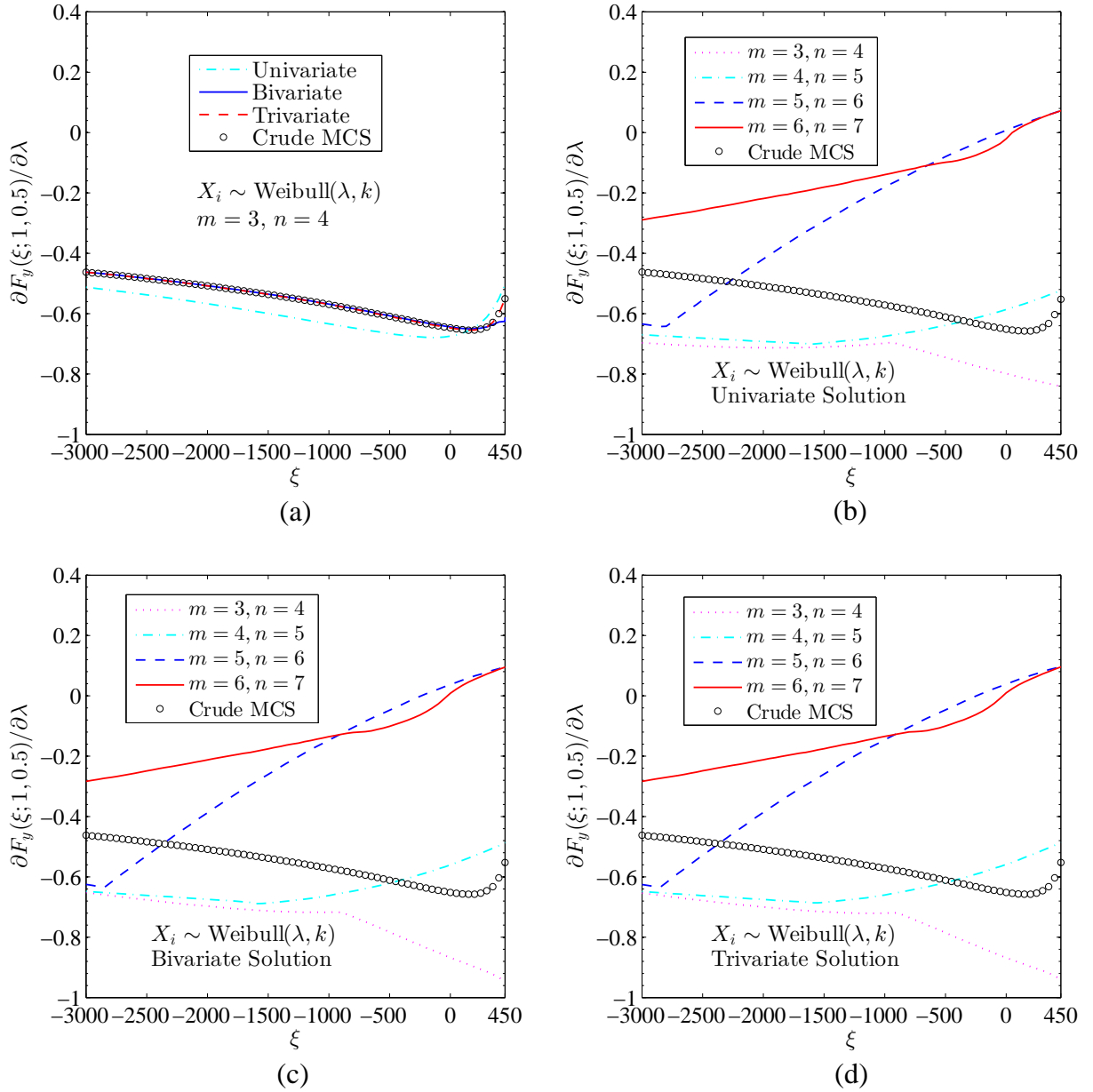
Figure 3.3: Sensitivities of the probability distribution of y with respect to λ for Weibull distributions of input variables; (a) direct approach; (b) indirect approach-univariate; (c) indirect approach-bivariate; (d) indirect approach-trivariate (Example 2)
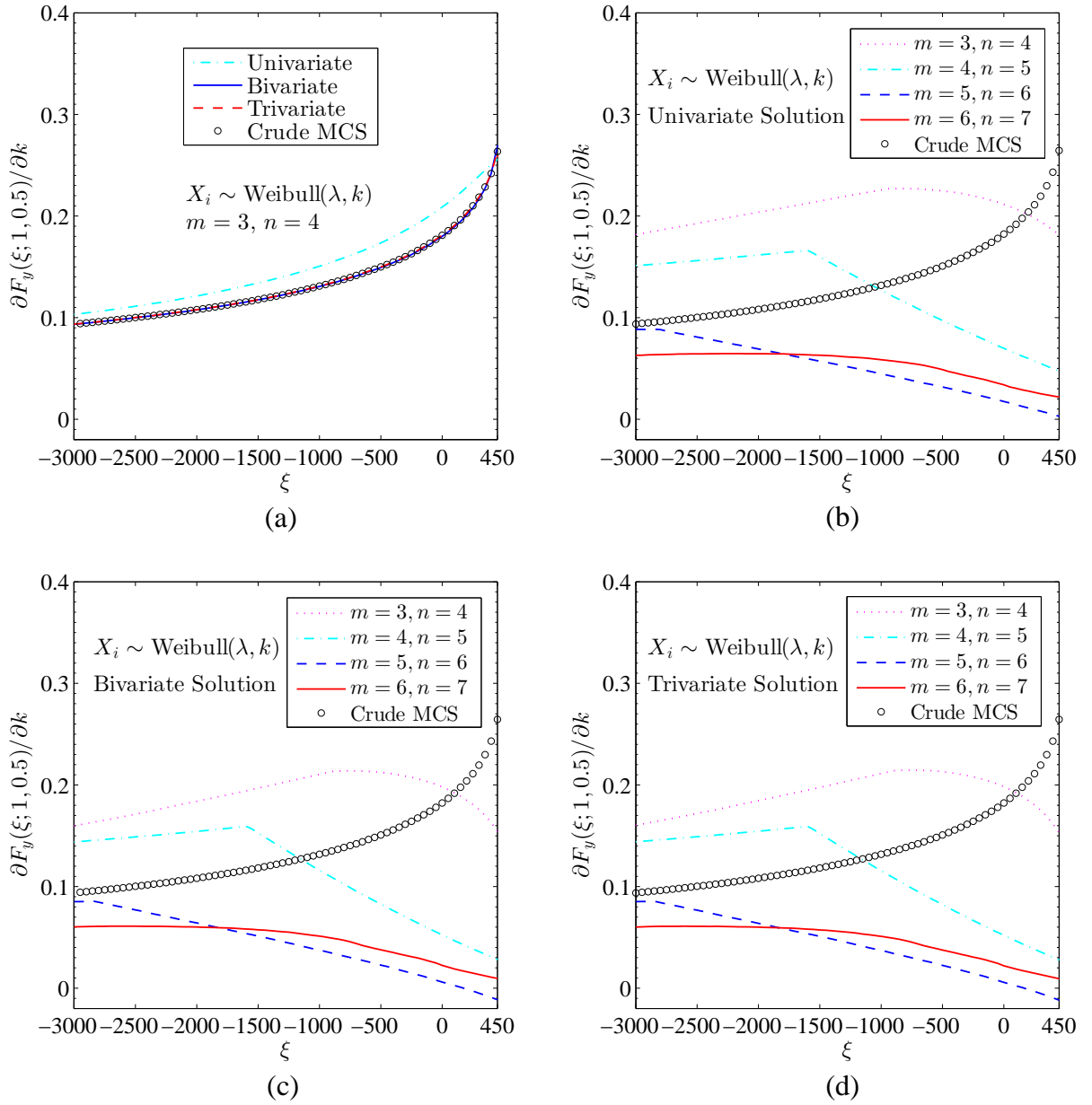
Figure 3.4: Sensitivities of the probability distribution of y with respect to k for Weibull distributions of input variables; (a) direct approach; (b) indirect approach-univariate; (c) indirect approach-bivariate; (d) indirect approach-trivariate (Example 2)

3.7.3 Example 3: a function of Gaussian variables

Consider a component reliability problem with the performance function

$$y(\mathbf{X}) = \frac{1}{1000 + \sum\limits_{i=1}^{N} X_i} - \frac{1}{1000 + 3\sqrt{N}}, \tag{3.78}$$

where $\mathbf{X} \sim N(\boldsymbol{\mu}, \boldsymbol{\Sigma})$ is an N-dimensional Gaussian random vector with mean vector $\boldsymbol{\mu} = (\mu, \cdots, \mu)^T$ and covariance matrix $\boldsymbol{\Sigma} = \sigma^2 \mathrm{diag}[1, \cdots, 1] =: \sigma^2 \mathbf{I}$, and $\mathbf{d} = (\mu, \sigma)^T$. The objective of this example is to evaluate the accuracy of the proposed PDD-SPA and PDD-MCS methods in calculating the failure probability $P_F(\mathbf{d}) := P_{\mathbf{d}}[y(\mathbf{X}) < 0]$ and its sensitivities $\partial P_F(\mathbf{d}_0) / \partial \mu$ and $\partial P_F(\mathbf{d}_0) / \partial \sigma$ at $\mathbf{d}_0 = (0, 1)^T$ for two problem sizes or dimensions: $N = 10$ and $N = 100$. The exact solutions for a general N-dimensional problem are

$$P_F(\mathbf{d}) = \Phi(-\beta), \frac{\partial P_F(\mathbf{d})}{\partial \mu} = \frac{\phi(-\beta)\sqrt{N}}{\sigma}, \frac{\partial P_F(\mathbf{d})}{\partial \sigma} = \frac{\phi(-\beta)(3 - \mu\sqrt{N})}{\sigma^2}, \tag{3.79}$$

where $\beta = (3 - \mu\sqrt{N})/\sigma$, provided that $0 < \sigma^2 < \infty$.

Since y in Equation (3.78) is a non-polynomial function, the univariate ($S = 1$) or bivariate ($S = 2$) truncation of PDD for a finite value of m, regardless how large, provides only an approximation. Nonetheless, using only $m = 3$ and $n = 4$, the univariate and bivariate estimates of the failure probability and its two sensitivities by the PDD-SPA and PDD-MCS methods for $N = 10$ are listed in Table 3.3. The measure-consistent Hermite polynomials and associated Gauss-Hermite quadrature rule were used in both methods. The results of the PDD-SPA method are further broken down according to Options I (Equation (3.59)) and II (Equation (3.60)) for calculating all moments of order up to four to approximate the CGF of $y(\mathbf{X})$, as

explained in Algorithm 3.1. Option I requires at most eight-dimensional integrations in the bivariate PDD-SPA method for calculating the moments of $y(\mathbf{X})$, whereas Option II entails at most two-dimensional integrations for the values of $\bar{S} = 2$ and $\bar{m} = 6$ selected. However, the differences between the two respective estimates of the failure probability and its sensitivities by these options, in conjunction with either the univariate or the bivariate PDD approximation, are negligibly small. Therefore, Option II is not only accurate, but also facilitates efficient solutions by the PDD-SPA method, at least in this example. Compared with the results of crude MCS/SF (10^6 samples) or the exact solution, also listed in Table 3.3, both univariate and bivariate versions of the PDD-SPA method, regardless of the option, are satisfactory. The same trend holds for the univariate and bivariate PDD-MCS methods. No meaningful difference is found between the respective accuracies of the PDD-SPA and PDD-MCS solutions for a given truncation S. Indeed, the agreement between the bivariate solutions from the PDD-SPA or PDD-MCS method and the benchmark results is excellent.

Table 3.3: Component failure probability and sensitivities at $\mathbf{d}_0 = (0, 1)^T$ for $N = 10$ (Example 3)

	PDD-SPA (Univariate, Option I)	PDD-SPA (Univariate, Option II)	PDD-SPA (Bivariate, Option I)	PDD-SPA (Bivariate, Option II)	PDD-MCS (Univariate)	PDD-MCS (Bivariate)	Crude MCS/SF	Exact
$P_F(\mathbf{d}_0)$ ($\times 10^{-3}$)	1.349	1.453	1.349	1.347	1.510	1.397	1.397	1.350
$\partial P_F(\mathbf{d}_0)/\partial\mu$ ($\times 10^{-2}$)	1.401	1.529	1.401	1.550	1.553	1.447	1.447	1.401
$\partial P_F(\mathbf{d}_0)/\partial\sigma$ ($\times 10^{-2}$)	1.330	1.409	1.330	1.326	1.472	1.371	1.371	1.330
No. of function eval.	41	41	761	761	41	761	10^6	-

For high-dimensional problems, such as $N = 100$, Table 3.4 summarizes the estimates of the failure probability and its sensitivities by the PDD-SPA and PDD-MCS methods using $m = 3$. Due to the higher dimension, the PDD-SPA method with Option I requires numerous eight-dimensional integrations for calculating moments of $y(\mathbf{X})$ and is no longer practical. Therefore, the PDD-SPA method with Option II requiring only two-dimensional ($\bar{S} = 2$, $\bar{m} = 6$) integrations was used for $N = 100$. Again both univariate and bivariate approximations were invoked for the PDD-SPA and PDD-MCS methods. Compared with the benchmark results of crude MCS/SF (10^6 samples) or the exact solution, listed in Table 3.4, the bivariate PDD-SPA method and the bivariate PDD-MCS method provide highly accurate solutions for this high-dimensional reliability problem.

Table 3.4: Component failure probability and sensitivities at $\mathbf{d}_0 = (0, 1)^T$ for $N = 100$ (Example 3)

	PDD-SPA (Univariate, Option II)	PDD-SPA (Bivariate, Option II)	PDD-MCS (Univariate)	PDD-MCS (Bivariate)	Crude MCS/SF	Exact
$P_F(\mathbf{d}_0)$ $(\times 10^{-3})$	1.731	1.320	1.724	1.344	1.352	1.350
$\partial P_F(\mathbf{d}_0)/\partial\mu$ $(\times 10^{-2})$	5.994	6.412	5.538	4.413	4.437	4.432
$\partial P_F(\mathbf{d}_0)/\partial\sigma$ $(\times 10^{-2})$	1.612	1.277	1.556	1.291	1.302	1.330
No. of function eval.	401	79,601	401	79,601	10^6	-

Tables 3.3 and 3.4 also specify the relative computational efforts of the PDD-SPA and PDD-MCS methods, measured in terms of numbers of original function evaluations, when $N = 10$ and $N = 100$. Given the truncation parameter S, the PDD-SPA and PDD-MCS methods require identical numbers of function evaluations, meaning that their computational costs are practically the same. Although the bivariate approximation is significantly more expensive than the univariate approximation, the former generates highly accurate solutions, as expected. However, both versions of the PDD-SPA or PDD-MCS method are markedly more economical than the crude MCS/SF method for solving this high-dimensional reliability problem.

3.7.4 Example 4 : a function of non-Gaussian variables

Consider the univariate function [79]

$$y(\mathbf{X}) = X_1 + 2X_2 + 2X_3 + X_4 - 5X_5 - 5X_6 \tag{3.80}$$

of six statistically independent and lognormally distributed random variables X_i with means μ_i and standard deviations $c\mu_i$, $i = 1, \cdots, 6$, where $c > 0$ is a constant, representing the coefficient of variation of X_i. The design vector $\mathbf{d} = (\mu_1, \cdots \mu_6, \sigma_1, \cdots, \sigma_6)^T$. The objective of this example is to evaluate the accuracy of the proposed PDD-SPA method in estimating the failure probability $P_F(\mathbf{d}) := P_{\mathbf{d}}[y(\mathbf{X}) < 0]$ and its sensitivities $\partial P_F(\mathbf{d}) / \partial \mu_i$ and $\partial P_F(\mathbf{d}) / \partial \sigma_i$, $i = 1, \cdots, 6$, at $\mathbf{d} = \mathbf{d}_0 = (120, 120, 120, 120, 50, 40, 120c, 120c, 120c, 120c, 50c, 40c)^T$ for $0.1 \leq c \leq 0.7$.

The function y, being both univariate and linear, is exactly reproduced by the univariate ($S = 1$), first-order ($m = 1$) PDD approximation when orthonormal polynomials consistent with lognormal probability measures are used. Therefore, the univariate, first-order PDD approximation, along with Option I (Equation (3.59)), was employed in the PDD-SPA method to approximate $P_F(\mathbf{d}_0)$, $\partial P_F(\mathbf{d}_0) / \partial \mu_i$, and $\partial P_F(\mathbf{d}_0) / \partial \sigma_i$. All moments of order up to four were estimated according to Algorithm 3.1. The measure-consistent solutions by the PDD-SPA method and crude MCS/SF are presented in Figures 3.5(a), 3.5(b), and 3.5(c). Huang and Zhang [79], who solved the same problem, reported similar results, but at the expense of higher-order integrations stemming from transformation to Gaussian variables. No such transformation was required or performed in this work. According to Figure 3.5(a), the failure probability curve generated by the PDD-SPA method closely traces the path of crude MCS/SF (10^6 samples) for low coefficients of variation, although a slight deviation begins to appear when c exceeds about 0.4. The loss of accuracy becomes more pronounced when comparing the sensitivities of the failure probability

with respect to means and standard deviations in Figures 3.5(b) and 3.5(c). Indeed, for large coefficients of variation, that is, for $c > 0.4$, some of the sensitivities are no longer accurately calculated by the PDD-SPA method. This is because the fourth-order ($Q = 4$) approximation of the CGF of $y(\mathbf{X})$, used for constructing the PDD-SPA method, is inadequate. Indeed, Table 3.5 reveals that the relative errors in the fourth-order Taylor approximation of the CGF, obtained by MCS (10^8 samples) and evaluated at respective saddlepoints, rises with increasing values of the coefficient of variation from 0.2 to 0.7. Therefore, a truncation larger than four is warranted for higher-order approximations of CGF, but doing so engenders an added difficulty in finding a unique saddlepoint. The topic merits further study.

Table 3.5: Relative errors in calculating CGF (Example 4)

c	t_s	Relative error [a]
0.1	-1.0029×10^{-1}	0.0248
0.2	-2.5008×10^{-2}	0.0068
0.3	-1.1066×10^{-2}	0.0125
0.4	-6.1850×10^{-3}	0.0183
0.5	-3.9250×10^{-3}	0.0329
0.6	-2.6966×10^{-3}	0.0447
0.7	-1.9551×10^{-3}	0.2781

[a] The sample size of MCS is 10^8.

It is important to note that the univariate, first-order PDD-MCS method, employing measure-consistent orthonormal polynomials, should render the same solution

of crude MCS/SF. This is the primary reason why the PDD-MCS results are not depicted in Figures 3.5(a) through 3.5(c). Nonetheless, the PDD-MCS method should be more accurate than the PDD-SPA method in solving this problem, especially at larger coefficients of variation.
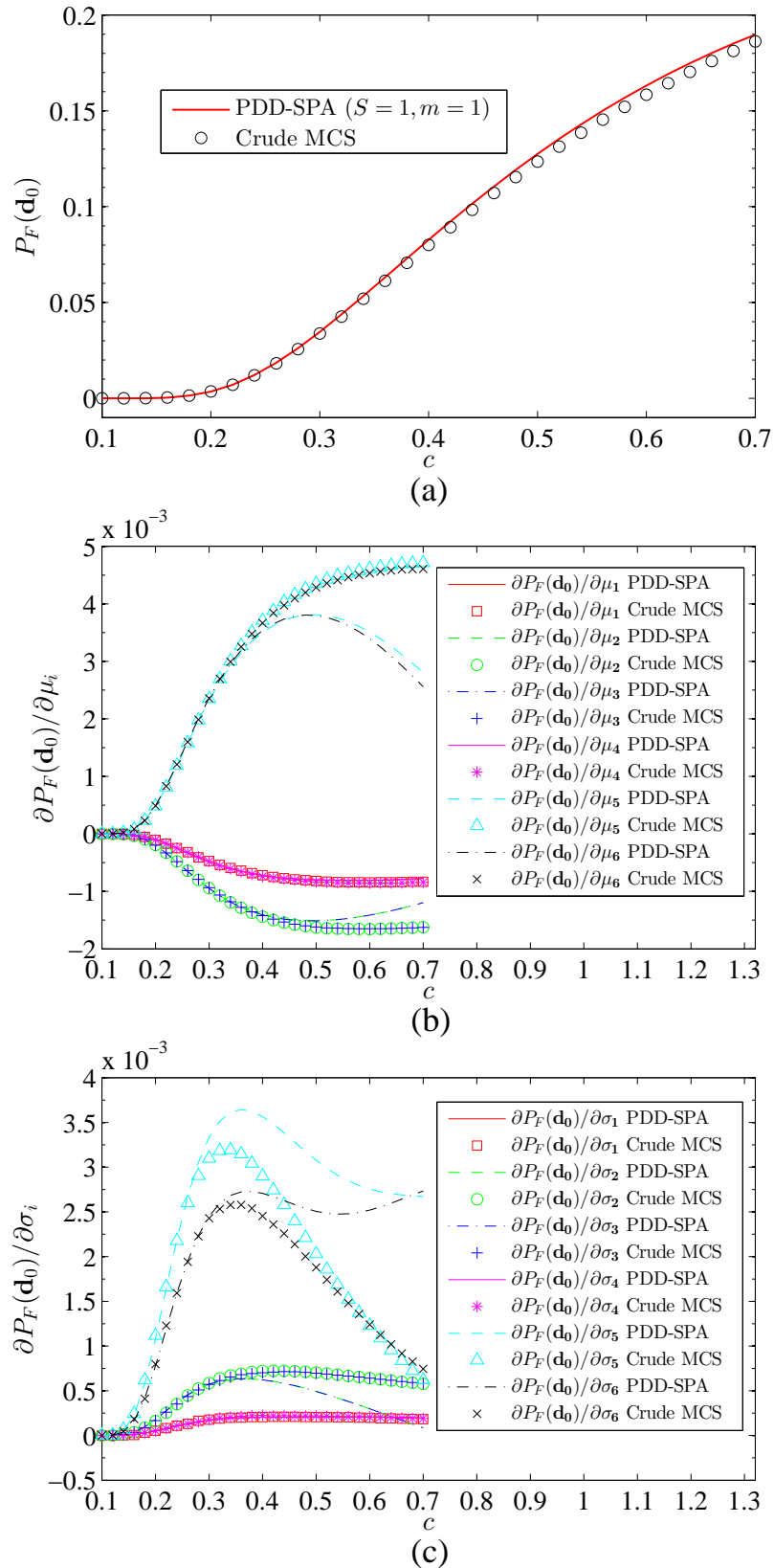
Figure 3.5: Results of the reliability and sensitivity analyses by the PDD-SPA method and crude MCS/SF; (a) failure probability; (b) sensitivities of failure probability with respect to means; (c) sensitivities of failure probability with respect to standard deviations (Example 4)

3.7.5 Example 5: a six-bay, twenty-one-bar truss

This example demonstrates how system reliability and its sensitivities can be efficiently estimated with the PDD-MCS method. A linear-elastic, six-bay, twenty-one-bar truss structure, with geometric properties shown in Figure 3.6, is simply supported at nodes 1 and 12, and is subjected to four concentrated loads of 10,000 lb (44,482 N) at nodes 3, 5, 9, and 11 and a concentrated load of 16,000 lb (71,172 N) at node 7. The truss material is made of an aluminum alloy with the Young's modulus $E = 10^7$ psi (68.94 GPa). The random input is $\mathbf{X} = (X_1, \cdots, X_{21})^T \in \mathbb{R}^{21}$, where X_i is the cross-sectional areas of the ith truss member. The random variables are independent and lognormally distributed with means μ_i, $i = 1, \cdots, 21$, each of which has a ten percent coefficient of variation. From linear-elastic finite-element analysis (FEA), the maximum vertical displacement $v_{\max}(\mathbf{X})$ and maximum axial stress $\sigma_{\max}(\mathbf{X})$ occur at node 7 and member 3 or 4, respectively, where the permissible displacement and stress are limited to $d_{\mathrm{allow}} = 0.266$ in (6.76 mm) and $\sigma_{\mathrm{allow}} = 37,680$ psi (259.8 MPa), respectively. The system-level failure set is defined as $\Omega_F := \{\mathbf{x} : \{y_1(\mathbf{x}) < 0\} \cup \{y_2(\mathbf{x}) < 0\}\}$, where the performance functions

$$y_1(\mathbf{X}) = 1 - \frac{|v_{\max}(\mathbf{X})|}{d_{\mathrm{allow}}}, \; y_2(\mathbf{X}) = 1 - \frac{|\sigma_{\max}(\mathbf{X})|}{\sigma_{\mathrm{allow}}}. \tag{3.81}$$

The design vector is $\mathbf{d} = (\mu_1, \cdots, \mu_{21})^T$. The objective of this example is to evaluate the accuracy of the proposed PDD-MCS method in estimating the system failure probability $P_F(\mathbf{d}) := P_{\mathbf{d}} [\{y_1(\mathbf{X}) < 0\} \cup \{y_2(\mathbf{X}) < 0\}]$ and its sensitivities $\partial P_F(\mathbf{d})/\partial \mu_i$, $i = 1, \ldots, 21$ at $\mathbf{d} = \mathbf{d}_0 = (2, 2, 2, 2, 2, 2, 10, 10, 10, 10, 10, 10, 3, 3, 3, 3, 3, 1, 1, 1, 1)^T$ in^2 ($\times 2.54^2$ cm^2).
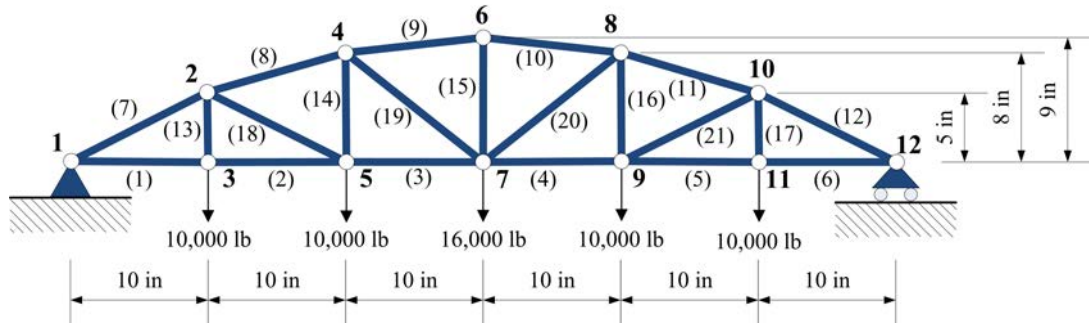
Figure 3.6: A six-bay, twenty-one-bar truss structure (Example 5)

Table 3.6 presents the system failure probability and its 21 sensitivities obtained using the bivariate ($S = 2$), third-order ($m = 3$) PDD approximations of $y_1(\mathbf{X})$ and $y_2(\mathbf{X})$ and two versions of crude MCS: crude MCS/SF and crude MCS/FD, providing benchmark solutions. The crude MCS/FD method does not depend on score functions and, therefore, facilitates an independent verification of the PDD-MCS method. The respective sensitivities obtained by the PDD-MCS method and crude MCS/SF are practically the same. However, crude MCS/FD typically gives biased sensitivity estimates, where slight fluctuations in the results are expected due to a finite variance of the estimator. For two instances, such as when the sensitivities are too small, crude MCS/FD produces trivial solutions and hence cannot be used as reference solutions. Nonetheless, the general quality of agreement between the results of the PDD-MCS method and crude MCS/FD is very good. Comparing the computational efforts, only 3445 FEA were required to produce the results of the PDD-MCS method in Table 3.6, whereas 10^7 and 22×10^7 FEA (samples) were incurred by crude MCS/SF and crude MCS/FD, respectively. The 22-fold increase in the number of

FEA in crude MCS/FD is due to forward finite-difference calculations entailing all 21 sensitivities. Therefore, the PDD-MCS method provides not only highly accurate, but also vastly efficient, solutions of system reliability problems.

Table 3.6: System failure probability and sensitivities for the six-bay, twenty-one-bar truss (Example 5)

	PDD-MCS	Crude MCS/SF	Crude MCS/FD
$P_F(\mathbf{d}_0)$	8.1782×10^{-3}	8.3890×10^{-3}	8.3890×10^{-3}
$\partial P_F(\mathbf{d}_0)/\partial\mu_1$	-2.6390×10^{-2}	-2.6546×10^{-2}	-2.3895×10^{-2}
$\partial P_F(\mathbf{d}_0)/\partial\mu_2$	-2.6385×10^{-2}	-2.6505×10^{-2}	-2.3810×10^{-2}
$\partial P_F(\mathbf{d}_0)/\partial\mu_3$	-1.0010×10^{-1}	-1.0320×10^{-1}	-8.8875×10^{-2}
$\partial P_F(\mathbf{d}_0)/\partial\mu_4$	-3.5684×10^{-2}	-3.5972×10^{-2}	-3.1960×10^{-2}
$\partial P_F(\mathbf{d}_0)/\partial\mu_5$	-2.6356×10^{-2}	-2.6469×10^{-2}	-2.3825×10^{-2}
$\partial P_F(\mathbf{d}_0)/\partial\mu_6$	-2.6266×10^{-2}	-2.6364×10^{-2}	-2.3950×10^{-2}
$\partial P_F(\mathbf{d}_0)/\partial\mu_7$	-1.3189×10^{-3}	-1.3213×10^{-3}	-1.1970×10^{-3}
$\partial P_F(\mathbf{d}_0)/\partial\mu_8$	-1.3294×10^{-3}	-1.3244×10^{-3}	-1.2820×10^{-3}
$\partial P_F(\mathbf{d}_0)/\partial\mu_9$	-1.6665×10^{-3}	-1.6514×10^{-3}	-1.5610×10^{-3}
$\partial P_F(\mathbf{d}_0)/\partial\mu_{10}$	-1.7554×10^{-3}	-1.7576×10^{-3}	-1.5670×10^{-3}
$\partial P_F(\mathbf{d}_0)/\partial\mu_{11}$	-1.3892×10^{-3}	-1.3945×10^{-3}	-1.2530×10^{-3}
$\partial P_F(\mathbf{d}_0)/\partial\mu_{12}$	-1.3136×10^{-3}	-1.3140×10^{-3}	-1.2060×10^{-3}
$\partial P_F(\mathbf{d}_0)/\partial\mu_{13}$	9.1378×10^{-5}	7.2857×10^{-5}	0.0
$\partial P_F(\mathbf{d}_0)/\partial\mu_{14}$	2.3126×10^{-4}	2.0942×10^{-4}	1.3000×10^{-4}
$\partial P_F(\mathbf{d}_0)/\partial\mu_{15}$	-6.3125×10^{-4}	-6.2761×10^{-4}	-5.8333×10^{-4}
$\partial P_F(\mathbf{d}_0)/\partial\mu_{16}$	2.2333×10^{-4}	2.2261×10^{-4}	1.3333×10^{-4}
$\partial P_F(\mathbf{d}_0)/\partial\mu_{17}$	-3.0844×10^{-5}	-3.9551×10^{-5}	0.0
$\partial P_F(\mathbf{d}_0)/\partial\mu_{18}$	-2.0729×10^{-4}	-2.6582×10^{-4}	-8.8000×10^{-4}
$\partial P_F(\mathbf{d}_0)/\partial\mu_{19}$	-3.5881×10^{-3}	-3.4714×10^{-3}	-3.2900×10^{-3}
$\partial P_F(\mathbf{d}_0)/\partial\mu_{20}$	-4.1604×10^{-3}	-4.0774×10^{-3}	-3.2200×10^{-3}
$\partial P_F(\mathbf{d}_0)/\partial\mu_{21}$	-7.7002×10^{-4}	-7.2830×10^{-4}	-8.5000×10^{-4}
No. of FEA	3445	10^7	22×10^7

It is important to recognize that the PDD-SPA method can be applied to solve this series-system reliability problem by interpreting the failure domain as $\Omega_F :=$ $\{\mathbf{x} : \{y_s(\mathbf{x}) < 0\}$, where $y_s(\mathbf{X}) := \min\{y_1(\mathbf{X}), y_2(\mathbf{X})\}$ and then constructing a PDD approximation of $y_s(\mathbf{X})$. In so doing, however, y_s is no longer a smooth function of $\mathbf{X}$, meaning that the convergence properties of the PDD-SPA method can be significantly deteriorated. More importantly, the PDD-SPA method is not suitable for a general system reliability problem involving multiple, interdependent component performance functions. This is the primary reason why the results of the PDD-SPA method are not included in this example.

3.8   Conclusion

Three novel computational methods grounded in PDD were developed for design sensitivity analysis of high-dimensional complex systems subject to random input. The first method, capitalizing on a novel integration of PDD and score functions, provides analytical expressions of approximate design sensitivities of the first two moments that are mean-square convergent. Applied to higher-order moments, the method also estimates design sensitivities by two distinct options, depending on how the high-dimensional integrations are performed. The second method, the PDD-SPA method, integrates PDD, SPA, and score functions, leading to analytical formulae for calculating design sensitivities of probability distribution and component reliability. The third method, the PDD-MCS method, also relevant to probability distribution or reliability analysis, utilizes the embedded MCS of the PDD approximation and

score functions. Unlike the PDD-SPA method, however, the sensitivities in the PDD-MCS method are estimated via efficient sampling of approximate stochastic responses, thereby affording the method to address both component and system reliability problems. Furthermore, the PDD-MCS method is not influenced by any added approximations, involving calculations of the saddlepoint and higher-order moments, of the PDD-SPA method. For all three methods developed, both the statistical moments or failure probabilities and their design sensitivities are determined concurrently from a single stochastic analysis or simulation. Numerical results from mathematical examples corroborate fast convergence of the sensitivities of the first two moments. The same condition holds for the sensitivities of the tails of probability distributions when orthonormal polynomials are constructed consistent with the probability measure of random variables. Otherwise, the convergence properties may markedly degrade or even disappear when resorting to commonly used transformations. For calculating the sensitivities of reliability, the PDD-MCS method, especially its bivariate version, provides excellent solutions to all problems, including a 100-dimensional mathematical function, examined. In contrast, the PDD-SPA method also generates very good estimates of the sensitivities, but mostly for small to moderate uncertainties of random input. When the coefficient of variation is large, the PDD-SPA method may produce inaccurate results, suggesting a need for further improvements.

The computational effort of the univariate PDD method varies linearly with respect to the number of random variables and, therefore, the univariate method is highly economical. In contrast, the bivariate PDD method, which generally outper-

forms the univariate PDD method, demands a quadratic cost scaling, making it more expensive than the latter method. Nonetheless, both versions of the PDD method are substantially more efficient than crude MCS.

CHAPTER 4
ROBUST DESIGN OPTIMIZATION

4.1   Introduction

This chapter presents four new methods for robust design optimization of complex engineering systems. The methods are based on: (1) PDD of a high-dimensional stochastic response for statistical moment analysis; (2) a novel integration of PDD and score functions for calculating the second-moment sensitivities with respect to design variables; and (3) standard gradient-based optimization algorithms, encompassing direct, single-step, sequential, and multi-point single-step design processes. Section 4.2 formally defines one particular kind of RDO problem in which all design variables are distributional parameters, including a concomitant mathematical statement. Section 4.3 introduces four new design methods and explains how the stochastic analysis and design sensitivities from a PDD approximation are integrated with a gradient-based optimization algorithm in each method. Section 4.4 presents four numerical examples involving mathematical functions or solid-mechanics problems, contrasting the accuracy, convergence properties, and computational efforts of the proposed RDO methods. It is followed by Section 4.5, which discusses the efficiency and applicability of all four methods. Finally, the conclusions are drawn in Section 4.6.

4.2   RDO

Consider a measurable space $(\Omega_{\mathbf{d}}, \mathcal{F}_{\mathbf{d}})$, where $\Omega_{\mathbf{d}}$ is a sample space and $\mathcal{F}_{\mathbf{d}}$ is a σ-field on $\Omega_{\mathbf{d}}$. Defined over $(\Omega_{\mathbf{d}}, \mathcal{F}_{\mathbf{d}})$, let $\{P_{\mathbf{d}} : \mathcal{F} \to [0, 1]\}$ be a family of probability measures, where for $M \in \mathbb{N}$ and $N \in \mathbb{N}$, $\mathbf{d} = (d_1, \cdots, d_M)^T \in \mathcal{D}$ is an $\mathbb{R}^M$-valued design vector with non-empty closed set $\mathcal{D} \subseteq \mathbb{R}^M$, and let $\mathbf{X} := (X_1, \cdots, X_N)^T : (\Omega_{\mathbf{d}}, \mathcal{F}_{\mathbf{d}}) \to (\mathbb{R}^N, \mathcal{B}^N)$ be an $\mathbb{R}^N$-valued input random vector with $\mathcal{B}^N$ representing the Borel σ-field on $\mathbb{R}^N$, describing the statistical uncertainties in loads, material properties, and geometry of a complex mechanical system. The probability law of $\mathbf{X}$ is completely defined by a family of the joint probability density functions (PDF) $\{f_{\mathbf{X}}(\mathbf{x}; \mathbf{d}),\ \mathbf{x} \in \mathbb{R}^N,\ \mathbf{d} \in \mathcal{D}\}$ that are associated with probability measures $\{P_{\mathbf{d}},\ \mathbf{d} \in \mathcal{D}\}$, so that the probability triple $(\Omega_{\mathbf{d}}, \mathcal{F}_{\mathbf{d}}, P_{\mathbf{d}})$ of $\mathbf{X}$ depends on $\mathbf{d}$. A design variable d_k can be any distribution parameter or a statistic — for instance, the mean or standard deviation — of X_i.

Let $y_l(\mathbf{X})$, $l = 0, 1, 2, \cdots, K$, be a collection of $K + 1$ real-valued, square-integrable, measurable transformations on $(\Omega, \mathcal{F})$, describing the relevant geometry (*e.g.*, length, area, volume, mass) and performance functions of a complex system. It is assumed that $y_l : (\mathbb{R}^N, \mathcal{B}^N) \to (\mathbb{R}, \mathcal{B})$ is not an explicit function of $\mathbf{d}$, although y_l implicitly depends on $\mathbf{d}$ via the probability law of $\mathbf{X}$. This is not a major limitation, as most RDO problems involve means and/or standard deviations of random variables as design variables. Nonetheless, a common mathematical formulation for RDO problems involving an objective function $c_0 : \mathbb{R}^M \to \mathbb{R}$ and constraint functions

$c_l : \mathbb{R}^M \to \mathbb{R}$, where $l = 1, \cdots, K$ and $1 \leq K < \infty$, requires one to

$$\min_{\mathbf{d} \in \mathcal{D} \subseteq \mathbb{R}^M} \quad c_0(\mathbf{d}) := w_1 \frac{\mathbb{E}_\mathbf{d}[y_0(\mathbf{X})]}{\mu_0^*} + w_2 \frac{\sqrt{\mathrm{var}_\mathbf{d}[y_0(\mathbf{X})]}}{\sigma_0^*},$$

$$\text{subject to} \quad c_l(\mathbf{d}) := \alpha_l \sqrt{\mathrm{var}_\mathbf{d}[y_l(\mathbf{X})]} - \mathbb{E}_\mathbf{d}[y_l(\mathbf{X})] \leq 0, \ l = 1, \cdots, K,$$

$$d_{k,L} \leq d_k \leq d_{k,U}, \ k = 1, \cdots, M, \tag{4.1}$$

where $\mathbb{E}_\mathbf{d}[y_l(\mathbf{X})] := \int_{\mathbb{R}^N} y_l(\mathbf{x}) f_\mathbf{X}(\mathbf{x}; \mathbf{d}) d\mathbf{x}$ is the mean of $y_l(\mathbf{X})$ with $\mathbb{E}_\mathbf{d}$ denoting the expectation operator with respect to the probability measure $P_\mathbf{d}, \mathbf{d} \in \mathbb{R}^M$; $\mathrm{var}_\mathbf{d}[y_l(\mathbf{X})] := \mathbb{E}_\mathbf{d}[\{y_l(\mathbf{X}) - \mathbb{E}_\mathbf{d}[y_l(\mathbf{X})]\}^2]$ is the variance of $y_l(\mathbf{X})$; $g_l, \ l = 0, 1, \cdots, K$, are arbitrary functions of $\mathbb{E}_\mathbf{d}[y_l(\mathbf{X})]$ and $\mathrm{var}_\mathbf{d}[y_l(\mathbf{X})]$; $w_1 \in \mathbb{R}_0^+$ and $w_2 \in \mathbb{R}_0^+$ are two non-negative, real-valued weights, satisfying $w_1 + w_2 = 1$; $\mu_0^* \in \mathbb{R} \setminus \{0\}$ and $\sigma_0^* \in \mathbb{R}_0^+ \setminus \{0\}$ are two non-zero, real-valued scaling factors; $\alpha_l \in \mathbb{R}_0^+, \ l = 0, 1, \cdots, K$, are non-negative, real-valued constants associated with the probabilities of constraint satisfaction; and $d_{k,L}$ and $d_{k,U}$ are the lower and upper bounds, respectively, of d_k. Other formulations entailing nonlinear functions of the first two or higher-order moments can be envisioned, but they are easily tackled by the proposed methods. Nonetheless, the focus of this work is solving the RDO problem described by Equation (4.1) for arbitrary functions $y_l, \ l = 0, 1, 2, \cdots, K$, and arbitrary probability distributions of $\mathbf{X}$.

4.3 Proposed Methods for Design Optimization

The PDD approximations described in the preceding section provide a means to approximate the objective and constraint functions, including their design sensitivities, from a single stochastic analysis. Therefore, any gradient-based algorithm employing PDD approximations should render a convergent solution of the RDO

problem in Equation (4.1). However, there exist multiple ways to dovetail stochastic analysis with an optimization algorithm. Four such design optimization methods, all anchored in PDD, are presented in this section.

4.3.1 Direct PDD

The direct PDD method involves straightforward integration of the PDD-based stochastic analysis with design optimization. Given a design vector at the current iteration and the corresponding values of the objective and constraint functions and their sensitivities, the design vector at the next iteration is generated from a suitable gradient-based optimization algorithm. However, new statistical moment and sensitivity analyses, entailing re-calculations of the PDD expansion coefficients, are needed at every design iteration. Therefore, the direct PDD method is expensive, depending on the cost of evaluating the objective and constraint functions and the requisite number of design iterations.

4.3.2 Single-Step PDD

The single-step PDD method is motivated on solving the entire RDO problem from a single stochastic analysis by sidestepping the need to recalculate the PDD expansion coefficients at every design iteration. It subsumes two important assumptions: (1) an S-variate, mth-order PDD approximation $\tilde{y}_{S,m}$ of y at the initial design is acceptable for all possible designs; and (2) the expansion coefficients for one design, derived from those generated for another design, are accurate.

Consider a change of the probability measure of $\mathbf{X}$ from $f_{\mathbf{X}}(\mathbf{x}; \mathbf{d})d\mathbf{x}$ to $f_{\mathbf{X}}(\mathbf{x}; \mathbf{d}')d\mathbf{x}$,

where $\mathbf{d}$ and $\mathbf{d}'$ are two arbitrary design vectors corresponding to old and new designs, respectively. Let $\{\psi_{ij}(X_i; \mathbf{d}'); \ j = 0, 1, \cdots\}$ be a set of new orthonormal polynomial basis functions consistent with the marginal probability measure $f_{X_i}(x_i; \mathbf{d}')dx_i$ of X_i, producing new product polynomials $\psi_{u\mathbf{j}_{|u|}}(\mathbf{X}_u; \mathbf{d}') = \prod_{p=1}^{|u|} \psi_{i_p j_p}(X_{i_p}; \mathbf{d}')$, $\emptyset \neq u \subseteq \{1, \cdots, N\}$. Assume that the expansion coefficients, $y_\emptyset(\mathbf{d})$ and $C_{u\mathbf{j}_{|u|}}(\mathbf{d})$, for the old design have been calculated already. Then, the expansion coefficients for the new design are determined from

$$
\begin{aligned}
y_\emptyset(\mathbf{d}') = \int_{\mathbb{R}^N} \bigg[& \sum_{\emptyset \neq u \subseteq \{1, \cdots, N\}} \sum_{\substack{\mathbf{j}_{|u|} \in \mathbb{N}_0^{|u|} \\ j_1, \cdots, j_{|u|} \neq 0}} C_{u\mathbf{j}_{|u|}}(\mathbf{d}) \times \\
& \psi_{u\mathbf{j}_{|u|}}(\mathbf{x}_u; \mathbf{d}) + y_\emptyset(\mathbf{d}) \bigg] f_{\mathbf{X}}(\mathbf{x}; \mathbf{d}')d\mathbf{x}
\end{aligned}
\tag{4.2}
$$

and

$$
\begin{aligned}
C_{u\mathbf{j}_{|u|}}(\mathbf{d}') = \int_{\mathbb{R}^N} \bigg[& \sum_{\emptyset \neq v \subseteq \{1, \cdots, N\}} \sum_{\substack{\mathbf{j}_{|v|} \in \mathbb{N}_0^{|v|} \\ j_1, \cdots, j_{|v|} \neq 0}} C_{v\mathbf{j}_{|v|}}(\mathbf{d}) \times \\
& \psi_{v\mathbf{j}_{|v|}}(\mathbf{x}_v; \mathbf{d}) + y_\emptyset(\mathbf{d}) \bigg] \psi_{u\mathbf{j}_{|u|}}(\mathbf{x}_u; \mathbf{d}')f_{\mathbf{X}}(\mathbf{x}; \mathbf{d}')d\mathbf{x},
\end{aligned}
\tag{4.3}
$$

for all $\emptyset \neq u \subseteq \{1, \cdots, N\}$ by recycling the old expansion coefficients and using orthonormal polynomials associated with both designs. The relationship between the old and new coefficients, described by Equations (4.2) and (4.3), is exact and is obtained by replacing y with the right side of Equation (3.10) in Equations (2.7) and (3.7). However, in practice, when the S-variate, mth-order PDD approximation (Equation (3.11)) is used to replace y in Equations (2.7) and (3.7), then the new

expansion coefficients,

$$y_\emptyset(\mathbf{d}') \cong \int_{\mathbb{R}^N} \Bigg[\sum_{\substack{\emptyset \neq u \subseteq \{1,\cdots,N\} \\ 1 \le |u| \le S}} \sum_{\substack{\mathbf{j}_{|u|} \in \mathbb{N}_0^{|u|}, ||\mathbf{j}_{|u|}||_\infty \le m \\ j_1,\cdots,j_{|u|} \neq 0}} C_{u\mathbf{j}_{|u|}}(\mathbf{d})$$
$$\times\, \psi_{u\mathbf{j}_{|u|}}(\mathbf{X}_u; \mathbf{d}) + y_\emptyset(\mathbf{d}) \Bigg] f_{\mathbf{X}}(\mathbf{x}; \mathbf{d}') d\mathbf{x} \qquad (4.4)$$

and

$$C_{u\mathbf{j}_{|u|}}(\mathbf{d}') \cong \int_{\mathbb{R}^N} \Bigg[\sum_{\substack{\emptyset \neq v \subseteq \{1,\cdots,N\} \\ 1 \le |v| \le S}} \sum_{\substack{\mathbf{j}_{|v|} \in \mathbb{N}_0^{|v|}, ||\mathbf{j}_{|v|}||_\infty \le m \\ j_1,\cdots,j_{|v|} \neq 0}}$$
$$C_{v\mathbf{j}_{|v|}}(\mathbf{d})\psi_{v\mathbf{j}_{|v|}}(\mathbf{X}_v; \mathbf{d}) + y_\emptyset(\mathbf{d}) \Bigg]$$
$$\times \psi_{u\mathbf{j}_{|u|}}(\mathbf{x}_u; \mathbf{d}') f_{\mathbf{X}}(\mathbf{x}; \mathbf{d}') d\mathbf{x}, \qquad (4.5)$$

which are applicable for $\emptyset \neq u \subseteq \{1, \cdots, N\}$, $1 \le |u| \le S$, become approximate, although convergent. In the latter case, the integrals in Equations (4.4) and (4.5) consist of finite-order polynomial functions of at most S variables and can be evaluated inexpensively without having to compute the original function y for the new design. Therefore, new stochastic analyses, all employing S-variate, mth-order PDD approximation of y, are conducted with little additional cost during all design iterations, drastically curbing the computational effort in solving the RDO problem.

4.3.3   Sequential PDD

When the truncations parameters, S and/or m, of a PDD approximation are too low, the assumptions of the single-step PDD method are likely to be violated, resulting in a premature or inaccurate optimal solution. To overcome this problem, a sequential PDD method, combining the ideas of the single-step PDD and direct

PDD methods, was developed. It forms a sequential design process, where each sequence begins with a single-step PDD using the expansion coefficients calculated at an optimal design solution generated from the previous sequence. Although more expensive than the single-step PDD method, the sequential PDD method is expected to be more economical than the direct PDD method.

The sequential PDD method is outlined by the following steps. The flow chart of this method is shown in Figure 4.1.

Step 1: Select an initial design vector $\mathbf{d}_0$. Define a tolerance $\epsilon > 0$. Set the iteration $q = 1$, qth initial design vector $\mathbf{d}_0^{(q)} = \mathbf{d}_0$, and approximate optimal solution $\mathbf{d}_*^{(0)} = \mathbf{d}_0$ at $q = 0$.

Step 2: Select ($q = 1$) or use ($q > 1$) the PDD and Fourier truncation parameters S, m, and m'. At $\mathbf{d} = \mathbf{d}_0^{(q)}$, generate the PDD expansion coefficients, $y_\emptyset(\mathbf{d})$ and $C_{u\mathbf{j}_{|u|}}(\mathbf{d})$, where $\emptyset \neq u \subseteq \{1, \cdots, N\}$, $1 \leq |u| \leq S$, $\mathbf{j}_{|u|} \in \mathbb{N}_0^{|u|}$, $||\mathbf{j}_{|u|}||_\infty \leq m$, $j_1, \cdots, j_{|u|} \neq 0$, using dimension-reduction integration with $R = S$, $n = m + 1$, leading to S-variate, mth-order PDD approximations of $y_l(\mathbf{X})$, $l = 0, 1, \ldots, K$, in Equation (4.1). Calculate the expansion coefficients of the score functions, $s_{k,\emptyset}(\mathbf{d})$ and $D_{i_k,j}(\mathbf{d})$, where $k = 1, \cdots, M$ and $j = 1, \cdots, m'$, analytically, if possible, or numerically, resulting in m'th-order Fourier-polynomial approximations of $s_k(X_{i_k}; \mathbf{d})$, $k = 1, \cdots, M$.

Step 3: Solve the design problem in Equation (4.1) employing PDD approximations of y_l, $l = 0, 1, \cdots, K$ and a standard gradient-based optimization algorithm. In so doing, recycle the PDD expansion coefficients obtained from Step 2 in

Equations (4.4) and (4.5), producing approximations of the objective and constraint functions that stem from single calculation of these coefficients. To evaluate the gradients, recalculate the Fourier expansion coefficients of score functions as needed. Denote the approximate optimal solution by $\mathbf{d}_*^{(q)}$. Set $\mathbf{d}_0^{(q+1)} = \mathbf{d}_*^{(q)}$.

Step 4: If $||\mathbf{d}_*^{(q)} - \mathbf{d}_*^{(q-1)}||_2 < \epsilon$, then stop and denote the final approximate optimal solution as $\tilde{\mathbf{d}}^* = \mathbf{d}_*^{(q)}$. Otherwise, update $q = q + 1$ and go to Step 2.
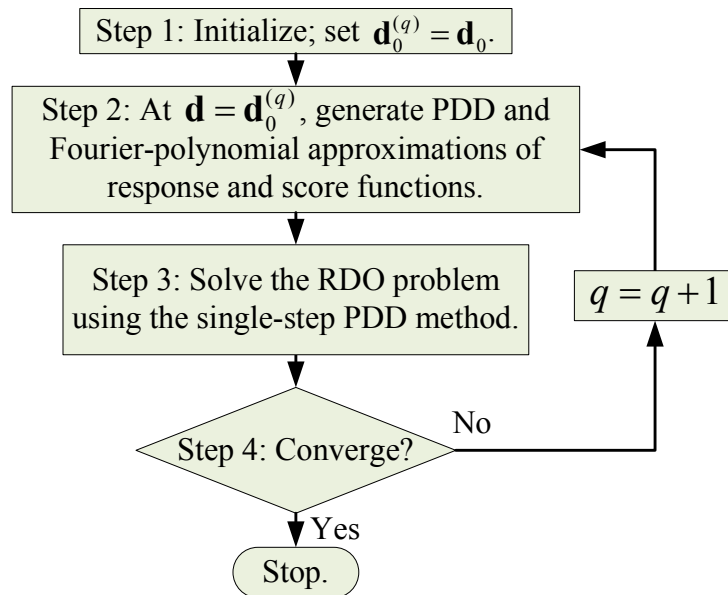
Figure 4.1: A flow chart of the sequential PDD method

4.3.4 Multi-Point Single-Step PDD

The optimization methods described in the preceding subsections are founded on PDD approximations of stochastic responses, supplying surrogates of objective and

constraint functions for the entire design space. Therefore, these methods are global and may not be cost-effective when the truncation parameters of PDD are required to be exceedingly large to capture high-order responses or high-variate interactions of input variables. Furthermore, a global method using a truncated PDD, obtained by retaining only low-order or low-variate terms, may not even find a true optimal solution. An attractive alternative method, developed in this work and referred to as the multi-point single-step PDD method, involves local implementations of the single-step PDD approximation that are built on a local subregion of the design space. According to this method, the original RDO problem is exchanged with a succession of simpler RDO sub-problems, where the objective and constraint functions in each sub-problem represent their multi-point approximations [84]. The design solution of an individual sub-problem, obtained by the single-step PDD method, becomes the initial design for the next sub-problem. Then, the move limits are updated, and the optimization is repeated iteratively until the optimal solution is attained. Due to its local approach, the multi-point single-step PDD method should solve practical engineering problems using low-order and/or low-variate PDD approximations.

Let $\mathcal{D} = \times_{k=1}^{k=M}[d_{k,L}, d_{k,U}] \subseteq \mathbb{R}^M$ be a rectangular domain, representing the design space of the RDO problem defined by Equation (4.1). For a scalar variable $0 < \beta_k^{(q)} \leq 1$ and an initial design vector $\mathbf{d}_0^{(q)} = (d_{1,0}^{(q)}, \cdots, d_{M,0}^{(q)})$, the subset $\mathcal{D}^{(q)} = \times_{k=1}^{k=M}[d_{k,0}^{(q)} - \beta_k^{(q)}(d_{k,U} - d_{k,L})/2, d_{k,0}^{(q)} + \beta_k^{(q)}(d_{k,U} - d_{k,L})/2] \subseteq \mathcal{D} \subseteq \mathbb{R}^M$ defines the qth subregion for $q = 1, 2, \cdots$. According to the multi-point single-step PDD method,

the RDO problem in Equation (4.1) is reformulated to

$$\min_{\mathbf{d} \in \mathcal{D}^{(q)} \subseteq \mathcal{D}} \quad \tilde{c}_{0,S,m}^{(q)}(\mathbf{d}) := w_1 \frac{\mathbb{E}_{\mathbf{d}}\left[\tilde{y}_{0,S,m}^{(q)}(\mathbf{X})\right]}{\mu_0^*} + w_2 \frac{\sqrt{\text{var}_{\mathbf{d}}\left[\tilde{y}_{0,S,m}^{(q)}(\mathbf{X})\right]}}{\sigma_0^*},$$

$$\text{subject to} \quad \tilde{c}_{l,S,m}^{(q)}(\mathbf{d}) := \alpha_l \sqrt{\text{var}_{\mathbf{d}}\left[\tilde{y}_{l,S,m}^{(q)}(\mathbf{X})\right]} - \mathbb{E}_{\mathbf{d}}\left[\tilde{y}_{l,S,m}^{(q)}(\mathbf{X})\right] \leq 0,$$

$$l = 1, \cdots, K,$$

$$d_{k,0}^{(q)} - \beta_k^{(q)}(d_{k,U} - d_{k,L})/2 \leq d_k \leq d_{k,0}^{(q)} + \beta_k^{(q)}(d_{k,U} - d_{k,L})/2,$$

$$k = 1, \cdots, M, \tag{4.6}$$

where $\tilde{y}_{l,S,m}^{(q)}(\mathbf{X})$ and $\tilde{c}_{l,S,m}^{(q)}(\mathbf{d})$, $l = 0, 1, 2, \cdots, K$, are local, S-variate, mth-order PDD approximations of $y_l(\mathbf{X})$ and $c_l(\mathbf{d})$, respectively, at iteration q, and $d_{k,0}^{(q)} - \beta_k^{(q)}(d_{k,U} - d_{k,L})/2$ and $d_{k,0}^{(q)} + \beta_k^{(q)}(d_{k,U} - d_{k,L})/2$, also known as the move limits, are the lower and upper bounds, respectively, of the subregion $\mathcal{D}^{(q)}$. The multi-point single-step PDD method solves the optimization problem in Equation (4.6) for $q = 1, 2, \cdots$ by successively employing the single-step PDD approximation at each subregion or iteration until convergence is attained. When $S \to N$ and $m \to \infty$, the second-moment properties of PDD approximations converge to their exact values, yielding coincident solutions of the optimization problems described by Equations (4.1) and (4.6). However, if the subregions are sufficiently small, then for finite and possibly low values of S and m, Equation (4.6) is expected to generate an accurate solution of Equation (4.1), the principal motivation of this method.

The multi-point single-step PDD method is outlined by the following steps. The flow chart of this method is shown in Figure 4.2.

Step 1: Select an initial design vector $\mathbf{d}_0$. Define tolerances $\epsilon_1 > 0$, $\epsilon_2 > 0$, and

$\epsilon_3 > 0$. Set the iteration $q = 1$, $\mathbf{d}_0^{(q)} = (d_{1,0}^{(q)}, \cdots, d_{M,0}^{(q)})^T = \mathbf{d}_0$. Define the subregion size parameters $0 < \beta_k^{(q)} \leq 1$, $k = 1, \cdots, M$, describing $\mathcal{D}^{(q)} = \times_{k=1}^{k=M} [d_{k,0}^{(q)} - \beta_k^{(q)}(d_{k,U} - d_{k,L})/2, d_{k,0}^{(q)} + \beta_k^{(q)}(d_{k,U} - d_{k,L})/2]$. Denote the subregion's increasing history by a set $H^{(0)}$ and set it to empty. Set two designs $\mathbf{d}_f = \mathbf{d}_0$ and $\mathbf{d}_{f,last} \neq \mathbf{d}_0$ such that $||\mathbf{d}_f - \mathbf{d}_{f,last}||_2 > \epsilon_1$. Set $\mathbf{d}_*^{(0)} = \mathbf{d}_0$, $q_{f,last} = 1$ and $q_f = 1$. Usually, a feasible design should be selected to be the initial design $\mathbf{d}_0$. However, when an infeasible initial design is chosen, a new feasible design can be obtained during the iteration if the initial subregion size parameters are large enough.

Step 2: Select ($q = 1$) or use ($q > 1$) the PDD truncation parameters S and m. At $\mathbf{d} = \mathbf{d}_0^{(q)}$, generate the PDD expansion coefficients, $y_\emptyset(\mathbf{d})$ and $C_{u\mathbf{j}_{|u|}}(\mathbf{d})$, where $\emptyset \neq u \subseteq \{1, \cdots, N\}$, $1 \leq |u| \leq S$, $\mathbf{j}_{|u|} \in \mathbb{N}_0^{|u|}$, $||\mathbf{j}_{|u|}||_\infty \leq m$, $j_1, \cdots, j_{|u|} \neq 0$, using dimension-reduction integration with $R = S$, $n = m + 1$, leading to S-variate, mth-order PDD approximations $\tilde{y}_{l,S,m}^{(q)}(\mathbf{X})$ of $y_l(\mathbf{X})$ and $\tilde{c}_{l,S,m}^{(q)}(\mathbf{d})$ of $c_l(\mathbf{d})$, $l = 0, 1, \cdots, K$, in Equation (4.1). Calculate the expansion coefficients of score functions, $s_{k,\emptyset}(\mathbf{d})$ and $D_{i_k,j}(\mathbf{d})$, where $k = 1, \cdots, M$ and $j = 1, \cdots, m'$, analytically, if possible, or numerically, resulting in m'th-order Fourier-polynomial approximations of $s_k(X_{i_k}; \mathbf{d})$, $k = 1, \cdots, M$.

Step 3: If $q = 1$ and $\tilde{c}_l^{(q)}(\mathbf{d}_0^{(q)}) < 0$ for $l = 1, \cdots, K$, then go to Step 4. If $q > 1$ and $\tilde{c}_l^{(q)}(\mathbf{d}_0^{(q)}) < 0$ for $l = 1, \cdots, K$, then set $\mathbf{d}_{f,last} = \mathbf{d}_f$, $\mathbf{d}_f = \mathbf{d}_0^{(q)}$, $q_{f,last} = q_f$, $q_f = q$ and go to Step 4. Otherwise, go to Step 5.

Step 4: If $||\mathbf{d}_f - \mathbf{d}_{f,last}||_2 < \epsilon_1$ or $\left|\left[\tilde{c}_0^{(q)}(\mathbf{d}_f) - \tilde{c}_0^{(q_{f,last})}(\mathbf{d}_{f,last})\right]/\tilde{c}_0^{(q)}(\mathbf{d}_f)\right| < \epsilon_3$, then stop and denote the final optimal solution as $\tilde{\mathbf{d}}^* = \mathbf{d}_f$. Otherwise, go to Step 6.

Step 5: Compare the infeasible design $\mathbf{d}_0^{(q)}$ with the feasible design $\mathbf{d}_f$ and interpolate between $\mathbf{d}_0^{(q)}$ and $\mathbf{d}_f$ to obtain a new feasible design and set it as $\mathbf{d}_0^{(q+1)}$. For dimensions with large differences between $\mathbf{d}_0^{(q)}$ and $\mathbf{d}_f$, interpolate aggressively. Reduce the size of the subregion $\mathcal{D}^{(q)}$ to obtain new subregion $\mathcal{D}^{(q+1)}$. For dimensions with large differences between $\mathbf{d}_0^{(q)}$ and $\mathbf{d}_f$, reduce aggressively. Also, for dimensions with large differences between the sensitivities of $\tilde{c}_{l,Sm}^{(q)}(\mathbf{d}_0^{(q)})$ and $\tilde{c}_{l,Sm}^{(q-1)}(\mathbf{d}_0^{(q)})$, reduce aggressively. Update $q = q + 1$ and go to Step 2.

Step 6: If the subregion size is small, that is, $\beta_k^{(q)}(d_{k,U} - d_{k,L}) < \epsilon_2$, and $\mathbf{d}_*^{(q-1)}$ is located on the boundary of the subregion, then go to Step 7. Otherwise, go to Step 9.

Step 7: If the subregion centered at $\mathbf{d}_0^{(q)}$ has been enlarged before, that is, $\mathbf{d}_0^{(q)} \in H^{(q-1)}$, then set $H^{(q)} = H^{(q-1)}$ and go to Step 9. Otherwise, set $H^{(q)} = H^{(q-1)} \bigcup \{\mathbf{d}_0^{(q)}\}$ and go to Step 8.

Step 8: For coordinates of $\mathbf{d}_0^{(q)}$ located on the boundary of the subregion and $\beta_k^{(q)}(d_{k,U} - d_{k,L}) < \epsilon_2$, increase the sizes of corresponding components of $\mathcal{D}^{(q)}$; for other coordinates, keep them as they are. Set the new subregion as $\mathcal{D}^{(q+1)}$.

Step 9: Solve the design problem in Equation (4.6) employing the single-step PDD method. In so doing, recycle the PDD expansion coefficients obtained from

Step 2 in Equations (4.4) and (4.5), producing approximations of the objective and constraint functions that stem from single calculation of these coefficients. To evaluate the gradients, recalculate the Fourier expansion coefficients of score functions as needed. Denote the optimal solution by $\mathbf{d}_*^{(q)}$ and set $\mathbf{d}_0^{(q+1)} = \mathbf{d}_*^{(q)}$. Update $q = q + 1$ and go to Step 2.

Table 4.1 summarizes several features of all four design methods developed in this work. It describes the design space of a method, how many times a method requires the PDD approximation, and whether the original problem or a sequence of subproblems are solved.
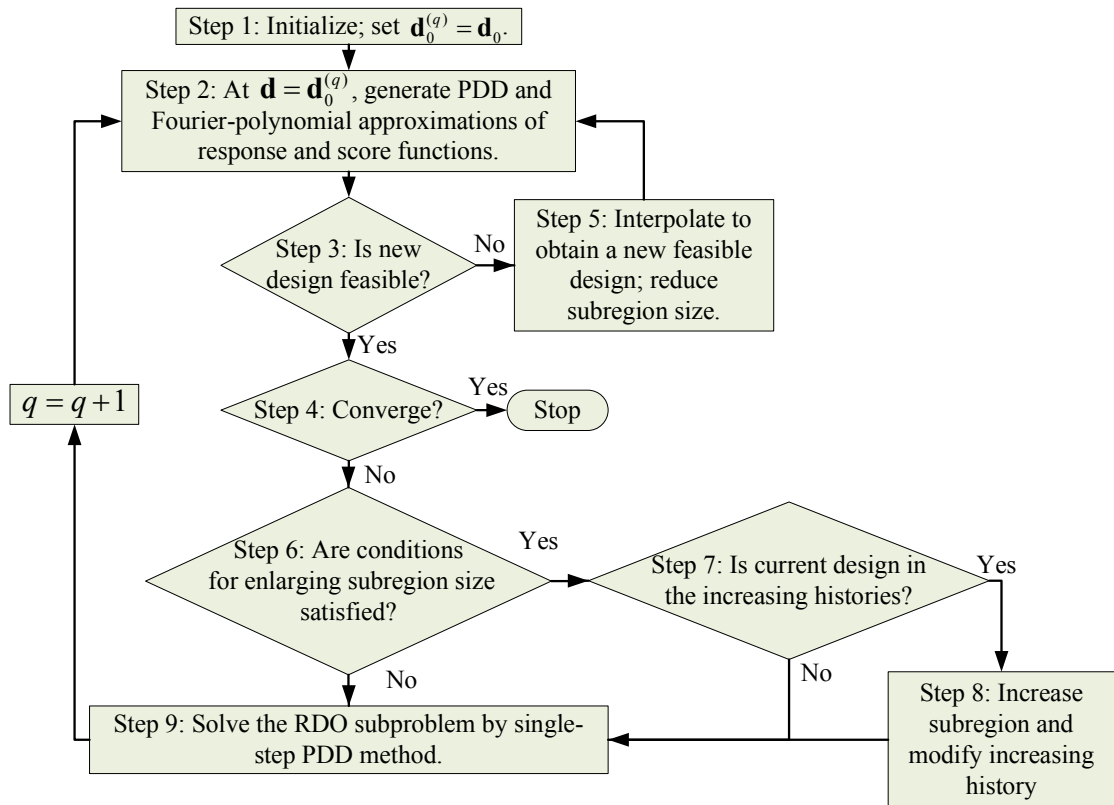
Figure 4.2: A flow chart of the multi-point single-step PDD method

Table 4.1: Summary of features of the four proposed methods

Feature	Direct PDD	Single-Step PDD	Sequential PDD	Multi-point Single-Step PDD
Design space	Global	Global	Global	Local
Frequency of PDD approximations	Every iteration	Only first iteration	A few iterations	For every subproblem
Problem solved in every iteration	Original problem	Original problem	Original problem	Subproblems

4.4 Numerical Examples

Four examples are presented to illustrate the PDD methods developed in solving various RDO problems. The objective and constraint functions are either elementary mathematical functions or relate to engineering problems, ranging from simple structural to complex FEA-aided mechanical designs. Both size and shape design problems are included. In Examples 1-4, orthonormal polynomials, consistent with the probability distributions of input random variables, were used as bases. For the Gaussian distribution, the Hermite polynomials were used. For random variables following non-Gaussian probability distributions, such as the Lognormal, Beta, and Gumbel distributions in Example 2, the orthonormal polynomials were obtained either analytically when possible or numerically, exploiting the Stieltjes procedure [97, 98]. However, in Examples 3 and 4, the original random variables were transformed into standard Gaussian random variables, facilitating the use of classical Hermite polynomials as orthonormal polynomials. The PDD truncation parameters S and m vary,

depending on the function or the example, but in all cases the PDD expansion coefficients were calculated using dimension-reduction integration with $R = S$ and the number of integration points $n = m + 1$. The Gauss-quadrature rules are consistent with the polynomial basis functions employed. Since the design variables are the means of Gaussian random variables, the order m' used for Fourier expansion coefficients of score functions in Examples 1, 3, and 4 is one. However, in Example 2, where the design variables describe both means and standard deviations of random variables, m' is two. The tolerances and initial subregion size parameters are as follows: (1) $\epsilon = 0.001$; $\epsilon_1 = 0.1$, $\epsilon_2 = 2$; $\epsilon_3 = 0$ (Example 3), $\epsilon_3 = 0.005$ (Example 4); and (2) $\beta_1^{(1)} = \cdots = \beta_M^{(1)} = 0.5$. The optimization algorithm selected is sequential quadratic programming [106] in all examples.

4.4.1 Example 1: optimization of a mathematical function

Consider a mathematical example, studied by Lee *et al.* [14], involving two independent Gaussian random variables X_1 and X_2 and two design variables $d_1 = \mathbb{E}_{\mathbf{d}}[X_1]$ and $d_2 = \mathbb{E}_{\mathbf{d}}[X_2]$, which requires to

$$
\begin{aligned}
\min_{\mathbf{d} \in \mathcal{D}} \qquad & c_0(\mathbf{d}) = \frac{\sqrt{\text{var}_{\mathbf{d}}[y_0(\mathbf{X})]}}{15}, \\
\text{subject to} \qquad & c_1(\mathbf{d}) = 3\sqrt{\text{var}_{\mathbf{d}}[y_1(\mathbf{X})]} - \mathbb{E}_{\mathbf{d}}[y_1(\mathbf{X})] \leq 0, \\
& 1 \leq d_1 \leq 10, \, 1 \leq d_2 \leq 10,
\end{aligned}
\tag{4.7}
$$

where

$$
y_0(\mathbf{X}) = (X_1 - 4)^3 + (X_1 - 3)^4 + (X_2 - 5)^2 + 10
\tag{4.8}
$$

and

$$y_1(\mathbf{X}) = X_1 + X_2 - 6.45 \tag{4.9}$$

are two random functions. The random variables X_1 and X_2 have respective means d_1 and d_2, but the same standard deviation, which is equal to 0.4. The design vector $\mathbf{d} = (d_1, d_2)^T \in \mathcal{D}$, where $\mathcal{D} = (1, 10) \times (1, 10) \subset \mathbb{R}^2$.

Two proposed RDO methods, the direct PDD and single-step PDD methods, were applied to solve this problem. Since y_0 and y_1 are both univariate functions, only univariate ($S = 1$) PDD approximations are required. The chosen PDD expansion orders are $m = 4$ for y_0 and $m = 1$ for y_1. The initial design vector $\mathbf{d}_0 = (5, 5)^T$ and, correspondingly, $\sqrt{\mathrm{var}_{\mathbf{d}_0}[y_0(\mathbf{X})]} = 18.2987$. The approximate optimal solution is denoted by $\tilde{\mathbf{d}}^* = (\tilde{d}_1^*, \tilde{d}_2^*)^T$.

Table 4.2 summarizes the approximate optimal solutions, including the numbers of design iterations and function evaluations, by the two PDD methods. For comparison, the results of a tensor product quadrature (TPQ) method and Taylor series approximation, proposed by and obtained from Lee *et al.* [14], are also included. From Table 4.2, all four methods engender close optimal solutions in four to five iterations. Hence, each method can be used to solve this optimization problem. Both PDD versions yield identical solutions due to the same truncation parameters selected. However, the numbers of function evaluations required to reach optimal solutions reduce dramatically when the single-step PDD is employed. This is because a univariate PDD approximation is adequate for the entire design space, facilitating exact calculations of the expansion coefficients by Equations (4.4) and (4.5) for any

design. In which case, the expansion coefficients need to be calculated only once during all design iterations. At respective optima, the exact values of objective functions for the PDD methods are smaller than those for the TPQ and first-order Taylor series methods. In addition, the numbers of function evaluations by the direct PDD or single-step PDD method are moderately or significantly lower than those by the TPQ method. Therefore, the PDD methods not only furnish a slightly better optimal solution, but also a more computationally efficient one than the TPQ method, at least in this example. Although the total numbers of function evaluations by the direct PDD and Taylor series methods are similar, the single-step PDD method is more efficient than the Taylor series method by almost a factor of six.

Table 4.2: Optimization results for the mathematical example

Results	Method			
	Direct PDD	Single-Step PDD	TPQ[a]	Taylor series[a]
$\tilde{d}_1^*$	3.3508	3.3508	3.4449	3.4983
$\tilde{d}_1^*$	4.9856	4.9856	5.000	4.9992
$c_0(\tilde{\mathbf{d}}^*)^{[b]}$	0.0756	0.0756	0.0861[c]	0.0902[c]
$c_1(\tilde{\mathbf{d}}^*)^{[b]}$	-0.1873	-0.1599	-0.2978[c]	-0.3504[c]
$\sqrt{\mathrm{var}_{\tilde{\mathbf{d}}^*}[y_0(\mathbf{X})]}^{[b]}$	1.1340	1.1340	1.2915[c]	1.3535[c]
No. of iterations	5	5	4	4
No. of y_0 evaluations	66	11	81	45
No. of y_1 evaluations	30	5	81	45

[a] The results of TPQ (DSA) and Taylor series were obtained from Lee *et al.* [14].

[b] The objective function, constraint functions, and $\sqrt{\mathrm{var}_{\tilde{\mathbf{d}}^*}[y_0(\mathbf{X})]}$ were evaluated exactly.

[c] The objective and constraint functions of optimal designs by TPQ(DSA) and Taylor series were evaluated exactly.

4.4.2 Example 2: size design of a two-bar truss

The second example, studied by Ramakrishnan and Rao [107] and Lee *et al.* [14], entails RDO of a two-bar truss structure, as shown in Figure 4.3. There are five independent random variables, comprising the cross-sectional area X_1, the half-horizontal span X_2, mass density X_3, load magnitude X_4, and material yield (tensile) strength X_5. Their probability distributions are listed in Table 4.3. The design variables are as follows: $d_1 = \mathbb{E}_{\mathbf{d}}[X_1]$ and $d_2 = \mathbb{E}_{\mathbf{d}}[X_2]$. The objective is to minimize the second-moment properties of the mass of the structure subject to constraints, limiting axial stresses of both members at or below the yield strength of the material with 99.875% probability if y_l, $l = 1, 2$, are Gaussian. The RDO problem is formulated to

$$\min_{\mathbf{d} \in \mathcal{D}} \; c_0(\mathbf{d}) = 0.5 \frac{\mathbb{E}_{\mathbf{d}}\left[y_0(\mathbf{X})\right]}{10} + 0.5 \frac{\sqrt{\mathrm{var}_{\mathbf{d}}\left[y_0(\mathbf{X})\right]}}{2},$$

$$\text{subject to} \quad c_1(\mathbf{d}) = 3\sqrt{\mathrm{var}_{\mathbf{d}}\left[y_1(\mathbf{X})\right]} - \mathbb{E}_{\mathbf{d}}\left[y_1(\mathbf{X})\right] \le 0,$$

$$c_2(\mathbf{d}) = 3\sqrt{\mathrm{var}_{\mathbf{d}}\left[y_2(\mathbf{X})\right]} - \mathbb{E}_{\mathbf{d}}\left[y_2(\mathbf{X})\right] \le 0 \tag{4.10}$$

$$0.2 \text{ cm}^2 \le d_1 \le 20 \text{ cm}^2, \; 0.1 \text{ m} \le d_2 \le 1.6 \text{ m},$$

where

$$y_0(\mathbf{X}) = X_3 X_1 \sqrt{1 + X_2^2}, \tag{4.11}$$

$$y_1(\mathbf{X}) = 1 - \frac{5 X_4 \sqrt{1 + X_2^2}}{\sqrt{65} X_5} \left(\frac{8}{X_1} + \frac{1}{X_1 X_2} \right), \tag{4.12}$$

and

$$y_2(\mathbf{X}) = 1 - \frac{5 X_4 \sqrt{1 + X_2^2}}{\sqrt{65} X_5} \left(\frac{8}{X_1} - \frac{1}{X_1 X_2} \right) \tag{4.13}$$

are three random response functions. The design vector $\mathbf{d} = (d_1, d_2)^T \in \mathcal{D}$, where $\mathcal{D} = (0.2 \text{ cm}^2, 20 \text{ cm}^2) \times (0.1 \text{ m}, 1.6 \text{ m}) \subset \mathbb{R}^2$. The initial design vector is $\mathbf{d}_0 =$

$(10 \text{ cm}^2, 1 \text{ m})^T$. The corresponding mean and standard deviation of $y_0(\mathbf{d}_0)$ at the initial design, calculated by crude MCS simulation with 10^8 samples, are 14.1422 kg and 2.8468 kg, respectively. The approximate optimal solution is denoted by $\tilde{\mathbf{d}}^* = (\tilde{d}_1^*, \tilde{d}_2^*)^T$.
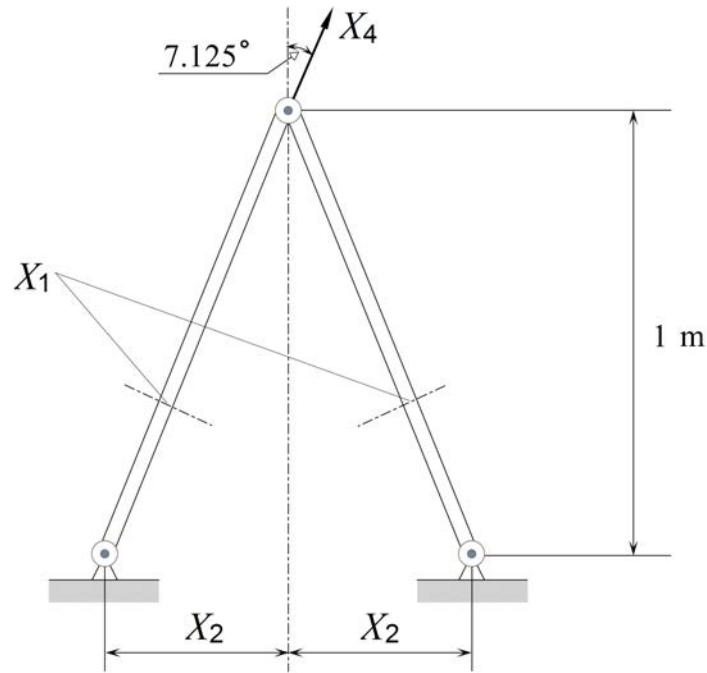
Figure 4.3: A two-bar truss structure

Table 4.4 presents detailed optimization results generated by the direct and sequential PDD methods, each entailing univariate, bivariate, and trivariate PDD approximations with $m = 2$, $n = 3$. The optimal solutions by all PDD methods or approximations are very close to each other, all indicating that the first constraint is active. Although there are slight constraint violations ($c_1 > 0$), they are negligi-

Table 4.3: Statistical properties of random input for the two-bar truss problem

Random variable	Mean	Standard deviation	Probability distribution
Cross-sectional area (X_1), cm^2	d_1	$0.02d_1$	Gaussian
Half-horizontal span(X_2), m	d_2	$0.02d_2$	Gaussian
Mass density (X_3), kg/m^3	10,000	2000	Beta
Load magnitude (X_4), kN	800	200	Gumbel
Yield strength (X_5), MPa	1050	250	Lognormal

bly small. The results of bivariate and trivariate PDD approximations confirm that the univariate solution by either the direct or sequential PDD method is valid and adequate. However, the numbers of function evaluations step up for higher-variate PDD approximations, as expected. When the sequential PDD method is employed, the respective numbers of function evaluations diminish by a factor of approximately two, regardless of the PDD approximation. While this reduction is not as dramatic as the one found in the single-step PDD method (Example 1), the sequential PDD method should still greatly improve the current state of the art of robust design.

Since this problem was also solved by the TPQ and Taylor series methods, comparing their reported solutions [14], listed in the last two columns of Table 4.4, with the PDD solutions should be intriguing. It appears that the TPQ method is also capable of producing a similar optimal solution, but by incurring a computational cost more than most of the PDD methods examined in this work. Comparing the numbers of function evaluations, the TPQ method is more expensive than the univariate direct PDD method by factors of three to seven. These factors grow into seven to 17 when graded against the univariate sequential PDD method. The Tay-

lor series method needs only 378 function evaluations, which is slightly more than 288 function evaluations by the univariate sequential PDD, but it violates the first constraint by at least six times more than all PDD and TPQ methods.

Table 4.4: Optimization results for the two-bar truss problem ($m = 2$, $n = 3$)

Results	Method							
	Direct PDD (Univariate)	Direct PDD (Bivariate)	Direct PDD (Trivariate)	Sequential PDD (Univariate)	Sequential PDD (Bivariate)	Sequential PDD (Trivariate)	TPQ[a]	Taylor series[a]
$\tilde{d}_1^*$, cm^2	11.4749	11.5561	11.5561	11.4811	11.5710	11.5714	11.5669	10.9573
$\tilde{d}_2^*$, m	0.3781	0.3791	0.3791	0.3777	0.3753	0.3752	0.3767	0.3770
$c_0(\tilde{\mathbf{d}}^*)$[b]	1.2300	1.2392	1.2391	1.2306	1.2392	1.2392	1.2393	1.1741
$c_1(\tilde{\mathbf{d}}^*)$[b]	0.0172	0.0096	0.0096	0.0167	0.0097	0.0096	0.0095	0.0657
$c_2(\tilde{\mathbf{d}}^*)$[b]	-0.4882	-0.4911	-0.4910	-0.4889	-0.4948	-0.4950	-0.4935	-0.4650
$\mathbb{E}_{\tilde{\mathbf{d}}^*}[y_0(\mathbf{X})]$, kg[b]	12.2684	12.3591	12.3591	12.2732	12.3589	12.3598	12.3608	11.7105
$\sqrt{\text{var}_{\tilde{\mathbf{d}}^*}[y_0(\mathbf{X})]}$, kg[b]	2.4666	2.4851	2.4851	2.4677	2.4849	2.4850	2.4852	2.3542
No. of iterations	19	14	14	8	7	7	10	8
No. of y_0 evaluations	190	518	896	80	259	448	594	108
Total no. of y_1 & y_2 evaluations	494	1876	4900	208	938	2450	3564	270

[a] The results of TPQ (DSA) and Taylor series were obtained from Lee *et al.* [14].
[b] The objective and constraint functions, $\mathbb{E}_{\tilde{\mathbf{d}}^*}[y_0(\mathbf{X})]$, and $\sqrt{\text{var}_{\tilde{\mathbf{d}}^*}[y_0(\mathbf{X})]}$ at respective optima, were evaluated by crude MCS (10^8 samples).

When the expansion order and the number of Gauss-quadrature points are increased to $m = 3$ and $n = 4$, respectively, the corresponding optimization results by all PDD, TPQ, and Taylor series methods are summarized in Table 4.5. The optimal solutions do not change greatly and, therefore, the results of Table 4.4 are adequate. However, the numbers of function evaluations rise for each method, as they

should for larger m or n. In which case, the univariate PDD methods are even more efficient than the TPQ method by orders of magnitude.

Table 4.5: Optimization results for the two-bar truss problem ($m = 3$, $n = 4$)

Results	Method							
	Direct PDD (Univariate)	Direct PDD (Bivariate)	Direct PDD (Trivariate)	Sequential PDD (Univariate)	Sequential PDD (Bivariate)	Sequential PDD (Trivariate)	TPQ[a]	Taylor series[a]
$\tilde{d}_1^*$, cm^2	11.5516	11.6439	11.6439	11.5650	11.6505	11.6498	11.6476	10.9573
$\tilde{d}_2^*$, m	0.3805	0.3779	0.3779	0.3754	0.3763	0.3763	0.3767	0.3770
$c_0(\tilde{\mathbf{d}}^*)$[b]	1.2393	1.2481	1.2481	1.2386	1.2481	1.2481	1.2480	1.1741
$c_1(\tilde{\mathbf{d}}^*)$[b]	0.0095	0.0024	0.0025	0.0101	0.0024	0.0024	0.0025	0.0657
$c_2(\tilde{\mathbf{d}}^*)$[b]	-0.4897	-0.4959	-0.4958	-0.4945	-0.4974	-0.4974	-0.4970	-0.4650
$\mathbb{E}_{\tilde{\mathbf{d}}^*}[y_0(\mathbf{X})]$[b], kg	12.3597	12.4480	12.4480	12.3538	12.4482	12.4477	12.4464	11.7150
$\sqrt{\mathrm{var}_{\tilde{\mathbf{d}}^*}[y_0(\mathbf{X})]}$[b], kg	2.4678	2.5025	2.5025	2.4836	2.5029	2.5028	2.5023	2.3542
No. of iterations	15	16	15	7	5	5	10	8
No. of y_0 evaluations	195	976	1875	91	305	625	2503	108
Total no. of y_1 & y_2 evaluations	510	3616	11,070	238	1130	3690	15,018	270

[a] The results of TPQ (DSA) were obtained from Lee *et al.* [14].
[b] The objective and constraint functions, $\mathbb{E}_{\tilde{\mathbf{d}}^*}[y_0(\mathbf{X})]$, and $\sqrt{\mathrm{var}_{\tilde{\mathbf{d}}^*}[y_0(\mathbf{X})]}$ at respective optima, were evaluated by crude MCS (10^8 samples).

4.4.3   Example 3: shape design of a three-hole bracket

The third example involves shape design optimization of a two-dimensional, three-hole bracket, where nine random shape parameters, X_i, $i = 1, \cdots, 9$, describe its inner and outer boundaries, while maintaining symmetry about the central vertical axis. The design variables, $d_k = \mathbb{E}_{\mathbf{d}}[X_k]$, $i = 1, \cdots, 9$, are the means of these

independent random variables with Figure 4.4(a) depicting the initial design of the bracket geometry at the mean values of the shape parameters. The bottom two holes are fixed, and a deterministic horizontal force $F = 15,000$ N is applied at the center of the top hole. The bracket material has a deterministic mass density $\rho = 7810$ kg/m^3, deterministic elastic modulus $E = 207.4$ GPa, deterministic Poisson's ratio $\nu = 0.3$, and deterministic uniaxial yield strength $S_y = 800$ MPa. The objective is to minimize the second-moment properties of the mass of the bracket by changing the shape of the geometry such that the maximum von Mises stress $\sigma_{e,\max}(\mathbf{X})$ does not exceed the yield strength S_y of the material with 99.875% probability if y_1 is Gaussian. Mathematically, the RDO for this problem is defined to

$$
\begin{aligned}
\min_{\mathbf{d} \in \mathcal{D}} \quad c_0(\mathbf{d}) \;&=\; 0.5 \frac{\mathbb{E}_{\mathbf{d}}\left[y_0(\mathbf{X})\right]}{\mathbb{E}_{\mathbf{d}_0}\left[y_0(\mathbf{X})\right]} + 0.5 \frac{\sqrt{\operatorname{var}_{\mathbf{d}}\left[y_0(\mathbf{X})\right]}}{\sqrt{\operatorname{var}_{\mathbf{d}_0}\left[y_0(\mathbf{X})\right]}}, \\
\text{subject to} \quad c_1(\mathbf{d}) \;&=\; 3\sqrt{\operatorname{var}_{\mathbf{d}}\left[y_1(\mathbf{X})\right]} - \mathbb{E}_{\mathbf{d}}\left[y_1(\mathbf{X})\right] \leq 0, \\
0 \text{ mm} \leq \; d_1 \;&\leq 14 \text{ mm}, \; 17 \text{ mm} \leq d_2 \leq 35 \text{ mm}, \\
10 \text{ mm} \leq \; d_3 \;&\leq 30 \text{ mm}, \; 30 \text{ mm} \leq d_4 \leq 40 \text{ mm}, \\
12 \text{ mm} \leq \; d_5 \;&\leq 30 \text{ mm}, \; 12 \text{ mm} \leq d_6 \leq 30 \text{ mm}, \\
50 \text{ mm} \leq \; d_7 \;&\leq 140 \text{ mm}, \; -15 \text{ mm} \leq d_8 \leq 10 \text{ mm}, \\
-8 \text{ mm} \leq \; d_9 \;&\leq 15 \text{ mm},
\end{aligned}
\tag{4.14}
$$

where

$$
y_0(\mathbf{X}) = \rho \int_{\mathcal{D}'(\mathbf{X})} d\mathcal{D}'
\tag{4.15}
$$

and

$$
y_1(\mathbf{X}) = S_y - \sigma_{e,\max}(\mathbf{X})
\tag{4.16}
$$

are two random response functions, and $\mathbb{E}_{\mathbf{d}_0}[y_0(\mathbf{X})]$ and $\mathrm{var}_{\mathbf{d}_0}[y_0(\mathbf{X})]$ are the mean and variance, respectively, of y_0 at the initial design $\mathbf{d}_0 = (0, 30, 10, 40, 20, 20, 75, 0, 0)^T$ mm of the design vector $\mathbf{d} = (d_1, \cdots, d_9)^T \in \mathcal{D} \subset \mathbb{R}^9$. The corresponding mean and standard deviation of y_0 of the original design, calculated by first-order bivariate PDD method, are 0.3415 kg and 0.00140 kg, respectively. Figure 4.4(b) portrays the contours of the von Mises stress calculated by FEA of the initial bracket design, which comprises 11,908 nodes and 3914 eight-noded quadrilateral elements. A plane stress condition was assumed. The approximate optimal solution is denoted by $\tilde{\mathbf{d}}^* = (\tilde{d}_1^*, \cdots, \tilde{d}_9^*)^T$.
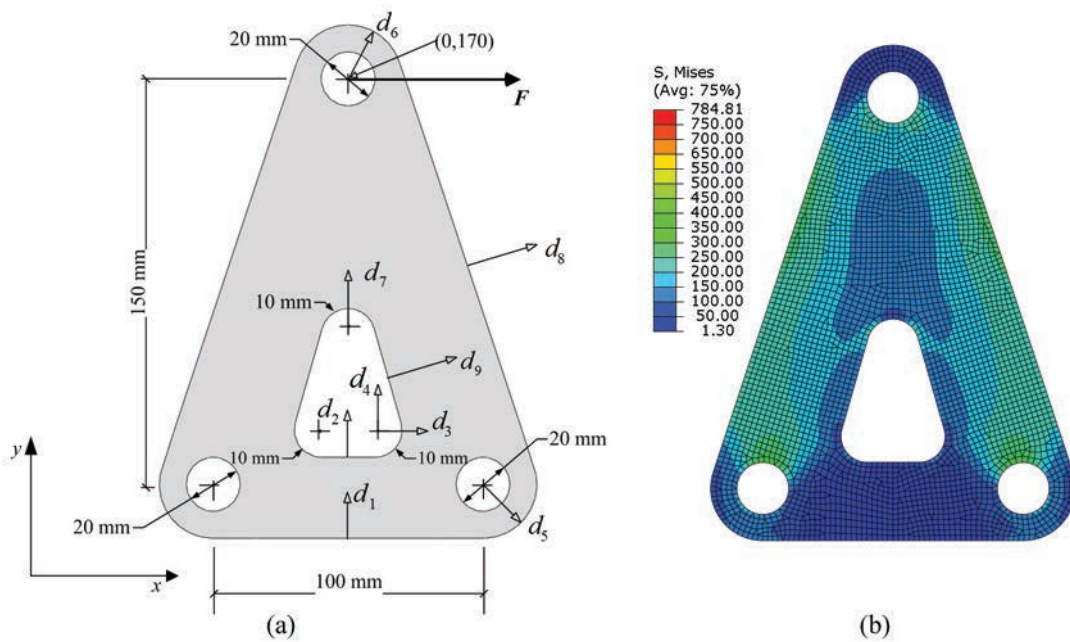
Figure 4.4: A three-hole bracket; (a) design parametrization; (b) von Mises stress at initial design

Due to their finite bounds, the random variables X_i, $i = 1, \cdots, N$, were assumed to follow truncated Gaussian distributions with densities

$$f_{X_i}(x_i) = \begin{cases} \dfrac{\phi(\frac{x_i - d_i}{\sigma_i})}{\Phi(D_i) - \Phi(-D_i)}, & a_i \leq x_i \leq b_i, \\ \\ 0, & \text{otherwise,} \end{cases} \tag{4.17}$$

where $\Phi(\cdot)$ and $\phi(\cdot)$ are the cumulative distribution and probability density functions, respectively, of a standard Gaussian variable; $\sigma_i = \sqrt{\text{var}_{\mathbf{d}}[X_i]} = \sqrt{\mathbb{E}_{\mathbf{d}}[(X_i - d_i)^2]} = 0.2$ is the standard deviation of X_i; and $a_i = d_i - D_i$ and $b_i = d_i + D_i$ are the lower and upper bounds, respectively, of X_i. To avoid unrealistic designs, the bounds were chosen to satisfy the following nine conditions: (1) $D_1 = (d_2 - d_1 - 1)/2$; (2) $D_2 = \max[\min\{(d_7 - d_2 - 2)/2, (d_4 - d_2 - 2)/2\}, 2\sigma_2]$; (3) $D_3 = \min\{(d_3 - 2)/2, (30 - d_3 - 2)/2\}$; (4) $D_4 = \min\{(d_7 - d_4 - 2)/2, (d_4 - d_1 - 2)/2\}$; (5) $D_5 = (d_5 - 11)/2$; (6) $D_6 = (d_6 - 11)/2$; (7) $D_7 = \min\{(d_7 - d_4 - 2)/2, (150 - d_7 - 5)/2\}$; (8) $D_8 = \max\{(25.57 + d_8 - d_9)/2, 2\sigma_8\}$; and (9) $D_9 = \max[\min\{(25.57 + d_8 - d_9)/2, (12.912 + d_9)/2\}, 2\sigma_9]$. These conditions are consistent with the bound constraints of design variables stated in Equation (4.14).

The proposed multi-point single-step PDD method was applied to solve this problem, employing three univariate and one bivariate PDD approximations for the underlying stochastic analysis: (1) $S = 1$, $m = 1$; (2) $S = 1$, $m = 2$; (3) $S = 1$, $m = 3$; and (4) $S = 2$, $m = 1$. Table 4.6 summarizes the optimization results by all four choices of the truncation parameters. The optimal design solutions rapidly converge as S or m increases. The univariate, first-order ($S = 1$, $m = 1$) PDD method, which is the most economical method, produces an optimal solution reasonably close

to those obtained from higher-order or bivariate PDD methods. For instance, the largest deviation from the average values of the objective function at four optimum points is only 2.5 percent. It is important to note that the coupling between single-step PDD and multi-point approximation is essential to find optimal solutions of this practical problem using low-variate, low-order PDD approximations.

Table 4.6: Optimization results for the three-hole bracket

Results	Multi-Point Single-Step PDD Method			
	Univariate $(S=1, m=1)$	Univariate $(S=1, m=2)$	Univariate $(S=1, m=3)$	Bivariate $(S=2, m=1)$
$\tilde{d}_1^*$, mm	12.8168	13.6828	13.9996	13.9936
$\tilde{d}_2^*$, mm	17.0112	17.0071	17.5236	17.0133
$\tilde{d}_3^*$, mm	26.6950	28.3935	28.8053	28.6254
$\tilde{d}_4^*$, mm	30.1908	30.2860	30.0009	30.0083
$\tilde{d}_5^*$, mm	12.0069	12.0003	12.0000	12.0000
$\tilde{d}_6^*$, mm	12.0003	12.0000	12.0000	12.0000
$\tilde{d}_7^*$, mm	118.1200	118.0900	117.4930	117.7929
$\tilde{d}_8^*$, mm	-13.7400	-13.8900	-13.8680	-13.9053
$\tilde{d}_9^*$, mm	14.9124	14.9573	14.9991	14.9966
$\tilde{c}_0(\tilde{\mathbf{d}}^*)$[a]	0.6686	0.6430	0.6364	0.6602
$\tilde{c}_1(\tilde{\mathbf{d}}^*)$[a]	-1.6671	-0.8289	-1.8599	-8.8978
$\mathbb{E}_{\tilde{\mathbf{d}}^*}[y_0(\mathbf{X})]$,[a] kg	0.1230	0.1185	0.1181	0.1176
$\sqrt{\text{var}_{\tilde{\mathbf{d}}^*}[y_0(\mathbf{X})]}$,[a] kg	0.00137	0.00132	0.00130	0.00137
No. of iterations	42	43	36	39
No. of FEA	798	1204	1332	6357

[a] The objective and constraint functions, $\mathbb{E}_{\tilde{\mathbf{d}}^*}[y_0(\mathbf{X})]$, and $\sqrt{\text{var}_{\tilde{\mathbf{d}}^*}[y_0(\mathbf{X})]}$ at respective optima, were evaluated by respective approximations.
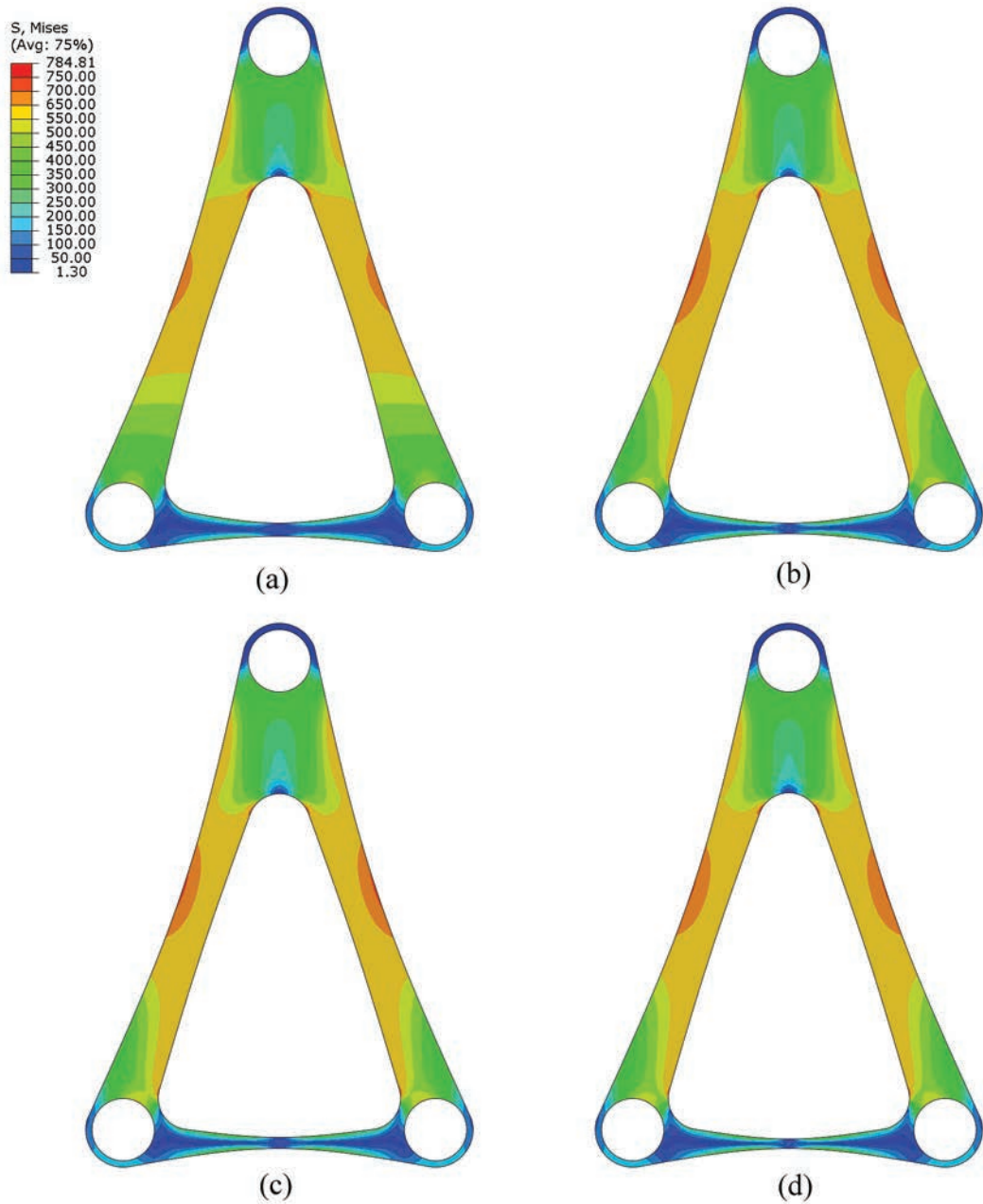
Figure 4.5: von Mises stress contours at mean values of optimal bracket designs by the multi-point single-step PDD method; (a) univariate approximation ($S = 1$, $m = 1$); (b) univariate approximation ($S = 1$, $m = 2$); (c) univariate approximation($S = 1$, $m = 3$); (d) bivariate approximation ($S = 2$, $m = 1$)

Figures 4.5(a) through 4.5(d) illustrate the contour plots of the von Mises

stress for the four optimal designs at the mean values of random shape parameters. Regardless of S or m, the overall area of an optimal design has been substantially reduced, mainly due to significant alteration of the inner boundary and moderate alteration of the outer boundary of the bracket. All nine design variables have undergone moderate to significant changes from their initial values. The optimal masses of the bracket vary as 0.1230 kg, 0.1185 kg, 0.1181 kg, and 0.1186 kg − about a 65 percent reduction from the initial mass of 0.3415 kg. Compared with the conservative design in Figure 4(b), larger stresses − for example, 800 MPa − are safely tolerated by the final designs in Figures 4.5(a) through 4.5(d).

4.4.4   Example 4: shape design of a lever arm

The final example demonstrates the usefulness of the RDO methods advocated in designing an industrial-scale mechanical component, known as a lever arm, commonly found in wheel loaders, as shown in Figure 4.6(a). Twenty-two random shape parameters, X_i, $i = 1, \cdots, 22$, resulting from manufacturing variability, describe the shape of a lever arm in three dimensions, including two rounded quadrilateral holes introduced to reduce the mass of the lever arm as much as possible. The design variables, $d_k = \mathbb{E}_{\mathbf{d}}[X_k]$, $k = 1, \cdots, 22$, are the means of these independent random variables, with Figures 4.6(b) and 4.6(c) depicting the initial design of the lever arm geometry at mean values of the shape parameters. The centers of the central and right circular holes are fixed, and a deterministic horizontal force, $F = 1600$ kN, was applied at the center of the left circular hole with a 71.5° angle from the horizontal

line, as shown in Figure 6(b). These boundary conditions are determined from the interaction of the lever arm with other mechanical components of the wheel loader. The lever arm is made of cast steel with deterministic material properties, as follows: mass density $\rho = 7800$ kg/m^3, elastic modulus $E = 203$ GPa, Poisson's ratio $\nu = 0.3$, fatigue strength coefficient $\sigma'_f = 1332$ MPa, fatigue strength exponent $b = -0.1085$, fatigue ductility coefficient $\epsilon'_f = 0.375$, and fatigue ductility exponent $c = -0.6354$. The performance of the lever arm was determined by its fatigue durability obtained by (1) calculating maximum principal strain and mean stress at a point; and (2) calculating the fatigue crack-initiation life at that point from the well-known Coffin-Manson-Morrow equation [108]. The objective is to minimize the second-moment properties of the mass of the lever arm by changing the shape of the geometry such that the minimum fatigue crack-initiation life $N_{\min}(\mathbf{X})$ exceeds a design threshold of $N_c = 10^6$ loading cycles with 99.875% probability if y_1 is Gaussian. Mathematically,

the RDO for this problem is defined to

$$\min_{\mathbf{d} \in \mathcal{D}} \ c_0(\mathbf{d}) = 0.5 \frac{\mathbb{E}_{\mathbf{d}}\left[y_0(\mathbf{X})\right]}{\mathbb{E}_{\mathbf{d}_0}\left[y_0(\mathbf{X})\right]} + 0.5 \frac{\sqrt{\mathrm{var}_{\mathbf{d}}\left[y_0(\mathbf{X})\right]}}{\sqrt{\mathrm{var}_{\mathbf{d}_0}\left[y_0(\mathbf{X})\right]}},$$

$$\text{subject to} \quad c_1(\mathbf{d}) = 3\sqrt{\mathrm{var}_{\mathbf{d}}\left[y_1(\mathbf{X})\right]} - \mathbb{E}_{\mathbf{d}}\left[y_1(\mathbf{X})\right] \leq 0,$$

$$382 \text{ mm} \leq d_1 \leq 458 \text{ mm}, \ 532 \text{ mm} \leq d_2 \leq 563 \text{ mm},$$

$$1075 \text{ mm} \leq d_3 \leq 1185 \text{ mm}, \ 152 \text{ mm} \leq d_4 \leq 178 \text{ mm},$$

$$305 \text{ mm} \leq d_5 \leq 795 \text{ mm}, \ 55 \text{ mm} \leq d_6 \leq 357.5 \text{ mm},$$

$$241 \text{ mm} \leq d_7 \leq 630 \text{ mm}, \ 435 \text{ mm} \leq d_8 \leq 689 \text{ mm},$$

$$241 \text{ mm} \leq d_9 \leq 630 \text{ mm}, \ 850 \text{ mm} \leq d_{10} \leq 1023 \text{ mm}, \qquad (4.18)$$

$$818 \text{ mm} \leq d_{11} \leq 1131 \text{ mm}, \ 850 \text{ mm} \leq d_{12} \leq 1013 \text{ mm},$$

$$818 \text{ mm} \leq d_{13} \leq 1131 \text{ mm}, \ 702 \text{ mm} \leq d_{14} \leq 748 \text{ mm},$$

$$637 \text{ mm} \leq d_{15} \leq 755 \text{ mm}, \ 816 \text{ mm} \leq d_{16} \leq 888 \text{ mm},$$

$$637 \text{ mm} \leq d_{17} \leq 755 \text{ mm}, \ 1006 \text{ mm} \leq d_{18} \leq 1116 \text{ mm},$$

$$239 \text{ mm} \leq d_{19} \leq 447 \text{ mm}, \ 947 \text{ mm} \leq d_{20} \leq 1097 \text{ mm},$$

$$257 \text{ mm} \leq d_{21} \leq 447 \text{ mm}, \ 505 \text{ mm} \leq d_{22} \leq 833 \text{ mm},$$

where

$$y_0(\mathbf{X}) = \rho \int_{\mathcal{D}'(\mathbf{X})} d\mathcal{D}' \qquad (4.19)$$

and

$$y_1(\mathbf{X}) = N_{\min}(\mathbf{X}) - N_c \qquad (4.20)$$

are two random response functions, and $\mathbb{E}_{\mathbf{d}_0}[y_0(\mathbf{X})]$ and $\mathrm{var}_{\mathbf{d}_0}[y_0(\mathbf{X})]$ are the mean and variance, respectively, of y_0 at the initial design $\mathbf{d}_0 = (450, 562, 1075, 170, 795, 365, 630,$

$689, 630, 850, 818, 850, 818, 748, 637, 888, 637, 1006, 447, 947, 447, 833)^T$ mm of the design vector $\mathbf{d} = (d_1, \cdots, d_{22})^T \in \mathcal{D} \subset \mathbb{R}^{22}$. Figure 4.7 portrays the FEA mesh for the initial lever-arm design, which comprises 126,392 nodes and 75,114 ten-noded, quadratic, tetrahedral elements.

As in Example 3, the random variables X_i, $i = 1, \cdots, 22$, are truncated Gaussian and have probability densities described by Equation (4.17) with $a_i = d_i - D_i$ and $b_i = d_i + D_i$ denoting the lower and upper bounds, respectively. To avoid unrealistic designs, $D_i = 2$ when $i = 1, 2, 4, 14, 16$, and $D_i = 5$ otherwise.

The proposed multi-point single-step PDD method was applied to solve this lever-arm design problem employing only a univariate, first-order PDD approximation, that is, selecting $S = 1$, $m = 1$, for second-moment analyses of y_0 and y_1. Figures 4.8(a) through 4.8(d) show the contour plots of the logarithm of fatigue crack-initiation life at mean shapes of several design iterations, including the initial design, throughout the RDO process. Due to a conservative initial design, with fatigue life contour depicted in Figure 8(a), the minimum fatigue crack-initiation life of 1.068×10^{12} cycles is much larger than the required fatigue crack-initiation life of a million cycles. For the tolerance and subregion size parameters selected, 15 iterations and 675 FEA led to a final optimal design with the corresponding mean shape presented in Figure 8(d). The mean optimal mass of the lever arm is 1263 kg − about a 79 percent reduction from the initial mass of 6036 kg. Correspondingly, the standard deviation of the mass drops from 2.1031 kg to 1.8016 kg.
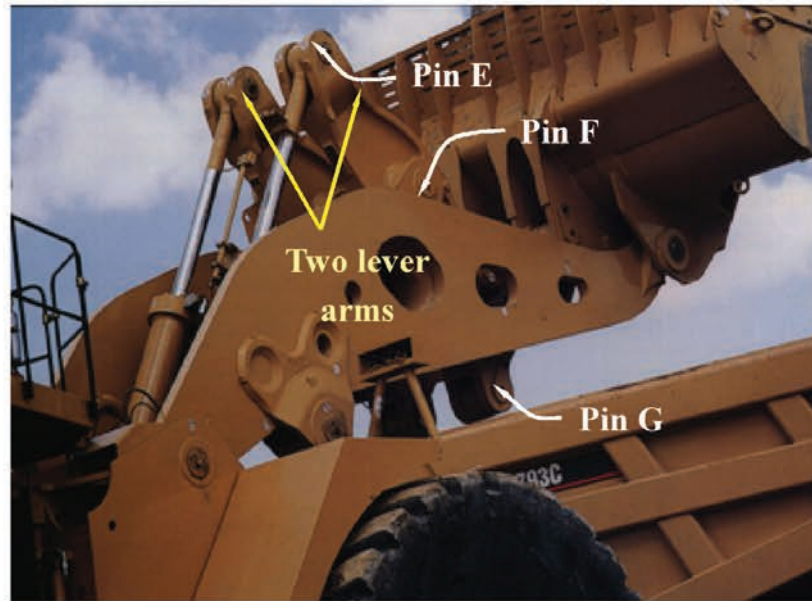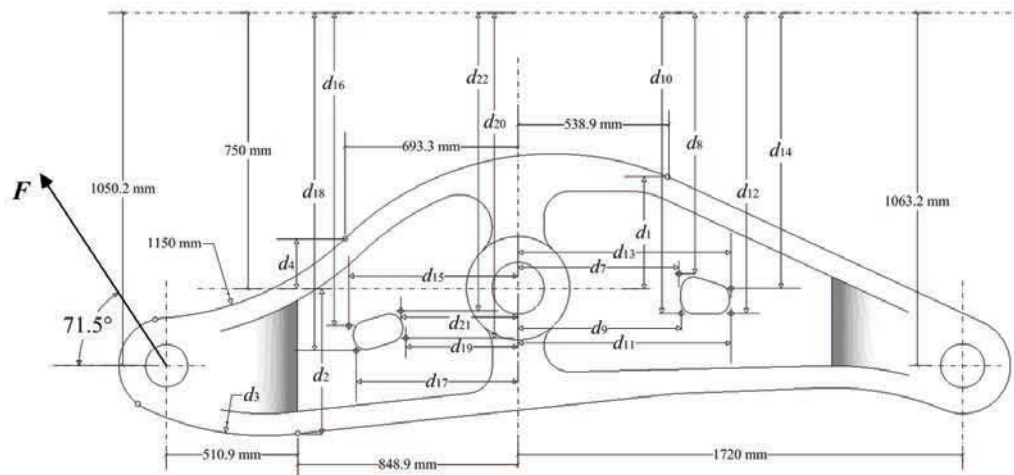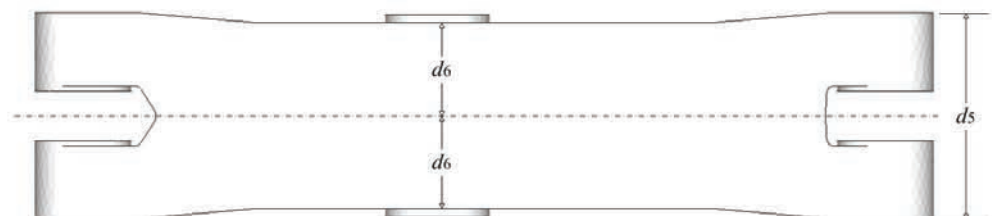
Figure 4.6: Fatigue durability analysis of a lever arm in a wheel loader; (a) two lever arms; (b) design parametrization in front view; (c) design parametrization in top view

Figure 4.7: An FEA mesh of a lever arm

Figures 4.9(a) through 4.9(d) present the iteration histories of the objective function, constraint function, and 22 design variables during the RDO process. The objective function c_0 is reduced from 0.9838 at initial design to 0.5238 at optimal design, an almost 50 percent change. At optimum, the constraint function c_1 is -0.0342×10^6 cycles and is, therefore, close to being active. The design variables d_5, d_6, d_7, d_9, d_{19}, and d_{21} have undergone the most significant changes from their initial values, prompting substantial modifications of the shapes or sizes of the rounded quadrilateral holes and thickness of the lever arm. The outer boundaries of the profile of the lever arm, controlled by the design variables d_1, d_2, d_3, and d_4 have undergone slight changes because the initial design used is the result of a traditional deterministic optimization. This final example demonstrates that the RDO methods developed – in particular, the multi-point single-step PDD method – are capable of solving industrial-scale engineering design problems using only a few hundred FEA.
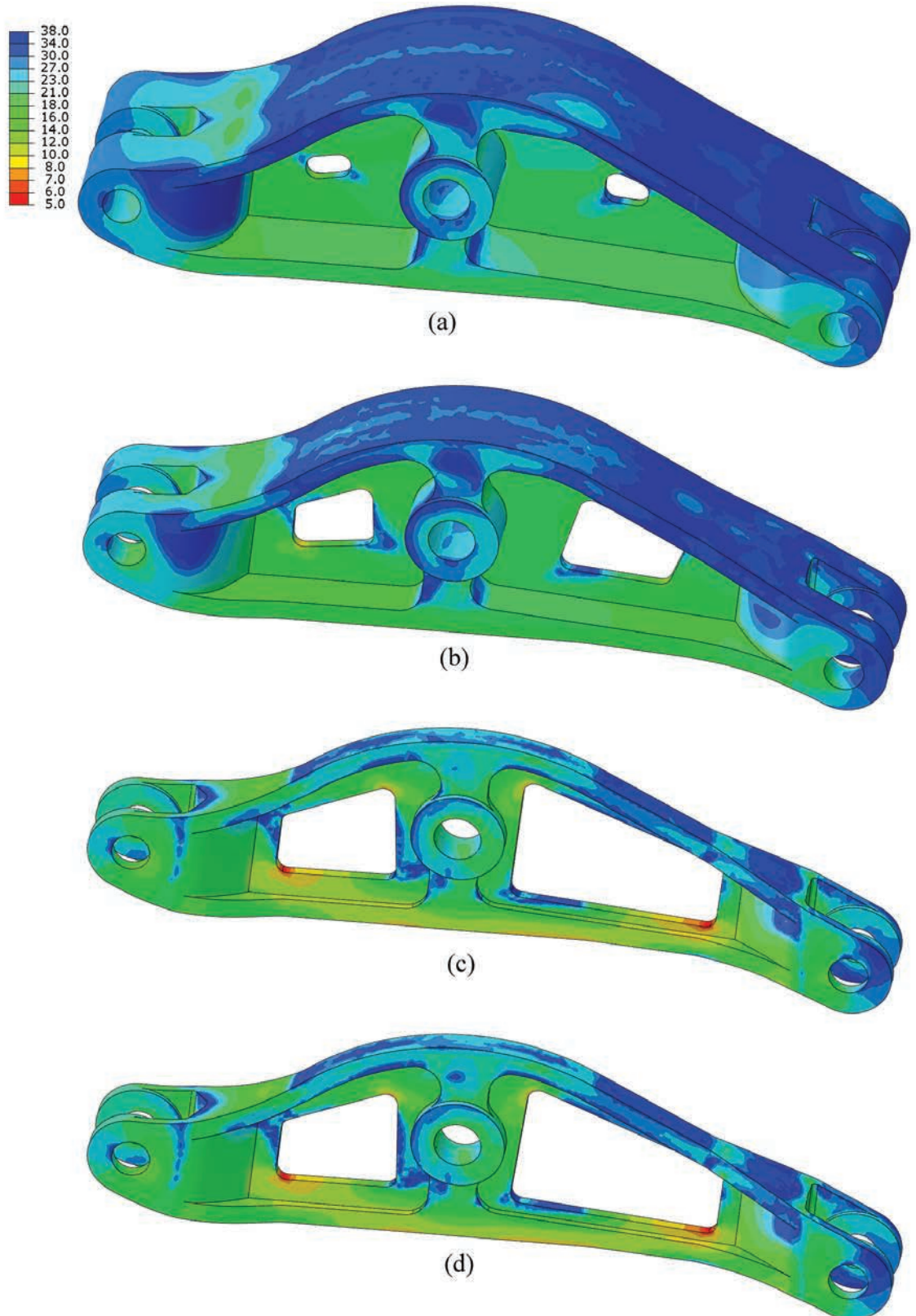
Figure 4.8: Contours of logarithmic fatigue crack-initiation life at mean shapes of the lever arm by the multi-point single-step PDD method; (a) iteration 1; (b) iteration 3; (c) iteration 9; (d) iteration 15 (optimum)

Table 4.7 lists percentage changes in the mean and standard deviation of y_0 from initial to optimal designs in all four examples. The second-moment statistics at optimal designs are averages of all PDD solutions described earlier. Due to robust design, the largest reduction of the mean is 78.81 percent, whereas the standard deviation diminishes by at most 93.80 percent. The moderate drop in the standard deviations of Examples 2-4 is attributed to the objective function that combines both the mean and standard deviation of y_0.
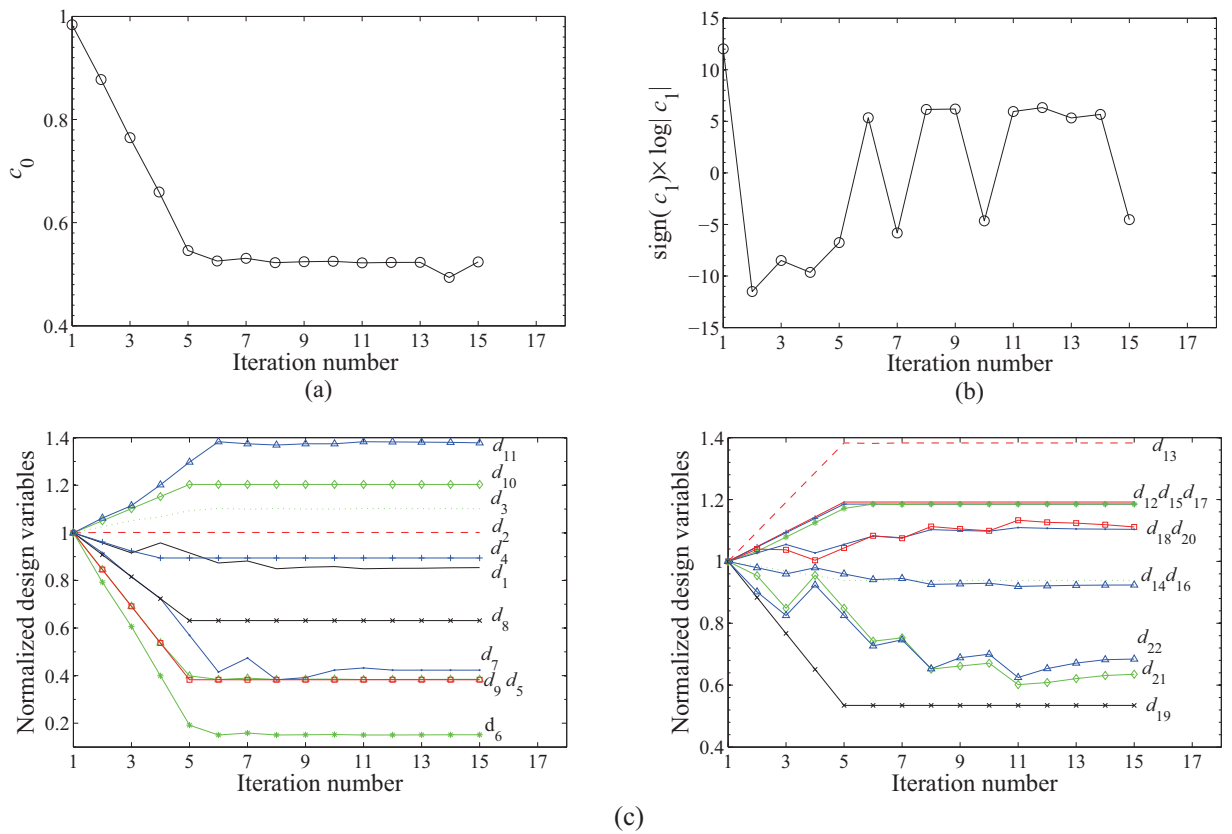
Figure 4.9: RDO iteration histories for the lever arm; (a) objective function; (b) constraint function; (c) normalized design variables; note: design variables are normalized with respect to their initial values

Table 4.7: Reductions in the mean and standard deviation of y_0 from initial to optimal designs.

Example	$\dfrac{\mathbb{E}_{\tilde{\mathbf{d}}^*}[y_0(\mathbf{X})]-\mathbb{E}_{\mathbf{d}_0}[y_0(\mathbf{X})]}{\mathbb{E}_{\mathbf{d}_0}[y_0(\mathbf{X})]}$	$\dfrac{\sqrt{\mathrm{var}_{\tilde{\mathbf{d}}^*}[y_0(\mathbf{X})]}-\sqrt{\mathrm{var}_{\mathbf{d}_0}[y_0(\mathbf{X})]}}{\sqrt{\mathrm{var}_{\mathbf{d}_0}[y_0(\mathbf{X})]}}$
$1^{(a)}$	Not applicable	-93.80%
$2^{(b)}$	-12.51%	-12.66%
$3^{(c)}$	-65.07%	-4.35%
4	-78.81%	-14.34%

[a] The value of $\mathbb{E}_{\tilde{\mathbf{d}}^*}[y_0(\mathbf{X})]$ and $\sqrt{\mathrm{var}_{\tilde{\mathbf{d}}^*}[y_0(\mathbf{X})]}$ is the average of all corresponding PDD results in Table 4.2.

[b] The value of $\mathbb{E}_{\tilde{\mathbf{d}}^*}[y_0(\mathbf{X})]$ and $\sqrt{\mathrm{var}_{\tilde{\mathbf{d}}^*}[y_0(\mathbf{X})]}$ is the average of all corresponding PDD results in Tables 4.4 and 4.5.

[c] The value of $\mathbb{E}_{\tilde{\mathbf{d}}^*}[y_0(\mathbf{X})]$ and $\sqrt{\mathrm{var}_{\tilde{\mathbf{d}}^*}[y_0(\mathbf{X})]}$ is the average of all corresponding PDD results in Table 4.6.

4.5 Discussion

Since multiple methods and examples are presented in the chapter, it is useful to summarize the efficiency and applicability of each method under different conditions. Table 4.8 presents such a summary, including a few qualitative comments inspired by the examples of the preceding section. Furthermore, the numerical results indicate the following:

(1) The direct and single-step PDD methods generate identical optimal solutions for the polynomial functions, but the latter method is substantially more efficient than the former method.

(2) The direct and sequential PDD methods, both employing univariate, bivariate, and trivariate PDD approximations, produce very close optimal solutions for the non-polynomial functions, but at vastly differing expenses. For either

method, the univariate solution is accurate and most economical, even though the stochastic responses are multivariate functions. Given a PDD approximation, the sequential PDD method furnishes an optimal solution incurring at most half the computational cost of the direct PDD method.

(3) For both polynomial and non-polynomial functions, the TPQ method, although accurate, is more expensive than most variants of the direct, single-step, and sequential PDD methods examined. Considering the non-polynomial functions, the univariate direct PDD and univariate sequential PDD methods are more economical than the TPQ method by an order of magnitude or more.

(4) The multi-point single-step PDD method employing low-variate or low-order PDD approximations, including a univariate, first-order PDD approximation, is able to solve practical engineering problems with a reasonable computational effort.

Table 4.8: Efficiency and applicability of the four proposed methods

Method	Efficiency	Applicability	Comments
Direct PDD	Low	Both polynomial and non-polynomial functions with small design spaces	Expensive due to recalculation of expansion coefficients. Impractical for complex system designs.
Single-Step PDD	Highest	Low-order polynomial functions with small design spaces	Highly economical due to recycling of expansion coefficients, but may produce premature solutions for complex system designs.
Sequential PDD	Medium	Polynomial or non-polynomial functions with small to medium design spaces	More expensive than single-step PDD, but substantially more economical than direct PDD. May require high-variate and high-order PDD approximations for complex system designs.
Multi-point Single-Step PDD	High	Polynomial or non-polynomial functions with large design spaces	Capable of solving complex, practical design problems using low-variate and/or low-order PDD approximations.

4.6   Conclusion

Four new methods are proposed for robust design optimization of complex engineering systems. The methods involve PDD of a high-dimensional stochastic response for statistical moment analysis, a novel integration of PDD and score functions for calculating the second-moment sensitivities with respect to the design variables, and standard gradient-based optimization algorithms, encompassing direct, single-step, sequential, and multi-point single-step design processes. Because they are rooted in ANOVA dimensional decomposition, the PDD approximations for arbitrary truncations predict the exact mean and generate a convergent sequence of variance approximations for any square-integrable function. When blended with score functions, PDD leads to explicit formulae, expressed in terms of the expansion coefficients, for approximating the second-moment design sensitivities that are also theoretically convergent. More importantly, the statistical moments and design sensitivities are both determined concurrently from a single stochastic analysis or simulation.

Among the four design methods developed, the direct PDD method is the simplest of all, but requires re-calculations of the expansion coefficients at each design iteration and is, therefore, expensive, depending on the cost of evaluating the objective and constraint functions and the requisite number of design iterations. The single-step PDD method eliminates the need to re-calculate the expansion coefficients from scratch by recycling the old expansion coefficients, consequently holding the potential to significantly curtail the computational effort. However, it depends heavily on the quality of a PDD approximation and the accuracy of the estimated expansion

coefficients during design iterations. The sequential PDD method upholds the merits of both the direct and single-step PDD methods by re-calculating the expansion coefficients a few times more than the single-step PDD, incurring a computational complexity that is lower than the direct PDD method. However, all three methods just described are global and may not work if the design space is too large for a PDD approximation, with a chosen degree of interaction or expansion order, to be sufficiently accurate. The multi-point single-step PDD method mitigates this problem by adopting a local implementation of PDD approximations, where an RDO problem with a large design space is solved in succession. Precisely for this reason, the method is capable of solving practical engineering problems using low-order and/or low-variate PDD approximations of stochastic responses.

CHAPTER 5
RELIABILITY-BASED DESIGN OPTIMIZATION

5.1   Introduction

This chapter presents two new methods — the adaptive-sparse PDD-saddlepoint approximation (SPA), or AS-PDD-SPA, method and the adaptive-sparse PDD-Monte Carlo simulation (MCS), or AS-PDD-MCS, method — for reliability-based design optimization of complex engineering systems. Both methods are based on (1) an adaptive-sparse PDD approximation of a high-dimensional stochastic response for reliability analysis; (2) a novel integration of the adaptive-sparse PDD approximation and score functions for calculating the sensitivities of the failure probability with respect to design variables; and (3) standard gradient-based optimization algorithms, encompassing a multi-point, single-step design process. Section 5.2 formally defines a general RBDO problem, including a concomitant mathematical statement. Section 5.3 starts with a brief exposition of PDD and explains how it leads up to the AS-PDD approximation. Section 5.4 formally introduces the AS-PDD-SPA and AS-PDD-MCS methods for reliability analysis. Exploiting score functions, Section 5.5 explains how the effort required to calculate the failure probability by these two methods also delivers its design sensitivities, sustaining no additional cost. The calculation of PDD expansion coefficients, required for reliability and design sensitivity analysis, is discussed in Section 5.6. Section 5.7 introduces a multi-point, single-step iterative scheme for RBDO and explains how the reliability analysis and design sen-

sitivities from the AS-PDD-SPA and AS-PDD-MCS methods are integrated with a gradient-based optimization algorithm. Section 5.8 presents four numerical examples, including shape design of a 79-dimensional engine bracket problem, to evaluate the accuracy, convergence properties, and computational efforts of the proposed RBDO methods. Finally, the conclusions are drawn in Section 5.9.

5.2 Reliability-Based Design Optimization

Consider a measurable space $(\Omega_{\mathbf{d}}, \mathcal{F}_{\mathbf{d}})$, where $\Omega_{\mathbf{d}}$ is a sample space and $\mathcal{F}_{\mathbf{d}}$ is a σ-field on $\Omega_{\mathbf{d}}$. Defined over $(\Omega_{\mathbf{d}}, \mathcal{F}_{\mathbf{d}})$, let $\{P_{\mathbf{d}} : \mathcal{F} \to [0,1]\}$ be a family of probability measures, where for $M \in \mathbb{N}$ and $N \in \mathbb{N}$, $\mathbf{d} = (d_1, \cdots, d_M)^T \in \mathcal{D}$ is an $\mathbb{R}^M$-valued design vector with non-empty closed set $\mathcal{D} \subseteq \mathbb{R}^M$ and let $\mathbf{X} := (X_1, \cdots, X_N)^T :$ $(\Omega_{\mathbf{d}}, \mathcal{F}_{\mathbf{d}}) \to (\mathbb{R}^N, \mathcal{B}^N)$ be an $\mathbb{R}^N$-valued input random vector with $\mathcal{B}^N$ representing the Borel σ-field on $\mathbb{R}^N$, describing the statistical uncertainties in loads, material properties, and geometry of a complex mechanical system. The probability law of $\mathbf{X}$ is completely defined by a family of the joint probability density functions (PDF) $\{f_{\mathbf{X}}(\mathbf{x}; \mathbf{d}), \mathbf{x} \in \mathbb{R}^N, \mathbf{d} \in \mathcal{D}\}$ that are associated with probability measures $\{P_{\mathbf{d}}, \mathbf{d} \in \mathcal{D}\}$, so that the probability triple $(\Omega_{\mathbf{d}}, \mathcal{F}_{\mathbf{d}}, P_{\mathbf{d}})$ of $\mathbf{X}$ depends on $\mathbf{d}$. A design variable d_k can be any distribution parameter or a statistic — for instance, the mean or standard deviation — of X_i.

Let $y_l(\mathbf{X})$, $l = 1, 2, \cdots, K$, be a collection of $K + 1$ real-valued, square-integrable, measurable transformations on $(\Omega_{\mathbf{d}}, \mathcal{F}_{\mathbf{d}})$, describing the performance functions of a complex system. It is assumed that $y_l : (\mathbb{R}^N, \mathcal{B}^N) \to (\mathbb{R}, \mathcal{B})$ is not an explicit

function of $\mathbf{d}$, although y_l implicitly depends on $\mathbf{d}$ via the probability law of $\mathbf{X}$. This is not a major limitation, as most RBDO problems involve means and/or standard deviations of random variables as design variables. Nonetheless, the mathematical formulation for RBDO in most engineering applications involving an objective function $c_0 : \mathbb{R}^M \to \mathbb{R}$ and probabilistic constraint functions $c_l : \mathbb{R}^M \to \mathbb{R}$, where $l = 1, \cdots, K$ and $1 \leq K < \infty$, requires one to

$$
\begin{aligned}
\min_{\mathbf{d} \in \mathcal{D} \subseteq \mathbb{R}^M} \quad & c_0(\mathbf{d}), \\
\text{subject to} \quad & c_l(\mathbf{d}) := P_{\mathbf{d}}\left[\mathbf{X} \in \Omega_{F,l}(\mathbf{d})\right] - p_l \leq 0, \quad l = 1, \cdots, K, \\
& d_{k,L} \leq d_k \leq d_{k,U}, \ k = 1, \cdots, M,
\end{aligned}
\tag{5.1}
$$

where $\Omega_{F,l}(\mathbf{d})$ is the lth failure domain, $0 \leq p_l \leq 1$ is the lth target failure probability, and $d_{k,L}$ and $d_{k,U}$ are the lower and upper bounds of the kth design variable d_k. The objective function c_0 is commonly prescribed as a deterministic function of $\mathbf{d}$, describing relevant system geometry, such as area, volume, and mass. In contrast, the constraint functions c_l, $l = 1, 2, \cdots, K$, are generally more complicated than the objective function. Depending on the failure domain $\Omega_{F,l}$, a component or a system failure probability can be envisioned. For component reliability analysis, the failure domain is often adequately described by a single performance function $y_l(\mathbf{X})$, for instance, $\Omega_{F,l} := \{\mathbf{x} : y_l(\mathbf{x}) < 0\}$, whereas multiple, interdependent performance functions $y_{l,i}(\mathbf{x})$, $i = 1, 2, \cdots$, are required for system reliability analysis, leading, for example, to $\Omega_{F,l} := \{\mathbf{x} : \cup_i y_{l,i}(\mathbf{x}) < 0\}$ and $\Omega_{F,l} := \{\mathbf{x} : \cap_i y_{l,i}(\mathbf{x}) < 0\}$ for series and parallel systems, respectively. In any case, the evaluation of the failure probability in

Equation (5.1) is fundamentally equivalent to calculating a high-dimensional integral over a complex failure domain.

The evaluation of probabilistic constraints $c_l(\mathbf{d})$, $l = 1, 2, \cdots, K$, requires calculating component or system probabilities of failure defined by respective performance functions. Coupling with gradient-based optimization algorithms mandates that the gradients of $c_l(\mathbf{d})$ also be formulated, thus requiring design sensitivity analysis of failure probability. The focus of this work is to solve a general high-dimensional RBDO problem described by Equation (5.1) for arbitrary functions $y_l(\mathbf{X})$, $l = 1, 2, \cdots, K$, and arbitrary probability distributions of $\mathbf{X}$.

5.3 Polynomial Dimensional Decomposition

Let $y(\mathbf{X}) := y(X_1, \cdots, X_N)$ represent any one of the random functions y_l, $l = 1, \cdots, K$, introduced in Section 2, and let $\mathcal{L}_2(\Omega_{\mathbf{d}}, \mathcal{F}_{\mathbf{d}}, P_{\mathbf{d}})$ represent a Hilbert space of square-integrable functions y with respect to the probability measure $f_{\mathbf{X}}(\mathbf{x}; \mathbf{d})d\mathbf{x}$ supported on $\mathbb{R}^N$. Assuming independent coordinates, the joint probability density function of $\mathbf{X}$ is expressed by the product, $f_{\mathbf{X}}(\mathbf{x}; \mathbf{d}) = \prod_{i=1}^{i=N} f_{X_i}(x_i; \mathbf{d})$, of marginal probability density functions $f_{X_i} : \mathbb{R} \to \mathbb{R}_0^+$ of X_i, $i = 1, \cdots, N$, defined on its probability triple $(\Omega_{i,\mathbf{d}}, \mathcal{F}_{i,\mathbf{d}}, P_{i,\mathbf{d}})$ with a bounded or an unbounded support on $\mathbb{R}$. Then, for a given subset $u \subseteq \{1, \cdots, N\}$, $f_{\mathbf{X}_u}(\mathbf{x}_u; \mathbf{d}) := \prod_{p=1}^{|u|} f_{i_p}(x_{i_p}; \mathbf{d})$ defines the marginal density function of the subvector $\mathbf{X}_u = (X_{i_1}, \cdots, X_{i_{|u|}})^T$ of $\mathbf{X}$.

Let $\{\psi_{ij}(X_i; \mathbf{d}); \ j = 0, 1, \cdots\}$ be a set of univariate orthonormal polynomial basis functions in the Hilbert space $\mathcal{L}_2(\Omega_{i,\mathbf{d}}, \mathcal{F}_{i,\mathbf{d}}, P_{i,\mathbf{d}})$ that is consistent with

the probability measure $P_{i,\mathbf{d}}$ of X_i for a given design $\mathbf{d}$, where $i = 1, \cdots, N$. For a given $\emptyset \neq u = \{i_1, \cdots, i_{|u|}\} \subseteq \{1, \cdots, N\}$, $1 \leq |u| \leq N$, $1 \leq i_1 < \cdots < i_{|u|} \leq N$, denote by $(\times_{p=1}^{p=|u|}\Omega_{i_p,\mathbf{d}}, \times_{p=1}^{p=|u|}\mathcal{F}_{i_p,\mathbf{d}}, \times_{p=1}^{p=|u|}P_{i_p,\mathbf{d}})$ the product probability triple of the subvector $\mathbf{X}_u$. Since the probability density function of $\mathbf{X}_u$ is separable (independent), the product polynomial $\psi_{u\mathbf{j}_{|u|}}(\mathbf{X}_u; \mathbf{d}) := \prod_{p=1}^{|u|} \psi_{i_p j_p}(X_{i_p}; \mathbf{d})$, where $\mathbf{j}_{|u|} = (j_1, \cdots, j_{|u|}) \in \mathbb{N}_0^{|u|}$ is a $|u|$-dimensional multi-index, constitutes an orthonormal basis in $\mathcal{L}_2(\times_{p=1}^{p=|u|}\Omega_{i_p,\mathbf{d}}, \times_{p=1}^{p=|u|}\mathcal{F}_{i_p,\mathbf{d}}, \times_{p=1}^{p=|u|}P_{i_p,\mathbf{d}})$.

The PDD of a square-integrable function y represents a hierarchical expansion [97, 99]

$$y(\mathbf{X}) = y_\emptyset(\mathbf{d}) + \sum_{\emptyset \neq u \subseteq \{1,\cdots,N\}} \sum_{\substack{\mathbf{j}_{|u|} \in \mathbb{N}_0^{|u|} \\ j_1,\cdots,j_{|u|} \neq 0}} C_{u\mathbf{j}_{|u|}}(\mathbf{d})\psi_{u\mathbf{j}_{|u|}}(\mathbf{X}_u; \mathbf{d}), \qquad (5.2)$$

in terms of a set of random multivariate orthonormal polynomials of input variables with increasing dimensions, where

$$y_\emptyset(\mathbf{d}) = \int_{\mathbb{R}^N} y(\mathbf{x}) f_{\mathbf{X}}(\mathbf{x}; \mathbf{d}) d\mathbf{x} \qquad (5.3)$$

and

$$C_{u\mathbf{j}_{|u|}}(\mathbf{d}) := \int_{\mathbb{R}^N} y(\mathbf{x})\psi_{u\mathbf{j}_{|u|}}(\mathbf{x}_u; \mathbf{d}) f_{\mathbf{X}}(\mathbf{x}; \mathbf{d}) d\mathbf{x},$$
$$\emptyset \neq u \subseteq \{1, \cdots, N\}, \mathbf{j}_{|u|} \in \mathbb{N}_0^{|u|}, \qquad (5.4)$$

are various expansion coefficients. The inner sum of Equation (5.2) precludes $j_1, \cdots, j_{|u|} \neq 0$, that is, the individual degree of each variable X_i in $\psi_{u\mathbf{j}_{|u|}}$, $i \in u$, cannot be *zero* since $\psi_{u\mathbf{j}_{|u|}}(\mathbf{X}_u; \mathbf{d})$ is a *zero*-mean strictly $|u|$-variate function. Derived from

the ANOVA dimensional decomposition [62], Equation (5.2) provides an exact representation because it includes all main and interactive effects of input variables. For instance, $|u| = 0$ corresponds to the constant component function $y_\emptyset$, representing the mean effect of y; $|u| = 1$ leads to the univariate component functions, describing the main effects of input variables, and $|u| = S$, $1 < S \leq N$, results in the S-variate component functions, facilitating the interaction among at most S input variables $X_{i_1}, \cdots, X_{i_S}$, $1 \leq i_1 < \cdots < i_S \leq N$. Further details of PDD are available elsewhere [97, 99].

Equation (5.2) contains an infinite number of coefficients, emanating from infinite numbers of orthonormal polynomials. In practice, the number of coefficients must be finite, say, by retaining finite-order polynomials and reduced-degree interaction among input variables. Doing so results in a truncated PDD and concomitant approximation, but there is more than one way to perform the truncation, described as follows.

5.3.1   Truncated PDD approximation

The PDD in Equation (5.2) is grounded on a fundamental conjecture known to be true in many real-world applications: given a high-dimensional function y, its $|u|$-variate component functions decay rapidly with respect to $|u|$, leading to accurate lower-variate approximations of y. Furthermore, the largest order of polynomials in each variable can be restricted to a finite integer. Indeed, given the integers $0 \leq S < N$ and $1 \leq m < \infty$ for all $1 \leq |u| \leq S$ and the ∞-norm $||\mathbf{j}_{|u|}||_\infty := \max\left(j_1, \cdots, j_{|u|}\right)$,

the truncated PDD [97, 99]

$$\tilde{y}_{S,m}(\mathbf{X}) := y_{\emptyset}(\mathbf{d}) + \sum_{\substack{\emptyset \neq u \subseteq \{1, \cdots, N\} \\ 1 \leq |u| \leq S}} \sum_{\substack{\mathbf{j}_{|u|} \in \mathbb{N}_0^{|u|}, \|\mathbf{j}_{|u|}\|_{\infty} \leq m \\ j_1, \cdots, j_{|u|} \neq 0}} C_{u\mathbf{j}_{|u|}}(\mathbf{d}) \psi_{u\mathbf{j}_{|u|}}(\mathbf{X}_u; \mathbf{d}) \qquad (5.5)$$

leads to the S-variate, mth-order PDD approximation, which for $S > 0$ includes interactive effects of at most S input variables $X_{i_1}, \cdots, X_{i_S}$, $1 \leq i_1 < \cdots < i_S \leq N$, on y. It is elementary to show that when $S \to N$ and/or $m \to \infty$, $\tilde{y}_{S,m}$ converges to y in the mean-square sense, generating a hierarchical and convergent sequence of approximations of y. The truncation parameters S and m depend on the dimensional structure and nonlinearity of a stochastic response. The higher the values of S and m, the higher the accuracy, but also the computational cost that is endowed with an Sth-order polynomial computational complexity [97, 99]. The S-variate, mth-order PDD approximation will be referred to as simply *truncated PDD approximation* in this chapter.

5.3.2 Adaptive-Sparse PDD approximation

In practice, the dimensional hierarchy or nonlinearity, in general, is not known *apriori*. Therefore, indiscriminately assigning the truncation parameters S and m is not desirable, nor is it possible to do so when a stochastic solution is obtained via complex numerical algorithms. In which case, one should perform these truncations adaptively by progressively drawing in higher-variate or higher-order contributions as appropriate. Furthermore, given $1 \leq S < N$, all S-variate component functions of PDD may not contribute equally or even appreciably to be considered in the resulting approximation. Therefore, a sparse approximation, expelling component

functions with negligible contributions, is possible. Indeed, addressing these issues, Yadav and Rahman [109] developed two AS-PDD approximations, but they have yet to be exploited for solving RBDO problems.

Based on the author's past experience, an S-variate PDD approximation, where $S \ll N$, is adequate, when solving real-world engineering problems, with the computational cost varying polynomially (S-order) with respect to the number of variables [97, 99]. As an example, consider the selection of $S = 2$ for solving a stochastic problem in 100 dimensions by a bivariate PDD approximation, comprising $100 \times 99/2 = 4950$ bivariate component functions. If all such component functions are included, then the computational effort for even a full bivariate PDD approximation may exceed the computational budget allocated to solving this problem. However, many of these component functions contribute little to the probabilistic characteristics sought and can be safely ignored. Similar conditions may prevail for higher-variate component functions. Henceforth, define an S-variate, partially AS-PDD approximation [109]

$$\bar{y}_S(\mathbf{X}) : = y_\emptyset(\mathbf{d}) + \sum_{\substack{\emptyset \neq u \subseteq \{1,\cdots,N\} \\ 1 \leq |u| \leq S}} \sum_{m_u=1}^{\infty} \sum_{\substack{\left\|\mathbf{j}_{|u|}\right\|_\infty = m_u, j_1,\cdots,j_{|u|} \neq 0 \\ \tilde{G}_{u,m_u} > \epsilon_1, \Delta\tilde{G}_{u,m_u} > \epsilon_2}} C_{u\mathbf{j}_{|u|}}(\mathbf{d})\psi_{u\mathbf{j}_{|u|}}(\mathbf{X}_u;\mathbf{d}) \quad (5.6)$$

of $y(\mathbf{X})$, where

$$\tilde{G}_{u,m_u} : = \frac{1}{\sigma^2(\mathbf{d})} \sum_{\substack{\mathbf{j}_{|u|} \in \mathbb{N}_0^{|u|}, \left\|\mathbf{j}_{|u|}\right\|_\infty \leq m_u \\ j_1,\cdots,j_{|u|} \neq 0}} C_{u\mathbf{j}_{|u|}}^2(\mathbf{d}), \quad m_u \in \mathbb{N}, \ 0 < \sigma^2(\mathbf{d}) < \infty, \quad (5.7)$$

defines the approximate m_uth-order approximation of the global sensitivity index of

$y(\mathbf{X})$ for a subvector $\mathbf{X}_u$, $\emptyset \neq u \subseteq \{1, \cdots, N\}$, of input variables $\mathbf{X}$ and

$$\Delta \tilde{G}_{u,m_u} := \frac{\tilde{G}_{u,m_u} - \tilde{G}_{u,m_u-1}}{\tilde{G}_{u,m_u-1}} \tag{5.8}$$

defines the relative change in the approximate global sensitivity index when the largest polynomial order increases from $m_u - 1$ to m_u, provided that $2 \leq m_u < \infty$ and $\tilde{G}_{u,m_u-1} \neq 0$. Here,

$$\sigma^2(\mathbf{d}) = \sum_{\emptyset \neq u \subseteq \{1, \cdots, N\}} \sum_{\substack{\mathbf{j}_{|u|} \in \mathbb{N}_0^{|u|} \\ j_1, \cdots, j_{|u|} \neq 0}} C_{u\mathbf{j}_{|u|}}^2(\mathbf{d}) \tag{5.9}$$

is the variance of $y(\mathbf{X})$. Then the sensitivity indices $\tilde{G}_{u,m_u}$ and $\Delta \tilde{G}_{u,m_u}$ provide an effective means to truncate the PDD in Equation (5.2) both adaptively and sparsely. Equation (5.6) is attained by subsuming at most S-variate component functions, but fulfilling two inclusion criteria: (1) $\tilde{G}_{u,m_u} > \epsilon_1$ for $1 \leq |u| \leq S \leq N$, and (2) $\Delta \tilde{G}_{u,m_u} > \epsilon_2$ for $1 \leq |u| \leq S \leq N$, where $\epsilon_1 \geq 0$ and $\epsilon_2 \geq 0$ are two non-negative tolerances. The resulting approximation is partially adaptive because the truncations are restricted to at most S-variate component functions of y. When $S = N$, Equation (5.6) becomes the fully AS-PDD approximation [109]. Figure 5.1 presents a computational flowchart to accomplish the numerical implementation of both variants of the AS-PDD approximation. The algorithmic details of the iterative process are available elsewhere [109] and are not included here for brevity.

The S-variate, partially AS-PDD approximation behaves differently from the S-variate, mth-order PDD approximation. While the latter approximation includes a sum containing at most S-variate component functions, the former approximation may or may not include all such component functions, depending on the tolerances

$\epsilon_1 > 0$ and $\epsilon_2 > 0$. It is elementary to show that $\bar{y}_S$ approaches $\tilde{y}_{S,m}$ in the mean-square sense as $\epsilon_1 \to 0, \epsilon_2 \to 0$, and $m \to \infty$. The S-variate, partially adaptive-sparse PDD approximation will be referred to as simply *AS-PDD approximation* in this chapter.
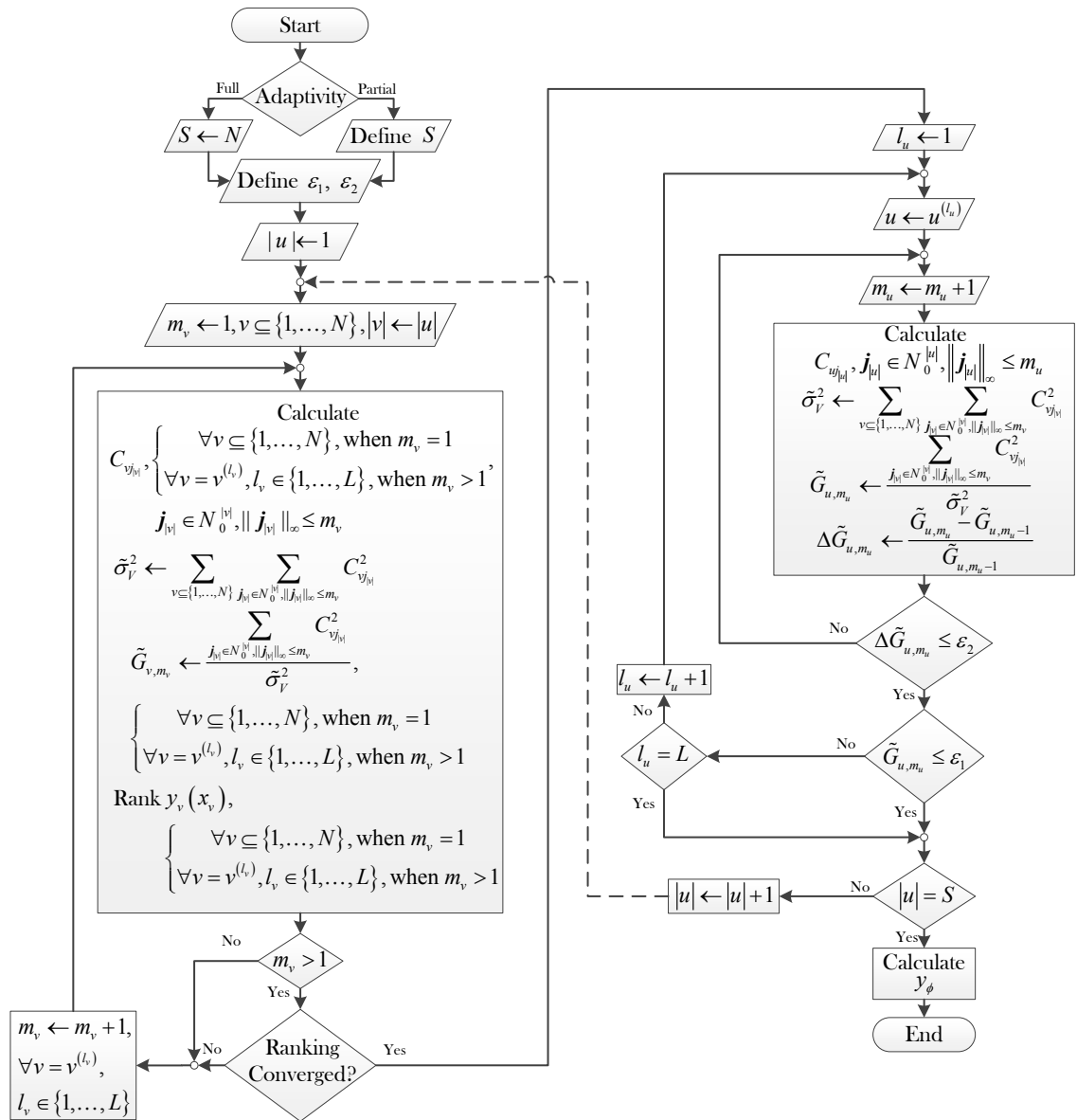
Figure 5.1: A flowchart for constructing AS-PDD approximations

5.4 Reliability Analysis

A fundamental problem in reliability analysis, required for evaluating the probabilistic constraints in Equation (5.1), entails calculation of the failure probability

$$
\begin{aligned}
P_F(\mathbf{d}) &:= P_\mathbf{d}\left[\mathbf{X} \in \Omega_F\right] = \int_{\mathbb{R}^N} I_{\Omega_F}(\mathbf{x}) f_\mathbf{X}(\mathbf{x}; \mathbf{d}) d\mathbf{x} \\
&=: \mathbb{E}_\mathbf{d}\left[I_{\Omega_F}(\mathbf{X})\right],
\end{aligned} \tag{5.10}
$$

where Ω_F is the failure domain and $I_{\Omega_F}(\mathbf{x})$ is the associated indicator function, which is equal to *one* when $\mathbf{x} \in \Omega_F$ and *zero* otherwise. Depending on the failure domain, as explained in Section 2, $\Omega_F := \{\mathbf{x} : y(\mathbf{x}) < 0\}$ for component reliability analysis and $\Omega_F := \{\mathbf{x} : \cup_i y_i(\mathbf{x}) < 0\}$ and $\Omega_F := \{\mathbf{x} : \cap_i y_i(\mathbf{x}) < 0\}$ for series- and parallel-type system reliability analyses, respectively. In this section, two methods are presented for estimating the failure probability. The AS-PDD-SPA method, which blends the AS-PDD approximation with SPA, is described first. Then the AS-PDD-MCS method, which exploits the AS-PDD approximation for MCS, is elucidated.

5.4.1 The AS-PDD-SPA method

Let $F_y(\xi) := P_\mathbf{d}[y \leq \xi]$ be the cumulative distribution function (CDF) of $y(\mathbf{X})$. Assume that the PDF $f_y(\xi) := dF_y(\xi)/d\xi$ exists and suppose that the cumulant generating function (CGF)

$$
K_y(t) := \ln\left\{\int_{-\infty}^{+\infty} \exp(t\xi) f_y(\xi) d\xi\right\} \tag{5.11}
$$

of y converges for $t \in \mathbb{R}$ in some non-vanishing interval containing the origin. Using inverse Fourier transformation, exponential power series expansion, and Hermite

polynomial approximation, Daniels [56] developed an SPA formula to approximately evaluate $f_y(\xi)$. However, the success of such a formula is predicated on how accurately the CGF and its derivatives, if they exist, are calculated. In fact, determining $K_y(t)$ is immensely difficult because it is equivalent to knowing all higher-order moments of y. To mitigate this problem, consider the Taylor series expansion of

$$K_y(t) = \sum_{r \in \mathbb{N}} \frac{\kappa^{(r)} t^r}{r!} \tag{5.12}$$

at $t = 0$, where $\kappa^{(r)} := d^r K_y(0)/dt^r$, $r \in \mathbb{N}$, is known as the rth-order cumulant of $y(\mathbf{X})$. If some of these cumulants are effectively estimated, then a truncated Taylor series provides a useful means to approximate $K_y(t)$. For instance, given a positive integer $Q < \infty$, the approximate raw moments $\bar{m}_S^{(r)}(\mathbf{d}) := \int_{\mathbb{R}^N} \bar{y}_S^r(\mathbf{x}) f_{\mathbf{X}}(\mathbf{x}; \mathbf{d}) d\mathbf{x} =: \mathbb{E}_{\mathbf{d}} [\bar{y}_S^r(\mathbf{X})]$ of order $1 \leq r \leq Q$ can be calculated based on an S-variate, AS-PDD approximation $\bar{y}_S(\mathbf{X})$ of $y(\mathbf{X})$, involving integrations of elementary polynomial functions and requiring no expensive evaluation of the original function $y(\mathbf{X})$. Nonetheless, because $\bar{y}_S(\mathbf{X})$ is a superposition of at most S-variate component functions of independent variables, the largest dimension of the integrals is $\min(rS, N)$. Therefore, many high-dimensional integrations are involved if $\min(rS, N)$ is large, even though the $\bar{y}_S(\mathbf{X})$ is known analytically. An alternative approach, adopted in this chapter, is dimension-reduction integration, approximating the N-dimensional integral by

$$\bar{m}_S^{(r)}(\mathbf{d}) \cong \sum_{i=0}^{T} (-1)^i \binom{N - T + i - 1}{i} \\ \sum_{\substack{v \subseteq \{1, \cdots, N\} \\ |v| = T - i}} \sum_{\mathbf{k}_{|v|} \in P^{(n_v)}} w^{(\mathbf{k}_{|v|})} \bar{y}_S^r(\mathbf{x}_v^{(\mathbf{k}_{|v|})}, \mathbf{c}_{-v}), \tag{5.13}$$

and hence involving at most T-dimensional lower-variate Gauss quadratures, where $T \leq N$ is a positive integer. When $T \ll N$, the computational cost of statistical moment analysis is markedly reduced. Then the corresponding approximate cumulants are easily obtained from the well-known cumulant-moment relationship,

$$\bar{\kappa}_S^{(r)}(\mathbf{d}) = \begin{cases} \bar{m}_S^{(1)}(\mathbf{d}) & : \quad r = 1, \\ \bar{m}_S^{(r)}(\mathbf{d}) - \sum_{p=1}^{r-1} \binom{r-1}{p-1} \times & : \quad 2 \leq r \leq Q, \\ \quad \bar{\kappa}_S^{(p)}(\mathbf{d}) \bar{m}_S^{(r-p)}(\mathbf{d}) & \end{cases} \tag{5.14}$$

where the functional argument $\mathbf{d}$ serves as a reminder that the moments and cumulants all depend on the design vector $\mathbf{d}$. Setting $\kappa^{(r)} = \bar{\kappa}_S^{(r)}$ for $r = 1, \cdots, Q$, and *zero* otherwise in Equation (5.12), the result is an S-variate, AS-PDD approximation

$$\bar{K}_{y,Q,S}(t; \mathbf{d}) = \sum_{r=1}^{Q} \frac{\bar{\kappa}_S^{(r)}(\mathbf{d}) t^r}{r!} \tag{5.15}$$

of the Qth-order Taylor series expansion of $K_y(t)$. It is elementary to show that $\bar{K}_{y,Q,S}(t; \mathbf{d}) \to K_y(t)$ when $\epsilon_1 \to 0$, $\epsilon_2 \to 0$, $S \to N$, and $Q \to \infty$.

Using the CGF approximation in Equation (5.15), Daniels' SPA leads to the explicit formula [56],

$$\bar{f}_{y,APS}(\xi; \mathbf{d}) = \left[2\pi \bar{K}_{y,Q,S}''(t_s; \mathbf{d}) \right]^{-\frac{1}{2}} \exp \left[\bar{K}_{y,Q,S}(t_s; \mathbf{d}) - t_s \xi \right], \tag{5.16}$$

for the approximate PDF of y, where the subscript 'APS' stands for AS-PDD-SPA and t_s is the saddlepoint that is obtained from solving

$$\bar{K}_{y,Q,S}'(t_s; \mathbf{d}) = \xi \tag{5.17}$$

with $\bar{K}_{y,Q,S}'(t; \mathbf{d}) := d\bar{K}_{y,Q,S}(t; \mathbf{d})/dt$ and $\bar{K}_{y,Q,S}''(t; \mathbf{d}) := d^2\bar{K}_{y,Q,S}(t; \mathbf{d})/dt^2$ defining the first- and second-order derivatives, respectively, of the approximate CGF of y

with respect to t. Furthermore, based on a related work of Lugannani [101], the approximate CDF of y becomes

$$
\begin{aligned}
\bar{F}_{y,APS}(\xi; \mathbf{d}) &= \Phi(w) + \phi(w)\left(\frac{1}{w} - \frac{1}{v}\right), \\
w &= \operatorname{sgn}(t_s)\left\{2\left[t_s\xi - \bar{K}_{y,Q,S}(t_s; \mathbf{d})\right]\right\}^{\frac{1}{2}}, \\
v &= t_s\left[\bar{K}''_{y,Q,S}(t_s; \mathbf{d})\right]^{\frac{1}{2}},
\end{aligned}
\tag{5.18}
$$

where $\Phi(\cdot)$ and $\phi(\cdot)$ are the CDF and PDF, respectively, of the standard Gaussian variable and $\operatorname{sgn}(t_s) = +1, -1,$ or 0, depending on whether t_s is positive, negative, or zero. According to Equation (5.18), the CDF of y at a point ξ is obtained using solely the corresponding saddlepoint t_s, that is, without the need to integrate Equation (5.16) from $-\infty$ to ξ.

Finally, using Lugannani and Rice's formula, the AS-PDD-SPA estimate $\bar{P}_{F,APS}$ ($\mathbf{d}$) of the component failure probability $P_F(\mathbf{d}) := P_{\mathbf{d}}[y(\mathbf{X}) < 0]$ is obtained as

$$
\bar{P}_{F,APS}(\mathbf{d}) = \bar{F}_{y,APS}(0; \mathbf{d}),
\tag{5.19}
$$

the AS-PDD-SPA generated CDF of y at $\xi = 0$. It is important to recognize that no similar SPA-based formulae are available for the joint PDF or joint CDF of dependent stochastic responses. Therefore, the AS-PDD-SPA method in the current form cannot be applied to general system reliability analysis.

The AS-PDD-SPA method contains several truncation parameters that should be carefully selected. For instance, if Q is too small, then the truncated CGF from Equation (5.15) may spoil the method, regardless of how large is the S chosen in the AS-PDD approximation. On the other hand, if Q is overly large, then many higher-

order moments involved may not be accurately calculated by the PDD approximation. More significantly, a finite-order truncation of CGF may cause loss of convexity of the actual CGF, meaning that the one-to-one relationship between ξ and t_s in Equation (5.17) is not ensured for every threshold ξ. Furthermore, the important property $\bar{K}''_{y,Q,S}(t_s; \mathbf{d}) > 0$ may not be maintained. To resolve this quandary, Yuen [102] presented for $Q = 4$ several distinct cases of the cumulants, describing the interval (t_l, t_u), where $-\infty \leq t_l \leq 0$ and $0 \leq t_u \leq \infty$, such that $t_l \leq t_s \leq t_u$ and $\bar{K}''_{y,Q,S}(t_s; \mathbf{d}) > 0$, ruling out any complex values of the square root in Equation (5.16) or (5.18). If ξ falls into these specified thresholds, then the saddlepoint t_s is uniquely determined from Equation (5.17), leading to the CDF or reliability in Equation (5.18) or (5.19). Otherwise, the AS-PDD-SPA method will fail to provide a solution. Further details of these thresholds can be found elsewhere [110].

5.4.2 The AS-PDD-MCS method

Depending on component or system reliability analysis, let $\bar{\Omega}_{F,S} := \{\mathbf{x} : \bar{y}_S(\mathbf{x}) < 0\}$ or $\bar{\Omega}_{F,S} := \{\mathbf{x} : \cup_i \bar{y}_{i,S}(\mathbf{x}) < 0\}$ or $\bar{\Omega}_{F,S} := \{\mathbf{x} : \cap_i \bar{y}_{i,S}(\mathbf{x}) < 0\}$ be an approximate failure set as a result of S-variate, AS-PDD approximations $\bar{y}_S(\mathbf{X})$ of $y(\mathbf{X})$ or $\bar{y}_{i,S}(\mathbf{X})$ of $y_i(\mathbf{X})$. Then the AS-PDD-MCS estimate of the failure probability $P_F(\mathbf{d})$ is

$$\bar{P}_{F,APM}(\mathbf{d}) = \mathbb{E}_\mathbf{d}\left[I_{\bar{\Omega}_{F,S}}(\mathbf{X})\right] = \lim_{L\to\infty} \frac{1}{L}\sum_{l=1}^{L} I_{\bar{\Omega}_{F,S}}(\mathbf{x}^{(l)}), \tag{5.20}$$

where the subscript 'APM' stands for AS-PDD-MCS, L is the sample size, $\mathbf{x}^{(l)}$ is the lth realization of $\mathbf{X}$, and $I_{\bar{\Omega}_{F,S}}(\mathbf{x})$ is another indicator function, which is equal to *one*

when $\mathbf{x} \in \bar{\Omega}_{F,S}$ and *zero* otherwise.

Note that the simulation of the PDD approximation in Equation (5.20) should not be confused with crude MCS commonly used for producing benchmark results. The crude MCS, which requires numerical calculations of $y(\mathbf{x}^{(l)})$ or $y_i(\mathbf{x}^{(l)})$ for input samples $\mathbf{x}^{(l)}, l = 1, \cdots, L$, can be expensive or even prohibitive, particularly when the sample size L needs to be very large for estimating small failure probabilities. In contrast, the MCS embedded in the AS-PDD approximation requires evaluations of simple polynomial functions that describe $\bar{y}_S(\mathbf{x}^{(l)})$ or $\bar{y}_{i,S}(\mathbf{x}^{(l)})$. Therefore, an arbitrarily large sample size can be accommodated in the AS-PDD-MCS method. In which case, the AS-PDD-MCS method also furnishes the approximate CDF $\bar{F}_{y,PM}(\xi; \mathbf{d})$:= $P_{\mathbf{d}}[\bar{y}_S(\mathbf{X}) \leq \xi]$ of $y(\mathbf{X})$ or even joint CDF of dependent stochastic responses, if desired.

Although the AS-PDD-SPA and AS-PDD-MCS methods are both rooted in the same PDD approximation, the former requires additional layers of approximations to calculate the CGF and saddlepoint. Therefore, the AS-PDD-SPA method, when it works, is expected to be less accurate than the AS-PDD-MCS method at comparable computational efforts. However, the AS-PDD-SPA method facilitates an analytical means to estimate the probability distribution and reliability — a convenient process not supported by the AS-PDD-MCS method. The respective properties of both methods extend to sensitivity analysis, presented in the following section.

5.5 Design Sensitivity Analysis

When solving RBDO problems employing gradient-based optimization algorithms, at least first-order derivatives of the failure probability with respect to each design variable are required. Therefore, the AS-PDD-SPA and AS-PDD-MCS methods for reliability analysis in Section 5.4 are expanded for sensitivity analysis of the failure probability in the following subsections.

5.5.1 Score functions

Let

$$h(\mathbf{d}) = \mathbb{E}_{\mathbf{d}}[g(\mathbf{X})] := \int_{\mathbb{R}^N} g(\mathbf{x}) f_{\mathbf{X}}(\mathbf{x}; \mathbf{d}) d\mathbf{x} \tag{5.21}$$

be a generic probabilistic response, where $h(\mathbf{d})$ and $g(\mathbf{x})$ are either $P_F(\mathbf{d})$ and $I_{\Omega_F}(\mathbf{x})$ for reliability analysis, or $m^{(r)}(\mathbf{d})$ and $y^r(\mathbf{x})$ for statistical moment analysis, where $m^{(r)}(\mathbf{d}) = \mathbb{E}_{\mathbf{d}} [y_S^r(\mathbf{X})]$, $r = 1, \cdots, Q$, is the rth-order raw moment of $y(\mathbf{X})$. Suppose that the first-order derivative of $h(\mathbf{d})$ with respect to a design variable d_k, $1 \le k \le M$, is sought. Taking the partial derivative of $h(\mathbf{d})$ with respect to d_k and then applying the Lebesgue dominated convergence theorem [76], which permits the differential and integral operators to be interchanged, yields the sensitivity

$$
\begin{aligned}
\frac{\partial h(\mathbf{d})}{\partial d_k} &:= \frac{\partial \mathbb{E}_{\mathbf{d}} [g(\mathbf{X})]}{\partial d_k} \\
&= \frac{\partial}{\partial d_k} \int_{\mathbb{R}^N} g(\mathbf{x}) f_{\mathbf{X}}(\mathbf{x}; \mathbf{d}) d\mathbf{x} \\
&= \int_{\mathbb{R}^N} g(\mathbf{x}) \frac{\partial \ln f_{\mathbf{X}}(\mathbf{x}; \mathbf{d})}{\partial d_k} f_{\mathbf{X}}(\mathbf{x}; \mathbf{d}) d\mathbf{x} \\
&=: \mathbb{E}_{\mathbf{d}} \left[g(\mathbf{X}) s_{d_k}^{(1)}(\mathbf{X}; \mathbf{d}) \right],
\end{aligned}
\tag{5.22}
$$

provided that $f_{\mathbf{X}}(\mathbf{x}; \mathbf{d}) > 0$ and the derivative $\partial \ln f_{\mathbf{X}}(\mathbf{x}; \mathbf{d}) / \partial d_k$ exists. In the last line of Equation (5.22), $s_{d_k}^{(1)}(\mathbf{X}; \mathbf{d}) := \partial \ln f_{\mathbf{X}}(\mathbf{X}; \mathbf{d}) / \partial d_k$ is known as the first-order score function for the design variable d_k [74, 111]. According to Equations (5.21) and (5.22), the generic probabilistic response and its sensitivities have both been formulated as expectations of stochastic quantities with respect to the same probability measure, facilitating their concurrent evaluations in a single stochastic simulation or analysis.

Remark 5.1. The evaluation of score functions, $s_{d_k}^{(1)}(\mathbf{X}; \mathbf{d})$, $k = 1, \cdots, M$, requires differentiating only the PDF of $\mathbf{X}$. Therefore, the resulting score functions can be determined easily and, in many cases, analytically — for instance, when $\mathbf{X}$ follows classical probability distributions [111]. If the density function of $\mathbf{X}$ is arbitrarily prescribed, the score functions can be calculated numerically, yet inexpensively, since no evaluation of the performance function is involved.

When $\mathbf{X}$ comprises independent variables, as assumed here, $\ln f_{\mathbf{X}}(\mathbf{X}; \mathbf{d}) = \sum_{i=1}^{i=N} \ln f_{X_i}(x_i; \mathbf{d})$ is a sum of N univariate log-density (marginal) functions of random variables. Hence, in general, the score function for the kth design variable, expressed by

$$s_{d_k}^{(1)}(\mathbf{X}; \mathbf{d}) = \sum_{i=1}^{N} \frac{\partial \ln f_{X_i}(X_i; \mathbf{d})}{\partial d_k} = \sum_{i=1}^{N} s_{ki}(X_i; \mathbf{d}), \tag{5.23}$$

is also a sum of univariate functions $s_{ki}(X_i; \mathbf{d}) := \partial \ln f_{X_i}(X_i; \mathbf{d}) / \partial d_k$, $i = 1, \cdots, N$, which are the derivatives of log-density (marginal) functions. If d_k is a distribution parameter of a single random variable X_{i_k}, then the score function reduces to $s_{d_k}^{(1)}(\mathbf{X}; \mathbf{d}) = \partial \ln f_{X_{i_k}}(X_{i_k}; \mathbf{d}) / \partial d_k =: s_{ki_k}(X_{i_k}; \mathbf{d})$, the derivative of the log-density

(marginal) function of X_{i_k}, which remains a univariate function. Nonetheless, combining Equations (5.22) and (5.23), the sensitivity of the generic probabilistic response $h(\mathbf{d})$ is obtained as

$$\frac{\partial h(\mathbf{d})}{\partial d_k} = \sum_{i=1}^{N} \mathbb{E}_{\mathbf{d}} \left[g(\mathbf{X}) s_{ki}(X_i; \mathbf{d}) \right], \tag{5.24}$$

the sum of expectations of products comprising stochastic response and log-density derivative functions with respect to the probability measure $P_{\mathbf{d}}$, $\mathbf{d} \in \mathcal{D}$.

5.5.2 The AS-PDD-SPA method

Suppose that the first-order derivative $\partial \bar{F}_{y,APS}(\xi; \mathbf{d})/\partial d_k$ of the CDF $\bar{F}_{y,APS}(\xi; \mathbf{d})$ of $\bar{y}_S(\mathbf{X})$, obtained by the AS-PDD-SPA method, with respect to a design variable d_k, is desired. Applying the chain rule on the derivative of Equation (5.18),

$$\frac{\partial \bar{F}_{y,APS}(\xi; \mathbf{d})}{\partial d_k} = \sum_{r=1}^{Q} \left(\frac{\partial \bar{F}_{y,APS}}{\partial w} \frac{\partial w}{\partial \bar{\kappa}_S^{(r)}} + \frac{\partial \bar{F}_{y,APS}}{\partial v} \frac{\partial v}{\partial \bar{\kappa}_S^{(r)}} \right) \frac{\partial \bar{\kappa}_S^{(r)}}{\partial d_k} \tag{5.25}$$

is obtained via the partial derivatives

$$\frac{\partial \bar{F}_{y,APS}}{\partial w} = \phi(w) \left(\frac{w}{v} - \frac{1}{w^2} \right), \quad \frac{\partial \bar{F}_{y,APS}}{\partial v} = \frac{\phi(w)}{v^2}, \tag{5.26}$$

$$\frac{\partial \bar{\kappa}_S^{(r)}}{\partial d_k} = \begin{cases} \dfrac{\partial \bar{m}_S^{(1)}(\mathbf{d})}{\partial d_k} & : \quad r = 1, \\[2ex] \dfrac{\partial \bar{m}_S^{(r)}(\mathbf{d})}{\partial d_k} - \sum\limits_{p=1}^{r-1} \binom{r-1}{p-1} \times & \\ \left(\dfrac{\partial \bar{\kappa}_S^{(r)}}{\partial d_k} \bar{m}_S^{(r-p)}(\mathbf{d}) + \bar{\kappa}_S^{(p)} \dfrac{\partial \bar{m}_S^{(r-p)}}{\partial d_k} \right) & : \quad 2 \leq r \leq Q, \end{cases}$$

where the derivatives of moments, that is, $\partial \bar{m}_S^{(r)}/\partial d_k$, $r = 1, \cdots, Q$, required to calculate the derivatives of cumulants, are obtained by the dimension-reduction numerical

integration, given by

$$
\begin{aligned}
\frac{\partial \bar{m}_S^{(r)}(\mathbf{d})}{\partial d_k} &= \mathbb{E}_{\mathbf{d}}\left[\bar{y}_S^r(\mathbf{X}) s_{d_k}^{(1)}(\mathbf{X}; \mathbf{d})\right] \\
&= \int_{\mathbb{R}^N} \bar{y}_S^r(\mathbf{x}) s_{d_k}^{(1)}(\mathbf{x}; \mathbf{d}) f_{\mathbf{X}}(\mathbf{x}; \mathbf{d}) d\mathbf{x} \\
&\cong \sum_{i=0}^{T}(-1)^i \binom{N-T+i-1}{i} \sum_{\substack{v \subseteq \{1,\cdots,N\} \\ |v|=T-i}} \\
&\quad \sum_{\mathbf{k}_{|v|} \in P^{(n_v)}} w^{(\mathbf{k}_{|v|})} \bar{y}_S^r(\mathbf{x}_v^{(\mathbf{k}_{|v|})}, \mathbf{c}_{-v}) s_{d_k}^{(1)}(\mathbf{x}_v^{(\mathbf{k}_{|v|})}, \mathbf{c}_{-v}; \mathbf{d}),
\end{aligned}
\tag{5.27}
$$

involving the AS-PDD approximation and score functions and requiring also at most T-dimensional lower-variate Gauss quadratures. The remaining two partial derivatives in Equation (5.25) are expressed by

$$
\frac{\partial w}{\partial \bar{\kappa}_S^{(r)}} = \frac{\partial w}{\partial t_s}\frac{\partial t_s}{\partial \bar{\kappa}_S^{(r)}} + \frac{\partial w}{\partial \bar{K}_{y,Q,S}}\left[\frac{\partial \bar{K}_{y,Q,S}}{\partial \bar{\kappa}_S^{(r)}} + \frac{\partial \bar{K}_{y,Q,S}}{\partial t_s}\frac{\partial t_s}{\partial \bar{\kappa}_S^{(r)}}\right],
\tag{5.28}
$$

and

$$
\frac{\partial v}{\partial \bar{\kappa}_S^{(r)}} = \frac{\partial v}{\partial t_s}\frac{\partial t_s}{\partial \bar{\kappa}_S^{(r)}} + \frac{\partial v}{\partial \bar{K}_{y,Q,S}''}\left[\frac{\partial \bar{K}_{y,Q,S}''}{\partial \bar{\kappa}_S^{(r)}} + \frac{\partial \bar{K}_{y,Q,S}''}{\partial t_s}\frac{\partial t_s}{\partial \bar{\kappa}_S^{(r)}}\right],
\tag{5.29}
$$

where

$$
\begin{aligned}
\frac{\partial w}{\partial t_s} &= \frac{\xi}{w}, \quad \frac{\partial w}{\partial \bar{K}_{y,Q,S}} = -\frac{1}{w}, \\
\frac{\partial \bar{K}_{y,Q,S}}{\partial t_s} &= \xi, \quad \frac{\partial v}{\partial t_s} = \left[\bar{K}_{y,Q,S}''\right]^{\frac{1}{2}},
\end{aligned}
\tag{5.30}
$$

$$
\frac{\partial v}{\partial \bar{K}_{y,Q,S}''} = \frac{t_s}{2\sqrt{\bar{K}_{y,Q,S}''}}, \quad \frac{\partial t_s}{\partial \bar{\kappa}_S^{(r)}} = -\frac{\dfrac{\partial \bar{K}_{y,Q,S}'}{\partial \bar{\kappa}_S^{(r)}}}{\dfrac{\partial \bar{K}_{y,Q,S}'}{\partial t_s}}.
\tag{5.31}
$$

The expressions of the partial derivatives $\partial \bar{K}_{y,Q,S}/\partial \bar{\kappa}_S^{(r)}$, $\partial \bar{K}_{y,Q,S}'/\partial \bar{\kappa}_S^{(r)}$, and $\partial \bar{K}_{y,Q,S}''/\partial \bar{\kappa}_S^{(r)}$, not explicitly presented here, can be easily derived from Equation (5.15) once the cumulants $\bar{\kappa}_S^{(r)}$, $r = 1, \cdots, Q$, and the saddlepoint t_s are obtained.

Henceforth, the first-order derivative of the failure probability estimate by the AS-PDD-SPA method is easily determined from

$$\frac{\partial \bar{P}_{F,APS}(\mathbf{d})}{\partial d_k} = \frac{\partial \bar{F}_{y,APS}(0;\mathbf{d})}{\partial d_k}, \tag{5.32}$$

the sensitivity of the CDF evaluated at $\xi = 0$.

5.5.3   The AS-PDD-MCS method

Taking the partial derivative of the AS-PDD-MCS estimate of the failure probability in Equation (5.20) with respect to d_k and then following the same arguments in deriving Equation (5.22) produces

$$
\begin{aligned}
\frac{\partial \bar{P}_{F,APM}(\mathbf{d})}{\partial d_k} &:= \frac{\partial \mathbb{E}_{\mathbf{d}}\left[I_{\bar{\Omega}_{F,S}}(\mathbf{X}) \right]}{\partial d_k} \\
&= \mathbb{E}_{\mathbf{d}}\left[I_{\bar{\Omega}_{F,S}}(\mathbf{X}) s_{d_k}^{(1)}(\mathbf{X};\mathbf{d}) \right] \\
&= \lim_{L \to \infty} \frac{1}{L} \sum_{l=1}^{L} \left[I_{\bar{\Omega}_{F,S}}(\mathbf{x}^{(l)}) s_{d_k}^{(1)}(\mathbf{x}^{(l)};\mathbf{d}) \right],
\end{aligned} \tag{5.33}
$$

where L is the sample size, $\mathbf{x}^{(l)}$ is the lth realization of $\mathbf{X}$, and $I_{\bar{\Omega}_{F,S}}(\mathbf{x})$ is the AS-PDD-generated indicator function. Again, they are easily and inexpensively determined by sampling analytical functions that describe $\bar{y}_S$ and $s_{d_k}^{(1)}$. A similar sampling procedure can be employed to calculate the sensitivity of the AS-PDD-MCS-generated CDF $\bar{F}_{y,APM}(\xi;\mathbf{d}) := P_{\mathbf{d}}[\bar{y}_S(\mathbf{X}) \leq \xi]$. It is important to note that the effort required to calculate the failure probability or CDF also delivers their sensitivities, incurring no additional cost. Setting $S = 1$ or 2 in Equations (5.20) and (5.33), the univariate or bivariate AS-PDD approximation of the failure probability and its sensitivities are determined.

Remark 5.2. The score function method has the nice property that it requires differentiating only the underlying PDF $f_{\mathbf{X}}(\mathbf{x}; \mathbf{d})$. The resulting score functions can be easily and, in most cases, analytically determined. If the performance function is not differentiable or discontinuous − for example, the indicator function that comes from reliability analysis − the proposed method still allows evaluation of the sensitivity if the density function is differentiable. In reality, the density function is often smoother than the performance function, and therefore the proposed sensitivity methods will be able to calculate sensitivities for a wide variety of complex mechanical systems.

Remark 5.3. The AS-PDD-SPA and AS-PDD-MCS methods, discussed in Sections 4 and 5, are predicated on the S-variate, AS-PDD approximation $\bar{y}_S(\mathbf{X})$ (Equation (5.6)) and are, therefore, new. The author and his colleagues had developed in a prequel similar methods, called the PDD-SPA and PDD-MCS methods [110], employing the truncated PDD approximation $\tilde{y}_{S,m}(\mathbf{X})$ ((5.5)). The new methods will be contrasted with the existing ones in the Numerical Examples section.

5.6 Expansion Coefficients by Dimension-Reduction Integration

The determination of AS-PDD expansion coefficients $y_{\emptyset}(\mathbf{d})$ and $C_{u\mathbf{j}_{|u|}}(\mathbf{d})$ is vitally important for reliability analysis, including its design sensitivities. As defined in Equations (5.3) and (5.4), the coefficients involve various N-dimensional integrals over $\mathbb{R}^N$. For large N, a multivariate numerical integration employing an N-dimensional tensor product of a univariate quadrature formula is computationally prohibitive and is, therefore, ruled out. An attractive alternative approach entails

dimension-reduction integration, which was originally developed by Xu and Rahman [22] for high-dimensional numerical integration. For calculating $y_\emptyset$ and $C_{u\mathbf{j}_{|u|}}$, this is accomplished by replacing the N-variate function y in Equations (5.3) and (5.4) with an R-variate RDD approximation at a chosen reference point, where $R \leq N$. The result is a reduced integration scheme, requiring evaluations of at most R-dimensional integrals.

Let $\mathbf{c} = (c_1, \cdots, c_N)^T \in \mathbb{R}^N$, which is commonly adopted as the mean of $\mathbf{X}$, be a reference point, and $y(\mathbf{x}_v, \mathbf{c}_{-v})$ represent an $|v|$-variate RDD component function of $y(\mathbf{x})$, where $v \subseteq \{1, \cdots, N\}$ [64, 83]. Given a positive integer $S \leq R \leq N$, when $y(\mathbf{x})$ in Equations (5.3) and (5.4) is replaced with its R-variate RDD approximation, the coefficients $y_\emptyset(\mathbf{d})$ and $C_{u\mathbf{j}_{|u|}}(\mathbf{d})$ are estimated from [22]

$$
\begin{aligned}
y_\emptyset(\mathbf{d}) \cong & \sum_{i=0}^{R} (-1)^i \binom{N-R+i-1}{i} \times \\
& \sum_{\substack{v \subseteq \{1,\cdots,N\} \\ |v|=R-i}} \int_{\mathbb{R}^{|v|}} y(\mathbf{x}_v, \mathbf{c}_{-v}) f_{\mathbf{X}_v}(\mathbf{x}_v; \mathbf{d}) d\mathbf{x}_v
\end{aligned}
\tag{5.34}
$$

and

$$
\begin{aligned}
C_{u\mathbf{j}_{|u|}}(\mathbf{d}) \cong & \sum_{i=0}^{R} (-1)^i \binom{N-R+i-1}{i} \sum_{\substack{v \subseteq \{1,\cdots,N\} \\ |v|=R-i, u \subseteq v}} \\
& \int_{\mathbb{R}^{|v|}} y(\mathbf{x}_v, \mathbf{c}_{-v}) \psi_{u\mathbf{j}_{|u|}}(\mathbf{x}_u; \mathbf{d}) f_{\mathbf{X}_v}(\mathbf{x}_v; \mathbf{d}) d\mathbf{x}_v,
\end{aligned}
\tag{5.35}
$$

respectively, requiring evaluation of at most R-dimensional integrals. The reduced integration facilitates calculation of the coefficients approaching their exact values as $R \to N$ and is significantly more efficient than performing one N-dimensional integration, particularly when $R \ll N$. Hence, the computational effort is significantly

lowered using the dimension-reduction integration. For instance, when $R = 1$ or 2, Equations (5.34) and (5.35) involve one-, or at most, two-dimensional integrations, respectively. Nonetheless, numerical integrations are still required for performing various $|v|$-dimensional integrals over $\mathbb{R}^{|v|}$, where $0 \leq |v| \leq R$. When $R > 1$, the multivariate integrations involved can be approximated using full-grid and sparse-grid quadratures, including their combination, described as follows.

5.6.1 Full-grid integration

The full-grid dimension-reduction integration entails constructing a tensor product of the underlying univariate quadrature rules. For a given $v \subseteq \{1, \cdots, N\}$, $1 < |v| \leq R$, let $v = \{i_1, \cdots i_{|v|}\}$, where $1 \leq i_1 < \cdots < i_{|v|} \leq N$. Denote by $\{x_{i_p}^{(1)}, \cdots, x_{i_p}^{(n_v)}\} \subset \mathbb{R}$ a set of integration points of x_{i_p} and by $\{w_{i_p}^{(1)}, \cdots, w_{i_p}^{(n_v)}\}$ the associated weights generated from a chosen univariate quadrature rule and a positive integer $n_v \in \mathbb{N}$. Denote by $P^{(n_v)} = \times_{p=1}^{p=|v|} \{x_{i_p}^{(1)}, \cdots, x_{i_p}^{(n_v)}\}$ the rectangular grid consisting of all integration points generated by the variables indexed by the elements of v. Then the coefficients using dimension-reduction numerical integration with a full grid are approximated by

$$y_\emptyset(\mathbf{d}) \cong \sum_{i=0}^{R} (-1)^i \binom{N-R+i-1}{i} \sum_{\substack{v \subseteq \{1,\cdots,N\} \\ |v|=R-i}} \sum_{\mathbf{k}_{|v|} \in P^{(n_v)}} w^{(\mathbf{k}_{|v|})} y(\mathbf{x}_v^{(\mathbf{k}_{|v|})}, \mathbf{c}_{-v}), \quad (5.36)$$

$$C_{u\mathbf{j}_{|u|}}(\mathbf{d}) \cong \sum_{i=0}^{R} (-1)^i \binom{N-R+i-1}{i} \times$$
$$\sum_{\substack{v \subseteq \{1,\cdots,N\} \\ |v|=R-i, u \subseteq v}} \sum_{\mathbf{k}_{|v|} \in P^{(n_v)}} w^{(\mathbf{k}_{|v|})} y(\mathbf{x}_v^{(\mathbf{k}_{|v|})}, \mathbf{c}_{-v}) \psi_{u\mathbf{j}_{|u|}}(\mathbf{x}_u^{(\mathbf{k}_{|u|})}; \mathbf{d}), \quad (5.37)$$

where $\mathbf{x}_v^{(\mathbf{k}_{|v|})} = \{x_{i_1}^{(k_1)}, \cdots, x_{i_{|v|}}^{(k_{|v|})}\}$ and $w^{(\mathbf{k}_{|v|})} = \prod_{p=1}^{p=|v|} w_{i_p}^{(k_p)}$ is the product of integration weights generated by the variables indexed by the elements of v. For independent coordinates of $\mathbf{X}$, as assumed here, a univariate Gauss quadrature rule is commonly used, where the integration points and associated weights depend on the probability distribution of X_i. The quadrature rule is readily available, for example, as the Gauss-Hermite or Gauss-Legendre quadrature rule, when X_i follows Gaussian or uniform distribution [98]. For an arbitrary probability distribution of X_i, the Stieltjes procedure can be employed to generate the measure-consistent Gauss quadrature formulae [98]. An n_v-point Gauss quadrature rule exactly integrates a polynomial of total degree at most $2n_v - 1$.

The calculation of $y_\emptyset$ and $C_{u\mathbf{j}_{|u|}}$ from Equations (5.36) and (5.37) involves at most R-dimensional tensor products of an n_v-point univariate quadrature rule, requiring the following deterministic responses or function evaluations: $y(\mathbf{c})$, $y(\mathbf{x}_v^{(\mathbf{j}_{|v|})}, \mathbf{c}_{-v})$ for $i = 0, \cdots, R$, $v \subseteq \{1, \cdots, N\}$, $|v| = R - i$, and $\mathbf{j}_{|v|} \in P^{(n_v)}$. Accordingly, the total cost for estimating the PDD expansion coefficients entails

$$L_{FG} = \sum_{i=0}^{R} \sum_{\substack{v \subseteq \{1,\cdots,N\} \\ |v|=R-i}} n_v^{|v|} \tag{5.38}$$

function evaluations, encountering a computational complexity that is an Rth-order polynomial − for instance, linear or quadratic when $R = 1$ or 2 − with respect to the number of random variables or integration points. For $R < N$, the technique alleviates the curse of dimensionality to an extent determined by R. The dimension-reduction integration in conjunction with the full-grid quadrature rule was used for

constructing truncated PDD approximations [97, 99].

5.6.2   Sparse-grid integration

Although the full-grid dimension-reduction integration has been successfully applied to the calculation of the PDD expansion coefficients in the past [97, 99, 112], it faces a major drawback when the polynomial order m_u for a PDD component function y_u needs to be modulated for adaptivity. As the value of m_u is incremented by one, a completely new set of integration points is generated by the univariate Gauss quadrature rule, rendering all expensive function evaluations on prior integration points as useless. Therefore, a nested Gauss quadrature rule, such as the fully symmetric interpolatory rule capable of exploiting dimension-reduction integration, becomes desirable.

The fully symmetric interpolatory (FSI) rule, developed by Genz and his associates [113, 114], is a sparse-grid integration technique for performing high-dimensional numerical integration. Applying this rule to the $|v|$-dimensional integrations in Equations (5.34) and (5.35), the PDD expansion coefficients are approximated by

$$
\begin{aligned}
y_\emptyset &\cong \sum_{i=0}^{R} (-1)^i \binom{N-R+i-1}{i} \sum_{\substack{v \subseteq \{1,\cdots,N\} \\ |v|=R-i}} \sum_{\mathbf{p}_{|v|} \in P^{(\tilde{n}_v,|v|)}} w_{\mathbf{p}_{|v|}} \\
&\times \sum_{\mathbf{q}_{|v|} \in \Pi_{\mathbf{p}_{|v|}}} \sum_{\mathbf{t}_{|v|}} y\left(t_{i_1} \alpha_{q_{i_1}}, \cdots, t_{i_{|v|}} \alpha_{q_{i_{|v|}}}, \mathbf{c}_{-v} \right),
\end{aligned} \tag{5.39}
$$

$$C_{u\mathbf{j}_{|u|}} \cong \sum_{i=0}^{R}(-1)^i \binom{N-R+i-1}{i} \sum_{\substack{v\subseteq\{1,\cdots,N\}\\|v|=R-i,u\subseteq v}}$$

$$\sum_{\mathbf{p}_{|v|}\in P^{(\tilde{n}_v,|v|)}} w_{\mathbf{p}_{|v|}} \sum_{\mathbf{q}_{|v|}\in\Pi_{\mathbf{p}_{|v|}}} \sum_{\mathbf{t}_{|v|}} y\left(t_{i_1}\alpha_{q_{i_1}},\cdots,t_{i_{|v|}}\alpha_{q_{i_{|v|}}},\mathbf{c}_{-v}\right)$$

$$\times \psi_{u\mathbf{j}_{|u|}}\left(t_{i_1}\alpha_{q_{i_1}},\cdots,t_{i_{|u|}}\alpha_{q_{i_{|u|}}}\right), \tag{5.40}$$

where $v=\{i_1,\cdots i_{|v|}\}$, $\mathbf{t}_{|v|}=(t_{i_1},\cdots,t_{i_{|v|}})$, $\mathbf{p}_{|v|}=(p_{i_1},\cdots,p_{i_{|v|}})$, and

$$P^{(\tilde{n}_v,|v|)} = \left\{\mathbf{p}_{|v|}:\tilde{n}_v\geq p_{i_1}\geq\cdots\geq p_{i_{|v|}}\geq 0,\left\|\mathbf{p}_{|v|}\right\|\leq\tilde{n}_v\right\} \tag{5.41}$$

with $\left\|\mathbf{p}_{|v|}\right\|:=\sum_{r=1}^{|v|}p_{i_r}$ is the set of all distinct $|v|$-partitions of the integers $0,1,\cdots,\tilde{n}_v$, and $\Pi_{\mathbf{p}_{|v|}}$ is the set of all permutations of $\mathbf{p}_{|v|}$. The innermost sum over $\mathbf{t}_{|v|}$ is taken over all of the sign combinations that occur when $t_{i_r}=\pm 1$ for those values of i_r with generators $\alpha_{q_{i_r}}\neq 0$ [114]. The weight

$$w_{\mathbf{p}_{|v|}} = 2^{-K} \sum_{\left\|\mathbf{k}_{|v|}\right\|\leqslant\tilde{n}_v-\left\|\mathbf{p}_{|v|}\right\|} \prod_{r=1}^{|v|} \frac{a_{k_{i_r}+p_{i_r}}}{\displaystyle\prod_{j=0,j\neq p_{i_r}}^{k_{i_r}+p_{i_r}}\left(\alpha_{p_{i_r}}^2-\alpha_j^2\right)}, \tag{5.42}$$

where K is the number of nonzero components in $\mathbf{p}_{|v|}$ and a_i is a constant that depends on the probability measure of X_i, for instance,

$$a_i = \frac{1}{\sqrt{2\pi}}\int_{\mathbb{R}}\exp\left(-\frac{\xi^2}{2}\right)\prod_{j=0}^{i-1}\left(\xi^2-\alpha_j^2\right)d\xi \tag{5.43}$$

for $i>0$ and $a_0=1$ when X_i follows the standard Gaussian distribution [114]. An $\tilde{n}_v$-parameter FSI rule exactly integrates a polynomial of degree at most $2\tilde{n}_v-1$.

The number of function evaluations by the original FSI rule [113] increases rapidly as $|v|$ and $\tilde{n}_v$ increase. To enhance the efficiency, Genz [114] proposed an extended FSI rule in which the function evaluations are significantly reduced if the

generator set is chosen such that some of the weights $w_{\mathbf{p}|\mathbf{v}|}$ are *zero*. The pivotal step in constructing such an FSI rule is to extend a $(2\beta+1)$-point Gauss-Hermite quadrature rule by adding 2γ points or generators $\pm\alpha_{\beta+1}, \pm\alpha_{\beta+2}, \ldots, \pm\alpha_{\beta+\gamma}$ with the objective of maximizing the degree of polynomial exactness of the extended rule, where $\beta \in \mathbb{N}$ and $\gamma \in \mathbb{N}$. Genz [114] presented a special case of initiating the FSI rule from the univariate Gauss-Hermite rule over the interval $(-\infty, \infty)$. The additional generators in this case are determined as roots of the monic polynomial $\zeta^{2\gamma} + t_{\gamma-1}\zeta^{2\gamma-1} + \cdots + t_0$, where the coefficients $t_{\gamma-1}, \cdots, t_0$ are obtained by invoking the condition

$$\frac{1}{\sqrt{2\pi}} \int_{\mathbb{R}} \exp\left(-\frac{\xi^2}{2}\right) \prod_{j=0}^{\beta} \xi^{2b} \left(\xi^2 - \alpha_j^2\right) d\xi = 0, \qquad (5.44)$$

where $\gamma > \beta$. A new set of generators is propagated based on the prior rule and, therefore, as the polynomial degree of exactness of the rule increases, all the previous points and the expensive function evaluations over those points are preserved. A remarkable feature of the extended FSI rule is that the choice of generators is such that some of the weights $w_{\mathbf{p}|v|} = 0$ in each step of the extension [114], thus eliminating the need for function evaluations at the integration points corresponding to *zero* weights, making the extended FSI rule significantly more efficient than its earlier version. The dimension-reduction integration in conjunction with the sparse-grid quadrature rule was used for constructing AS-PDD approximations of high-dimensional complex systems [109].

5.6.3 Combined sparse- and full-grids

The adaptive-sparse algorithm [109] described by Figure 5.1, in tandem with the sparse-grid quadrature, should be employed to calculate the requisite AS-PDD expansion coefficients and hence determine the largest polynomial orders of PDD component functions retained. However, due to potential approximation errors, the expansion coefficients may need to be recalculated for at least two reasons.

The first source of error is low values of R set in the dimension-reduction integration. According to the algorithm, the largest polynomial orders $\max_u m_u$, $\emptyset \neq u \subseteq \{1, \cdots, N\}$, $1 \leq |u| \leq S$, associated with all S-variate PDD component functions, are determined using the expansion coefficients estimated by the dimension-reduction integration with $R = |u|$. For instance, the largest polynomial orders $\max_{\{i\}} m_{\{i\}}$, $i = 1, \cdots, N$, of univariate ($S = 1$) PDD component functions are ascertained employing the univariate expansion coefficients C_{ij}, $i = 1, \cdots, N$, $j = 1, 2, \cdots$, estimated with $R = 1$ to keep the computational effort at minimum. However, from the author's recent experience, the setting $R = 1$ is too low to warrant convergent solutions of complex RBDO problems, especially when the original function y contains significant interactive effects among input random variables. For an illustration, consider the function

$$y(X_1, X_2, X_3) = X_1^3 + X_2 + X_3^2 + (1 + X_1)^2(1 + X_2)^2 \qquad (5.45)$$

of three independent standard Gaussian random variables X_1, X_2, and X_3 with zero means and unit variances. Selecting $S = 2$ and sufficiently small tolerance parameters, let $\bar{y}_2(X_1, X_2, X_3)$ denote a bivariate, AS-PDD approximation, reproducing all terms

of $y(X_1, X_2, X_3)$. By definition, Equation (5.4) yields the exact univariate, first-order coefficient $C_{11} = 7$. However, setting $R = 1$ for the dimension-reduction integration in Equation (5.35), the adaptive-sparse algorithm produces an estimate of 5. The underestimation of C_{11} originates from the failure to include the bivariate interactive term $(1 + X_1)^2(1 + X_2)^2$ of Equation (5.45). Indeed, when $R = 2$ is employed, Equation (5.35) reproduces the exact value of 7. Therefore, the value of R must be raised to two to capture the two-variable interaction in this case and, in general, to S, which is the largest degree of interaction retained in a concomitant S-variate AS-PDD approximation. In other words, after the largest polynomial orders are determined by the adaptive-sparse algorithm, the AS-PDD coefficients need to be recalculated when $S \geq 2$. The author proposes doing so using full-grid dimension-reduction integration with $R = S$.

The second source of error is low-order Gauss quadrature. When calculating AS-PDD expansion coefficients $C_{u\mathbf{j}_{|u|}}$ by Equation (5.35), a low-order Gauss quadrature, selected merely according to the order of $\psi_{u\mathbf{j}_{|u|}}(\mathbf{x}_u; \mathbf{d})$ without accounting for $\max_u m_u$ (reflecting the nonlinearity of $y(\mathbf{x}_v, \mathbf{c}_{-v})$), may result in inadequate or erroneous estimates. For example, consider the bivariate, first-order expansion coefficient C_{1211} for the function in Equation (5.45). According to Equation (5.4), the exact value of $C_{1211} = 4$. However, when the 2×2 Gauss quadrature is used in the dimension-reduction integration with $R = 2$, the adaptive-sparse algorithm produces an estimate of 1. This is due to not accounting for the third-order term X_1^3 ($\max_{\{1\}} m_{\{1\}} = 3$) in Equation (5.45), resulting in an under-integration by the order of Gauss quadrature

chosen. Indeed, when the 3×2 Gauss quadrature is employed, the resulting estimate becomes 4, which is the exact value of C_{1211}. Therefore, the order of Gauss quadrature for the ith dimension in the dimension-reduction integration must be selected according to both $\max_{i \in u} m_u$ and the order of the corresponding polynomial basis to accurately estimate all $|u|$-variate expansion coefficients. In other words, after the largest polynomial orders are determined by the adaptive-sparse algorithm, the AS-PDD coefficients need to be recalculated. Again, the author proposes doing so using full-grid dimension-reduction integration with a Gauss quadrature rule commensurate with $\max_{i \in u} m_u$.

5.6.4 Computational expense

For the AS-PDD approximation, the computational effort is commonly determined by the total number of original function evaluations required for calculating all necessary expansion coefficients. In solving an RBDO problem, which is presented in Section 5.7, the total computational effort stems from two types of calculations: (1) initial calculations involved in the adaptive-sparse algorithm to automatically determine the truncation parameters of PDD; and (2) final calculations of the AS-PDD expansion coefficients based on the knowledge of truncation parameters. The computational cost required by the initial calculations, that is, by the S-variate, adaptive-sparse algorithm, is discussed by Yadav and Rahman [109], although an explicit formula for the number of original function evaluations remains elusive. However, the

computational cost can be bounded from above by

$$L_I \leq \sum_{k=0}^{S} \binom{N}{k} (m_{\max} + 1)^k, \tag{5.46}$$

the number of function evaluations in the truncated S-variate, $m_{\max}$th-order PDD approximation, where

$$m_{\max} = \max_{\substack{\emptyset \neq u \subseteq \{1, \cdots, N\},\, 1 \leq |u| \leq S \\ \tilde{G}_{u,m_u} > \epsilon_1,\, \Delta\tilde{G}_{u,m_u} > \epsilon_2}} m_u < \infty \tag{5.47}$$

is the largest order of polynomial expansions for all PDD component functions $y_u(\mathbf{X}_u)$, $\emptyset \neq u \subseteq \{1, \cdots, N\}$, $1 \leq |u| \leq S$, such that $\tilde{G}_{u,m_u} > \epsilon_1$, $\Delta\tilde{G}_{u,m_u} > \epsilon_2$. It is assumed here that the number of integration points at each dimension is $m_{\max} + 1$. Therefore, the computational complexity of the S-variate AS-PDD approximation is at most an Sth-order polynomial with respect to the number of input variables or the largest order of polynomial. Therefore, S-variate AS-PDD approximation alleviates the curse of dimensionality to an extent determined by S, ϵ_1, and ϵ_2.

The number of original function evaluations required by the final calculations, that is, by recalculations of the AS-PDD expansion coefficients based on the known truncation parameters, can be obtained from another bound

$$
\begin{aligned}
L_{II} \;\leq\; & 1 + \sum_{\substack{v \subseteq \{1, \cdots, N\} \\ 1 \leq |v| \leq S \\ \max m_v \neq 0}} \prod_{i \in v} \max_{\substack{u \subseteq \{1, \cdots, N\},\, 1 \leq |u| \leq S,\, i \in u \\ \tilde{G}_{u,m_u} > \epsilon_1,\, \Delta\tilde{G}_{u,m_u} > \epsilon_2,\, m_u \in \mathbb{N}}} \\
& \left\lceil \frac{m_u + \max m_v + 1}{2} \right\rceil
\end{aligned} \tag{5.48}
$$

when full-grid Gauss quadrature is employed. Here, the symbol $\lceil t \rceil$ refers to the ceiling function, which is the smallest integer not less than t. Therefore, the recalculation

of the expansion coefficients results in a computational expense in addition to that incurred by the adaptive-sparse algorithm. The total computational effort, measured in terms of the total number of function evaluations, is bounded by $L_I + L_{II}$, and will be discussed in the Numerical Examples section.

5.7 Proposed RBDO Methods

The PDD approximations described in the preceding sections provide a means to evaluate the constraint functions, including their design sensitivities, from a single stochastic analysis. No such approximation is required for the objective function, when it is a simple and explicit deterministic function of design variables. However, for complex mechanical design problems, for instance, Example 4 in the Numerical Examples section, the objective function is usually determined implicitly by intrinsic calculations from a computer-aided design code. In which case, the objective function and its design sensitivities may also be simultaneously evaluated by constructing PDD approximations of $c_0(\mathbf{d})$ in the space of design variables $\mathbf{d}$. Additional details of the PDD approximations of the objective function and its design sensitivities are not included here for brevity.

An integration of reliability analysis, design sensitivity analysis, and a suitable optimization algorithm should render a convergent solution of the RBDO problem in Equation (5.1). However, new reliability and sensitivity analyses, entailing re-calculations of the PDD expansion coefficients, are needed at every design iteration. Therefore, a straightforward integration is expensive, depending on the cost

of evaluating the objective and constraint functions and the requisite number of design iterations. In this section, a multi-point design process [84, 112], where a series of single-step, AS-PDD approximations are built on a local subregion of the design space, are presented for solving the RBDO problem.

5.7.1   Multi-point approximation

Let

$$\mathcal{D} = \times_{k=1}^{k=M} [d_{k,L}, d_{k,U}] \subseteq \mathbb{R}^M \tag{5.49}$$

be a rectangular domain, representing the design space of the RBDO problem defined by Equation (5.1). For a scalar variable $0 < \beta_k^{(q)} \leq 1$ and an initial design vector $\mathbf{d}_0^{(q)} = (d_{1,0}^{(q)}, \cdots, d_{M,0}^{(q)})$, the subset

$$
\begin{aligned}
\mathcal{D}^{(q)} \;=\; &\times_{k=1}^{k=M} \Big[d_{k,0}^{(q)} - \beta_k^{(q)}(d_{k,U} - d_{k,L})/2, \\
&\quad d_{k,0}^{(q)} + \beta_k^{(q)}(d_{k,U} - d_{k,L})/2 \Big] \subseteq \mathcal{D} \subseteq \mathbb{R}^M
\end{aligned}
\tag{5.50}
$$

defines the qth subregion for $q = 1, 2, \cdots$. Using the multi-point approximation [84, 112], the original RBDO problem in Equation (5.1) is exchanged with a succession of simpler RBDO subproblems, expressed by

$$
\begin{aligned}
\min_{\mathbf{d} \in \mathcal{D}^{(q)} \subseteq \mathcal{D}} \quad & \bar{c}_{0,S}^{(q)}(\mathbf{d}), \\
\text{subject to} \quad & \bar{c}_{l,S}^{(q)}(\mathbf{d}) := P_{\mathbf{d}} \Big[\mathbf{X} \in \bar{\Omega}_{F,l,S}^{(q)}(\mathbf{d}) \Big] - p_l \leq 0 \\
& l = 1, \cdots, K, \\
& d_{k,0}^{(q)} - \beta_k^{(q)}(d_{k,U} - d_{k,L})/2 \leq d_k \leq d_{k,0}^{(q)} + \\
& \quad \beta_k^{(q)}(d_{k,U} - d_{k,L})/2, \; k = 1, \cdots, M,
\end{aligned}
\tag{5.51}
$$

where $\bar{c}_{0,S}^{(q)}(\mathbf{d})$, $\bar{\Omega}_{F,l,S}^{(q)}(\mathbf{d})$ and $\bar{c}_{l,S}^{(q)}(\mathbf{d})$, $l = 1, 2, \cdots, K$, are local S-variate, AS-PDD approximations of $c_0(\mathbf{d})$, $\Omega_{F,l}(\mathbf{d})$ and $c_l(\mathbf{d})$, respectively, at iteration q, where $\bar{\Omega}_{F,l,S}^{(q)}(\mathbf{d})$ is defined using local, S-variate, AS-PDD approximations of $\bar{y}_{l,S}^{(q)}(\mathbf{X})$ of $y_l(\mathbf{X})$, and $d_{k,0}^{(q)} - \beta_k^{(q)}(d_{k,U} - d_{k,L})/2$ and $d_{k,0}^{(q)} + \beta_k^{(q)}(d_{k,U} - d_{k,L})/2$, also known as the move limits, are the lower and upper bounds, respectively, of the kth coordinate of subregion $\mathcal{D}^{(q)}$. In Equation (5.51), the original objective and constraint functions are replaced with those derived locally from respective AS-PDD approximations. Since the PDD approximations are mean-square convergent [97, 99], they also converge in probability and in distribution. Therefore, given a subregion $\mathcal{D}^{(q)}$, the solution of the associated RBDO subproblem also converges when $\epsilon_1 \to 0$, $\epsilon_2 \to 0$, and $S \to N$.

5.7.2 Single-step procedure

The single-step procedure is motivated on solving each RBDO subproblem in Equation (5.51) from a single stochastic analysis by sidestepping the need to recalculate the PDD expansion coefficients at every design iteration. It subsumes two important assumptions: (1) an S-variate, AS-PDD approximation $\bar{y}_S$ of y at the initial design is acceptable for all possible designs in the subregion; and (2) the expansion coefficients for one design, derived from those generated for another design, are accurate.

Consider a change of the probability measure of $\mathbf{X}$ from $f_{\mathbf{X}}(\mathbf{x}; \mathbf{d})d\mathbf{x}$ to $f_{\mathbf{X}}(\mathbf{x}; \mathbf{d}')$ $d\mathbf{x}$, where $\mathbf{d}$ and $\mathbf{d}'$ are two arbitrary design vectors corresponding to old and new designs, respectively. Let $\{\psi_{ij}(X_i; \mathbf{d}'); j = 0, 1, \cdots\}$ be a set of new orthonormal poly-

nomial basis functions consistent with the marginal probability measure $f_{X_i}(x_i; \mathbf{d}')dx_i$ of X_i, producing new product polynomials $\psi_{u\mathbf{j}_{|u|}}(\mathbf{X}_u; \mathbf{d}') = \prod_{p=1}^{|u|} \psi_{i_p j_p}(X_{i_p}; \mathbf{d}')$, $\emptyset \neq u \subseteq \{1, \cdots, N\}$. Assume that the expansion coefficients, $y_{\emptyset}(\mathbf{d})$ and $C_{u\mathbf{j}_{|u|}}(\mathbf{d})$, for the old design have been calculated already. Then, the expansion coefficients for the new design are determined from

$$
y_{\emptyset}(\mathbf{d}') = \int_{\mathbb{R}^N} \Bigg[\sum_{\emptyset \neq u \subseteq \{1, \cdots, N\}} \sum_{\substack{\mathbf{j}_{|u|} \in \mathbb{N}_0^{|u|} \\ j_1, \cdots, j_{|u|} \neq 0}} C_{u\mathbf{j}_{|u|}}(\mathbf{d})
$$
$$
\times \psi_{u\mathbf{j}_{|u|}}(\mathbf{x}_u; \mathbf{d}) + y_{\emptyset}(\mathbf{d}) \Bigg] f_{\mathbf{X}}(\mathbf{x}; \mathbf{d}')d\mathbf{x} \tag{5.52}
$$

and

$$
C_{u\mathbf{j}_{|u|}}(\mathbf{d}') = \int_{\mathbb{R}^N} \Bigg[\sum_{\emptyset \neq v \subseteq \{1, \cdots, N\}} \sum_{\substack{\mathbf{j}_{|v|} \in \mathbb{N}_0^{|v|} \\ j_1, \cdots, j_{|v|} \neq 0}} C_{v\mathbf{j}_{|v|}}(\mathbf{d})
$$
$$
\times \psi_{v\mathbf{j}_{|v|}}(\mathbf{x}_v; \mathbf{d}) + y_{\emptyset}(\mathbf{d}) \Bigg] \psi_{u\mathbf{j}_{|u|}}(\mathbf{x}_u; \mathbf{d}') f_{\mathbf{X}}(\mathbf{x}; \mathbf{d}')d\mathbf{x}, \tag{5.53}
$$

for all $\emptyset \neq u \subseteq \{1, \cdots, N\}$ by recycling the old expansion coefficients and using orthonormal polynomials associated with both designs. The relationship between the old and new coefficients, described by Equations (5.52) and (5.53), is exact and is obtained by replacing y in Equations (5.3) and (5.4) with the right side of Equation (5.2). However, in practice, when the S-variate, AS-PDD approximation (Equation (5.6)) is used to replace y in Equations (5.3) and (5.4), then the new expansion

coefficients,

$$y_\emptyset(\mathbf{d}') \cong \int_{\mathbb{R}^N} \Bigg[\sum_{\substack{\emptyset \neq u \subseteq \{1,\cdots,N\} \\ 1 \leq |u| \leq S}} \sum_{m_u=1}^{\infty} \sum_{\substack{\|\mathbf{j}_{|u|}\|_\infty = m_u, j_1,\cdots,j_{|u|} \neq 0 \\ \tilde{G}_{u,m_u} > \epsilon_1, \Delta\tilde{G}_{u,m_u} > \epsilon_2}} C_{u\mathbf{j}_{|u|}}(\mathbf{d})$$
$$\times\, \psi_{u\mathbf{j}_{|u|}}(\mathbf{X}_u; \mathbf{d}) + y_\emptyset(\mathbf{d}) \Bigg] f_\mathbf{X}(\mathbf{x}; \mathbf{d}')d\mathbf{x} \tag{5.54}$$

and

$$C_{u\mathbf{j}_{|u|}}(\mathbf{d}') \cong \int_{\mathbb{R}^N} \Bigg[\sum_{\substack{\emptyset \neq v \subseteq \{1,\cdots,N\} \\ 1 \leq |v| \leq S}} \sum_{m_v=1}^{\infty} \sum_{\substack{\|\mathbf{j}_{|v|}\|_\infty = m_v, j_1,\cdots,j_{|v|} \neq 0 \\ \tilde{G}_{v,m_v} > \epsilon_1, \Delta\tilde{G}_{v,m_v} > \epsilon_2}}$$
$$C_{v\mathbf{j}_{|v|}}(\mathbf{d})\psi_{v\mathbf{j}_{|v|}}(\mathbf{X}_v; \mathbf{d}) + y_\emptyset(\mathbf{d}) \Bigg]$$
$$\times \psi_{u\mathbf{j}_{|u|}}(\mathbf{x}_u; \mathbf{d}') f_\mathbf{X}(\mathbf{x}; \mathbf{d}')d\mathbf{x}, \tag{5.55}$$

which are applicable for $\emptyset \neq u \subseteq \{1,\cdots,N\}$, $1 \leq |u| \leq S$, become approximate, although convergent. In the latter case, the integrals in Equations (5.54) and (5.55) consist of finite-order polynomial functions of at most S variables and can be evaluated inexpensively without having to compute the original function y for the new design. Therefore, new stochastic analyses, all employing S-variate, AS-PDD approximation of y, are conducted with little additional cost during all design iterations, drastically curbing the computational effort in solving an RBDO subproblem.

5.7.3 The AS-PDD-SPA and AS-PDD-MCS methods

When the multi-point approximation is combined with the single-step procedure, the result is an accurate and efficient design process to solve the RBDO problem defined by (5.1). Depending on whether the AS-PDD-SPA or AS-PDD-MCS method is employed for reliability and design sensitivity analyses in the combined multi-point,

single-step design process, two distinct RBDO methods are proposed: the AS-PDD-SPA method and the AS-PDD-MCS method. Using the single-step procedure in both methods, the design solution of an individual RBDO subproblem becomes the initial design for the next RBDO subproblem. Then, the move limits are updated, and the optimization is repeated iteratively until an optimal solution is attained. The method is schematically depicted in Figure 5.2. Given an initial design $\mathbf{d}_0$, a sequence of design solutions, obtained successively for each subregion $\mathcal{D}^{(q)}$ and using the S-variate, AS-PDD approximation, leads to an approximate optimal solution $\bar{\mathbf{d}}^*$ of the RBDO problem. In contrast, an AS-PDD approximation constructed for the entire design space $\mathcal{D}$, if it commits large approximation errors, may possibly lead to a premature or erroneous design solution. The multi-point approximation in the proposed methods overcomes this quandary by adopting smaller subregions and local AS-PDD approximations, whereas the single-step procedure diminishes the computational requirement as much as possible by recycling the PDD expansion coefficients.

When $\epsilon_1 \to 0$, $\epsilon_2 \to 0$, $S \to N$, and $q \to \infty$, the reliability and its design sensitivities by the AS-PDD approximations converge to their exactness, yielding coincident solutions of the optimization problems described by Equations (5.1) and (5.51). However, if the subregions are sufficiently small, then for finite and possibly low values of S and nonzero values of ϵ_1 and ϵ_2, Equation (5.51) is expected to generate an accurate solution of Equation (5.1), the principal motivation for developing the AS-PDD-SPA and AS-PDD-MCS methods.
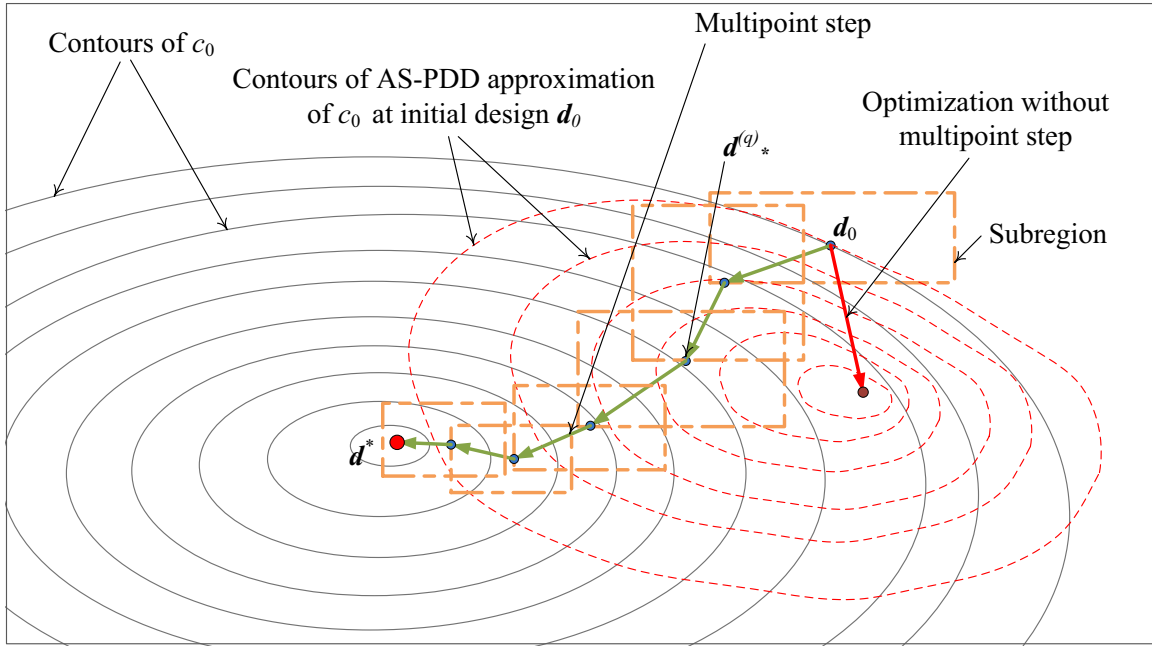
Figure 5.2: A schematic description of the multi-point, single-step design process

The AS-PDD-SPA and AS-PDD-MCS methods in conjunction with the combined multi-point, single-step design process is outlined by the following steps. The flow chart of this method is shown in Figure 5.3.

Step 1: Select an initial design vector $\mathbf{d}_0$. Define tolerances $\epsilon^{(1)} > 0$, $\epsilon^{(2)} > 0$, and $\epsilon^{(3)} > 0$. Set the iteration $q = 1$, $\mathbf{d}_0^{(q)} = (d_{1,0}^{(q)}, \cdots, d_{M,0}^{(q)})^T = \mathbf{d}_0$. Define the subregion size parameters $0 < \beta_k^{(q)} \leq 1$, $k = 1, \cdots, M$, describing $\mathcal{D}^{(q)} = \times_{k=1}^{k=M}[d_{k,0}^{(q)} - \beta_k^{(q)}(d_{k,U} - d_{k,L})/2, d_{k,0}^{(q)} + \beta_k^{(q)}(d_{k,U} - d_{k,L})/2]$. Denote the subregion's increasing history by a set $H^{(0)}$ and set it to empty. Set two designs $\mathbf{d}_f = \mathbf{d}_0$ and $\mathbf{d}_{f,last} \neq \mathbf{d}_0$ such that $||\mathbf{d}_f - \mathbf{d}_{f,last}||_2 > \epsilon^{(1)}$. Set $\mathbf{d}_*^{(0)} = \mathbf{d}_0$, $q_{f,last} = 1$ and $q_f = 1$. Usually, a feasible design should be selected to be the initial design $\mathbf{d}_0$. However, when an infeasible initial

design is chosen, a new feasible design can be obtained during the iteration if the initial subregion size parameters are large enough.

Step 2: Define tolerances $\epsilon_1 > 0$ and $\epsilon_2 > 0$. Use the adaptive PDD algorithm together with sparse-grid integration to obtain truncation parameters of $c_0(\mathbf{d})$ and $y_l(\mathbf{X})$, $l = 1, \cdots, K$ at current design $\mathbf{d}_0^{(q)}$. Set $\mathbf{d}_{AS} = \mathbf{d}_0^{(q)}$.

Step 3: Use ($q > 1$) the PDD truncation parameters obtained in Step 2. At $\mathbf{d} = \mathbf{d}_0^{(q)}$, generate the AS-PDD expansion coefficients, $y_\emptyset(\mathbf{d})$ and $C_{u\mathbf{j}_{|u|}}(\mathbf{d})$, where $\emptyset \neq u \subseteq \{1, \cdots, N\}$, $1 \leq |u| \leq S$, and $\mathbf{j}_{|u|} \in \mathbb{N}_0^{|u|}$, $j_1, \cdots, j_{|u|} \neq 0$ was determined in Step 2, using dimension-reduction integration with $R = S$, leading to S-variate, AS-PDD approximations $\bar{c}_{0,S}^{(q)}(\mathbf{d})$ of $c_0(\mathbf{d})$ and $\bar{y}_{l,S}^{(q)}(\mathbf{X})$ of $y_l(\mathbf{X})$, $l = 1, \cdots, K$.

Step 4: Evaluate $\bar{c}_{l,S}^{(q)}(\mathbf{d})$ of $c_l(\mathbf{d})$, $l = 1, \cdots, K$, in Equation (5.51) and their sensitivities by the AS-PDD-MCS or AS-PDD-SPA methods based on AS-PDD approximations $\bar{y}_{l,S}^{(q)}(\mathbf{X})$ in Step 3.

Step 5: If $q = 1$ and $\bar{c}_{l,S}^{(q)}(\mathbf{d}_0^{(q)}) < 0$ for $l = 1, \cdots, K$, then go to Step 7. If $q > 1$ and $\bar{c}_{l,S}^{(q)}(\mathbf{d}_0^{(q)}) < 0$ for $l = 1, \cdots, K$, then set $\mathbf{d}_{f,last} = \mathbf{d}_f$, $\mathbf{d}_f = \mathbf{d}_0^{(q)}$, $q_{f,last} = q_f$, $q_f = q$ and go to Step 7. Otherwise, go to Step 6.

Step 6: Compare the infeasible design $\mathbf{d}_0^{(q)}$ with the feasible design $\mathbf{d}_f$ and interpolate between $\mathbf{d}_0^{(q)}$ and $\mathbf{d}_f$ to obtain a new feasible design and set it as $\mathbf{d}_0^{(q+1)}$. For dimensions with large differences between $\mathbf{d}_0^{(q)}$ and $\mathbf{d}_f$, interpolate aggressively, that is, interpolate close to $\mathbf{d}_f$. Reduce the size of the subregion $\mathcal{D}^{(q)}$ to obtain new subregion $\mathcal{D}^{(q+1)}$. For dimensions with large

differences between $\mathbf{d}_0^{(q)}$ and $\mathbf{d}_f$, reduce aggressively. Also, for dimensions with large differences between the sensitivities of $\bar{c}_{l,S}^{(q)}(\mathbf{d}_0^{(q)})$ and $\bar{c}_{l,S}^{(q-1)}(\mathbf{d}_0^{(q)})$, reduce aggressively. Update $q = q + 1$ and go to Step 3.

Step 7: If $||\mathbf{d}_f - \mathbf{d}_{f,last}||_2 < \epsilon^{(1)}$ or $|[\bar{c}_{0,S}^{(q)}(\mathbf{d}_f) - \bar{c}_{0,S}^{(q_{f,last})}(\mathbf{d}_{f,last})]/\bar{c}_{0,S}^{(q)}(\mathbf{d}_f)| < \epsilon^{(3)}$, then stop and denote the final optimal solution as $\bar{\mathbf{d}}^* = \mathbf{d}_f$. Otherwise, go to Step 8.

Step 8: If the subregion size is small, that is, $\beta_k^{(q)}(d_{k,U} - d_{k,L}) < \epsilon^{(2)}$, and $\mathbf{d}_*^{(q-1)}$ is located on the boundary of the subregion, then go to Step 9. Otherwise, go to Step 11.

Step 9: If the subregion centered at $\mathbf{d}_0^{(q)}$ has been enlarged before, that is, $\mathbf{d}_0^{(q)} \in H^{(q-1)}$, then set $H^{(q)} = H^{(q-1)}$ and go to Step 11. Otherwise, set $H^{(q)} = H^{(q-1)} \bigcup \{\mathbf{d}_0^{(q)}\}$ and go to Step 10.

Step 10: For coordinates of $\mathbf{d}_0^{(q)}$ located on the boundary of the subregion and $\beta_k^{(q)}(d_{k,U} - d_{k,L}) < \epsilon^{(2)}$, increase the sizes of corresponding components of $\mathcal{D}^{(q)}$; for other coordinates, keep them as they are. Set the new subregion as $\mathcal{D}^{(q+1)}$.

Step 11: Solve the design problem in Equation (5.51) employing the single-step procedure. In so doing, recycle the PDD expansion coefficients obtained from Step 3 in Equations (5.54) and (5.55), producing approximations of the objective and constraint functions that stem from single calculation of these coefficients. Denote the optimal solution by $\mathbf{d}_*^{(q)}$ and set $\mathbf{d}_0^{(q+1)} = \mathbf{d}_*^{(q)}$. Update $q = q + 1$ and go to Step 12.

Step 12: If the form of a response function changes, go to Step 2; otherwise, go to Step 3. A threshold $t \in [0, 1]$ was used to determine whether the form changed. Only when the relative change of the objective function is greater than t, that is, $|c_0(\mathbf{d}_0^{(q)}) - c_0(\mathbf{d}_{AS})|/|c_0(\mathbf{d}_{AS})| > t$, then it is assumed that the form of the response function changes.
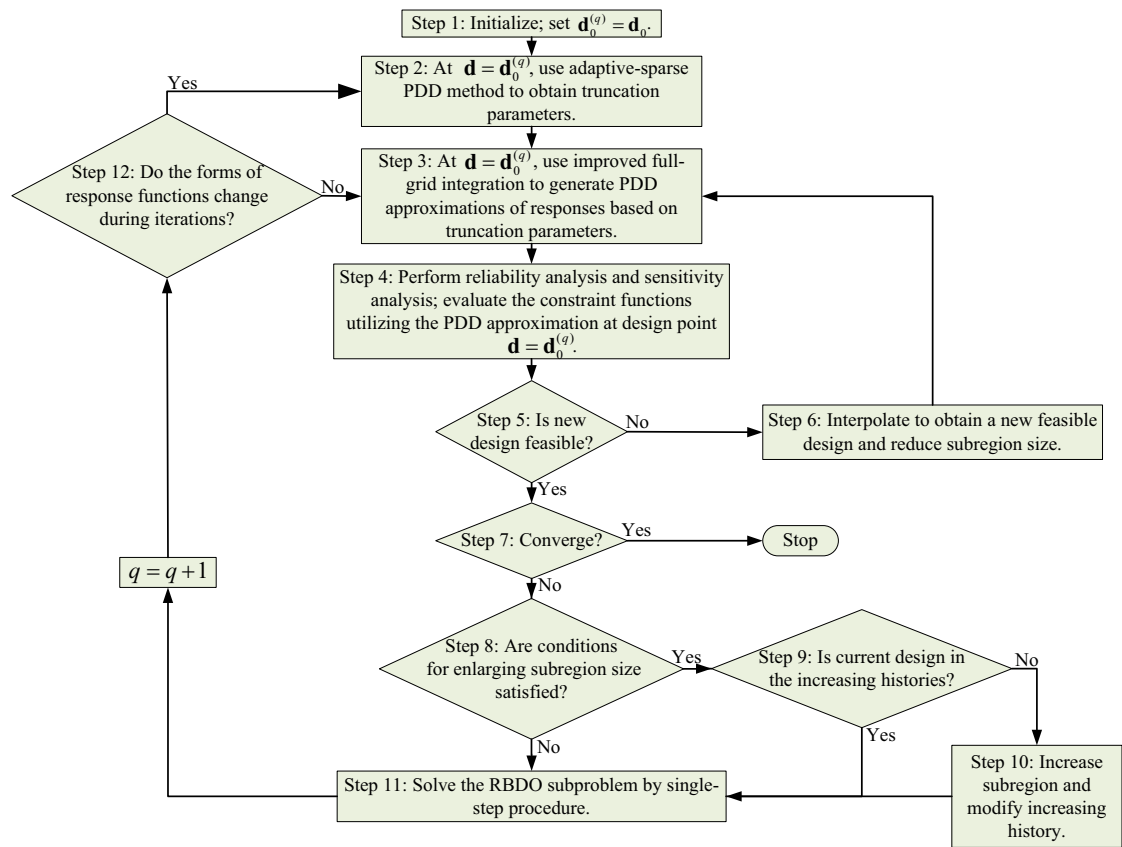
Figure 5.3: A flow chart of the proposed AS-PDD-SPA and AS-PDD-MCS methods

5.8 Numerical Examples

Four examples are presented to illustrate the AS-PDD-SPA and AS-PDD-MCS methods developed in solving various RBDO problems. The objective and constraint functions are either elementary mathematical functions or relate to engineering problems, ranging from simple structures to complex FEA-aided mechanical designs. Both size and shape design problems are included. In Examples 1 through 4, orthonormal polynomials, consistent with the probability distributions of input random variables, were used as bases. For the Gaussian distribution, the Hermite polynomials were used. For random variables following non-Gaussian probability distributions, such as the Lognormal distribution in Example 3 and truncated Gaussian distribution in Example 4, the orthonormal polynomials were obtained either analytically when possible or numerically, exploiting the Stieltjes procedure [98]. The value of S for AS-PDD approximation varies, depending on the function or the example, but in all cases the tolerances are as follows: $\epsilon_1 = \epsilon_2 = 10^{-4}$. The AS-PDD expansion coefficients were calculated using dimension-reduction integration with $R = S$ and the Gauss quadrature rule of the ith dimension consistent with $\max_{i \in u} m_u$. The moments and their sensitivities required by the AS-PDD-SPA method in Examples 1 and 2 were calculated using dimension-reduction integration with $R = 2$. The sample size for the embedded simulation of the AS-PDD-MCS method is 10^6 in all examples. In Examples 1-3, the design sensitivities of the objective functions were obtained analytically. Since the objective function in Example 4 is an implicit function, the truncated PDD approximation of the objective function was employed to obtain design sensitivities.

The multi-point, single-step PDD method was used in all examples. The tolerances, initial subregion size, and threshold parameters for the multi-point, single-step PDD method are as follows: (1) $\epsilon^{(1)} = 0.1$ (Examples 1 and 2), $\epsilon^{(1)} = 0.01$ (Example 3), $\epsilon^{(1)} = 0.2$ (Example 4); $\epsilon^{(2)} = 2$; $\epsilon^{(3)} = 0.005$ (Examples 1, 2, and 3), $\epsilon^{(3)} = 0.05$ (Example 4); (2) $\beta_1^{(1)} = \cdots = \beta_M^{(1)} = 0.5$; and (3) $t = 0.99$ (Example 1-3); $t = 0.6$ (Example 4). The optimization algorithm selected is sequential quadratic programming [106] in all examples.

5.8.1 Example 1: optimization of a mathematical problem

Consider a mathematical example, involving a 100-dimensional random vector $\mathbf{X}$, where X_i, $i = 1, \cdots, 100$, are independent and identically distributed Gaussian random variables, each with the mean value μ and the standard deviation s. Given the design vector $\mathbf{d} = (\mu, s)$, the objective of this problem is to

$$
\begin{aligned}
\min_{\mathbf{d} \in \mathcal{D}} \quad & c_0(\mathbf{d}) = d_1^2 + 5d_2, \\
\text{subject to} \quad & c_1(\mathbf{d}) = P_{\mathbf{d}}(y_1(\mathbf{X}) < 0) - 10^{-3} \le 0, \\
& -9 \le d_1 \le 9, \ 0.5 \le d_2 \le 4,
\end{aligned}
\tag{5.56}
$$

where

$$
y_1(\mathbf{X}) \ = \ \frac{1}{1000 + \sum\limits_{i=1}^{100} X_i} - \frac{1}{1000 + 3\sqrt{100}}
\tag{5.57}
$$

is a random function. The design vector $\mathbf{d} \in \mathcal{D}$, where $\mathcal{D} = [-9, 9] \times [0.5, 4] \subset \mathbb{R}^2$. The exact solution of the RBDO problem in Equation (5.56) is as follows: $\mathbf{d}^* = (0, 0.5)^T$; $c_0(\mathbf{d}^*) = 2.5$; and $c_1(\mathbf{d}^*) = \Phi(-6) - 10^{-3} \approx -10^{-3}$. The AS-PDD-SPA and AS-PDD-

MCS methods with $S = 1$ were employed to solve this elementary RBDO problem. The approximate optimal solution is denoted by $\bar{\mathbf{d}}^* = (\bar{d}_1^*, \bar{d}_2^*)^T$.

Four different initial designs were selected to study the robustness of the proposed methods in obtaining optimal design solutions. The first two initial designs $\mathbf{d}_0 = (-9, 4)^T$ and $\mathbf{d}_0 = (-4.5, 2)^T$ lie in the feasible region, whereas the last two initial designs $\mathbf{d}_0 = (9, 4)^T$ and $\mathbf{d}_0 = (4.5, 2)^T$ are located in the infeasible region. Table 5.1 summarizes the optimization results, including the numbers of function evaluations, by the AS-PDD-SPA and AS-PDD-MCS methods for all four initial designs. The exact solution, existing for this particular problem, is also listed in Table 5.1 to verify the approximate solutions. From Table 5.1, the proposed methods, starting from four different initial designs, engender identical optima, which is the exact solution. Hence, each method can be used to solve this optimization problem, regardless of feasible or infeasible initial designs.

Table 5.1: Optimization results for the 100-dimensional mathematical problem

	$\mathbf{d}_0 = (-9, 4)^T$		$\mathbf{d}_0 = (-4.5, 2)^T$		$\mathbf{d}_0 = (9, 4)^T$		$\mathbf{d}_0 = (4.5, 2)^T$		Exact
	AS-PDD-SPA	AS-PDD-MCS	AS-PDD-SPA	AS-PDD-MCS	AS-PDD-SPA	AS-PDD-MCS	AS-PDD-SPA	AS-PDD-MCS	
$\bar{d}_1^*$	0.0	0.0	0.0	0.0	0.0	0.0	0.0	0.0	0.0
$\bar{d}_2^*$	0.5	0.5	0.5	0.5	0.5	0.5	0.5	0.5	0.5
c_0	2.5	2.5	2.5	2.5	2.5	2.5	2.5	2.5	2.5
c_1	-0.001	-0.001	-0.001	-0.001	-0.001	-0.001	-0.001	-0.001	$\Phi(-6) -$ 0.001
No. of y_1 eval.	3211	3211	1706	1706	2910	2007	1706	1405	–

Figures 5.4 and 5.5 depict the iteration histories of the AS-PDD-SPA and AS-PDD-MCS methods, respectively, for all four initial designs. When starting from the feasible initial designs $\mathbf{d}_0 = (-9, 4)^T$ and $\mathbf{d}_0 = (-4.5, 2)^T$, both methods experience nearly identical iteration steps. This is because at every step of the design iteration the AS-PDD-SPA method provides estimates of the failure probability and its design sensitivities very close to those obtained by the AS-PDD-MCS method. Consequently, both methods incur the same number of function evaluations in reaching respective optimal solutions. In contrast, when the infeasible initial designs $\mathbf{d}_0 = (9, 4)^T$ and $\mathbf{d}_0 = (4.5, 2)^T$ are chosen, there exist some discrepancies in the iteration paths produced by the AS-PDD-SPA and AS-PDD-MCS methods. This is primarily due to the failure of SPA, where the existence of the saddlepoint is not guaranteed for some design iterations. In which case, the MCS, instead of SPA, were used to calculate the failure probability and its design sensitivities. Therefore, the computational cost by the AS-PDD-SPA method should increase, depending on the frequency of the failure of SPA. Indeed, when the discrepancy is large, as exhibited for the initial design $\mathbf{d}_0 = (9, 4)^T$, nearly 900 more function evaluations are needed by the AS-PDD-SPA method. For the initial design $\mathbf{d}_0 = (4.5, 2)^T$, the discrepancy is small, and consequently, the AS-PDD-SPA method requires almost 300 more function evaluations than the AS-PDD-MCS method. In general, the AS-PDD-MCS method should be more efficient than the AS-PDD-SPA method in solving RBDO problems since an added layer of approximation is involved when evaluating CGF in the latter method.
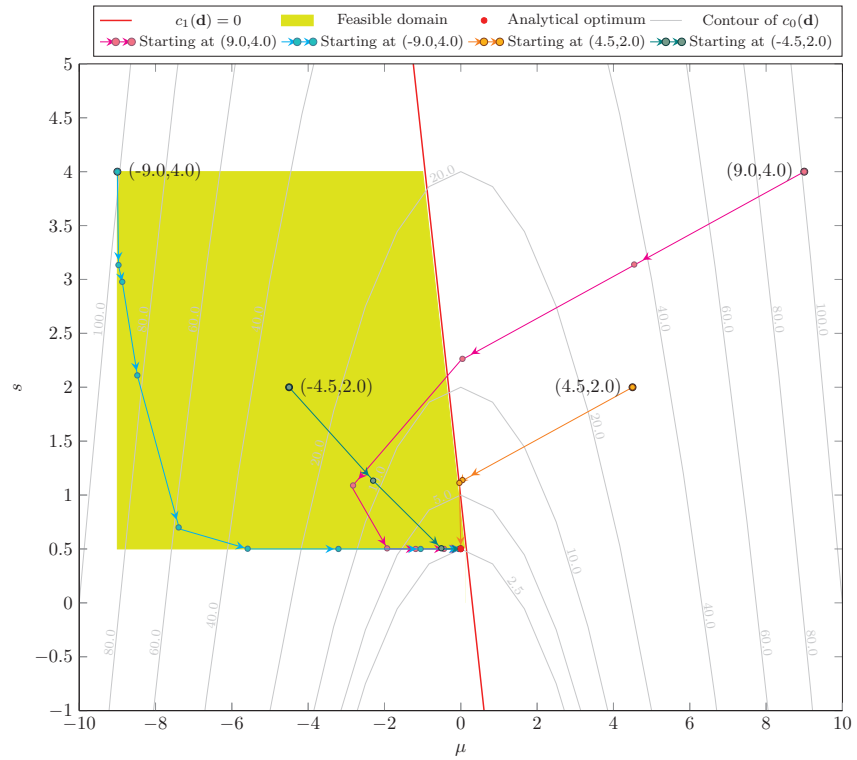
Figure 5.4: Iteration histories of the AS-PDD-SPA method for four different initial designs (Example 1)
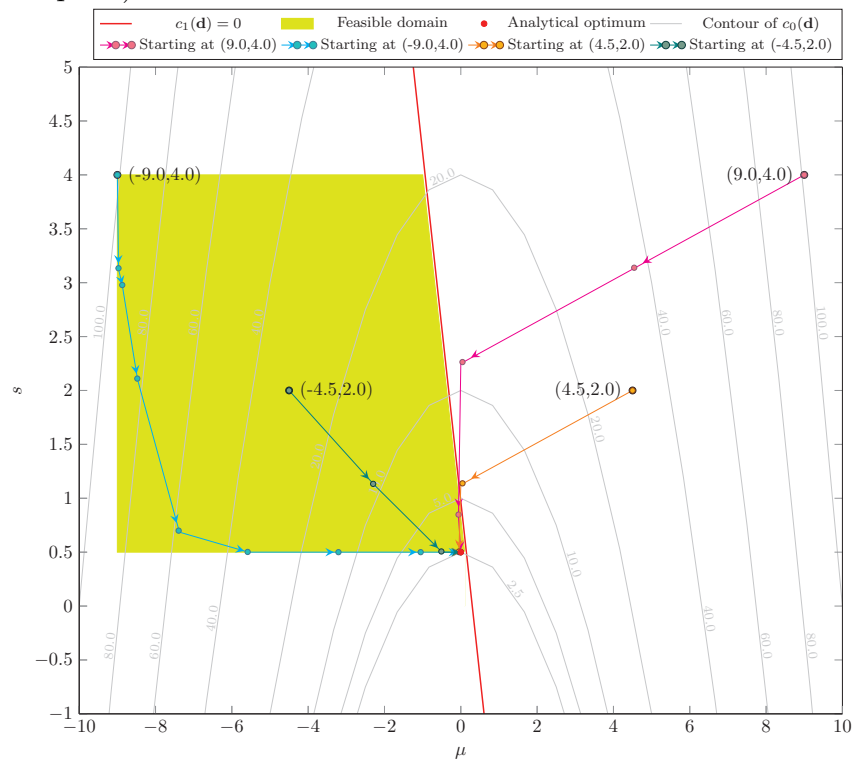
Figure 5.5: Iteration histories of the AS-PDD-MCS method for four different initial designs (Example 1)

5.8.2   Example 2 : optimization of a speed reducer

The second example, studied by Lee et al. [115], entails RBDO of a speed reducer, which was originally formulated as a deterministic optimization problem by Golinski [116]. Seven random variables, as shown in Figure 5.6, comprise the gear width X_1 (cm), the teeth module X_2 (cm), the number of teeth in the pinion X_3, the distances between bearings X_4 (cm) and X_5 (cm), and the axis diameters X_6 (cm) and X_7 (cm). They are independent Gaussian random variables with means $\mathbb{E}_{\mathbf{d}}[X_k]$, $k = 1, \cdots, 7$, and a standard deviation of 0.005. It is important to notice that in reality X_3 should be a discrete random variable, but here it is treated as a continuous Gaussian random variable. The design variables are the means of $\mathbf{X}$, that is, $d_k = \mathbb{E}_{\mathbf{d}}[X_k]$. The objective is to minimize the weight of the speed reducer subject to 11 probabilistic constraints, limiting the bending stress and surface stress of the gear teeth, transverse deflections of shafts 1 and 2, and stresses in shafts 1 and 2.

Mathematically, the RBDO problem is formulated to

$$\min_{\mathbf{d}\in\mathcal{D}} \quad c_0(\mathbf{d}) = 0.7854 d_1 d_2^2 (3.3333 d_3^2 + 14.9334 d_3$$

$$-43.0934) - 1.508 d_1 (d_6^2 + d_7^2)$$

$$+7.477(d_6^3 + d_7^3) + 0.7854(d_4 d_6^2 + d_5 d_7^2)$$

$$\text{subject to} \quad c_l(\mathbf{d}) = P_{\mathbf{d}}(y_l(\mathbf{X}) \leq 0) - \Phi(-\beta_l) \leq 0,$$

$$l = 1, \cdots, 11$$

$$2.6 \text{ cm} \leq d_1 \leq 3.6 \text{ cm}, \ 0.7 \text{ cm} \leq d_2 \leq 0.8 \text{ cm},$$

$$17 \ \leq d_3 \leq 28 \ , \ \ 7.3 \text{ cm} \leq d_4 \leq 8.3 \text{ cm},$$

$$7.3 \text{ cm} \leq d_5 \leq 8.3 \text{ cm}, \ 2.9 \text{ cm} \leq d_6 \leq 3.9 \text{ cm},$$

$$5.0 \text{ cm} \leq d_7 \leq 5.5 \text{ cm}, \tag{5.58}$$

where

$$y_1(\mathbf{X}) = 1 - \frac{27}{X_1 X_2^2 X_3}, \tag{5.59}$$

$$y_2(\mathbf{X}) = 1 - \frac{397.5}{X_1 X_2^2 X_3^2}, \tag{5.60}$$

$$y_3(\mathbf{X}) = 1 - \frac{1.93 X_4}{X_2 X_3 X_6^4}, \tag{5.61}$$

$$y_4(\mathbf{X}) = 1 - \frac{1.93 X_5}{X_2 X_3 X_7^4}, \tag{5.62}$$

$$y_5(\mathbf{X}) = 1100 - \frac{\sqrt{(745 X_4/(X_2 X_3))^2 + 16.9 \times 10^6}}{0.1 X_6^3}, \tag{5.63}$$

$$y_6(\mathbf{X}) = 850 - \frac{\sqrt{(745 X_5/(X_2 X_3))^2 + 157.5 \times 10^6}}{0.1 X_7^3}, \tag{5.64}$$

$$y_7(\mathbf{X}) = 40 - X_2 X_3, \tag{5.65}$$

$$y_8(\mathbf{X}) = \frac{X_1}{X_2} - 5, \tag{5.66}$$

$$y_9(\mathbf{X}) = 12 - \frac{X_1}{X_2}, \tag{5.67}$$

$$y_{10}(\mathbf{X}) = 1 - \frac{1.5 X_6 + 1.9}{X_4}, \tag{5.68}$$

$$y_{11}(\mathbf{X}) = 1 - \frac{1.1 X_7 + 1.9}{X_5}, \tag{5.69}$$

are 11 random performance functions and $\beta_l = 3$, $l = 1, \cdots, 11$. The initial design vector is $\mathbf{d}_0 = (3.1 \text{ cm}, 0.75 \text{ cm}, 22.5, 7.8 \text{ cm}, 7.8 \text{ cm}, 3.4 \text{ cm}, 5.25 \text{ cm})^T$. The approximate optimal solution is denoted by $\bar{\mathbf{d}}^* = (\bar{d}_1^*, \bar{d}_2^*, \cdots, \bar{d}_7^*)^T$.
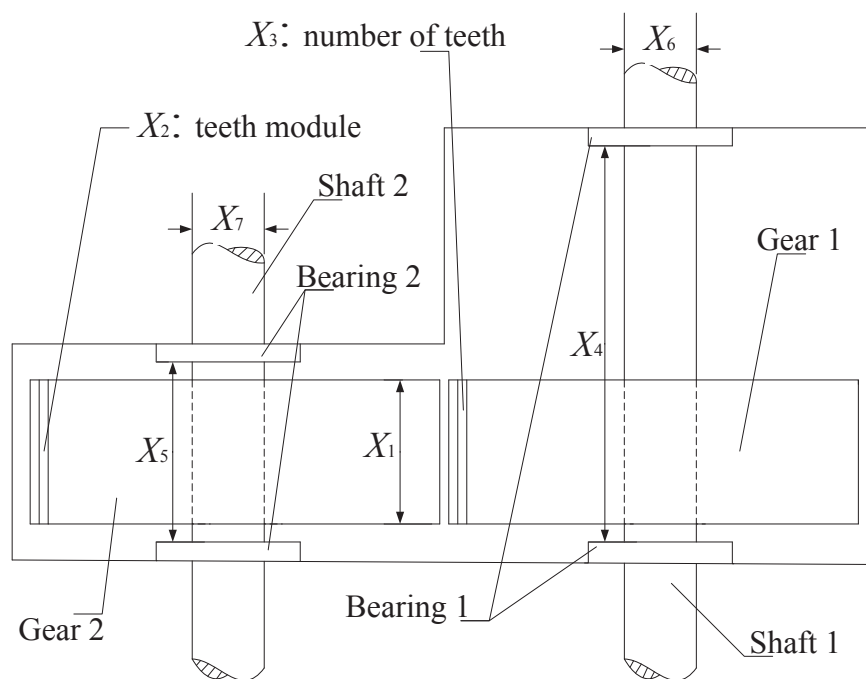
Figure 5.6: A schematic illustration of the speed reducer (Example 2)

Table 5.2 presents detailed optimization results generated by the AS-PDD-SPA and AS-PDD-MCS methods, each entailing $S = 1$ and $S = 2$, in the second through fifth columns. The optimal solutions by both proposed methods, regardless of S, are very close to each other, all indicating no constraints are active. The objective function values of optimal solutions by the AS-PDD-MCS method are slightly lower than those by the AS-PDD-SPA method. Although there is a constraint violation, that is, $\max_l c_l > 0$ in the AS-PDD-MCS method with $S = 1$, it is negligibly small. The results of both versions ($S = 1$ and $S = 2$) of the AS-PDD-SPA and AS-PDD-MCS methods confirm that the solutions obtained using the univariate ($S = 1$), AS-PDD approximation are accurate and hence adequate. However, the numbers of function evaluations step up for the bivariate ($S = 2$), AS-PDD approximation, as expected. When the univariate, AS-PDD approximation is employed, the respective numbers of function evaluations diminish by more than a factor of five, regardless of method selected.

Since this problem was also solved by the RIA, PMA, RIA envelope method, and PMA envelope method, comparing their reported solutions [115], listed in the sixth through ninth columns of Table 5.2, with the proposed solutions should be intriguing. These existing methods are commonly used in conjunction with FORM for solving RBDO problems. It appears that RIA and PMA and their respective enhancements are also capable of producing optimal solutions similar to those obtained by the AS-PDD-SPA and AS-PDD-MCS methods, but by incurring computational costs markedly higher than those by the latter two methods. Comparing the num-

bers of function evaluations, the RIA and PMA methods are more expensive than the AS-PDD-SPA methods by factors of 20 to 120. These factors grow into 25 to 150 when graded against the AS-PDD-MCS methods. The dramatic reduction of computational cost by the proposed methods indicates that the AS-PDD approximations, in cooperation with the multi-point, single-step design process, should greatly improve the current state of the art of reliability-based design optimization.

Table 5.2: Optimization results for speed reducer problem

	AS-PDD-SPA $S=1$	AS-PDD-SPA $S=2$	AS-PDD-MCS $S=1$	AS-PDD-MCS $S=2$	RIA[a]	PMA[a]	RIA envelope[a]	PMA envelope[a]
$\bar{d}_1^*$, cm	3.5767	3.5767	3.5784	3.5793	3.58	3.60	3.60	3.60
$\bar{d}_2^*$, cm	0.7000	0.7000	0.7000	0.7006	0.7	0.7	0.7	0.7
$\bar{d}_3^*$	17.0000	17.0000	17.0016	17.0024	17.0	17.8	17.0	17.2
$\bar{d}_4^*$, cm	8.2983	8.2984	7.3000	7.5062	7.43	7.30	7.61	8.30
$\bar{d}_5^*$, cm	7.9782	7.9783	8.2901	8.2713	8.24	7.79	8.15	8.30
$\bar{d}_6^*$, cm	3.8627	3.8645	3.4815	3.3630	3.37	3.40	3.43	3.43
$\bar{d}_7^*$, cm	5.3355	5.3394	5.3018	5.3018	5.31	5.34	5.50	5.45
c_0, g	3224	3227	3082	3059	3039	3037	3207	3100
Max value of c_l, $l = 1, \cdots, 11$ [b]	-3.67×10^{-5}	-3.27×10^{-5}	9.62×10^{-6}	-7.53×10^{-6}	-4.97×10^{-4}	1.43×10^{-2}	-1.31×10^{-3}	-1.31×10^{-3}
No. of y_l eval., $l = 1 \cdots, 11$	748	4132	517	3337	89,303	81,520	5304	10,917

[a] The results of RIA, PMA, RIA envelope, and PMA envelope are from Lee et al. [115].
[b] The constraint values are calculated by MCS with 10^8 sample size.

5.8.3 Example 3: size design of a six-bay, twenty-one-bar truss

This example demonstrates how an RBDO problem entailing system reliability constraints can be efficiently solved by the AS-PDD-MCS method. A linear-elastic, six-bay, twenty-one-bar truss structure, with geometric properties shown in Figure 5.7, is simply supported at nodes 1 and 12, and is subjected to four concentrated loads of 10,000 lb (44,482 N) at nodes 3, 5, 9, and 11 and a concentrated load of 16,000 lb (71,172 N) at node 7. The truss material is made of an aluminum alloy with the Young's modulus $E = 10^7$ psi (68.94 GPa). Considering the symmetry properties of the structure, the random input is selected as $\mathbf{X} = (X_1, \cdots, X_{11})^T$ $\in \mathbb{R}^{11}$, where $X_i,\ i = 1, \cdots, 11$, is the cross-sectional area of the ith truss member. The random variables are independent and lognormally distributed with means μ_i in^2, and standard deviations $\sigma_i = 0.1$ in^2, $i = 1, \cdots, 11$. From linear-elastic finite-element analysis (FEA), the maximum vertical displacement $v_{\max}(\mathbf{X})$ and maximum axial stress $\sigma_{\max}(\mathbf{X})$ occur at node 7 and member 3 or 12, respectively, where the permissible displacement and stress are limited to $d_{\text{allow}} = 0.266$ in (6.76 mm) and $\sigma_{\text{allow}} = 37,680$ psi (259.8 MPa), respectively. The system-level failure set is defined as $\Omega_F := \{\mathbf{x} : \{y_1(\mathbf{x}) < 0\} \cup \{y_2(\mathbf{x}) < 0\}\}$, where the performance functions

$$y_1(\mathbf{X}) = 1 - \frac{|v_{\max}(\mathbf{X})|}{d_{\text{allow}}},\ \ y_2(\mathbf{X}) = 1 - \frac{|\sigma_{\max}(\mathbf{X})|}{\sigma_{\text{allow}}}. \tag{5.70}$$

Due to symmetry, the design vector is $\mathbf{d} = (\mu_1, \cdots, \mu_{11})^T \in \mathcal{D} \subset \mathbb{R}^{11}$. The objective is to minimize the volume of the truss structure subject to a system reliability constraint, limiting the maximum vertical displacement and the maximum axial stress.

Therefore, the RBDO problem is formulated to

$$\min_{\mathbf{d}\in\mathcal{D}} \quad c_0(\mathbf{d}) = V(\mathbf{d}),$$

$$\text{subject to} \quad c_1(\mathbf{d}) = P_{\mathbf{d}}\left[\{y_1(\mathbf{X}) < 0\} \cup \{y_2(\mathbf{X}) < 0\}\right] - \Phi(-3) \leq 0,$$

$$1.0 \leq d_k \leq 30.0, \quad k = 1, \cdots, 11, \tag{5.71}$$

where $V(\mathbf{d})$ is the total volume of the truss. The initial design is $\mathbf{d}_0 = (15, 15, 15, 15, 15, 15, 15, 15, 15, 15, 15)^T$ in^2 ($\times 2.54^2$ cm^2). The approximate optimal solution is denoted by $\bar{\mathbf{d}}^* = (\bar{d}_1^*, \cdots, \bar{d}_{11}^*)^T$.
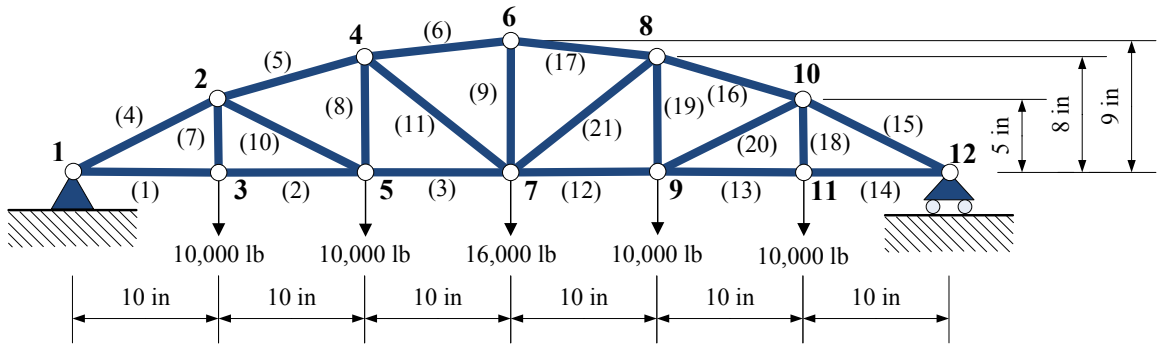
Figure 5.7: A six-bay, twenty-one-bar truss structure (Example 3)

The second column of Table 5.3 presents detailed optimization results generated by the proposed AS-PDD-MCS method employing $S = 2$. For comparison, the optimization results from the multi-point, single-step method using an existing truncated PDD-MCS approximation ($S = 2$, $m = 2$) for reliability and sensitivity analyses [110] are also tabulated in the third column. According to Table 5.3, both solutions reveal no constraint violations, but there are moderate to significant dif-

ferences in the design variables at respective optima. This is possible because the surrogate approximations grounded in adaptive-sparse and truncated PDD approximations are not necessarily the same or even similar. Therefore, when the original performance functions in Equation (5.70) are replaced with two different variants of the PDD approximation, the same initial condition may lead to distinct local optima, as found in this specific example. To seek further credibility for this reasoning, the RBDO problem, using these two optimal solutions as initial designs, was re-solved by crude MCS (10^6 samples) for evaluating the constraint and its design sensitivities in Equation (5.71). The optimal solutions from crude MCS, listed in the fourth and fifth columns of Table 5.3, are the same as the initial designs, indicating that the optimal solutions generated by the proposed and existing RBDO methods pertain to two distinct local optima. Comparing the values of objective functions at the two optima, the proposed AS-PDD-MCS method yields a slightly lower volume of the truss than the existing method. Furthermore, the AS-PDD-MCS method accomplishes this feat by reducing the number of function evaluations by 42 percent.

It is important to recognize that the AS-PDD-SPA method can be applied to solve this RBDO problem involving series-system reliability analysis by interpreting the failure domain as $\Omega_F := \{\mathbf{x} : y_{sys}(\mathbf{x}) < 0\}$, where $y_{sys}(\mathbf{X}) := \min\{y_1(\mathbf{X}), y_2(\mathbf{X})\}$ and then constructing an AS-PDD approximation of $y_{sys}(\mathbf{X})$. In doing so, however, $y_{sys}(\mathbf{X})$ is no longer a smooth function of $\mathbf{X}$, meaning that the convergence properties of the resulting AS-PDD-SPA method can be significantly deteriorated. More importantly, the AS-PDD-SPA method is not suitable for a general system reliability

problem involving multiple, interdependent component performance functions. This is the primary reason why the AS-PDD-SPA method was not used in this example.

Table 5.3: Optimization results for the six-bay, twenty-one-bar truss problem

	AS-PDD-MCS	Truncated PDD-MCS $S = 2,\ m = 2$	Crude-MCS-I[a]	Crude-MCS-II[b]
$\bar{d}_1^*$, in^2	5.0071	4.3799	5.0071	4.3799
$\bar{d}_2^*$, in^2	4.7132	3.9511	4.7132	3.9511
$\bar{d}_3^*$, in^2	2.7500	2.5637	2.7500	2.5637
$\bar{d}_4^*$, in^2	2.8494	3.6468	2.8494	3.6468
$\bar{d}_5^*$, in^2	2.7354	3.4131	2.7354	3.4131
$\bar{d}_6^*$, in^2	5.2246	3.8784	5.2246	3.8784
$\bar{d}_7^*$, in^2	1.8607	4.8285	1.8607	4.8285
$\bar{d}_8^*$, in^2	1.6262	3.1202	1.6262	3.1202
$\bar{d}_9^*$, in^2	3.2716	5.1164	3.2716	5.1164
$\tilde{d}_{10}^*$, in^2	1.3084	3.2883	1.3084	3.2883
$\bar{d}_{11}^*$, in^2	2.4425	2.1743	2.4425	2.1743
c_0, in^3	641.14	722.14	641.14	722.14
c_1 [c]	-0.2000×10^{-4}	-0.5400×10^{-4}	-0.2000×10^{-4}	-0.5400×10^{-4}
No. of y_i eval., $i = 1 \cdots, 2$	4,886	8,464	264,000,000	280,000,000

[a] Crude-MCS-I: initial design is set to the optimal solution of AS-PDD-MCS, i.e., the optimal solution in the second column.
[b] Crude-MCS-II: initial design is set to the optimal solution of truncated PDD-MCS, i.e., the optimal solution in the third column.
[b] The constraint values are calculated by MCS with 10^6 sample size.

5.8.4   Example 4: shape design of a jet engine bracket

The final example demonstrates the usefulness of the RBDO methods advocated in designing an industrial-scale mechanical component, known as a jet engine bracket, as shown in Figure 5.8(a). Seventy-nine random shape parameters, X_i, $i = 1, \cdots, 79$, resulting from manufacturing variability, describe the shape of a jet engine bracket in three dimensions, including two rounded quadrilateral holes introduced to reduce the mass of the jet engine bracket as much as possible. The design variables, $d_k = \mathbb{E}_{\mathbf{d}}[X_k]$, $k = 1, \cdots, 79$, as shown in Figure 5.9, are the means (mm) of these 79 independent random variables, with Figures 5.8(b)-(d) depicting the initial design of the jet engine bracket geometry at mean values of the shape parameters. The centers of the four bottom circular holes are fixed. A deterministic horizontal force, $F = 43.091$ kN, was applied at the center of the top circular hole with a 48° angle from the horizontal line, as shown in Figure 5.8(c), and a deterministic torque, $T = 0.1152$ kN-m, was applied at the center of the top circular hole, as shown in Figure 5.8(d). These boundary conditions are determined from the interaction of the jet engine bracket with other mechanical components of the jet engine. The jet engine bracket is made of Titanium Alloy Ti-6Al-4V with deterministic material properties, as follows: mass density $\rho = 4430$ kg/m³, elastic modulus $E = 113.8$ GPa, Poisson's ratio $\nu = 0.342$, fatigue strength coefficient $\sigma'_f = 2030$ MPa, fatigue strength exponent $b = -0.104$, fatigue ductility coefficient $\epsilon'_f = 0.841$, and fatigue ductility exponent $c = -0.69$. The performance of the jet engine bracket was determined by its fatigue durability obtained by (1) calculating maximum principal strain and mean stress at

a point; and (2) calculating the fatigue crack-initiation life at that point from the well-known Coffin-Manson-Morrow equation [108]. The objective is to minimize the mass of the jet engine bracket by changing the shape of the geometry such that the minimum fatigue crack-initiation life $N_{\min}(\mathbf{X})$ exceeds a design threshold of $N_c = 10^6$ loading cycles with 99.865% probability. Mathematically, the RBDO for this problem is defined to

$$
\min_{\mathbf{d} \in \mathcal{D}} \quad c_0(\mathbf{d}) = \rho \int_{\mathcal{D}'(\mathbf{d})} d\mathcal{D}',
$$

$$
\text{subject to} \quad c_1(\mathbf{d}) = P_{\mathbf{d}} \left[y_1(\mathbf{X}) < 0 \right] - \Phi(-3) \leq 0,
$$

$$
d_{k,L} \leq d_k \leq d_{k,U} \qquad i = 1, ..., 79, \tag{5.72}
$$

where

$$
y_1(\mathbf{X}) = N_{\min}(\mathbf{X}) - N_c \tag{5.73}
$$

is a high-dimensional random response function. The initial design $\mathbf{d}_0 = (d_{0,1}, \cdots, d_{0,79})^T$ mm; the upper and lower bounds of the design vector $\mathbf{d} = (d_1, \cdots, d_{79})^T \in \mathcal{D} \subset \mathbb{R}^{79}$ are listed in Table 5.4. Figure 5.10 portrays the FEA mesh for the initial jet engine bracket design, which comprises 341,112 nodes and 212,716 ten-noded, quadratic, tetrahedral elements.
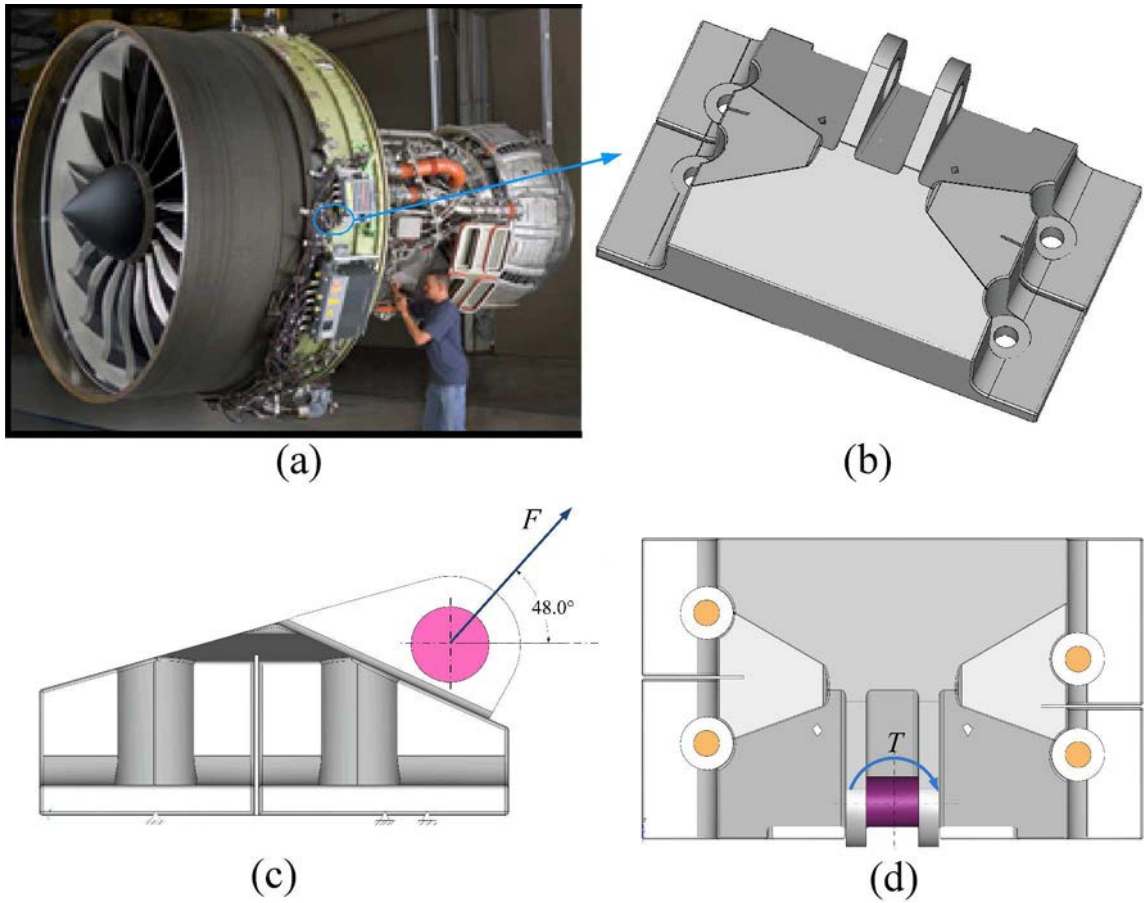
Figure 5.8: A jet engine bracket; (a) a jet engine; (b) isometric view; (c) lateral view; (d) top view

Figure 5.9: Definitions of 79 design variables

Table 5.4: Initial values, optimal values, and bounds of design variables for the jet engine bracket problem

i	$d_{0,i}$ mm	$\bar{d}_i^*$ mm	$d_{i,L}$ mm	$d_{i,U}$ mm	i	$d_{0,i}$ mm	$\bar{d}_i^*$ mm	$d_{i,L}$ mm	$d_{i,U}$ mm	i	$d_{0,i}$ mm	$\bar{d}_i^*$ mm	$d_{i,L}$ mm	$d_{i,U}$ mm
1	75	58.00	58	75	28	45	20.00	20	45	55	1	15.00	1	15
2	60	67.00	60	67	29	64	60.00	60	64	56	28	23.00	23	28
3	38	58.00	26	58	30	45	24.00	24	45	57	-2	5.00	-2	5
4	75	45.00	45	75	31	59.5	35.00	35	59.5	58	30	23.00	23	30
5	75	18.00	18	75	32	45	30.00	30	45	59	4	22.00	4	22
6	38	58.00	26	58	33	28	22.00	22	34	60	32	46.00	32	46
7	75	27.00	27	75	34	45	38.00	38	45	61	1	10.00	1	10
8	60	67.00	60	67	35	100	87.00	87	100	62	28	23.00	23	28
9	75	40.00	40	75	36	20	32.00	20	32	63	0	5.00	0	5
10	100	87.00	87	100	37	64	60.00	60	64	64	30	40.00	30	40
11	8.5	14.00	8.5	14	38	20	36.00	20	36	65	1	15.00	1	15
12	64	63.92	60	64	39	59.5	48.00	48	59.5	66	32	46.00	32	46
13	8.5	19.00	8.5	19	40	20	25.00	20	25	67	1	16.00	1	16
14	59.5	44.00	44	59.5	41	59.5	48.00	48	59.5	68	30	23.00	23	30
15	8.5	19.00	8.5	19	42	19	-8	-8	19	69	4	20.00	4	20
16	59.5	48.00	48	59.5	43	64	64.00	60	64	70	40	10.00	10	40
17	7.5	-14	-14	7.5	44	19	0.00	0	19	71	48	40.00	40	48
18	64	64.00	60	64	45	19	7.00	7	19	72	40	10.00	10	40
19	7.5	-3.5	-3.5	7.5	46	15	62.62	15	65	73	48	40.00	40	48
20	7.5	1.50	1.5	7.5	47	1	16.57	1	18	74	40	10.00	10	40
21	45	25.00	25	45	48	1	18.00	1	18	75	48	40.00	40	48
22	64	60.00	60	64	49	15	61.82	15	65	76	40	10.00	10	40
23	45	24.00	24	45	50	15	65.00	15	65	77	48	40.00	40	48
24	59.5	35.00	35	59.5	51	1	80.00	1	80	78	33	-2	-2	33
25	45	30.00	30	45	52	1	46.73	1	80	79	52	40.00	40	52
26	28	22.00	22	34	53	15	59.33	15	65					
27	45	38.00	38	45	54	30	40.00	30	40					
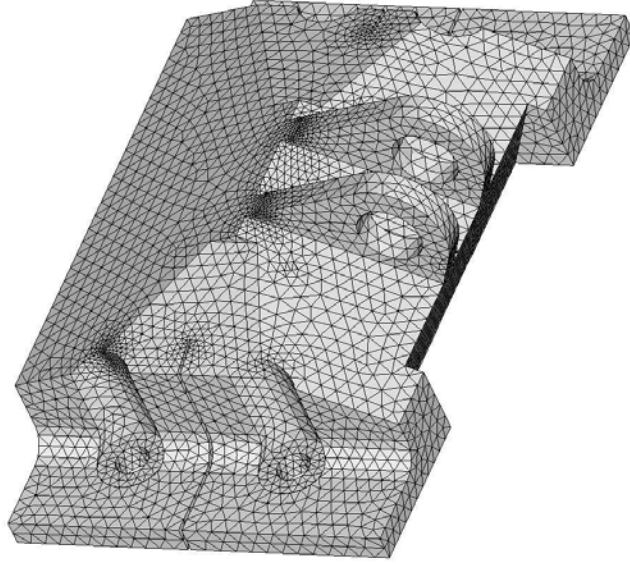
Figure 5.10: FEA mesh of the initial jet engine bracket design

Due to their finite bounds, the random variables X_i, $i = 1, \cdots, 79$, were assumed to follow truncated Gaussian distributions with densities

$$f_{X_i}(x_i) = \frac{\phi\left(\dfrac{x_i - d_i}{\sigma_i}\right)}{\Phi\left(\dfrac{D_i}{\sigma_i}\right) - \Phi\left(-\dfrac{D_i}{\sigma_i}\right)} \tag{5.74}$$

when $a_i \leq x_i \leq b_i$ and *zero* otherwise, where $\Phi(\cdot)$ and $\phi(\cdot)$ are the cumulative distribution and probability density functions, respectively, of a standard Gaussian random variable; $\sigma_i = 0.2$ are constants; $a_i = d_i - D_i$ and $b_i = d_i + D_i$ are the lower and upper bounds, respectively, of X_i; and $D_i = 2$.

The proposed AS-PDD-MCS method was applied to solve this jet engine bracket design problem employing $S = 1$ since employing $S \geq 2$ demands a large number of FEAs leading to a prohibitive computational cost for this 79-dimensional

problem. Figures 5.11(a) through (d) show the contour plots of the logarithm of fatigue crack-initiation life at mean shapes of several design iterations, including the initial design, throughout the RBDO process. Due to a conservative initial design, with fatigue life contour depicted in Figure 5.11(a), the minimum fatigue crack-initiation life of 0.665×10^{10} cycles is much larger than the required fatigue crack-initiation life of a million cycles. For the tolerance and subregion size parameters selected, 14 iterations and 2,808 FEA led to a final optimal design with the corresponding mean shape presented in Figure 5.11(d).
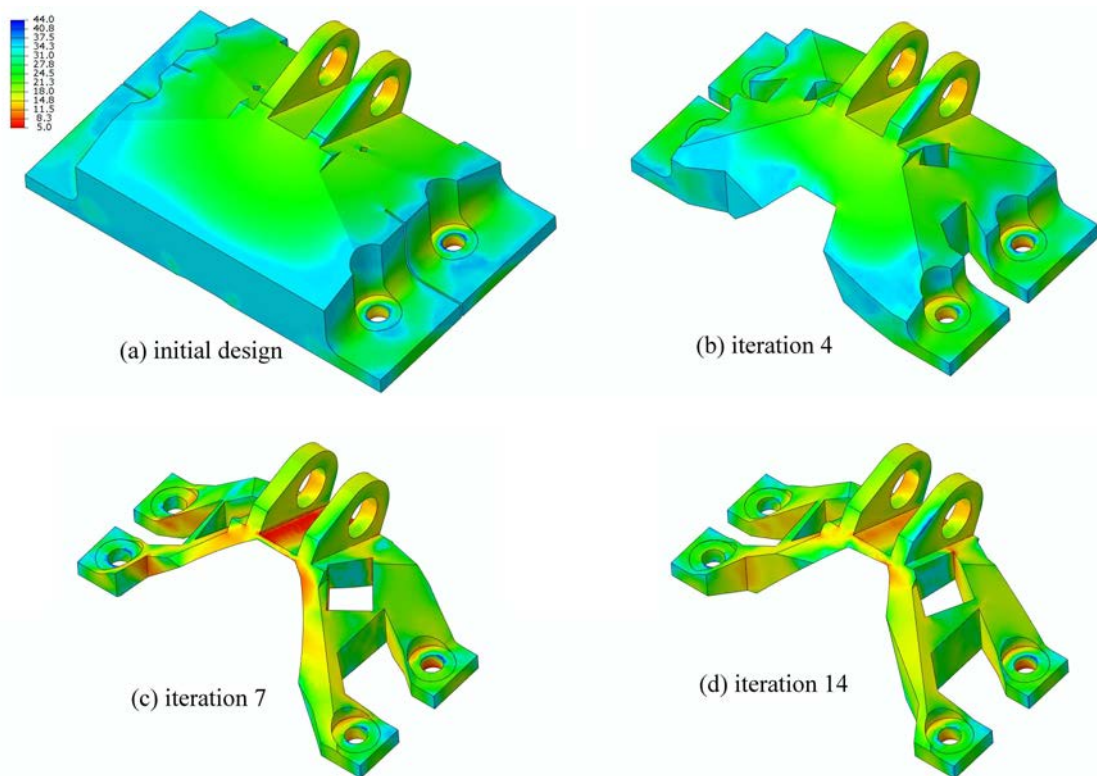
Figure 5.11: Contours of logarithmic fatigue crack-initiation life at mean shapes of the jet engine bracket by the multi-point, single-step PDD method; (a) initial design; (b) iteration 4; (c) iteration 7; (d) iteration 14 (optimum)

Table 5.4 exhibits the values of design variables, objective function, and constraint function for both the optimal and initial designs. The objective function c_0 is reduced from 2.9977 kg at initial design to 0.4904 kg at optimal design — an almost 84 percent change. At optimum, the constraint function c_1 is -1.35×10^{-3} and is, therefore, close to being active. Most of the design variables, except for d_{12}, d_{18}, and d_{43}, have undergone the most significant changes from their initial values, prompting substantial modifications of the shapes or sizes of the outer boundaries, rounded quadrilateral holes, and bottom surfaces of the engine bracket. The design variables d_{12}, d_{18}, and d_{43}, controlling minor features of outer boundaries, are virtually unchanged, because the associated initial values used are close to or the same as their lower or upper bounds, which the design process is seeking. This final example demonstrates that the RBDO methods developed — in particular, the AS-PDD-MCS method — are capable of solving industrial-scale engineering design problems with affordable computational cost.

5.9   Conclusion

Two new methods, namely, the AS-PDD-SPA method and the AS-PDD-MCS method, are proposed for reliability-based design optimization of complex engineering systems. The methods involve an adaptive-sparse polynomial dimensional decomposition of a high-dimensional stochastic response for reliability analysis, a novel integration of AS-PDD and score functions for calculating the sensitivities of the probability failure with respect to design variables, and standard gradient-based optimization al-

gorithms, encompassing a multi-point, single-step design process. The AS-PDD-SPA method capitalizes on a novel integration of AS-PDD, SPA, and score functions. The result is analytical formulae for calculating the failure probability and design sensitivities, solving component-level RBDO problems. In contrast, the AS-PDD-MCS method utilizes the embedded MCS of AS-PDD approximations and score functions. Unlike the AS-PDD-SPA method, however, the failure probability and design sensitivities in the AS-PDD-MCS method are estimated via efficient sampling of approximate stochastic responses, thereby affording the method the capability to address either component- or system-level RBDO problems. Furthermore, the AS-PDD-MCS method is not influenced by any added approximations, involving calculations of the saddlepoint and higher-order moments, of the AS-PDD-SPA method. Since both methods are rooted in the AS-PDD approximation, a dimension-reduction approach combining sparse- and full-grid quadratures is proposed to estimate the expansion coefficients more accurately than existing techniques. For the two methods developed, both the failure probability and its design sensitivities are determined concurrently from a single stochastic analysis or simulation. Consequently, the methods provide not only more accurate, but also more computationally efficient, design solutions than existing methods. Moreover, the multi-point, single-step design process embedded in the proposed methods facilitates a solution of an RBDO problem with a large design space. Precisely for this reason, the methods developed are capable of solving high-dimensional practical engineering problems, as demonstrated by the shape design of a jet engine bracket with 79 design variables.

CHAPTER 6
STOCHASTIC DESIGN OPTIMIZATION INVOLVING MIXED DESIGN VARIABLES

6.1　Introduction

This chapter presents a new method for RDO and RBDO involving both distributional and structural design variables. The method comprises: (1) a new augmented PDD of a high-dimensional stochastic response for statistical moment and reliability analyses; (2) an integration of the augmented PDD, score functions, and finite-difference approximation for calculating the sensitivities of the first two moments and the failure probability with respect to distributional and structural design variables; and (3) standard gradient-based optimization algorithms, encompassing a multi-point, single-step design process. Section 6.2 formally defines general RDO and RBDO problems involving mixed design variables, including their concomitant mathematical statements. Section 6.3 introduces the augmented PDD and its truncation in terms of both input random variables and new random variables affiliated with the distributional and structural design variables. The section also explains how the truncated augmented PDD leads to stochastic analysis consisting of analytical formulae for evaluating the first two moments and the embedded Monte Carlo simulation (MCS) for reliability analysis. Section 6.4 demonstrates that the effort required to calculate statistical moments or failure probability also delivers their design sensitivities. Section 6.5 introduces a multi-point, single-step iterative scheme for RDO and RBDO and elucidates how the stochastic analysis and design sensitivities are

integrated with a gradient-based optimization algorithm. Section 6.6 presents four numerical examples involving mathematical functions or solid-mechanics problems, and contrasts the accuracy and computational efforts of the proposed methods for sensitivity analysis of moments and reliability as well as solutions of two RDO/RBDO problems, all entailing mixed design variables. Finally, the conclusions are drawn in Section 6.7.

6.2   Design under Uncertainty

Consider a measurable space $(\Omega_{\mathbf{d}}, \mathcal{F}_{\mathbf{d}})$, where $\Omega_{\mathbf{d}}$ is a sample space and $\mathcal{F}_{\mathbf{d}}$ is a σ-field on $\Omega_{\mathbf{d}}$. For $M \in \mathbb{N}$ and $N \in \mathbb{N}$, let $\mathbf{d}_T = (\mathbf{d}, \mathbf{s}) = (d_1, \cdots, d_{M_d}, s_1, \cdots, s_{M_s})^T \in \mathcal{D}$ be an $\mathbb{R}^M$-valued design vector with non-empty closed set $\mathcal{D} \subseteq \mathbb{R}^M$, where $M_d, M_s \in \mathbb{N}$ and $M = M_d + M_s$, and let $\mathbf{X} := (X_1, \cdots, X_N)^T : (\Omega_{\mathbf{d}}, \mathcal{F}_{\mathbf{d}}) \rightarrow (\mathbb{R}^N, \mathcal{B}^N)$ be an $\mathbb{R}^N$-valued input random vector with $\mathcal{B}^N$ representing the Borel σ-field on $\mathbb{R}^N$, describing the statistical uncertainties in loads, material properties, and geometry of a complex mechanical system. The design variables are grouped into two major classes: (1) distributional design vector $\mathbf{d}$ with dimensionality M_d, and (2) structural design vector $\mathbf{s}$ with dimensionality M_s. A distributional design variable d_k, $k = 1, \cdots, M_d$, can be any distribution parameter or a statistic—for instance, the mean and standard deviation—of one or more random variables. A structural design variable s_p, $p = 1, \cdots, M_s$, can be any deterministic parameter of a performance function. Defined over $(\Omega_{\mathbf{d}}, \mathcal{F}_{\mathbf{d}})$, let $\{P_{\mathbf{d}} : \mathcal{F} \rightarrow [0, 1]\}$ be a family of probability measures. The probability law of $\mathbf{X}$ is completely defined by a family of the joint probability density

functions (PDF) $\{f_{\mathbf{X}}(\mathbf{x}; \mathbf{d}), \mathbf{x} \in \mathbb{R}^N, \mathbf{d} \in \mathcal{D}\}$ that are associated with corresponding probability measures $\{P_{\mathbf{d}}, \mathbf{d} \in \mathbb{R}^{M_d}\}$, so that the probability triple $(\Omega_{\mathbf{d}}, \mathcal{F}_{\mathbf{d}}, P_{\mathbf{d}})$ of $\mathbf{X}$ depends on $\mathbf{d}$.

Let $y_l(\mathbf{X}; \mathbf{d}, \mathbf{s})$, $l = 0, 1, 2, \cdots, K$, be a collection of $K + 1$ real-valued, square-integrable, measurable transformations on $(\Omega_{\mathbf{d}}, \mathcal{F}_{\mathbf{d}})$, describing relevant geometry (*e.g.*, length, area, volume, mass) and performance functions of a complex system. The function $y_l : (\mathbb{R}^N, \mathcal{B}^N) \to (\mathbb{R}, \mathcal{B})$ in general is not only an explicit function of distributional and structural design variables $\mathbf{d}$ and $\mathbf{s}$, but also implicitly depends on distributional design variables $\mathbf{d}$ via the probability law of $\mathbf{X}$. There exist two prominent variants of design optimization under uncertainty, described as follows.

6.2.1   Robust Design Optimization

The mathematical formulation of a general RDO problem involving an objective function $c_0 : \mathbb{R}^M \to \mathbb{R}$ and constraint functions $c_l : \mathbb{R}^M \to \mathbb{R}$, where $l = 1, \cdots, K$ and $1 \leq K < \infty$, requires one to

$$\min_{(\mathbf{d}, \mathbf{s}) \in \mathcal{D} \subseteq \mathbb{R}^M} \quad c_0(\mathbf{d}, \mathbf{s}) := w_1 \frac{\mathbb{E}_{\mathbf{d}} [y_0(\mathbf{X}; \mathbf{d}, \mathbf{s})]}{\mu_0^*} + w_2 \frac{\sqrt{\text{var}_{\mathbf{d}} [y_0(\mathbf{X}; \mathbf{d}, \mathbf{s})]}}{\sigma_0^*},$$

$$\text{subject to} \quad c_l(\mathbf{d}, \mathbf{s}) := \alpha_l \sqrt{\text{var}_{\mathbf{d}} [y_l(\mathbf{X}; \mathbf{d}, \mathbf{s})]} - \mathbb{E}_{\mathbf{d}} [y_l(\mathbf{X}; \mathbf{d}, \mathbf{s})] \leq 0, \ l = 1, \cdots, K,$$

$$d_{k,L} \leq d_k \leq d_{k,U}, \ k = 1, \cdots, M_d,$$

$$s_{p,L} \leq s_p \leq s_{p,U}, \ p = 1, \cdots, M_s, \tag{6.1}$$

where $\mathbb{E}_{\mathbf{d}}[y_l(\mathbf{X}; \mathbf{d}, \mathbf{s})] := \int_{\mathbb{R}^N} y_l(\mathbf{x}; \mathbf{d}, \mathbf{s}) f_{\mathbf{X}}(\mathbf{x}; \mathbf{d}) d\mathbf{x}$ is the mean of $y_l(\mathbf{X}; \mathbf{d}, \mathbf{s})$ with $\mathbb{E}_{\mathbf{d}}$ denoting the expectation operator with respect to the probability measure $f_{\mathbf{X}}(\mathbf{x}; \mathbf{d}) d\mathbf{x}$ of $\mathbf{X}$; $\text{var}_{\mathbf{d}}[y_l(\mathbf{X}; \mathbf{d}, \mathbf{s})] := \mathbb{E}_{\mathbf{d}}[\{y_l(\mathbf{X}; \mathbf{d}, \mathbf{s}) - \mathbb{E}_{\mathbf{d}}[y_l(\mathbf{X}; \mathbf{d}, \mathbf{s})]\}^2]$ is the variance of $y_l(\mathbf{X}; \mathbf{d}, \mathbf{s})$;

$w_1 \in \mathbb{R}_0^+$ and $w_2 \in \mathbb{R}_0^+$ are two non-negative, real-valued weights, satisfying $w_1 + w_2 = 1$; $\mu_0^* \in \mathbb{R} \setminus \{0\}$ and $\sigma_0^* \in \mathbb{R}_0^+ \setminus \{0\}$ are two non-zero, real-valued scaling factors; $\alpha_l \in \mathbb{R}_0^+$, $l = 0, 1, \cdots, K$, are non-negative, real-valued constants associated with the probabilities of constraint satisfaction; $d_{k,L}$ and $d_{k,U}$ are the lower and upper bounds, respectively, of d_k; and $s_{p,L}$ and $s_{p,U}$ are the lower and upper bounds, respectively, of s_p.

In Equation (6.1), $c_0(\mathbf{d}, \mathbf{s})$ describes the objective robustness, and $c_l(\mathbf{d}, \mathbf{s})$, $l = 1, \cdots, K$, describes the feasibility robustness of a given design. Evaluations of both objective robustness and feasibility robustness, involving the first two moments of various responses, are required for solving RDO problems, consequently demanding statistical moment analysis.

6.2.2 Reliability-based Design Optimization

The mathematical formulation of a general RBDO problem involving an objective function $c_0 : \mathbb{R}^M \to \mathbb{R}$ and constraint functions $c_l : \mathbb{R}^M \to \mathbb{R}$, where $l = 1, \cdots, K$ and $1 \leq K < \infty$, requires one to

$$
\begin{aligned}
&\min_{(\mathbf{d},\mathbf{s}) \in \mathcal{D} \subseteq \mathbb{R}^M} && c_0(\mathbf{d}, \mathbf{s}) \\
&\text{subject to} && c_l(\mathbf{d}, \mathbf{s}) := P_{\mathbf{d}}\left[\mathbf{X} \in \Omega_{F,l}(\mathbf{d}, \mathbf{s})\right] - p_l \leq 0, \; l = 1, \cdots, K, \\
& && d_{k,L} \leq d_k \leq d_{k,U}, \; k = 1, \cdots, M_d, \\
& && s_{p,L} \leq s_p \leq s_{p,U}, \; p = 1, \cdots, M_s,
\end{aligned}
\tag{6.2}
$$

where $\Omega_{F,l}(\mathbf{d}, \mathbf{s}) \subseteq \Omega$ is the lth failure set that, in general, may depend on $\mathbf{d}$ and $\mathbf{s}$, and $0 \leq p_l \leq 1$, $l = 1, \cdots, K$, are target failure probabilities.

In Equation (6.2), the objective function $c_0(\mathbf{d}, \mathbf{s})$ is commonly prescribed as a deterministic function of $\mathbf{d}$ and $\mathbf{s}$, describing relevant system geometry, such as area, volume, and mass. In contrast, the constraint functions $c_l(\mathbf{d}, \mathbf{s})$, $l = 1, 2, \cdots, K$, are generally more complicated than the objective function. Depending on the failure domain $\Omega_{F,l}(\mathbf{d}, \mathbf{s})$, a component or a system reliability analysis can be envisioned. For component reliability analysis, the failure domain is often adequately described by a single performance function $y_l(\mathbf{X}; \mathbf{d}, \mathbf{s})$, for instance, $\Omega_{F,l}(\mathbf{d}, \mathbf{s}) := \{\mathbf{x} : y_l(\mathbf{x}; \mathbf{d}, \mathbf{s}) < 0\}$, whereas multiple, interdependent performance functions $y_{l,i}(\mathbf{x}; \mathbf{d}, \mathbf{s})$, $i = 1, 2, \cdots$, are required for system reliability analysis, leading, for example, to $\Omega_{F,l}(\mathbf{d}, \mathbf{s}) := \{\mathbf{x} : \cup_i y_{l,i}(\mathbf{x}; \mathbf{d}, \mathbf{s}) < 0\}$ and $\Omega_{F,l}(\mathbf{d}, \mathbf{s}) := \{\mathbf{x} : \cap_i y_{l,i}(\mathbf{x}; \mathbf{d}, \mathbf{s}) < 0\}$ for series and parallel systems, respectively.

The RDO and RBDO problems described by Equations (6.1) or (6.2) entail mixed design variables, and, therefore, they constitute more general stochastic design problems than those studied in the past [1–6, 9, 12–14, 86, 89, 91, 93, 112, 117–124]. Solving such an RDO or RBDO problem using gradient-based optimization algorithms mandates not only statistical moment and reliability analyses, but also the gradients of moments and failure probability with respect to both distributional and structural design variables. The focus of this work is to solve a general high-dimensional RDO or RBDO problem described by Equation (6.1) or (6.2) for arbitrary square-integrable functions $y_l(\mathbf{X}; \mathbf{d}, \mathbf{s})$, $l = 0, 1, 2, \cdots, K$, and arbitrary probability distributions of $\mathbf{X}$, provided that a few regularity conditions are met.

6.3 Stochastic Analysis

6.3.1 Augmented PDD

Consider two additional measurable spaces $(\Omega_1, \mathcal{F}_1)$ and $(\Omega_2, \mathcal{F}_2)$, where Ω_1 and Ω_2 are two sample spaces and $\mathcal{F}_1$ and $\mathcal{F}_2$ are two σ-fields on Ω_1 and Ω_2, respectively. Let $\mathbf{D} := (D_1, \cdots, D_{M_d})^T : (\Omega_1, \mathcal{F}_1) \to (\mathbb{R}^{M_d}, \mathcal{B}^{M_d})$ and $\mathbf{S} := (S_1, \cdots, S_{M_s})^T : (\Omega_2, \mathcal{F}_2) \to (\mathbb{R}^{M_s}, \mathcal{B}^{M_s})$ be two affiliated random vectors with $\mathcal{B}^{M_d}$ and $\mathcal{B}^{M_s}$ representing the Borel σ-fields on $\mathbb{R}^{M_d}$ and $\mathbb{R}^{M_s}$, respectively. The probability laws of $\mathbf{D}$ and $\mathbf{S}$ are completely defined by selecting two families of the joint PDFs $\{f_{\mathbf{D}}(\mathbf{d}; \boldsymbol{\mu}_{\mathbf{D}}), \mathbf{d} \in \mathbb{R}^{M_d}\}$ and $\{f_{\mathbf{S}}(\mathbf{s}; \boldsymbol{\mu}_{\mathbf{S}}), \mathbf{s} \in \mathbb{R}^{M_s}\}$ with probability measures P_1 and P_2, and corresponding mean vectors $\mathbb{E}_1[\mathbf{D}] = \boldsymbol{\mu}_{\mathbf{D}}$ and $\mathbb{E}_2[\mathbf{S}] = \boldsymbol{\mu}_{\mathbf{S}}$, respectively.

Introduce an augmented measurable space $(\Omega_A, \mathcal{F}_A)$, where $\Omega_A := \Omega_{\mathbf{d}} \times \Omega_1 \times \Omega_2$ is the augmented sample space and $\mathcal{F}_A = \mathcal{F}_{\mathbf{d}} \times \mathcal{F}_1 \times \mathcal{F}_2$ is the corresponding σ-field on Ω_A. Let $y(\mathbf{X}; \mathbf{d}, \mathbf{s}) := y(X_1, \cdots, X_N; \mathbf{d}, \mathbf{s})$ represent any one of the random functions y_l, $l = 0, 1, \cdots, K$, introduced in Section 6.2. Then $y(\mathbf{X}; \mathbf{D}, \mathbf{S}) := y(X_1, \cdots, X_N; \mathbf{D}, \mathbf{S})$, obtained by simply replacing deterministic vectors $\mathbf{d}$ and $\mathbf{s}$ with random vectors $\mathbf{D}$ and $\mathbf{S}$ in $y(\mathbf{X}; \mathbf{d}, \mathbf{s})$, has the same functional form of $y(\mathbf{X}; \mathbf{d}, \mathbf{s})$. Let $\mathcal{L}_2(\Omega_A, \mathcal{F}_A, P_A)$ represent a Hilbert space of square-integrable functions $y(\mathbf{X}; \mathbf{D}, \mathbf{S})$ with respect to the probability measure $P_A = P_{\mathbf{d}} \times P_1 \times P_2$ supported on $\mathbb{R}^{N+M}$. Assuming independent coordinates, the joint PDFs of $\mathbf{X}$, $\mathbf{D}$, and $\mathbf{S}$ are expressed by the products,

$$f_A(\mathbf{x}, \mathbf{d}, \mathbf{s}) = f_{\mathbf{X}}(\mathbf{x}; \mathbf{d}) f_{\mathbf{D}}(\mathbf{d}; \boldsymbol{\mu}_{\mathbf{D}}) f_{\mathbf{S}}(\mathbf{s}; \boldsymbol{\mu}_{\mathbf{S}}) = \prod_{i=1}^{N} f_{X_i}(x_i; \mathbf{d}) \prod_{k=1}^{M_d} f_{D_k}(d_k; \boldsymbol{\mu}_{\mathbf{D}}) \prod_{p=1}^{M_s} f_{S_p}(s_p; \boldsymbol{\mu}_{\mathbf{S}}),$$

$$(6.3)$$

of marginal PDFs $f_{X_i} : \mathbb{R} \to \mathbb{R}_0^+$ of X_i, $f_{D_k} : \mathbb{R} \to \mathbb{R}_0^+$ of D_k, and $f_{S_p} : \mathbb{R} \to \mathbb{R}_0^+$ of S_p, $i = 1, \cdots, N$, $k = 1, \cdots, M_d$, and $p = 1, \cdots, M_s$. Then, for three given subsets $u \subseteq \{1, \cdots, N\}$, $v \subseteq \{1, \cdots, M_d\}$, and $w \subseteq \{1, \cdots, M_s\}$,

$$f_{uvw}(\mathbf{x}_u, \mathbf{d}_v, \mathbf{s}_w) := \prod_{q=1}^{|u|} f_{X_{i_q}}(x_{i_q}; \mathbf{d}) \prod_{r=1}^{|v|} f_{D_{k_r}}(d_{k_r}; \boldsymbol{\mu_D}) \prod_{t=1}^{|w|} f_{S_{q_t}}(s_{q_t}; \boldsymbol{\mu_S}) \tag{6.4}$$

defines the marginal density function of the subvector $(X_{i_1}, \cdots, X_{i_{|u|}}, D_{k_1}, \cdots, D_{k_{|v|}},$ $S_{p_1}, \cdots, S_{p_{|w|}})^T$, where $|\cdot|$ denotes cardinality.

Let $\{\psi_{i_q j_q}(X_{i_q}; \mathbf{d}); \ j_q = 0, 1, \cdots\}$, $\{\phi_{k_r l_r}(D_{k_r}; \boldsymbol{\mu_D}); \ l_r = 0, 1, \cdots\}$, and $\{\varphi_{p_t n_t}$ $(S_{p_t}; \boldsymbol{\mu_S}); \ n_t = 0, 1, \cdots\}$ be three sets of univariate orthonormal polynomial basis functions in the Hilbert spaces $\mathcal{L}_2(\Omega_{i_q, \mathbf{d}}, \mathcal{F}_{i_q, \mathbf{d}}, P_{i_q, \mathbf{d}})$, $\mathcal{L}_2(\Omega_{k_r, 1}, \mathcal{F}_{k_r, 1}, P_{k_r, 1})$, and $\mathcal{L}_2(\Omega_{p_t, 2}, \mathcal{F}_{p_t, 2}, P_{p_t, 2})$, respectively, which are consistent with the probability measures $P_{i_q, \mathbf{d}}$, $P_{k_r, 1}$, and $P_{q_t, 2}$, respectively, where $i_q = 1, \cdots, N$, $k_r = 1, \cdots, M_d$, and $q_t = 1, \cdots, M_s$. For given $\emptyset \neq u = \{i_1, \cdots, i_{|u|}\} \subseteq \{1, \cdots, N\}$, $\emptyset \neq v = \{k_1, \cdots, k_{|v|}\} \subseteq \{1, \cdots, M_d\}$ and $\emptyset \neq w = \{p_1, \cdots, p_{|w|}\} \subseteq \{1, \cdots, M_s\}$, define three associated multi-indices $\mathbf{j}_{|u|} = (j_1, \cdots, j_{|u|}) \in \mathbb{N}_0^{|u|}$, $\mathbf{l}_{|v|} = (l_1, \cdots, l_{|v|}) \in \mathbb{N}_0^{|v|}$, and $\mathbf{n}_{|w|} = (n_1, \cdots, n_{|w|}) \in \mathbb{N}_0^{|w|}$. Denote the product polynomials by

$$\psi_{u\mathbf{j}_{|u|}}(\mathbf{X}_u; \mathbf{d}) = \begin{cases} 1 & u = \emptyset, \\ \prod_{q=1}^{|u|} \psi_{i_q j_q}(X_{i_p}; \mathbf{d}) & \emptyset \neq u = \{i_1, \cdots, i_{|u|}\} \subseteq \{1, \cdots, N\}, \end{cases} \tag{6.5}$$

$$\phi_{v\mathbf{l}_{|v|}}(\mathbf{d}_v; \boldsymbol{\mu_D}) = \begin{cases} 1 & v = \emptyset, \\ \prod_{r=1}^{|v|} \phi_{k_r l_r}(d_{k_r}; \boldsymbol{\mu_D}) & \emptyset \neq v = \{k_1, \cdots, k_{|v|}\} \subseteq \{1, \cdots, M_d\}, \end{cases} \tag{6.6}$$

and

$$\varphi_{w\mathbf{n}_{|w|}}(\mathbf{s}_w;\boldsymbol{\mu}_{\mathbf{S}}) \;\;=\;\; \begin{cases} 1 & w = \emptyset, \\ \\ \prod_{t=1}^{|w|} \varphi_{p_t n_t}(s_{p_t};\boldsymbol{\mu}_{\mathbf{S}}) & \emptyset \neq w = \{p_1,\cdots,p_{|w|}\} \subseteq \{1,\cdots,M_s\}, \end{cases} \tag{6.7}$$

which form three orthonormal basis functions in $\mathcal{L}_2(\times_{q=1}^{|u|}\Omega_{i_q,\mathbf{d}}, \times_{q=1}^{|u|}\mathcal{F}_{i_q,\mathbf{d}}, \times_{q=1}^{|u|}P_{i_q,\mathbf{d}})$,

$\mathcal{L}_2(\times_{r=1}^{|v|}\Omega_{k_r,1}, \times_{r=1}^{|v|}\mathcal{F}_{k_r,1}, \times_{r=1}^{|v|}P_{k_r,1})$, and $\mathcal{L}_2(\times_{t=1}^{|w|}\Omega_{p_t,2}, \times_{t=1}^{|w|}\mathcal{F}_{p_t,2}, \times_{t=1}^{|w|}P_{p_t,2})$, respec-

tively. Since the PDF of the subvector $(X_{i_1},\cdots,X_{i_{|u|}}, D_{k_1},\cdots,D_{k_{|v|}}, S_{p_1},\cdots,S_{p_{|w|}})^T$

is separable (independent), the product polynomial

$$\psi_{uvw\mathbf{j}_{|u|}\mathbf{l}_{|v|}\mathbf{n}_{|w|}}(\mathbf{X}_u,\mathbf{D}_v,\mathbf{S}_w) := \psi_{u\mathbf{j}_{|u|}}(\mathbf{X}_u;\mathbf{d})\phi_{v\mathbf{l}_{|v|}}(\mathbf{d}_v;\boldsymbol{\mu}_{\mathbf{D}})\varphi_{w\mathbf{n}_{|w|}}(\mathbf{s}_w;\boldsymbol{\mu}_{\mathbf{S}}) \tag{6.8}$$

is consistent with the PDF $f_{uvw}(\mathbf{x}_u,\mathbf{d}_v,\mathbf{s}_w)$ and constitutes an orthonormal basis in

$$\mathcal{L}_2(\times_{q=1}^{|u|}\Omega_{i_q,\mathbf{d}}\times_{r=1}^{|v|}\Omega_{k_r,1}\times_{t=1}^{|w|}\Omega_{p_t,2}, \times_{q=1}^{|u|}\mathcal{F}_{i_q,\mathbf{d}}\times_{r=1}^{|v|}\mathcal{F}_{k_r,1}\times_{t=1}^{|w|}\mathcal{F}_{p_t,2}, \times_{q=1}^{|u|}P_{i_q,\mathbf{d}}\times_{r=1}^{|v|}P_{k_r,1}\times_{t=1}^{|w|}P_{p_t,2}).$$
$$\tag{6.9}$$

The augmented PDD of a square-integrable function y represents a hierarchical

expansion

$$y(\mathbf{X};\mathbf{D},\mathbf{S}) \;\;=\;\; y_\emptyset(\mathbf{d},\boldsymbol{\mu}_{\mathbf{D}},\boldsymbol{\mu}_{\mathbf{S}}) + \sum_{\substack{u\subseteq\{1,\cdots,N\},v\subseteq\{1,\cdots,M_d\} \\ w\subseteq\{1,\cdots,M_s\},|u|+|v|+|w|\geq 1}} \sum_{\substack{\mathbf{j}_{|u|}\in\mathbb{N}_0^{|u|},\mathbf{l}_{|v|}\in\mathbb{N}_0^{|v|},\mathbf{n}_{|w|}\in\mathbb{N}_0^{|w|} \\ j_1,\cdots,j_{|u|},l_1,\cdots,l_{|v|},n_1,\cdots,n_{|w|}\neq 0}}$$
$$C_{uvw\mathbf{j}_{|u|}\mathbf{l}_{|v|}\mathbf{n}_{|w|}}(\mathbf{d},\boldsymbol{\mu}_{\mathbf{D}},\boldsymbol{\mu}_{\mathbf{S}})\psi_{u\mathbf{j}_{|u|}}(\mathbf{X}_u;\mathbf{d})\phi_{v\mathbf{l}_{|v|}}(\mathbf{D}_v;\boldsymbol{\mu}_{\mathbf{D}})\varphi_{w\mathbf{n}_{|w|}}(\mathbf{S}_w;\boldsymbol{\mu}_{\mathbf{S}}), \tag{6.10}$$

in terms of a set of random multivariate orthonormal polynomials of input variables

with increasing dimensions, where

$$y_\emptyset(\mathbf{d},\boldsymbol{\mu}_{\mathbf{D}},\boldsymbol{\mu}_{\mathbf{S}}) := \int_{\mathbb{R}^N} y(\mathbf{x};\mathbf{d},\mathbf{s})f_A(\mathbf{x},\mathbf{d},\mathbf{s})d\mathbf{x}d\mathbf{d}d\mathbf{s} \tag{6.11}$$

and

$$C_{uvw\mathbf{j}_{|u|}\mathbf{l}_{|v|}\mathbf{n}_{|w|}}(\mathbf{d}, \boldsymbol{\mu}_{\mathbf{D}}, \boldsymbol{\mu}_{\mathbf{S}}) := \int_{\mathbb{R}^{N+M}} y(\mathbf{x}; \mathbf{d}, \mathbf{s}) \psi_{u\mathbf{j}_{|u|}}(\mathbf{x}_u; \mathbf{d}) \phi_{v\mathbf{l}_{|v|}}(\mathbf{d}_v; \boldsymbol{\mu}_{\mathbf{D}}) \varphi_{w\mathbf{n}_{|w|}}(\mathbf{s}_w; \boldsymbol{\mu}_{\mathbf{S}})$$
$$\times f_A(\mathbf{x}, \mathbf{d}, \mathbf{s}) d\mathbf{x} d\mathbf{d} d\mathbf{s},$$

$$u \subseteq \{1, \cdots, N\}, v \subseteq \{1, \cdots, M_d\}, w \subseteq \{1, \cdots, M_s\}, |u| + |v| + |w| \geq 1,$$

$$\mathbf{j}_{|u|} \in \mathbb{N}_0^{|u|}, \mathbf{l}_{|v|} \in \mathbb{N}_0^{|v|}, \mathbf{n}_{|w|} \in \mathbb{N}_0^{|w|}, j_1, \cdots, j_{|u|}, l_1, \cdots, l_{|v|}, n_1, \cdots, n_{|w|} \neq 0 \qquad (6.12)$$

are various expansion coefficients. The inner sum of Equation (6.10) precludes $j_1, \cdots, j_{|u|}$ $\neq 0$, $l_1, \cdots, l_{|v|} \neq 0$, and $n_1, \cdots, n_{|w|} \neq 0$, that is, the individual degree of involved variables cannot be *zero* since $\psi_{u\mathbf{j}_{|u|}}(\mathbf{X}_u; \mathbf{d})$, $\phi_{v\mathbf{l}_{|v|}}(\mathbf{D}_v; \boldsymbol{\mu}_{\mathbf{D}})$, and $\varphi_{w\mathbf{n}_{|w|}}(\mathbf{S}_w; \boldsymbol{\mu}_{\mathbf{S}})$ are *zero*-mean strictly $|u|$-variate, $|v|$-variate, $|w|$-variate functions, respectively. Derived from the ANOVA dimensional decomposition [62], Equation (6.10) provides an exact representation because it includes all main and interactive effects of input and affiliated variables. For instance, $|u| + |v| + |w| = 0$ corresponds to the constant component function $y_\emptyset$, representing the mean effect of y; $|u| + |v| + |w| = 1$ leads to the univariate component functions, describing the main effects of input and affiliated variables; and $|u| + |v| + |w| = S$, $1 < S \leq N + M$, results in the S-variate component functions, facilitating the interaction among at most S input and affiliated variables. The augmented PDD expansion in Equation (6.10) can be used to reproduce the function $y(\mathbf{X}; \mathbf{d}, \mathbf{s})$ by simply replacing the random vectors $\mathbf{D}$ and $\mathbf{S}$ in Equation (6.10) with deterministic vectors $\mathbf{d}$ and $\mathbf{s}$, that is,

$$y(\mathbf{X}; \mathbf{d}, \mathbf{s}) = y_\emptyset(\mathbf{d}, \boldsymbol{\mu}_{\mathbf{D}}, \boldsymbol{\mu}_{\mathbf{S}}) + \sum_{\substack{u \subseteq \{1, \cdots, N\}, v \subseteq \{1, \cdots, M_d\} \\ w \subseteq \{1, \cdots, M_s\}, |u| + |v| + |w| \geq 1}} \sum_{\substack{\mathbf{j}_{|u|} \in \mathbb{N}_0^{|u|}, \mathbf{l}_{|v|} \in \mathbb{N}_0^{|v|}, \mathbf{n}_{|w|} \in \mathbb{N}_0^{|w|} \\ j_1, \cdots, j_{|u|}, l_1, \cdots, l_{|v|}, n_1, \cdots, n_{|w|} \neq 0}}$$
$$C_{uvw\mathbf{j}_{|u|}\mathbf{l}_{|v|}\mathbf{n}_{|w|}}(\mathbf{d}, \boldsymbol{\mu}_{\mathbf{D}}, \boldsymbol{\mu}_{\mathbf{S}}) \psi_{u\mathbf{j}_{|u|}}(\mathbf{X}_u; \mathbf{d}) \phi_{v\mathbf{l}_{|v|}}(\mathbf{d}_v; \boldsymbol{\mu}_{\mathbf{D}}) \varphi_{w\mathbf{n}_{|w|}}(\mathbf{s}_w; \boldsymbol{\mu}_{\mathbf{S}}) \quad (6.13)$$

6.3.2 Truncated Augmented PDD Approximation

The augmented PDD in Equation (6.10) is grounded on a fundamental conjecture known to be true in many real-world applications: given a high-dimensional function y, its $(|u|+|v|+|w|)$-variate component functions decay rapidly with respect to $|u| + |v| + |w|$, leading to accurate lower-variate approximations of y. Furthermore, the largest order of polynomials in each variable can be restricted to a finite integer. Indeed, given the integers $0 \leq S < N + M$ and $1 \leq m < \infty$ for all $1 \leq |u| + |v| + |w| \leq S$ and the ∞-norms $1 \leq ||\mathbf{j}_{|u|}||_\infty := \max\left(j_1, \cdots, j_{|u|}\right) \leq m$, $1 \leq ||\mathbf{l}_{|v|}||_\infty := \max\left(l_1, \cdots, l_{|v|}\right) \leq m$, and $1 \leq ||\mathbf{n}_{|w|}||_\infty := \max\left(n_1, \cdots, n_{|w|}\right) \leq m$, the truncated augmented PDD

$$
\tilde{y}_{S,m}(\mathbf{X}; \mathbf{D}, \mathbf{S}) = y_\emptyset(\mathbf{d}, \boldsymbol{\mu}_\mathbf{D}, \boldsymbol{\mu}_\mathbf{S}) + \sum_{\substack{u \subseteq \{1, \cdots, N\}, v \subseteq \{1, \cdots, M_d\} \\ w \subseteq \{1, \cdots, M_s\}, 1 \leq |u|+|v|+|w| \leq S}} \sum_{\substack{\mathbf{j}_{|u|} \in \mathbb{N}_0^{|u|}, \mathbf{l}_{|v|} \in \mathbb{N}_0^{|v|}, \mathbf{n}_{|w|} \in \mathbb{N}_0^{|w|} \\ ||\mathbf{j}_{|u|}||_\infty, ||\mathbf{l}_{|v|}||_\infty, ||\mathbf{n}_{|w|}||_\infty \leq m \\ j_1, \cdots, j_{|u|}, l_1, \cdots, l_{|v|}, n_1, \cdots, n_{|w|} \neq 0}}
$$
$$
C_{uvw\mathbf{j}_{|u|}\mathbf{l}_{|v|}\mathbf{n}_{|w|}}(\mathbf{d}, \boldsymbol{\mu}_\mathbf{D}, \boldsymbol{\mu}_\mathbf{S}) \psi_{u\mathbf{j}_{|u|}}(\mathbf{X}_u; \mathbf{d}) \phi_{v\mathbf{l}_{|v|}}(\mathbf{D}_v; \boldsymbol{\mu}_\mathbf{D}) \varphi_{w\mathbf{n}_{|w|}}(\mathbf{S}_w; \boldsymbol{\mu}_\mathbf{S}), \quad (6.14)
$$

leads to the S-variate, mth-order augmented PDD approximation, which for $S > 0$ includes interactive effects of at most S input and affiliated variables, on y. It is elementary to show that when $S \to N + M$ and/or $m \to \infty$, $\tilde{y}_{S,m}$ converges to y in the mean-square sense, generating a hierarchical and convergent sequence of approximations of y. The truncation parameters S and m depend on the dimensional structure and nonlinearity of a stochastic response. The higher the values of S and m, the higher the accuracy, but also the computational cost that is endowed with an Sth-order polynomial computational complexity. Simply replacing the random vectors $\mathbf{D}$ and $\mathbf{S}$ in Equation (6.14) with deterministic vectors $\mathbf{d}$ and $\mathbf{s}$ renders an

S-variate, mth-order augmented PDD approximation

$$\tilde{y}_{S,m}(\mathbf{X};\mathbf{d},\mathbf{s}) = y_\emptyset(\mathbf{d},\boldsymbol{\mu}_\mathbf{D},\boldsymbol{\mu}_\mathbf{S}) + \sum_{\substack{u\subseteq\{1,\cdots,N\},v\subseteq\{1,\cdots,M_d\}\\ w\subseteq\{1,\cdots,M_s\},1\leq|u|+|v|+|w|\leq S}} \sum_{\substack{\mathbf{j}_{|u|}\in\mathbb{N}_0^{|u|},\mathbf{l}_{|v|}\in\mathbb{N}_0^{|v|},\mathbf{n}_{|w|}\in\mathbb{N}_0^{|w|}\\ \left\|\mathbf{j}_{|u|}\right\|_\infty,\left\|\mathbf{l}_{|v|}\right\|_\infty,\left\|\mathbf{n}_{|w|}\right\|_\infty\leq m\\ j_1,\cdots,j_{|u|},l_1,\cdots,l_{|v|},n_1,\cdots,n_{|w|}\neq0}}$$
$$C_{uvw\mathbf{j}_{|u|}\mathbf{l}_{|v|}\mathbf{n}_{|w|}}(\mathbf{d},\boldsymbol{\mu}_\mathbf{D},\boldsymbol{\mu}_\mathbf{S})\psi_{u\mathbf{j}_{|u|}}(\mathbf{X}_u;\mathbf{d})\phi_{v\mathbf{l}_{|v|}}(\mathbf{d}_v;\boldsymbol{\mu}_\mathbf{D})\varphi_{w\mathbf{n}_{|w|}}(\mathbf{s}_w;\boldsymbol{\mu}_\mathbf{S}) \quad (6.15)$$

of the original function $y(\mathbf{X};\mathbf{d},\mathbf{s})$. The S-variate, mth-order augmented PDD approximation will be referred to as *truncated augmented PDD approximation* in this chapter.

6.3.3   Statistical Moment Analysis

Let $m^{(r)}(\mathbf{d},\mathbf{s}):=\mathbb{E}_\mathbf{d}[y^r(\mathbf{X};\mathbf{d},\mathbf{s})]$, if it exists, define the raw moment of y of order r, where $r\in\mathbb{N}$. Given an S-variate, mth-order PDD approximation $\tilde{y}_{S,m}(\mathbf{X};\mathbf{d},\mathbf{s})$ of $y(\mathbf{X};\mathbf{d},\mathbf{s})$, let $\tilde{m}_{S,m}^{(r)}(\mathbf{d},\mathbf{s}):=\mathbb{E}_\mathbf{d}[\tilde{y}_{S,m}^r(\mathbf{X};\mathbf{d},\mathbf{s})]$ define the raw moment of $\tilde{y}_{S,m}$ of order r. The following paragraphs describe the explicit formulae or analytical expressions for calculating the first two moments by the PDD approximation.

Applying the expectation operator $\mathbb{E}_\mathbf{d}$ on $\tilde{y}_{S,m}(\mathbf{X};\mathbf{d},\mathbf{s})$ and $\tilde{y}_{S,m}^2(\mathbf{X};\mathbf{d},\mathbf{s})$, and recognizing the *zero*-mean and orthonormal properties of orthonormal basis, the first and second moments of the S-variate, mth-order augmented PDD approximation are

$$\tilde{m}_{S,m}^{(1)}(\mathbf{d},\mathbf{s}) := \mathbb{E}_\mathbf{d}\left[\tilde{y}_{S,m}(\mathbf{X};\mathbf{d},\mathbf{s})\right]$$

$$= y_\emptyset(\mathbf{d},\boldsymbol{\mu}_\mathbf{D},\boldsymbol{\mu}_\mathbf{S}) + \sum_{\substack{u\subseteq\{1,\cdots,N\},v\subseteq\{1,\cdots,M_d\},w\subseteq\{1,\cdots,M_s\}\\ |u|=0,1\leq|u|+|v|+|w|\leq S}} \sum_{\substack{\mathbf{j}_{|u|}\in\mathbb{N}_0^{|u|},\mathbf{l}_{|v|}\in\mathbb{N}_0^{|v|},\mathbf{n}_{|w|}\in\mathbb{N}_0^{|w|}\\ \left\|\mathbf{j}_{|u|}\right\|_\infty,\left\|\mathbf{l}_{|v|}\right\|_\infty,\left\|\mathbf{n}_{|w|}\right\|_\infty\leq m\\ j_1,\cdots,j_{|u|},l_1,\cdots,l_{|v|},n_1,\cdots,n_{|w|}\neq0}}$$
$$C_{uvw\mathbf{j}_{|u|}\mathbf{l}_{|v|}\mathbf{n}_{|w|}}(\mathbf{d},\boldsymbol{\mu}_\mathbf{D},\boldsymbol{\mu}_\mathbf{S})\phi_{v\mathbf{l}_{|v|}}(\mathbf{d}_v;\boldsymbol{\mu}_\mathbf{D})\varphi_{w\mathbf{n}_{|w|}}(\mathbf{s}_w;\boldsymbol{\mu}_\mathbf{S}) \quad (6.16)$$

and

$$\tilde{m}_{S,m}^{(2)}(\mathbf{d}, \mathbf{s}) := \mathbb{E}_{\mathbf{d}} \left[\tilde{y}_{S,m}^2(\mathbf{X}; \mathbf{d}, \mathbf{s}) \right]$$

$$= \left[\tilde{m}_{S,m}^{(1)}(\mathbf{d}, \mathbf{s}) \right]^2 + \sum_{\substack{u \subseteq \{1, \cdots, N\} \\ 1 \le |u| \le S}} \sum_{\substack{\mathbf{j}_{|u|} \in \mathbb{N}_0^{|u|}, \|\mathbf{j}_{|u|}\|_\infty \le m \\ j_1, \cdots, j_{|u|} \ne 0}} E_{u\mathbf{j}_{|u|}, S, m}^2(\mathbf{d}, \mathbf{s}), \quad (6.17)$$

respectively, where the second moment involves new expansion coefficients

$$E_{u\mathbf{j}_{|u|}, S, m}(\mathbf{d}, \mathbf{s}) = \sum_{\substack{v \subseteq \{1, \cdots, M_d\}, w \subseteq \{1, \cdots, M_s\} \\ 1 \le |u| + |v| + |w| \le S}} \sum_{\substack{\mathbf{l}_{|v|} \in \mathbb{N}_0^{|v|}, \mathbf{n}_{|w|} \in \mathbb{N}_0^{|w|}, \|\mathbf{l}_{|v|}\|_\infty, \|\mathbf{n}_{|w|}\|_\infty \le m \\ l_1, \cdots, l_{|v|}, n_1, \cdots, n_{|w|} \ne 0}} C_{uvw\mathbf{j}_{|u|}\mathbf{l}_{|v|}\mathbf{n}_{|w|}}(\mathbf{d}, \boldsymbol{\mu}_{\mathbf{D}}, \boldsymbol{\mu}_{\mathbf{S}})$$

$$\times \phi_{v\mathbf{l}_{|v|}}(\mathbf{d}_v; \boldsymbol{\mu}_{\mathbf{D}}) \varphi_{w\mathbf{n}_{|w|}}(\mathbf{s}_w; \boldsymbol{\mu}_{\mathbf{S}}), \quad (6.18)$$

via restructuring

$$\tilde{y}_{S,m}(\mathbf{X}; \mathbf{d}, \mathbf{s}) = \tilde{m}_{S,m}^{(1)}(\mathbf{d}, \mathbf{s}) + \sum_{\substack{u \subseteq \{1, \cdots, N\} \\ 1 \le |u| \le S}} \sum_{\substack{\mathbf{j}_{|u|} \in \mathbb{N}_0^{|u|} \|\mathbf{j}_{|u|}\|_\infty \le m \\ j_1, \cdots, j_{|u|} \ne 0}} E_{u\mathbf{j}_{|u|}, S, m}(\mathbf{d}, \mathbf{s}) \psi_{u\mathbf{j}_{|u|}}(\mathbf{X}_u; \mathbf{d}) \quad (6.19)$$

in terms of $\psi_{u\mathbf{j}_{|u|}}(\mathbf{X}_u; \mathbf{d})$. Clearly, the approximate moments in Equations (6.16) and (6.17) approach the exact moments

$$m^{(1)}(\mathbf{d}, \mathbf{s}) := \mathbb{E}_{\mathbf{d}} [y(\mathbf{X})] = y_\emptyset(\mathbf{d}, \boldsymbol{\mu}_{\mathbf{D}}, \boldsymbol{\mu}_{\mathbf{S}}) + \sum_{\substack{u \subseteq \{1, \cdots, N\}, v \subseteq \{1, \cdots, M_d\} \\ w \subseteq \{1, \cdots, M_s\}, |u| = 0 \\ |u| + |v| + |w| \ge 1}} \sum_{\substack{\mathbf{j}_{|u|} \in \mathbb{N}_0^{|u|}, \mathbf{l}_{|v|} \in \mathbb{N}_0^{|v|}, \mathbf{n}_{|w|} \in \mathbb{N}_0^{|w|} \\ j_1, \cdots, j_{|u|}, l_1, \cdots, l_{|v|}, n_1, \cdots, n_{|w|} \ne 0}}$$

$$C_{uvw\mathbf{j}_{|u|}\mathbf{l}_{|v|}\mathbf{n}_{|w|}}(\mathbf{d}, \boldsymbol{\mu}_{\mathbf{D}}, \boldsymbol{\mu}_{\mathbf{S}}) \phi_{v\mathbf{l}_{|v|}}(\mathbf{d}_v; \boldsymbol{\mu}_{\mathbf{D}}) \varphi_{w\mathbf{n}_{|w|}}(\mathbf{s}_w; \boldsymbol{\mu}_{\mathbf{S}}) \quad (6.20)$$

and

$$m^{(2)}(\mathbf{d}, \mathbf{s}) := \mathbb{E}_{\mathbf{d}} \left[y^2(\mathbf{X}; \mathbf{d}, \mathbf{s}) \right] = \left[m^{(1)}(\mathbf{d}, \mathbf{s}) \right]^2$$

$$+ \sum_{\substack{u \subseteq \{1, \cdots, N\} \\ |u| \ge 1}} \sum_{\substack{\mathbf{j}_{|u|} \in \mathbb{N}_0^{|u|} \\ j_1, \cdots, j_{|u|} \ne 0}} E_{u\mathbf{j}_{|u|}}^2(\mathbf{d}, \mathbf{s}) \quad (6.21)$$

of y when $S \to N + M$ and $m \to \infty$, where

$$
\begin{aligned}
E_{u\mathbf{j}_{|u|}}(\mathbf{d}, \mathbf{s}) \;=\; & \sum_{\substack{v \subseteq \{1, \cdots, M_d\}, w \subseteq \{1, \cdots, M_s\} \\ |u| + |v| + |w| \geq 1}} \sum_{\substack{\mathbf{l}_{|v|} \in \mathbb{N}_0^{|v|}, \mathbf{n}_{|w|} \in \mathbb{N}_0^{|w|} \\ l_1, \cdots, l_{|v|}, n_1, \cdots, n_{|w|} \neq 0}} C_{uvw\mathbf{j}_{|u|}\mathbf{l}_{|v|}\mathbf{n}_{|w|}}(\mathbf{d}, \boldsymbol{\mu}_{\mathbf{D}}, \boldsymbol{\mu}_{\mathbf{S}}) \\
& \times \phi_{v\mathbf{l}_{|v|}}(\mathbf{d}_v; \boldsymbol{\mu}_{\mathbf{D}}) \varphi_{w\mathbf{n}_{|w|}}(\mathbf{s}_w; \boldsymbol{\mu}_{\mathbf{S}})
\end{aligned}
\tag{6.22}
$$

is again derived from restructuring Equation (6.10) in terms of $\psi_{u\mathbf{j}_{|u|}}(\mathbf{X}_u; \mathbf{d})$, that is,

$$
y(\mathbf{X}; \mathbf{d}, \mathbf{s}) \;=\; m^{(1)}(\mathbf{d}, \mathbf{s}) + \sum_{\substack{u \subseteq \{1, \cdots, N\} \\ |u| \geq 1}} \sum_{\substack{\mathbf{j}_{|u|} \in \mathbb{N}_0^{|u|} \\ j_1, \cdots, j_{|u|} \neq 0}} E_{u\mathbf{j}_{|u|}}(\mathbf{d}, \mathbf{s}) \psi_{u\mathbf{j}_{|u|}}(\mathbf{X}_u; \mathbf{d}). \tag{6.23}
$$

The mean-square convergence of $\tilde{y}_{S,m}$ is guaranteed as y, and its component functions are all members of the associated Hilbert spaces. In other words, the mean and variance of $\tilde{y}_{S,m}$ are also convergent.

6.3.4   Reliability Analysis

A fundamental problem in reliability analysis entails calculation of the failure probability

$$
P_F(\mathbf{d}, \mathbf{s}) := P_{\mathbf{d}}\left[\mathbf{X} \in \Omega_F(\mathbf{d}, \mathbf{s})\right] = \int_{\mathbb{R}^N} I_{\Omega_F}(\mathbf{x}; \mathbf{d}, \mathbf{s}) f_{\mathbf{X}}(\mathbf{x}; \mathbf{d}) d\mathbf{x} =: \mathbb{E}_{\mathbf{d}}\left[I_{\Omega_F}(\mathbf{X}; \mathbf{d}, \mathbf{s})\right],
\tag{6.24}
$$

where $\Omega_F(\mathbf{d}, \mathbf{s})$ is the failure set and $I_{\Omega_F}(\mathbf{x}; \mathbf{d}, \mathbf{s})$ is the associated indicator function, which is equal to *one* when $\mathbf{x} \in \Omega_F(\mathbf{d}, \mathbf{s})$ and *zero* otherwise. In this subsection, the augmented PDD method for reliability analysis, which exploits the augmented PDD approximation for MCS, is elucidated.

Depending on component or system reliability analysis, let $\tilde{\Omega}_{F,S,m} := \{\mathbf{x} : \tilde{y}_{S,m}(\mathbf{x}; \mathbf{d}, \mathbf{s}) < 0\}$ or $\tilde{\Omega}_{F,S,m} := \{\mathbf{x} : \cup_i \tilde{y}_{i,S,m}(\mathbf{x}; \mathbf{d}, \mathbf{s}) < 0\}$ or $\tilde{\Omega}_{F,S,m} := \{\mathbf{x} : \cap_i \tilde{y}_{i,S,m}(\mathbf{x};$

$\mathbf{d}, \mathbf{s}) < 0\}$ be an approximate failure set as a result of S-variate, mth-order PDD approximations $\tilde{y}_{S,m}(\mathbf{X}; \mathbf{d}, \mathbf{s})$ of $y(\mathbf{X}; \mathbf{d}, \mathbf{s})$ or $\tilde{y}_{i,S,m}(\mathbf{X}; \mathbf{d}, \mathbf{s})$ of $y_i(\mathbf{X}; \mathbf{d}, \mathbf{s})$. Then the augmented PDD estimate of the failure probability $P_F(\mathbf{d}, \mathbf{s})$ is

$$\tilde{P}_{F,S,m}(\mathbf{d}, \mathbf{s}) = \mathbb{E}_{\mathbf{d}} \left[I_{\tilde{\Omega}_{F,S,m}}(\mathbf{X}; \mathbf{d}, \mathbf{s}) \right] = \lim_{L \to \infty} \frac{1}{L} \sum_{l=1}^{L} I_{\tilde{\Omega}_{F,S,m}}(\mathbf{x}^{(l)}; \mathbf{d}, \mathbf{s}), \qquad (6.25)$$

where L is the sample size, $\mathbf{x}^{(l)}$ is the lth realization of $\mathbf{X}$, and $I_{\tilde{\Omega}_{F,S,m}}(\mathbf{x}; \mathbf{d}, \mathbf{s})$ is another indicator function, which is equal to *one* when $\mathbf{x} \in \tilde{\Omega}_{F,S,m}$ and *zero* otherwise.

Note that the simulation of the augmented PDD approximation in Equation (6.25) should not be confused with the crude MCS commonly used for producing benchmark results. The crude MCS, which requires numerical calculations of $y(\mathbf{x}^{(l)}; \mathbf{d}, \mathbf{s})$ or $y_i(\mathbf{x}^{(l)}; \mathbf{d}, \mathbf{s})$ for input samples $\mathbf{x}^{(l)}, l = 1, \cdots, L$, can be expensive or even prohibitive, particularly when the sample size L needs to be very large for estimating small failure probabilities. In contrast, the MCS embedded in PDD requires evaluations of simple analytical functions that stem from an S-variate, mth-order approximation $\tilde{y}_{S,m}(\mathbf{x}^{(l)}; \mathbf{d}, \mathbf{s})$ or $\tilde{y}_{i,S,m}(\mathbf{x}^{(l)}; \mathbf{d}, \mathbf{s})$. Therefore, an arbitrarily large sample size can be accommodated in the augmented PDD method.

6.3.5   Expansion Coefficients

The determination of the augmented PDD expansion coefficients $y_\emptyset(\mathbf{d}, \boldsymbol{\mu}_{\mathbf{D}}, \boldsymbol{\mu}_{\mathbf{S}})$ and $C_{uvw\mathbf{j}_{|u|}\mathbf{l}_{|v|}\mathbf{n}_{|w|}}(\mathbf{d}, \boldsymbol{\mu}_{\mathbf{D}}, \boldsymbol{\mu}_{\mathbf{S}})$ is vitally important for moment and reliability analysis, including their design sensitivities. As defined in Equations (6.11) and (6.12), the coefficients involve various $(N + M)$-dimensional integrals over $\mathbb{R}^{N+M}$. For large $(N + M)$, a multivariate numerical integration employing an $(N + M)$-dimensional

tensor product of a univariate quadrature formula is computationally prohibitive and is, therefore, ruled out. An attractive alternative approach entails dimension-reduction integration, which was originally developed by Xu and Rahman [22] for high-dimensional numerical integration. For calculating $y_\emptyset$ and $C_{uvw\mathbf{j}_{|u|}\mathbf{l}_{|v|}\mathbf{n}_{|w|}}$, this is accomplished by replacing the $(N + M)$-variate function y in Equations (6.11) and (6.12) with an R-variate truncation of the referential dimensional decomposition (RDD) at a chosen reference point, where $R \leq N + M$. The result is a reduced integration scheme, requiring evaluations of at most R-dimensional integrals, described as follows.

Let $\mathbf{c} = (c_1, \cdots, c_N)^T \in \mathbb{R}^N$, $\mathbf{c}' = (c_1', \cdots, c_{M_d}')^T \in \mathbb{R}^{M_d}$, and $\mathbf{c}'' = (c_1'', \cdots, c_{M_s}'')^T$ $\in \mathbb{R}^{M_s}$, which are commonly adopted as the means of $\mathbf{X}$, $\mathbf{D}$, and $\mathbf{S}$, respectively, be the reference points. Let $y(\mathbf{x}_{u_1}, \mathbf{d}_{v_1}, \mathbf{s}_{w_1}, \mathbf{c}_{-u_1}, \mathbf{c}'_{-v_1}, \mathbf{c}''_{-w_1})$ represent an $(|u_1| + |v_1| + |w_1|)$-variate RDD component function of $y(\mathbf{x}, \mathbf{d}, \mathbf{s})$, where $u_1 \subseteq \{1, \cdots, N\}$, $v_1 \subseteq \{1, \cdots, M_d\}$, and $w_1 \subseteq \{1, \cdots, M_s\}$. Given a positive integer $S \leq R \leq N + M$, when $y(\mathbf{x}, \mathbf{d}, \mathbf{s})$ in Equations (6.11) and (6.12) is replaced with its R-variate RDD approximation, the coefficients $y_\emptyset(\mathbf{d}, \boldsymbol{\mu}_\mathbf{D}, \boldsymbol{\mu}_\mathbf{S})$ and $C_{uvw\mathbf{j}_{|u|}\mathbf{l}_{|v|}\mathbf{n}_{|w|}}(\mathbf{d}, \boldsymbol{\mu}_\mathbf{D}, \boldsymbol{\mu}_\mathbf{S})$ are estimated from [22]

$$
\begin{aligned}
y_\emptyset(\mathbf{d}, \boldsymbol{\mu}_\mathbf{D}, \boldsymbol{\mu}_\mathbf{S}) \cong{}& \sum_{i=0}^{R} (-1)^i \binom{N + M - R + i - 1}{i} \sum_{\substack{u_1 \subseteq \{1, \cdots, N\}, v_1 \subseteq \{1, \cdots, M_d\} \\ w_1 \subseteq \{1, \cdots, M_s\}, |u_1| + |v_1| + |w_1| = R - i}} \\
& \int_{\mathbb{R}^{|u_1| + |v_1| + |w_1|}} y(\mathbf{x}_{u_1}, \mathbf{d}_{v_1}, \mathbf{s}_{w_1}, \mathbf{c}_{-u_1}, \mathbf{c}'_{-v_1}, \mathbf{c}''_{-w_1}) \\
& \times f_{u_1 v_1 w_1}(\mathbf{x}_{u_1}, \mathbf{d}_{v_1}, \mathbf{s}_{w_1}) d\mathbf{x}_{u_1} d\mathbf{d}_{v_1} d\mathbf{s}_{w_1}
\end{aligned}
\tag{6.26}
$$

and

$$
\begin{aligned}
C_{uvw\mathbf{j}_{|u|}\mathbf{l}_{|v|}\mathbf{n}_{|w|}}(\mathbf{d}, \boldsymbol{\mu_D}, \boldsymbol{\mu_S}) \cong{}& \sum_{i=0}^{R}(-1)^i \binom{N+M-R+i-1}{i} \sum_{\substack{u_1 \subseteq \{1,\cdots,N\}, v_1 \subseteq \{1,\cdots,M_d\} \\ w_1 \subseteq \{1,\cdots,M_s\}, u \subseteq u_1, v \subseteq v_1, w \subseteq w_1 \\ |u_1|+|v_1|+|w_1|=R-i}} \\
& \int_{\mathbb{R}^{|u_1|+|v_1|+|w_1|}} y(\mathbf{x}_{u_1}, \mathbf{d}_{v_1}, \mathbf{s}_{w_1}, \mathbf{c}_{-u_1}, \mathbf{c}'_{-v_1}, \mathbf{c}''_{-w_1}) \psi_{uvw\mathbf{j}_{|u|}\mathbf{l}_{|v|}\mathbf{n}_{|w|}}(\mathbf{x}_u, \mathbf{d}_v, \mathbf{s}_w) \\
& \times f_{u_1 v_1 w_1}(\mathbf{x}_{u_1}, \mathbf{d}_{v_1}, \mathbf{s}_{w_1}) d\mathbf{x}_{u_1} d\mathbf{d}_{v_1} d\mathbf{s}_{w_1}, \quad\quad\quad (6.27)
\end{aligned}
$$

respectively, requiring evaluation of at most R-dimensional integrals. The reduced integration facilitates calculation of the coefficients approaching their exact values as $R \to N + M$ and is significantly more efficient than performing one $(N + M)$-dimensional integration, particularly when $R \ll N + M$. Hence, the computational effort is significantly lowered using the dimension-reduction integration. For instance, when $R = 1$ or 2, Equations (6.26) and (6.27) involve one-, or at most, two-dimensional integrations, respectively. For a general function y, numerical integrations are required for performing various low-dimensional integrations in Equations (6.26) and (6.27). See [22] for further details.

6.3.6   Computational Expense

The S-variate, mth-order augmented PDD approximation requires evaluations of $\sum_{k=0}^{k=S} \binom{N+M}{k} m^k$ expansion coefficients, including $y_\emptyset(\mathbf{d}, \boldsymbol{\mu_D}, \boldsymbol{\mu_S})$. If these coefficients are estimated by dimension-reduction integration with $R = S < N + M$ and, therefore, involve at most an S-dimensional tensor product of an n-point univariate quadrature rule depending on m, then the total cost for the S-variate, mth-order approximation entails a maximum of $\sum_{k=0}^{k=S} \binom{N+M}{k} n^k(m)$ function evaluations. If the

integration points include a common point in each coordinate $-$ a special case of symmetric input PDFs and odd values of n $-$ the number of function evaluations reduces to $\sum_{k=0}^{k=S} \binom{N+M}{k}(n(m)-1)^k$. Nonetheless, the computational complexity of the S-variate augmented PDD approximation is an Sth-order polynomial with respect to the number of random variables or integration points. Therefore, the augmented PDD with dimension-reduction integration of the expansion coefficients alleviates the curse of dimensionality to an extent determined by S.

6.4 Design Sensitivity Analysis

When solving RDO and RBDO problems employing gradient-based optimization algorithms, at least the first-order sensitivities of the first two moments of $y(\mathbf{X}; \mathbf{d}, \mathbf{s})$ and the failure probability with respect to each distributional and structural design variable are required. In this section, a new method involving the augmented PDD, score functions, and finite-difference approximation is presented. For such sensitivity analysis, the following regularity conditions are assumed.

1. The design variables $d_k \in \mathcal{D}_k \subset \mathbb{R}$, $k = 1, \cdots, M_d$ and $s_p \in \mathcal{S}_p \subset \mathbb{R}$, $p = 1, \cdots, M_s$, where $\mathcal{D}_k$ and $\mathcal{S}_p$ are open intervals of $\mathbb{R}$.

2. The PDF $f_{\mathbf{X}}(\mathbf{x}; \mathbf{d})$ of $\mathbf{X}$ is continuous. In addition, the partial derivative $\partial f_{\mathbf{X}}(\mathbf{x}; \mathbf{d}) / \partial d_k$, $k = 1, \cdots, M_d$, exists and is finite for all $\mathbf{x} \in \mathbb{R}^N$ and $d_k \in \mathcal{D}_k$. Furthermore, the statistical moments of y and failure probability are differentiable functions of $\mathbf{d} \in \mathbb{R}^{M_d}$.

3. The performance function $y(\mathbf{x}; \mathbf{d}, \mathbf{s})$ is continuous. In addition, the partial

derivative $\partial y(\mathbf{x}; \mathbf{d}, \mathbf{s}) / \partial s_p$, $p = 1, \cdots, M_s$, exists and is finite for all $\mathbf{x} \in \mathbb{R}^N$, $\mathbf{d} \in \mathbb{R}^{M_d}$, and $s_p \in \mathcal{S}_p$. Furthermore, the statistical moments of y and failure probability are differentiable functions of $\mathbf{s} \in \mathbb{R}^{M_s}$.

4. There exists a Lebesgue integrable dominating function $z(\mathbf{x})$ such that

$$\left| y^r(\mathbf{x}; \mathbf{d}, \mathbf{s}) \frac{\partial f_{\mathbf{X}}(\mathbf{x}; \mathbf{d})}{\partial d_k} \right| \leq z(\mathbf{x}), \qquad \left| I_{\Omega_F}(\mathbf{x}; \mathbf{d}, \mathbf{s}) \frac{\partial f_{\mathbf{X}}(\mathbf{x}; \mathbf{d})}{\partial d_k} \right| \leq z(\mathbf{x}),$$
$$r = 1, 2, \quad k = 1, \cdots, M_d. \tag{6.28}$$

6.4.1 Sensitivity of Moments

Suppose that the first-order derivative of a moment $m^{(r)}(\mathbf{d}, \mathbf{s})$, where $r = 1, 2$, of a generic stochastic response $y(\mathbf{X}; \mathbf{d}, \mathbf{s})$ with respect to a distributional design variable d_k, $1 \leq k \leq M_d$, or with respect to a structural design variable s_p, $1 \leq p \leq M_s$, is sought. Taking a partial derivative of the moment with respect to d_k and then applying the Lebesgue dominated convergence theorem [76], which permits the differential and integral operators to be interchanged, yields the sensitivity

$$
\begin{aligned}
\frac{\partial m^{(r)}(\mathbf{d}, \mathbf{s})}{\partial d_k} \; &:= \; \frac{\partial \mathbb{E}_{\mathbf{d}}[y^r(\mathbf{X}; \mathbf{d}, \mathbf{s})]}{\partial d_k} = \frac{\partial}{\partial d_k} \int_{\mathbb{R}^N} y^r(\mathbf{x}; \mathbf{d}, \mathbf{s}) f_{\mathbf{X}}(\mathbf{x}; \mathbf{d}) d\mathbf{x} \\
&= \; \int_{\mathbb{R}^N} y(\mathbf{x}; \mathbf{d}, \mathbf{s}) \frac{\partial \ln f(\mathbf{x}; \mathbf{d})}{\partial d_k} f_{\mathbf{X}}(\mathbf{x}; \mathbf{d}) d\mathbf{x} + \int_{\mathbb{R}^N} \frac{\partial y^r(\mathbf{x}; \mathbf{d}, \mathbf{s})}{\partial d_k} f_{\mathbf{X}}(\mathbf{x}; \mathbf{d}) d\mathbf{x} \\
&=: \; \mathbb{E}_{\mathbf{d}}\left[y^r(\mathbf{X}; \mathbf{d}, \mathbf{s}) s_{d_k}^{(1)}(\mathbf{X}; \mathbf{d}) \right] + \mathbb{E}_{\mathbf{d}}\left[\frac{\partial y^r(\mathbf{X}; \mathbf{d}, \mathbf{s})}{\partial d_k} \right]
\end{aligned}
\tag{6.29}
$$

with respect to the distributional design variables, provided that $f_{\mathbf{X}}(\mathbf{x}; \mathbf{d}) > 0$. In the last line of Equation (6.29), $s_{d_k}^{(1)}(\mathbf{X}; \mathbf{d}) := \partial \ln f_{\mathbf{X}}(\mathbf{X}; \mathbf{d}) / \partial d_k$ is known as the first-order score function for the design variable d_k [74, 97]. Compared with the existing sensitivity analysis [97, 110], the second term, $\mathbb{E}_{\mathbf{d}}[\partial y^r(\mathbf{X}; \mathbf{d}, \mathbf{s}) / \partial d_k]$, appears due to the permissible explicit dependence of y on the distributional design variables.

The evaluation of score functions, $s_{d_k}^{(1)}(\mathbf{X}; \mathbf{d})$, $k = 1, \cdots, M$, requires differentiating only the PDF of $\mathbf{X}$. Therefore, the resulting score functions can be determined easily and, in many cases, analytically − for instance, when $\mathbf{X}$ follows classical probability distributions [97]. If the density function of $\mathbf{X}$ is arbitrarily prescribed, the score functions can be calculated numerically, yet inexpensively, since no evaluation of the performance function is involved. When $\mathbf{X}$ comprises independent variables, as assumed here, $\ln f_{\mathbf{X}}(\mathbf{X}; \mathbf{d}) = \sum_{i=1}^{i=N} \ln f_{X_i}(x_i; \mathbf{d})$ is a sum of N univariate log-density (marginal) functions of random variables. Hence, in general, the score function for the kth design variable, expressed by

$$s_{d_k}^{(1)}(\mathbf{X}; \mathbf{d}) = \sum_{i=1}^{N} \frac{\partial \ln f_{X_i}(X_i; \mathbf{d})}{\partial d_k} = \sum_{i=1}^{N} s_{ki}(X_i; \mathbf{d}), \qquad (6.30)$$

is also a sum of univariate functions $s_{ki}(X_i; \mathbf{d}) := \partial \ln f_{X_i}(X_i; \mathbf{d}) / \partial d_k$, $i = 1, \cdots, N$, which are the derivatives of log-density (marginal) functions. If d_k is a distribution parameter of a single random variable X_{i_k}, then the score function reduces to $s_{d_k}^{(1)}(\mathbf{X}; \mathbf{d}) = \partial \ln f_{X_{i_k}}(X_{i_k}; \mathbf{d}) / \partial d_k =: s_{ki_k}(X_{i_k}; \mathbf{d})$, the derivative of the log-density (marginal) function of X_{i_k}, which remains a univariate function. Nonetheless, combining Equations (6.29) and (6.30), the sensitivity is obtained as

$$\frac{\partial m^{(r)}(\mathbf{d}, \mathbf{s})}{\partial d_k} = \sum_{i=1}^{N} \mathbb{E}_{\mathbf{d}} \left[y^r(\mathbf{X}; \mathbf{d}, \mathbf{s}) s_{ki}(X_i; \mathbf{d}) \right] + \mathbb{E}_{\mathbf{d}} \left[\frac{\partial y^r(\mathbf{X}; \mathbf{d}, \mathbf{s})}{\partial d_k} \right]. \qquad (6.31)$$

Similarly, taking a partial derivative of the moment with respect to s_p yields the sensitivity

$$\begin{aligned} \frac{\partial m^{(r)}(\mathbf{d}, \mathbf{s})}{\partial s_p} \quad &:= \quad \frac{\partial \mathbb{E}_{\mathbf{d}} \left[y^r(\mathbf{X}; \mathbf{d}, \mathbf{s}) \right]}{\partial s_p} = \frac{\partial}{\partial d_k} \int_{\mathbb{R}^N} y^r(\mathbf{x}; \mathbf{d}, \mathbf{s}) f_{\mathbf{X}}(\mathbf{x}; \mathbf{d}) d\mathbf{x} \\ &= \quad \int_{\mathbb{R}^N} \frac{\partial y^r(\mathbf{x}; \mathbf{d}, \mathbf{s})}{\partial s_p} f_{\mathbf{X}}(\mathbf{x}; \mathbf{d}) d\mathbf{x} =: \mathbb{E}_{\mathbf{d}} \left[\frac{\partial y^r(\mathbf{X}; \mathbf{d}, \mathbf{s})}{\partial s_p} \right] \end{aligned} \qquad (6.32)$$

with respect to the structural design variables, involving only one term because the PDF $f_{\mathbf{X}}(\mathbf{x};\mathbf{d})$ does not depend on $\mathbf{s}$. In general, these sensitivities are not available analytically since the moments are not either. Nonetheless, the moments and their sensitivities, whether in conjunction with the distributional or structural design variables, have both been formulated as expectations of stochastic quantities with respect to the same probability measure, facilitating their concurrent evaluations in a single stochastic simulation or analysis.

Given an S-variate, mth-order augmented PDD approximation $\tilde{y}_{S,m}(\mathbf{X};\mathbf{d},\mathbf{s})$ of $y(\mathbf{X};\mathbf{d},\mathbf{s})$, let $\partial\tilde{m}_{S,m}^{(r)}(\mathbf{d},\mathbf{s})/\partial d_k$ and $\partial\tilde{m}_{S,m}^{(r)}(\mathbf{d},\mathbf{s})/\partial s_p$ define the approximations of moment sensitivities. The following subsections describe the explicit formulae or analytical expressions for calculating the moments by augmented PDD approximations for $r = 1, 2$.

6.4.1.1 Sensitivity of the First Moment

Setting $r = 1$ in Equations (6.31) and (6.32), the sensitivities of the first moment are

$$\frac{\partial m^{(1)}(\mathbf{d},\mathbf{s})}{\partial d_k} = \sum_{i=1}^{N}\mathbb{E}_{\mathbf{d}}\left[y(\mathbf{X};\mathbf{d},\mathbf{s})s_{ki}(X_i;\mathbf{d})\right] + \mathbb{E}_{\mathbf{d}}\left[\frac{\partial y(\mathbf{X};\mathbf{d},\mathbf{s})}{\partial d_k}\right] \tag{6.33}$$

and

$$\frac{\partial m^{(1)}(\mathbf{d},\mathbf{s})}{\partial s_p} = \mathbb{E}_{\mathbf{d}}\left[\frac{\partial y(\mathbf{X};\mathbf{d},\mathbf{s})}{\partial s_p}\right], \tag{6.34}$$

where $k = 1, \cdots, M_d$ and $p = 1, \cdots, M_s$.

For independent coordinates of $\mathbf{X}$, consider the Fourier-polynomial expansion

of the kth log-density derivative function

$$s_{ki}(X_i; \mathbf{d}) = s_{ki,\emptyset}(\mathbf{d}) + \sum_{j=1}^{\infty} D_{k,ij}(\mathbf{d}) \psi_{ij}(X_i; \mathbf{d}), \qquad (6.35)$$

consisting of its own expansion coefficients

$$s_{ki,\emptyset}(\mathbf{d}) := \int_{\mathbb{R}} s_{ki}(x_i; \mathbf{d}) f_{X_i}(x_i; \mathbf{d}) dx_i \qquad (6.36)$$

and

$$D_{k,ij}(\mathbf{d}) := \int_{\mathbb{R}} s_{ki}(x_i; \mathbf{d}) \psi_{ij}(x_i; \mathbf{d}) f_{X_i}(x_i; \mathbf{d}) dx_i. \qquad (6.37)$$

The expansion is valid if s_{ki} is square integrable with respect to the probability measure of X_i. When blended with the PDD approximation, the score function leads to analytical or closed-form expressions of the exact or approximate sensitivities as follows.

6.4.1.1.1 Exact Sensitivities

Restructuring Equation (6.13) as

$$
\begin{aligned}
y(\mathbf{X}; \mathbf{d}, \mathbf{s}) =\ & m^{(1)}(\mathbf{d}, \mathbf{s}) + \sum_{\substack{u=\{i\}\subset\{1,\cdots,N\}}} \sum_{\substack{j\in\mathbb{N}_0 \\ j\neq 0}} C_{ij}(\mathbf{d}, \mathbf{s}) \psi_{ij}(X_i; \mathbf{d}) + \sum_{\substack{u\subseteq\{1,\cdots,N\},v\subseteq\{1,\cdots,M_d\} \\ w\subseteq\{1,\cdots,M_s\},|u|>1}} \\
& \sum_{\substack{\mathbf{j}_{|u|}\in\mathbb{N}_0^{|u|},\mathbf{l}_{|v|}\in\mathbb{N}_0^{|v|},\mathbf{n}_{|w|}\in\mathbb{N}_0^{|w|} \\ j_1,\cdots,j_{|u|},l_1,\cdots,l_{|v|},n_1,\cdots,n_{|w|}\neq 0}} C_{uvw\mathbf{j}_{|u|}\mathbf{l}_{|v|}\mathbf{n}_{|w|}}(\mathbf{d}, \boldsymbol{\mu}_{\mathbf{D}}, \boldsymbol{\mu}_{\mathbf{S}}) \psi_{u\mathbf{j}_{|u|}}(\mathbf{X}_u; \mathbf{d}) \phi_{v\mathbf{l}_{|v|}}(\mathbf{d}_v; \boldsymbol{\mu}_{\mathbf{D}}) \varphi_{w\mathbf{n}_{|w|}}(\mathbf{s}_w; \boldsymbol{\mu}_{\mathbf{S}}), \quad (6.38)
\end{aligned}
$$

where

$$
\begin{aligned}
C_{ij}(\mathbf{d}, \mathbf{s}) =\ & \sum_{\substack{u=\{i\},v\subseteq\{1,\cdots,M_d\} \\ w\subseteq\{1,\cdots,M_s\}}} \sum_{\substack{\mathbf{j}_{|u|}=j\in\mathbb{N}_0,\mathbf{l}_{|v|}\in\mathbb{N}_0^{|v|},\mathbf{n}_{|w|}\in\mathbb{N}_0^{|w|} \\ j,l_1,\cdots,l_{|v|},n_1,\cdots,n_{|w|}\neq 0}} C_{uvw\mathbf{j}_{|u|}\mathbf{l}_{|v|}\mathbf{n}_{|w|}}(\mathbf{d}, \boldsymbol{\mu}_{\mathbf{D}}, \boldsymbol{\mu}_{\mathbf{S}}) \\
& \times \phi_{v\mathbf{l}_{|v|}}(\mathbf{d}_v; \boldsymbol{\mu}_{\mathbf{D}}) \varphi_{w\mathbf{n}_{|w|}}(\mathbf{s}_w; \boldsymbol{\mu}_{\mathbf{S}}), \qquad (6.39)
\end{aligned}
$$

and employing Equations (6.35) and (6.38), the product appearing on the right side of Equation (6.33) expands to

$$
\begin{aligned}
y(\mathbf{X};\mathbf{d},\mathbf{s})s_{ki}(X_i;\mathbf{d}) = & \left(m^{(1)}(\mathbf{d},\mathbf{s}) + \sum_{u=\{i\}\subset\{1,\cdots,N\}} \sum_{\substack{j\in\mathbb{N}_0 \\ j\neq 0}} C_{ij}(\mathbf{d},\mathbf{s})\psi_{ij}(X_i;\mathbf{d}) \right. \\
& + \sum_{\substack{u\subseteq\{1,\cdots,N\},v\subseteq\{1,\cdots,M_d\} \\ w\subseteq\{1,\cdots,M_s\},|u|>1}} \sum_{\substack{\mathbf{j}_{|u|}\in\mathbb{N}_0^{|u|},\mathbf{l}_{|v|}\in\mathbb{N}_0^{|v|},\mathbf{n}_{|w|}\in\mathbb{N}_0^{|w|} \\ j_1,\cdots,j_{|u|},l_1,\cdots,l_{|v|},n_1,\cdots,n_{|w|}\neq 0}} C_{uvw\mathbf{j}_{|u|}\mathbf{l}_{|v|}\mathbf{n}_{|w|}}(\mathbf{d},\boldsymbol{\mu}_{\mathbf{D}},\boldsymbol{\mu}_{\mathbf{S}})\psi_{u\mathbf{j}_{|u|}}(\mathbf{X}_u;\mathbf{d}) \\
& \left. \times \phi_{v\mathbf{l}_{|v|}}(\mathbf{d}_v;\boldsymbol{\mu}_{\mathbf{D}})\varphi_{w\mathbf{n}_{|w|}}(\mathbf{s}_w;\boldsymbol{\mu}_{\mathbf{S}}) \right) \left(s_{ki,\emptyset}(\mathbf{d}) + \sum_{j=1}^{\infty} D_{k,ij}(\mathbf{d})\psi_{ij}(X_i;\mathbf{d}) \right),
\end{aligned} \qquad (6.40)
$$

encountering the same orthonormal polynomial bases that are consistent with the probability measure $f_{\mathbf{X}}(\mathbf{x};\mathbf{d})d\mathbf{x}$. Taking the expectation of Equation (6.40), aided by the *zero*-mean and orthonormal properties of orthonormal basis, leads to

$$
\mathbb{E}_{\mathbf{d}}\left[y(\mathbf{X};\mathbf{d},\mathbf{s})s_{ki}(X_i;\mathbf{d})\right] = m^{(1)}(\mathbf{d},\mathbf{s})s_{ki,\emptyset} + \sum_{j=1}^{\infty} D_{k,ij}(\mathbf{d})C_{ij}(\mathbf{d},\mathbf{s}). \qquad (6.41)
$$

In Equation (6.13), the PDD coefficients $y_{\emptyset}(\mathbf{d},\boldsymbol{\mu}_{\mathbf{D}},\boldsymbol{\mu}_{\mathbf{S}})$ and $C_{uvw\mathbf{j}_{|u|}\mathbf{l}_{|v|}\mathbf{n}_{|w|}}(\mathbf{d},\boldsymbol{\mu}_{\mathbf{D}},\boldsymbol{\mu}_{\mathbf{S}})$ and the polynomial basis $\psi_{u\mathbf{j}_{|u|}}(\mathbf{X}_u;\mathbf{d})$ are written as functions involving $\mathbf{d}$; however, they should be treated as constants when seeking the derivatives of $y(\mathbf{X};\mathbf{d},\mathbf{s})$ with respect to $\mathbf{d}$. Therefore, the term $\partial y(\mathbf{X};\mathbf{d},\mathbf{s})/\partial d_k$ can be written as

$$
\begin{aligned}
\frac{\partial y(\mathbf{X};\mathbf{d},\mathbf{s})}{\partial d_k} = & \sum_{\substack{u\subseteq\{1,\cdots,N\},k\in v\subseteq\{1,\cdots,M_d\} \\ w\subseteq\{1,\cdots,M_s\},|u|+|v|+|w|\geq 1}} \sum_{\substack{\mathbf{j}_{|u|}\in\mathbb{N}_0^{|u|},\mathbf{l}_{|v|}\in\mathbb{N}_0^{|v|},\mathbf{n}_{|w|}\in\mathbb{N}_0^{|w|} \\ j_1,\cdots,j_{|u|},l_1,\cdots,l_{|v|},n_1,\cdots,n_{|w|}\neq 0}} C_{uvw\mathbf{j}_{|u|}\mathbf{l}_{|v|}\mathbf{n}_{|w|}}(\mathbf{d},\boldsymbol{\mu}_{\mathbf{D}},\boldsymbol{\mu}_{\mathbf{S}}) \\
& \times \psi_{u\mathbf{j}_{|u|}}(\mathbf{X}_u;\mathbf{d})\frac{\partial\phi_{v\mathbf{l}_{|v|}}(\mathbf{d}_v;\boldsymbol{\mu}_{\mathbf{D}})}{\partial d_k}\varphi_{w\mathbf{n}_{|w|}}(\mathbf{s}_w;\boldsymbol{\mu}_{\mathbf{S}}).
\end{aligned} \qquad (6.42)
$$

Applying the expectation operator $\mathbb{E}_{\mathbf{d}}$ on $\partial y(\mathbf{X};\mathbf{d},\mathbf{s})/\partial d_k$ and recognizing again the *zero*-mean and orthonormal properties of orthonormal basis, leads to

$$
\mathbb{E}_{\mathbf{d}}\left[\frac{\partial y(\mathbf{X};\mathbf{d},\mathbf{s})}{\partial d_k}\right] = \sum_{\substack{u=\emptyset,k\in v\subseteq\{1,\cdots,M_d\}\\ w\subseteq\{1,\cdots,M_s\},|u|+|v|+|w|\geq 1}}\ \sum_{\substack{\mathbf{j}_{|u|}\in\mathbb{N}_0^{|u|},\mathbf{l}_{|v|}\in\mathbb{N}_0^{|v|},\mathbf{n}_{|w|}\in\mathbb{N}_0^{|w|}\\ j_1,\cdots,j_{|u|},l_1,\cdots,l_{|v|},n_1,\cdots,n_{|w|}\neq 0}} C_{uvw\mathbf{j}_{|u|}\mathbf{l}_{|v|}\mathbf{n}_{|w|}}(\mathbf{d},\boldsymbol{\mu_D},\boldsymbol{\mu_S})
$$
$$
\times\frac{\partial\phi_{v\mathbf{l}_{|v|}}(\mathbf{d}_v;\boldsymbol{\mu_D})}{\partial d_k}\varphi_{w\mathbf{n}_{|w|}}(\mathbf{s}_w;\boldsymbol{\mu_S}). \tag{6.43}
$$

Similarly, applying the expectation operator $\mathbb{E}_{\mathbf{d}}$ on $\partial y(\mathbf{X};\mathbf{d},\mathbf{s})/\partial s_p$ and recognizing the *zero*-mean and orthonormal properties of orthonormal basis, leads to

$$
\mathbb{E}_{\mathbf{d}}\left[\frac{\partial y(\mathbf{X};\mathbf{d},\mathbf{s})}{\partial s_p}\right] = \sum_{\substack{u=\emptyset,v\subseteq\{1,\cdots,M_d\}\\ p\in w\subseteq\{1,\cdots,M_s\},\\ |u|+|v|+|w|\geq 1}}\ \sum_{\substack{\mathbf{j}_{|u|}\in\mathbb{N}_0^{|u|},\mathbf{l}_{|v|}\in\mathbb{N}_0^{|v|},\mathbf{n}_{|w|}\in\mathbb{N}_0^{|w|}\\ j_1,\cdots,j_{|u|},l_1,\cdots,l_{|v|},n_1,\cdots,n_{|w|}\neq 0}} C_{uvw\mathbf{j}_{|u|}\mathbf{l}_{|v|}\mathbf{n}_{|w|}}(\mathbf{d},\boldsymbol{\mu_D},\boldsymbol{\mu_S})
$$
$$
\times\phi_{v\mathbf{l}_{|v|}}(\mathbf{d}_v;\boldsymbol{\mu_D})\frac{\partial\varphi_{w\mathbf{n}_{|w|}}(\mathbf{s}_w;\boldsymbol{\mu_S})}{\partial s_p}. \tag{6.44}
$$

Thus, the sensitivities of the first moment are

$$
\frac{\partial m^{(1)}(\mathbf{d},\mathbf{s})}{\partial d_k} = \sum_{i=1}^{N}\left[m^{(1)}(\mathbf{d},\mathbf{s})s_{ki,\emptyset}+\sum_{j=1}^{\infty}D_{k,ij}(\mathbf{d})C_{ij}(\mathbf{d},\mathbf{s})\right] + \sum_{\substack{u=\emptyset,k\in v\subseteq\{1,\cdots,M_d\}\\ w\subseteq\{1,\cdots,M_s\},|u|+|v|+|w|\geq 1}}
$$
$$
\sum_{\substack{\mathbf{j}_{|u|}\in\mathbb{N}_0^{|u|},\mathbf{l}_{|v|}\in\mathbb{N}_0^{|v|},\mathbf{n}_{|w|}\in\mathbb{N}_0^{|w|}\\ j_1,\cdots,j_{|u|},l_1,\cdots,l_{|v|},n_1,\cdots,n_{|w|}\neq 0}} C_{uvw\mathbf{j}_{|u|}\mathbf{l}_{|v|}\mathbf{n}_{|w|}}(\mathbf{d},\boldsymbol{\mu_D},\boldsymbol{\mu_S})\frac{\partial\phi_{v\mathbf{l}_{|v|}}(\mathbf{d}_v;\boldsymbol{\mu_D})}{\partial d_k}\varphi_{w\mathbf{n}_{|w|}}(\mathbf{s}_w;\boldsymbol{\mu_S}) \tag{6.45}
$$

and

$$
\frac{\partial m^{(1)}(\mathbf{d},\mathbf{s})}{\partial s_p} = \sum_{\substack{u=\emptyset,v\subseteq\{1,\cdots,M_d\}\\ p\in w\subseteq\{1,\cdots,M_s\},|u|+|v|+|w|\geq 1}}\ \sum_{\substack{\mathbf{j}_{|u|}\in\mathbb{N}_0^{|u|},\mathbf{l}_{|v|}\in\mathbb{N}_0^{|v|},\mathbf{n}_{|w|}\in\mathbb{N}_0^{|w|}\\ j_1,\cdots,j_{|u|},l_1,\cdots,l_{|v|},n_1,\cdots,n_{|w|}\neq 0}} C_{uvw\mathbf{j}_{|u|}\mathbf{l}_{|v|}\mathbf{n}_{|w|}}(\mathbf{d},\boldsymbol{\mu_D},\boldsymbol{\mu_S})
$$
$$
\times\phi_{v\mathbf{l}_{|v|}}(\mathbf{d}_v;\boldsymbol{\mu_D})\frac{\partial\varphi_{w\mathbf{n}_{|w|}}(\mathbf{s}_w;\boldsymbol{\mu_S})}{\partial s_p}, \tag{6.46}
$$

representing closed-form expressions of the sensitivities in terms of the augmented PDD or Fourier-polynomial expansion coefficients of the response or log-density derivative functions.

6.4.1.1.2 Approximate Sensitivities

When $y(\mathbf{X}; \mathbf{d}, \mathbf{s})$ and $s_{ki}(X_i; \mathbf{d})$ are replaced with their S-variate, mth-order augmented PDD and m'th-order Fourier-polynomial approximations, respectively, the resultant sensitivity equations, expressed by

$$
\begin{aligned}
\frac{\partial \tilde{m}_{S,m}^{(1)}(\mathbf{d}, \mathbf{s})}{\partial d_k} \ :=\ & \frac{\partial \mathbb{E}_{\mathbf{d}}\left[\tilde{y}_{S,m}(\mathbf{X}; \mathbf{d}, \mathbf{s})\right]}{\partial d_k} = \sum_{i=1}^{N}\left[\tilde{m}_{S,m}^{(1)}(\mathbf{d}, \mathbf{s})s_{ki,\emptyset} + \sum_{j=1}^{m_{\min}} D_{k,ij}(\mathbf{d})\tilde{C}_{ij}(\mathbf{d}, \mathbf{s})\right] \\
& + \sum_{\substack{u=\emptyset, k\in v\subseteq\{1,\cdots,M_d\} \\ w\subseteq\{1,\cdots,M_s\}, 1\leq|u|+|v|+|w|\leq S}} \ \sum_{\substack{\mathbf{j}_{|u|}\in\mathbb{N}_0^{|u|}, \mathbf{l}_{|v|}\in\mathbb{N}_0^{|v|}, \mathbf{n}_{|w|}\in\mathbb{N}_0^{|w|} \\ \left\|\mathbf{j}_{|u|}\right\|_{\infty}, \left\|\mathbf{l}_{|v|}\right\|_{\infty}, \left\|\mathbf{n}_{|w|}\right\|_{\infty}\leq m \\ j_1,\cdots,j_{|u|}, l_1,\cdots,l_{|v|}, n_1,\cdots,n_{|w|}\neq 0}} C_{uvw\mathbf{j}_{|u|}\mathbf{l}_{|v|}\mathbf{n}_{|w|}}(\mathbf{d}, \boldsymbol{\mu}_{\mathbf{D}}, \boldsymbol{\mu}_{\mathbf{S}}) \\
& \times \frac{\partial \phi_{v\mathbf{l}_{|v|}}(\mathbf{d}_v; \boldsymbol{\mu}_{\mathbf{D}})}{\partial d_k} \varphi_{w\mathbf{n}_{|w|}}(\mathbf{s}_w; \boldsymbol{\mu}_{\mathbf{S}}) \quad (6.47)
\end{aligned}
$$

and

$$
\begin{aligned}
\frac{\partial \tilde{m}_{S,m}^{(1)}(\mathbf{d}, \mathbf{s})}{\partial s_p} \ :=\ & \frac{\partial \mathbb{E}_{\mathbf{d}}\left[\tilde{y}_{S,m}(\mathbf{X}; \mathbf{d}, \mathbf{s})\right]}{\partial s_p} = \sum_{\substack{u=\emptyset, v\subseteq\{1,\cdots,M_d\} \\ p\in w\subseteq\{1,\cdots,M_s\} \\ 1\leq|u|+|v|+|w|\leq S}} \ \sum_{\substack{\mathbf{j}_{|u|}\in\mathbb{N}_0^{|u|}, \mathbf{l}_{|v|}\in\mathbb{N}_0^{|v|}, \mathbf{n}_{|w|}\in\mathbb{N}_0^{|w|} \\ \left\|\mathbf{j}_{|u|}\right\|_{\infty}, \left\|\mathbf{l}_{|v|}\right\|_{\infty}, \left\|\mathbf{n}_{|w|}\right\|_{\infty}\leq m \\ j_1,\cdots,j_{|u|}, l_1,\cdots,l_{|v|}, n_1,\cdots,n_{|w|}\neq 0}} \\
& C_{uvw\mathbf{j}_{|u|}\mathbf{l}_{|v|}\mathbf{n}_{|w|}}(\mathbf{d}, \boldsymbol{\mu}_{\mathbf{D}}, \boldsymbol{\mu}_{\mathbf{S}})\phi_{v\mathbf{l}_{|v|}}(\mathbf{d}_v; \boldsymbol{\mu}_{\mathbf{D}})\frac{\partial \varphi_{w\mathbf{n}_{|w|}}(\mathbf{s}_w; \boldsymbol{\mu}_{\mathbf{S}})}{\partial s_p}, \quad (6.48)
\end{aligned}
$$

where $m_{\min} := \min(m, m')$, and

$$
\begin{aligned}
\tilde{C}_{ij}(\mathbf{d}, \mathbf{s}) \ =\ & \sum_{\substack{u=\{i\}, v\subseteq\{1,\cdots,M_d\} \\ w\subseteq\{1,\cdots,M_s\}, |u|+|v|+|w|\leq S}} \ \sum_{\substack{\mathbf{j}_{|u|}=j\in\mathbb{N}_0, \mathbf{l}_{|v|}\in\mathbb{N}_0^{|v|}, \mathbf{n}_{|w|}\in\mathbb{N}_0^{|w|} \\ \left\|\mathbf{j}_{|u|}\right\|_{\infty}, \left\|\mathbf{l}_{|v|}\right\|_{\infty}, \left\|\mathbf{n}_{|w|}\right\|_{\infty}\leq m \\ j, l_1,\cdots,l_{|v|}, n_1,\cdots,n_{|w|}\neq 0}} C_{uvw\mathbf{j}_{|u|}\mathbf{l}_{|v|}\mathbf{n}_{|w|}}(\mathbf{d}, \boldsymbol{\mu}_{\mathbf{D}}, \boldsymbol{\mu}_{\mathbf{S}}) \\
& \times \phi_{v\mathbf{l}_{|v|}}(\mathbf{d}_v; \boldsymbol{\mu}_{\mathbf{D}})\varphi_{w\mathbf{n}_{|w|}}(\mathbf{s}_w; \boldsymbol{\mu}_{\mathbf{S}}), \quad (6.49)
\end{aligned}
$$

become approximate, relying on the truncation parameters S, m, and m' in general. It is elementary to show that the approximate sensitivities of the first moment, at appropriate limits, converge to the exact sensitivities when $S \to N + M$, $m \to \infty$, and $m' \to \infty$.

6.4.1.2 Sensitivity of the Second Moment

Setting $r = 2$ in Equations (6.31) and (6.32), the sensitivities of the second moment are

$$\frac{\partial m^{(2)}(\mathbf{d}, \mathbf{s})}{\partial d_k} = \sum_{i=1}^{N} \mathbb{E}_\mathbf{d} \left[y^2(\mathbf{X}; \mathbf{d}, \mathbf{s}) s_{ki}(X_i; \mathbf{d}) \right] + 2\mathbb{E}_\mathbf{d} \left[y(\mathbf{X}; \mathbf{d}, \mathbf{s}) \frac{\partial y(\mathbf{X}; \mathbf{d}, \mathbf{s})}{\partial d_k} \right] \tag{6.50}$$

and

$$\frac{\partial m^{(2)}(\mathbf{d}, \mathbf{s})}{\partial s_p} = 2\mathbb{E}_\mathbf{d} \left[y(\mathbf{X}; \mathbf{d}, \mathbf{s}) \frac{\partial y(\mathbf{X}; \mathbf{d}, \mathbf{s})}{\partial s_p} \right], \tag{6.51}$$

where $k = 1, \cdots, M_d$ and $p = 1, \cdots, M_s$.

6.4.1.2.1 Exact Sensitivities

Employing Equations (6.35) and (6.38), the first term $\mathbb{E}_\mathbf{d} \left[y^2(\mathbf{X}; \mathbf{d}, \mathbf{s}) s_{ki}(X_i; \mathbf{d}) \right]$ on the right hand side of Equation (6.50), aided by the *zero*-mean and orthonormal properties of orthonormal basis, can be expressed by

$$\mathbb{E}_\mathbf{d} \left[y^2(\mathbf{X}; \mathbf{d}, \mathbf{s}) s_{ki}(X_i; \mathbf{d}) \right] = m^{(2)}(\mathbf{d}, \mathbf{s}) s_{ki,\emptyset} + 2m^{(1)}(\mathbf{d}, \mathbf{s}) \sum_{j=1}^{\infty} C_{ij}(\mathbf{d}, \mathbf{s}) D_{k,ij}(\mathbf{d}) + T_{ki}, \tag{6.52}$$

where

$$\begin{aligned} T_{ki} &= \sum_{i_1=1}^{N} \sum_{i_2=1}^{N} \sum_{j_1=1}^{\infty} \sum_{j_2=1}^{\infty} \sum_{j_3=1}^{\infty} C_{i_1 j_1}(\mathbf{d}, \mathbf{s}) C_{i_2 j_2}(\mathbf{d}, \mathbf{s}) D_{k,i j_3}(\mathbf{d}) \\ &\quad \times \mathbb{E}_\mathbf{d} \left[\psi_{i_1 j_1}(X_{i_1}; \mathbf{d}) \psi_{i_2 j_2}(X_{i_2}; \mathbf{d}) \psi_{i j_3}(X_i; \mathbf{d}) \right], \end{aligned} \tag{6.53}$$

requiring expectations of various products of three random orthonormal polynomials as discussed in previous chapters.

The evaluation of the second term $\mathbb{E}_{\mathbf{d}}\left[y(\mathbf{X}; \mathbf{d}, \mathbf{s})\partial y(\mathbf{X}; \mathbf{d}, \mathbf{s})/\partial d_k\right]$ on the right hand side of Equation (6.50) requires restructuring Equation (6.42) as

$$\frac{\partial y(\mathbf{X}; \mathbf{d}, \mathbf{s})}{\partial d_k} = y_{d_k\emptyset}(\mathbf{d}, \mathbf{s}) + \sum_{\substack{u\subseteq\{1,\cdots,N\} \\ |u|\geq 1}} \sum_{\substack{\mathbf{j}_{|u|}\in\mathbb{N}_0^{|u|} \\ j_1,\cdots,j_{|u|}\neq 0}} F_{d_k u\mathbf{j}_{|u|}}(\mathbf{d}, \mathbf{s})\psi_{u\mathbf{j}_{|u|}}(\mathbf{X}_u; \mathbf{d}), \quad (6.54)$$

where

$$\begin{aligned} y_{d_k\emptyset}(\mathbf{d}, \mathbf{s}) &= \sum_{\substack{u=\emptyset, k\in v\subseteq\{1,\cdots,M_d\} \\ w\subseteq\{1,\cdots,M_s\}, |u|+|v|+|w|\geq 1}} \sum_{\substack{\mathbf{l}_{|v|}\in\mathbb{N}_0^{|v|}, \mathbf{n}_{|w|}\in\mathbb{N}_0^{|w|} \\ l_1,\cdots,l_{|v|}, n_1,\cdots,n_{|w|}\neq 0}} C_{uvw\mathbf{j}_{|u|}\mathbf{l}_{|v|}\mathbf{n}_{|w|}}(\mathbf{d}, \boldsymbol{\mu}_{\mathbf{D}}, \boldsymbol{\mu}_{\mathbf{S}}) \\ &\times \frac{\partial\phi_{v\mathbf{l}_{|v|}}(\mathbf{d}_v; \boldsymbol{\mu}_{\mathbf{D}})}{\partial d_k}\varphi_{w\mathbf{n}_{|w|}}(\mathbf{s}_w; \boldsymbol{\mu}_{\mathbf{S}}), \end{aligned} \quad (6.55)$$

and

$$\begin{aligned} F_{d_k u\mathbf{j}_{|u|}}(\mathbf{d}, \mathbf{s}) &= \sum_{\substack{k\in v\subseteq\{1,\cdots,M_d\}, w\subseteq\{1,\cdots,M_s\} \\ |u|+|v|+|w|\geq 1}} \sum_{\substack{\mathbf{l}_{|v|}\in\mathbb{N}_0^{|v|}, \mathbf{n}_{|w|}\in\mathbb{N}_0^{|w|} \\ l_1,\cdots,l_{|v|}, n_1,\cdots,n_{|w|}\neq 0}} C_{uvw\mathbf{j}_{|u|}\mathbf{l}_{|v|}\mathbf{n}_{|w|}}(\mathbf{d}, \boldsymbol{\mu}_{\mathbf{D}}, \boldsymbol{\mu}_{\mathbf{S}}) \\ &\times \frac{\partial\phi_{v\mathbf{l}_{|v|}}(\mathbf{d}_v; \boldsymbol{\mu}_{\mathbf{D}})}{\partial d_k}\varphi_{w\mathbf{n}_{|w|}}(\mathbf{s}_w; \boldsymbol{\mu}_{\mathbf{S}}). \end{aligned} \quad (6.56)$$

Hence, from Equations (6.23) and (6.54), and utilizing the orthonormal properties of $\psi_{u\mathbf{j}_{|u|}}(\mathbf{X}_u; \mathbf{d})$,

$$\begin{aligned} \mathbb{E}_{\mathbf{d}}\left[y(\mathbf{X}; \mathbf{d}, \mathbf{s})\frac{\partial y(\mathbf{X}; \mathbf{d}, \mathbf{s})}{\partial d_k}\right] &= m^{(1)}(\mathbf{d}, \mathbf{s})y_{d_k\emptyset}(\mathbf{d}, \mathbf{s}) \\ &+ \sum_{\substack{u\subseteq\{1,\cdots,N\} \\ |u|\geq 1}} \sum_{\substack{\mathbf{j}_{|u|}\in\mathbb{N}_0^{|u|} \\ j_1,\cdots,j_{|u|}\neq 0}} E_{u\mathbf{j}_{|u|}}(\mathbf{d}, \mathbf{s})F_{d_k u\mathbf{j}_{|u|}}(\mathbf{d}, \mathbf{s}). \end{aligned} \quad (6.57)$$

Similarly, the term $\mathbb{E}_{\mathbf{d}}\left[y(\mathbf{X}; \mathbf{d}, \mathbf{s})\partial y(\mathbf{X}; \mathbf{d}, \mathbf{s})/\partial s_p\right]$ on the right hand side of Equation (6.51) can be analytically derived as

$$\begin{aligned} \mathbb{E}_{\mathbf{d}}\left[y(\mathbf{X}; \mathbf{d}, \mathbf{s})\frac{\partial y(\mathbf{X}; \mathbf{d}, \mathbf{s})}{\partial s_p}\right] &= m^{(1)}(\mathbf{d}, \mathbf{s})y_{s_p\emptyset}(\mathbf{d}, \mathbf{s}) \\ &+ \sum_{\substack{u\subseteq\{1,\cdots,N\} \\ |u|\geq 1}} \sum_{\substack{\mathbf{j}_{|u|}\in\mathbb{N}_0^{|u|} \\ j_1,\cdots,j_{|u|}\neq 0}} E_{u\mathbf{j}_{|u|}}(\mathbf{d}, \mathbf{s})G_{s_p u\mathbf{j}_{|u|}}(\mathbf{d}, \mathbf{s}), \end{aligned} \quad (6.58)$$

where

$$y_{s_p\emptyset}(\mathbf{d}, \mathbf{s}) = \sum_{\substack{u=\emptyset, v\subseteq\{1,\cdots,M_d\} \\ p\in w\subseteq\{1,\cdots,M_s\}, |u|+|v|+|w|\geq 1}} \sum_{\substack{\mathbf{l}_{|v|}\in\mathbb{N}_0^{|v|}, \mathbf{n}_{|w|}\in\mathbb{N}_0^{|w|} \\ l_1,\cdots,l_{|v|}, n_1,\cdots,n_{|w|}\neq 0}} C_{uvw\mathbf{j}_{|u|}\mathbf{l}_{|v|}\mathbf{n}_{|w|}}(\mathbf{d}, \boldsymbol{\mu_D}, \boldsymbol{\mu_S})$$
$$\times \phi_{v\mathbf{l}_{|v|}}(\mathbf{d}_v; \boldsymbol{\mu_D}) \frac{\partial\varphi_{w\mathbf{n}_{|w|}}(\mathbf{s}_w; \boldsymbol{\mu_S})}{\partial s_p}, \tag{6.59}$$

and

$$G_{s_p u\mathbf{j}_{|u|}}(\mathbf{d}, \mathbf{s}) = \sum_{\substack{v\subseteq\{1,\cdots,M_d\}, p\in w\subseteq\{1,\cdots,M_s\} \\ |u|+|v|+|w|\geq 1}} \sum_{\substack{\mathbf{l}_{|v|}\in\mathbb{N}_0^{|v|}, \mathbf{n}_{|w|}\in\mathbb{N}_0^{|w|} \\ l_1,\cdots,l_{|v|}, n_1,\cdots,n_{|w|}\neq 0}} C_{uvw\mathbf{j}_{|u|}\mathbf{l}_{|v|}\mathbf{n}_{|w|}}(\mathbf{d}, \boldsymbol{\mu_D}, \boldsymbol{\mu_S})$$
$$\times \phi_{v\mathbf{l}_{|v|}}(\mathbf{d}_v; \boldsymbol{\mu_D}) \frac{\partial\varphi_{w\mathbf{n}_{|w|}}(\mathbf{s}_w; \boldsymbol{\mu_S})}{\partial s_p}. \tag{6.60}$$

Thus, the sensitivities of the second moment are

$$\frac{\partial m^{(2)}(\mathbf{d}, \mathbf{s})}{\partial d_k} = \sum_{i=1}^{N}\left[m^{(2)}(\mathbf{d}, \mathbf{s})s_{ki,\emptyset} + 2m^{(1)}(\mathbf{d}, \mathbf{s})\sum_{j=1}^{\infty}C_{ij}(\mathbf{d}, \mathbf{s})D_{k,ij}(\mathbf{d}) + T_{ki}\right]$$
$$+ m^{(1)}(\mathbf{d}, \mathbf{s})y_{d_k\emptyset}(\mathbf{d}, \mathbf{s}) + \sum_{\substack{u\subseteq\{1,\cdots,N\} \\ |u|\geq 1}} \sum_{\substack{\mathbf{j}_{|u|}\in\mathbb{N}_0^{|u|} \\ j_1,\cdots,j_{|u|}\neq 0}} E_{u\mathbf{j}_{|u|}}(\mathbf{d}, \mathbf{s})F_{d_k u\mathbf{j}_{|u|}}(\mathbf{d}, \mathbf{s}) \tag{6.61}$$

and

$$\frac{\partial m^{(2)}(\mathbf{d}, \mathbf{s})}{\partial s_p} = m^{(1)}(\mathbf{d}, \mathbf{s})y_{s_p\emptyset}(\mathbf{d}, \mathbf{s})$$
$$+ \sum_{\substack{u\subseteq\{1,\cdots,N\} \\ |u|\geq 1}} \sum_{\substack{\mathbf{j}_{|u|}\in\mathbb{N}_0^{|u|} \\ j_1,\cdots,j_{|u|}\neq 0}} E_{u\mathbf{j}_{|u|}}(\mathbf{d}, \mathbf{s})G_{s_p u\mathbf{j}_{|u|}}(\mathbf{d}, \mathbf{s}), \tag{6.62}$$

representing closed-form expressions of the sensitivities in terms of the augmented PDD or Fourier-polynomial expansion coefficients of the response or log-density derivative functions.

6.4.1.2.2 Approximate Sensitivities

When $y(\mathbf{X}; \mathbf{d}, \mathbf{s})$ and $s_{ki}(X_i; \mathbf{d})$ are replaced with their S-variate, mth-order augmented PDD and m'th-order Fourier-polynomial approximations, respectively, the resultant sensitivity equations, expressed by

$$
\begin{aligned}
\frac{\partial \tilde{m}_{S,m}^{(2)}(\mathbf{d}, \mathbf{s})}{\partial d_k} \quad &:= \quad \frac{\partial \mathbb{E}_{\mathbf{d}}\left[\tilde{y}_{S,m}^2(\mathbf{X}; \mathbf{d}, \mathbf{s})\right]}{\partial d_k} = \sum_{i=1}^{N}\left[\tilde{m}_{S,m}^{(2)}(\mathbf{d}, \mathbf{s})s_{ki,\emptyset} + 2\tilde{m}_{S,m}^{(1)}(\mathbf{d}, \mathbf{s})\right. \\
&\quad \left. \times \sum_{j=1}^{m_{\min}} \tilde{C}_{ij}(\mathbf{d}, \mathbf{s})D_{k,ij}(\mathbf{d}) + \tilde{T}_{ki,m,m'}\right] + \tilde{m}_{S,m}^{(1)}(\mathbf{d}, \mathbf{s})\tilde{y}_{d_k\emptyset,S,m}(\mathbf{d}, \mathbf{s}) \\
&\quad + \sum_{\substack{u\subseteq\{1,\cdots,N\}\\ 1\leq|u|\leq S}} \sum_{\substack{\mathbf{j}_{|u|}\in\mathbb{N}_0^{|u|}, \left\|\mathbf{j}_{|u|}\right\|_{\infty}\leq m\\ j_1,\cdots,j_{|u|}\neq 0}} E_{u\mathbf{j}_{|u|},S,m}(\mathbf{d}, \mathbf{s})F_{d_k u\mathbf{j}_{|u|},S,m}(\mathbf{d}, \mathbf{s}) \qquad (6.63)
\end{aligned}
$$

and

$$
\begin{aligned}
\frac{\partial \tilde{m}_{S,m}^{(2)}(\mathbf{d}, \mathbf{s})}{\partial s_p} \quad &:= \quad \frac{\partial \mathbb{E}_{\mathbf{d}}\left[\tilde{y}_{S,m}^2(\mathbf{X}; \mathbf{d}, \mathbf{s})\right]}{\partial s_p} = \tilde{m}_{S,m}^{(1)}(\mathbf{d}, \mathbf{s})\tilde{y}_{s_p\emptyset,S,m}(\mathbf{d}, \mathbf{s}) \\
&\quad + \sum_{\substack{u\subseteq\{1,\cdots,N\}\\ 1\leq|u|\leq S}} \sum_{\substack{\mathbf{j}_{|u|}\in\mathbb{N}_0^{|u|}, \left\|\mathbf{j}_{|u|}\right\|_{\infty}\leq m\\ j_1,\cdots,j_{|u|}\neq 0}} E_{u\mathbf{j}_{|u|},S,m}(\mathbf{d}, \mathbf{s})G_{s_p u\mathbf{j}_{|u|},S,m}(\mathbf{d}, \mathbf{s}), \qquad (6.64)
\end{aligned}
$$

where $m_{\min} := \min(m, m')$,

$$
\begin{aligned}
\tilde{y}_{d_k\emptyset,S,m}(\mathbf{d}, \mathbf{s}) \quad &= \quad \sum_{\substack{u=\emptyset, k\in v\subseteq\{1,\cdots,M_d\}\\ w\subseteq\{1,\cdots,M_s\}\\ 1\leq|u|+|v|+|w|\leq S}} \sum_{\substack{\mathbf{l}_{|v|}\in\mathbb{N}_0^{|v|}, \mathbf{n}_{|w|}\in\mathbb{N}_0^{|w|}\\ \left\|\mathbf{l}_{|v|}\right\|_{\infty}, \left\|\mathbf{n}_{|w|}\right\|_{\infty}\leq m\\ l_1,\cdots,l_{|v|}, n_1,\cdots,n_{|w|}\neq 0}} C_{uvw\mathbf{j}_{|u|}\mathbf{l}_{|v|}\mathbf{n}_{|w|}}(\mathbf{d}, \boldsymbol{\mu}_{\mathbf{D}}, \boldsymbol{\mu}_{\mathbf{S}}) \\
&\quad \times \frac{\partial \phi_{v\mathbf{l}_{|v|}}(\mathbf{d}_v; \boldsymbol{\mu}_{\mathbf{D}})}{\partial d_k}\varphi_{w\mathbf{n}_{|w|}}(\mathbf{s}_w; \boldsymbol{\mu}_{\mathbf{S}}), \qquad (6.65)
\end{aligned}
$$

$$
\begin{aligned}
\tilde{y}_{s_p\emptyset,S,m}(\mathbf{d}, \mathbf{s}) \quad &= \quad \sum_{\substack{u=\emptyset, v\subseteq\{1,\cdots,M_d\}\\ p\in w\subseteq\{1,\cdots,M_s\}\\ 1\leq|u|+|v|+|w|\leq S}} \sum_{\substack{\mathbf{l}_{|v|}\in\mathbb{N}_0^{|v|}, \mathbf{n}_{|w|}\in\mathbb{N}_0^{|w|}\\ \left\|\mathbf{l}_{|v|}\right\|_{\infty}, \left\|\mathbf{n}_{|w|}\right\|_{\infty}\leq m\\ l_1,\cdots,l_{|v|}, n_1,\cdots,n_{|w|}\neq 0}} C_{uvw\mathbf{j}_{|u|}\mathbf{l}_{|v|}\mathbf{n}_{|w|}}(\mathbf{d}, \boldsymbol{\mu}_{\mathbf{D}}, \boldsymbol{\mu}_{\mathbf{S}}) \\
&\quad \times \phi_{v\mathbf{l}_{|v|}}(\mathbf{d}_v; \boldsymbol{\mu}_{\mathbf{D}})\frac{\partial \varphi_{w\mathbf{n}_{|w|}}(\mathbf{s}_w; \boldsymbol{\mu}_{\mathbf{S}})}{\partial s_p}, \qquad (6.66)
\end{aligned}
$$

$$
\begin{aligned}
F_{d_k u \mathbf{j}_{|u|}, S, m}(\mathbf{d}, \mathbf{s}) \;=& \sum_{\substack{k \in v \subseteq \{1, \cdots, M_d\}, w \subseteq \{1, \cdots, M_s\} \\ 1 \le |u| + |v| + |w| \le S}} \sum_{\substack{\mathbf{l}_{|v|} \in \mathbb{N}_0^{|v|}, \mathbf{n}_{|w|} \in \mathbb{N}_0^{|w|} \\ \left\| \mathbf{l}_{|v|} \right\|_\infty, \left\| \mathbf{n}_{|w|} \right\|_\infty \le m \\ l_1, \cdots, l_{|v|}, n_1, \cdots, n_{|w|} \ne 0}} C_{uvw \mathbf{j}_{|u|} \mathbf{l}_{|v|} \mathbf{n}_{|w|}}(\mathbf{d}, \boldsymbol{\mu_D}, \boldsymbol{\mu_S}) \\
& \times \frac{\partial \phi_{v \mathbf{l}_{|v|}}(\mathbf{d}_v; \boldsymbol{\mu_D})}{\partial d_k} \varphi_{w \mathbf{n}_{|w|}}(\mathbf{s}_w; \boldsymbol{\mu_S}),
\end{aligned} \tag{6.67}
$$

$$
\begin{aligned}
\tilde{T}_{ki, m, m'} \;=& \sum_{i_1=1}^N \sum_{i_2=1}^N \sum_{j_1=1}^m \sum_{j_2=1}^m \sum_{j_3=1}^{m'} \tilde{C}_{i_1 j_1}(\mathbf{d}, \mathbf{s}) \tilde{C}_{i_2 j_2}(\mathbf{d}, \mathbf{s}) D_{k, i j_3}(\mathbf{d}) \times \\
& \mathbb{E}_{\mathbf{d}} \left[\psi_{i_1 j_1}(X_{i_1}; \mathbf{d}) \psi_{i_2 j_2}(X_{i_2}; \mathbf{d}) \psi_{i j_3}(X_i; \mathbf{d}) \right],
\end{aligned} \tag{6.68}
$$

$$
\begin{aligned}
G_{s_p u \mathbf{j}_{|u|}, S, m}(\mathbf{d}, \mathbf{s}) \;=& \sum_{\substack{v \subseteq \{1, \cdots, M_d\}, p \in w \subseteq \{1, \cdots, M_s\} \\ 1 \le |u| + |v| + |w| \le S}} \sum_{\substack{\mathbf{l}_{|v|} \in \mathbb{N}_0^{|v|}, \mathbf{n}_{|w|} \in \mathbb{N}_0^{|w|} \\ \left\| \mathbf{l}_{|v|} \right\|_\infty, \left\| \mathbf{n}_{|w|} \right\|_\infty \le m \\ l_1, \cdots, l_{|v|}, n_1, \cdots, n_{|w|} \ne 0}} C_{uvw \mathbf{j}_{|u|} \mathbf{l}_{|v|} \mathbf{n}_{|w|}}(\mathbf{d}, \boldsymbol{\mu_D}, \boldsymbol{\mu_S}) \\
& \times \phi_{v \mathbf{l}_{|v|}}(\mathbf{d}_v; \boldsymbol{\mu_D}) \frac{\partial \varphi_{w \mathbf{n}_{|w|}}(\mathbf{s}_w; \boldsymbol{\mu_S})}{\partial s_p}.
\end{aligned} \tag{6.69}
$$

become approximate, relying on the truncation parameters S, m, and m' in general. It is elementary to show that the approximate sensitivities of the second moment also converge, to the exact sensitivities when $S \to N + M$, $m \to \infty$, and $m' \to \infty$.

6.4.2 Sensitivity of Failure Probability

Taking a partial derivative of the augmented PDD estimate of the failure probability in Equation (6.25) with respect to d_k, $k = 1, \cdots, M_d$ or s_p, $p = 1, \cdots, M_s$, produces

$$
\frac{\partial \tilde{P}_{F, S, m}(\mathbf{d}, \mathbf{s})}{\partial d_k} \;:=\; \frac{\partial \mathbb{E}_{\mathbf{d}} \left[I_{\tilde{\Omega}_{F, S, m}}(\mathbf{X}; \mathbf{d}, \mathbf{s}) \right]}{\partial d_k} \tag{6.70}
$$

or

$$
\frac{\partial \tilde{P}_{F, S, m}(\mathbf{d}, \mathbf{s})}{\partial s_p} \;:=\; \frac{\partial \mathbb{E}_{\mathbf{d}} \left[I_{\tilde{\Omega}_{F, S, m}}(\mathbf{X}; \mathbf{d}, \mathbf{s}) \right]}{\partial s_p}, \tag{6.71}
$$

where $I_{\tilde{\Omega}_{F,S,m}}(\mathbf{x}; \mathbf{d}, \mathbf{s})$ is the augmented PDD-generated indicator function, which is equal to *one* when $\mathbf{x} \in \tilde{\Omega}_{F,S,m}$ and *zero* otherwise. Since $I_{\tilde{\Omega}_{F,S,m}}(\mathbf{x}; \mathbf{d}, \mathbf{s})$ depends on the design vectors $\mathbf{d}$ and $\mathbf{s}$ and their corresponding derivatives are infinite, the Lebesgue dominated convergence theorem is not applicable. Hence, the PDD-MCS method developed in previous works [75, 110, 124] for the reliability sensitivity of performance functions involving solely distributional design variables cannot be applied. The following finite-difference formulae, utilizing the augmented PDD expansion of the response function $y(\mathbf{X}; \mathbf{d}, \mathbf{s})$, are proposed to evaluate the sensitivity of reliability.

Assume that the design sensitivities at the design point $(\mathbf{d}, \mathbf{s})$ are sought. Let the small perturbations of the finite-difference approximation be Δd_k and Δs_p for the kth component of $\mathbf{d}$ and the pth component of $\mathbf{s}$, respectively, where $k = 1, \cdots, M_d$ and $p = 1, \cdots, M_s$. For the forward finite-difference approximation, the corresponding perturbed design vectors are $\mathbf{d} + \Delta d_k \cdot \mathbf{e}_k$ and $\mathbf{s} + \Delta s_p \cdot \mathbf{e}_p$, respectively, where $\mathbf{e}_k$ is the M_d-dimensional basis vector, in which the kth component is *one* and other components are *zeros*; similarly, $\mathbf{e}_p$ is the M_s-dimensional basis vector, in which the pth component is *one* and other components are *zeros*. Then, Equation (6.15) induces two additional approximate response functions

$$
\begin{aligned}
\tilde{y}_{S,m}(\mathbf{X}; \mathbf{d} + \Delta d_k \cdot \mathbf{e}_k, \mathbf{s}) &= y_\emptyset(\mathbf{d}, \boldsymbol{\mu}_{\mathbf{D}}, \boldsymbol{\mu}_{\mathbf{S}}) + \sum_{\substack{u \subseteq \{1,\cdots,N\}, v \subseteq \{1,\cdots,M_d\} \\ w \subseteq \{1,\cdots,M_s\}, 1 \le |u|+|v|+|w| \le S}} \\
&\quad \sum_{\substack{\mathbf{j}_{|u|} \in \mathbb{N}_0^{|u|}, \mathbf{l}_{|v|} \in \mathbb{N}_0^{|v|}, \mathbf{n}_{|w|} \in \mathbb{N}_0^{|w|} \\ \|\mathbf{j}_{|u|}\|_\infty, \|\mathbf{l}_{|v|}\|_\infty, \|\mathbf{n}_{|w|}\|_\infty \le m \\ j_1, \cdots, j_{|u|}, l_1, \cdots, l_{|v|}, n_1, \cdots, n_{|w|} \ne 0}} C_{uvw\mathbf{j}_{|u|}\mathbf{l}_{|v|}\mathbf{n}_{|w|}}(\mathbf{d}, \boldsymbol{\mu}_{\mathbf{D}}, \boldsymbol{\mu}_{\mathbf{S}}) \psi_{u\mathbf{j}_{|u|}}(\mathbf{X}_u; \mathbf{d}) \\
&\quad \times \phi_{v\mathbf{l}_{|v|}}((\mathbf{d} + \Delta d_k \cdot \mathbf{e}_k)_v; \boldsymbol{\mu}_{\mathbf{D}}) \varphi_{w\mathbf{n}_{|w|}}(\mathbf{s}_w; \boldsymbol{\mu}_{\mathbf{S}})
\end{aligned} \tag{6.72}
$$

and

$$
\begin{aligned}
\tilde{y}_{S,m}(\mathbf{X}; \mathbf{d}, \mathbf{s} + \Delta s_p \cdot \mathbf{e}_p) &= y_{i,\emptyset}(\mathbf{d}, \boldsymbol{\mu}_{\mathbf{D}}, \boldsymbol{\mu}_{\mathbf{S}}) + \sum_{\substack{u \subseteq \{1,\cdots,N\}, v \subseteq \{1,\cdots,M_d\} \\ w \subseteq \{1,\cdots,M_s\}, 1 \le |u|+|v|+|w| \le S}} \\
&\sum_{\substack{\mathbf{j}_{|u|} \in \mathbb{N}_0^{|u|}, \mathbf{l}_{|v|} \in \mathbb{N}_0^{|v|}, \mathbf{n}_{|w|} \in \mathbb{N}_0^{|w|} \\ \left\| \mathbf{j}_{|u|} \right\|_\infty, \left\| \mathbf{l}_{|v|} \right\|_\infty, \left\| \mathbf{n}_{|w|} \right\|_\infty \le m \\ j_1,\cdots,j_{|u|}, l_1,\cdots,l_{|v|}, n_1,\cdots,n_{|w|} \ne 0}} C_{uvw\mathbf{j}_{|u|}\mathbf{l}_{|v|}\mathbf{n}_{|w|}}(\mathbf{d}, \boldsymbol{\mu}_{\mathbf{D}}, \boldsymbol{\mu}_{\mathbf{S}}) \psi_{u\mathbf{j}_{|u|}}(\mathbf{X}_u; \mathbf{d}) \\
&\times \phi_{v\mathbf{l}_{|v|}}(\mathbf{d}_v; \boldsymbol{\mu}_{\mathbf{D}}) \varphi_{w\mathbf{n}_{|w|}}((\mathbf{s} + \Delta s_p \cdot \mathbf{e}_p)_w; \boldsymbol{\mu}_{\mathbf{S}}),
\end{aligned} \tag{6.73}
$$

owing to two finite-difference perturbations. The sensitivity of the probability of failure with respect to d_k by the forward finite-difference approximation is

$$
\begin{aligned}
\frac{\partial \tilde{P}_{F,S,m}(\mathbf{d}, \mathbf{s})}{\partial d_k} &= \lim_{\Delta d_k \to 0} \frac{1}{\Delta d_k} \left[\int_{\mathbb{R}^N} I_{\tilde{\Omega}_{F,S,m,\Delta d}}(\mathbf{X}; \mathbf{d} + \Delta d_k \cdot \mathbf{e}_k, \mathbf{s}) f_{\mathbf{X}}(\mathbf{x}; \mathbf{d} + \Delta d_k \cdot \mathbf{e}_k) \mathrm{d}\mathbf{x} \right. \\
&\qquad \left. - \int_{\mathbb{R}^N} I_{\tilde{\Omega}_{F,S,m}}(\mathbf{X}; \mathbf{d}, \mathbf{s}) f_{\mathbf{X}}(\mathbf{x}; \mathbf{d}) \mathrm{d}\mathbf{x} \right] \\
&= \lim_{\Delta d_k \to 0} \frac{1}{\Delta d_k} \lim_{L \to \infty} \frac{1}{L} \left[\sum_{l_1=1}^{L} I_{\tilde{\Omega}_{F,S,m,\Delta d}}(\mathbf{x}^{(l_1)}; \mathbf{d} + \Delta d_k \cdot \mathbf{e}_k, \mathbf{s}) \right. \\
&\qquad \left. - \sum_{l_2=1}^{L} I_{\tilde{\Omega}_{F,S,m}}(\mathbf{x}^{(l_2)}; \mathbf{d}, \mathbf{s}) \right], \quad k = 1, \cdots, M_d,
\end{aligned} \tag{6.74}
$$

where $\tilde{\Omega}_{F,S,m,\Delta d}$ and $\tilde{\Omega}_{F,S,m}$ are failure domains determined by $\tilde{y}_{S,m}(\mathbf{X}; \mathbf{d} + \Delta d_k \cdot \mathbf{e}_k, \mathbf{s})$ and $\tilde{y}_{S,m}(\mathbf{X}; \mathbf{d}, \mathbf{s})$, respectively, L is the sample size, $\mathbf{x}^{(l_1)}$ is the l_1th realization of $\mathbf{X}$ with respect to PDF $f_{\mathbf{X}}(\mathbf{x}; \mathbf{d} + \Delta d_k \cdot \mathbf{e}_k)$, and $\mathbf{x}^{(l_2)}$ is the l_2th realization of $\mathbf{X}$ with respect to PDF $f_{\mathbf{X}}(\mathbf{x}; \mathbf{d})$.

Similarly, the sensitivity of the probability of failure with respect to s_p by

finite-difference approximation is

$$
\begin{aligned}
\frac{\partial \tilde{P}_{F,S,m}(\mathbf{d},\mathbf{s})}{\partial s_p} &= \lim_{\Delta s_p \to 0} \frac{1}{\Delta s_p} \left[\int_{\mathbb{R}^N} I_{\tilde{\Omega}_{F,S,m,\Delta s}}(\mathbf{X};\mathbf{d},\mathbf{s}+\Delta s_p \cdot \mathbf{e}_p) f_{\mathbf{X}}(\mathbf{x};\mathbf{d}) \mathrm{d}\mathbf{x} \right. \\
&\qquad\qquad \left. - \int_{\mathbb{R}^N} I_{\tilde{\Omega}_{F,S,m}}(\mathbf{X};\mathbf{d},\mathbf{s}) f_{\mathbf{X}}(\mathbf{x};\mathbf{d}) \mathrm{d}\mathbf{x} \right] \\
&= \lim_{\Delta s_p \to 0} \frac{1}{\Delta s_p} \lim_{L \to \infty} \frac{1}{L} \sum_{l=1}^{L} \left[I_{\tilde{\Omega}_{F,S,m,\Delta s}}(\mathbf{x}^{(l)};\mathbf{d},\mathbf{s}+\Delta s_p \cdot \mathbf{e}_p) \right. \\
&\qquad\qquad \left. - I_{\tilde{\Omega}_{F,S,m}}(\mathbf{x}^{(l)};\mathbf{d},\mathbf{s}) \right], \quad p = 1, \cdots, M_s,
\end{aligned}
\tag{6.75}
$$

where $\tilde{\Omega}_{F,S,m,\Delta s}$ and $\tilde{\Omega}_{F,S,m}$ are failure domains determined by $\tilde{y}_{S,m}(\mathbf{X};\mathbf{d},\mathbf{s}+\Delta s_p \cdot \mathbf{e}_p)$ and $\tilde{y}_{S,m}(\mathbf{X};\mathbf{d},\mathbf{s})$, respectively, L is the sample size, and $\mathbf{x}^{(l)}$ is the lth realization of $\mathbf{X}$ with respect to PDF $f_{\mathbf{X}}(\mathbf{x};\mathbf{d})$.

It is important to note that two additional approximate response functions in Equations (6.72) and (6.73) are derived from the existing augmented PDD approximation used in Equation (6.25) for reliability analysis, requiring no additional original function evaluations. Therefore, the reliability and its sensitivities have both been formulated as embedded MCS based on the same PDD expansion, facilitating their concurrent evaluations in a single stochastic simulation or analysis.

6.5 Proposed Optimization Method

The augmented PDD approximations described in the preceding sections provide a means to evaluate the objective and constraint functions, including their design sensitivities, from a single stochastic analysis. An integration of reliability analysis, design sensitivity analysis, and a suitable optimization algorithm should render a convergent solution of the RDO and RBDO problems in Equations (6.1) and (6.2). However, new stochastic and design sensitivity analyses, entailing re-calculations of the

augmented PDD expansion coefficients, are needed at every design iteration. Therefore, a straightforward integration is expensive, depending on the cost of evaluating the objective and constraint functions and the requisite number of design iterations. In this section, a multi-point design process [84, 112, 124], where a series of single-step, augmented PDD approximations are built on a local subregion of the design space, is presented for solving the RDO and RBDO problems.

6.5.1 Multipoint Approximation

Let

$$\mathcal{D} = \times_{k=1}^{k=M_d} [d_{k,L}, d_{k,U}] \times_{p=1}^{p=M_s} [s_{p,L}, s_{p,U}] \subseteq \mathbb{R}^M \tag{6.76}$$

be a rectangular domain, representing the design space of the RDO and RBDO problems defined by Equations (6.1) and (6.2). For scalar variables $0 < \beta_{d,k}^{(q)} \leq 1$, $0 < \beta_{s,p}^{(q)} \leq 1$, and an initial design vector $\mathbf{d}_0^{(q)} = (d_{1,0}^{(q)}, \cdots, d_{M_d,0}^{(q)}, s_{1,0}^{(q)}, \cdots, s_{M_s,0}^{(q)})$, the subset

$$
\begin{aligned}
\mathcal{D}^{(q)} &= \times_{k=1}^{k=M_d} \left[d_{k,0}^{(q)} - \beta_{d,k}^{(q)}(d_{k,U} - d_{k,L})/2, \ d_{k,0}^{(q)} + \beta_{d,k}^{(q)}(d_{k,U} - d_{k,L})/2 \right] \\
&\quad \times_{p=1}^{p=M_s} \left[s_{p,0}^{(q)} - \beta_{s,p}^{(q)}(s_{p,U} - s_{p,L})/2, \ s_{p,0}^{(q)} + \beta_{s,p}^{(q)}(s_{p,U} - s_{p,L})/2 \right] \\
&\subseteq \mathcal{D} \subseteq \mathbb{R}^M
\end{aligned}
\tag{6.77}
$$

defines the qth subregion for $q = 1, 2, \cdots$. Using the multipoint approximation [84, 112, 124], the original RDO and RBDO problems in Equations (6.1) and (6.2) are exchanged with a succession of simpler subproblems, as follows.

1. RDO

$$\min_{(\mathbf{d},\mathbf{s})\in\mathcal{D}^{(q)}\subseteq\mathcal{D}} \quad \tilde{c}_{0,S,m}^{(q)}(\mathbf{d},\mathbf{s}) := w_1 \frac{\mathbb{E}_{\mathbf{d}}\left[\tilde{y}_{0,S,m}^{(q)}(\mathbf{X};\mathbf{d},\mathbf{s})\right]}{\mu_0^*} + w_2 \frac{\sqrt{\mathrm{var}_{\mathbf{d}}\left[\tilde{y}_{0,S,m}^{(q)}(\mathbf{X};\mathbf{d},\mathbf{s})\right]}}{\sigma_0^*},$$

$$\text{subject to} \quad \tilde{c}_{l,S,m}^{(q)}(\mathbf{d},\mathbf{s}) := \alpha_l \sqrt{\mathrm{var}_{\mathbf{d}}\left[\tilde{y}_{l,S,m}^{(q)}(\mathbf{X};\mathbf{d},\mathbf{s})\right]} - \mathbb{E}_{\mathbf{d}}\left[\tilde{y}_{l,S,m}^{(q)}(\mathbf{X};\mathbf{d},\mathbf{s})\right] \leq 0,$$

$$l = 1,\cdots,K,$$

$$d_{k,0}^{(q)} - \beta_{d,k}^{(q)}(d_{k,U} - d_{k,L})/2 \leq d_k \leq d_{k,0}^{(q)} + \beta_{d,k}^{(q)}(d_{k,U} - d_{k,L})/2,$$

$$k = 1,\cdots,M_d,$$

$$s_{p,0}^{(q)} - \beta_{s,p}^{(q)}(s_{p,U} - s_{p,L})/2 \leq s_p \leq s_{p,0}^{(q)} + \beta_{s,p}^{(q)}(s_{p,U} - s_{p,L})/2,$$

$$p = 1,\cdots,M_s. \tag{6.78}$$

2. RBDO

$$\min_{(\mathbf{d},\mathbf{s})\in\mathcal{D}^{(q)}\subseteq\mathcal{D}} \quad \tilde{c}_{0,S,m}^{(q)}(\mathbf{d},\mathbf{s}),$$

$$\text{subject to} \quad \tilde{c}_{l,S,m}^{(q)}(\mathbf{d},\mathbf{s}) := P_{\mathbf{d}}\left[\mathbf{X} \in \tilde{\Omega}_{F,l,S,m}^{(q)}(\mathbf{d},\mathbf{s})\right] - p_l \leq 0, \ l = 1,\cdots,K,$$

$$d_{k,0}^{(q)} - \beta_{d,k}^{(q)}(d_{k,U} - d_{k,L})/2 \leq d_k \leq d_{k,0}^{(q)} + \beta_{d,k}^{(q)}(d_{k,U} - d_{k,L})/2,$$

$$k = 1,\cdots,M_d,$$

$$s_{p,0}^{(q)} - \beta_{s,p}^{(q)}(s_{p,U} - s_{p,L})/2 \leq s_p \leq s_{p,0}^{(q)} + \beta_{s,p}^{(q)}(s_{p,U} - s_{p,L})/2,$$

$$p = 1,\cdots,M_s. \tag{6.79}$$

In Equations (6.78) and (6.79), $\tilde{c}_{0,S,m}^{(q)}$, $\tilde{y}_{0,S,m}^{(q)}$, $\tilde{c}_{l,S,m}^{(q)}$, $\tilde{y}_{l,S,m}^{(q)}$, and $\tilde{\Omega}_{F,l,S,m}^{(q)}$, $l = 1,2,\cdots,K$, are local S-variate, mth-order augmented PDD approximations of c_0, y_0, c_l, y_l, and $\Omega_{F,l}$, respectively, at iteration q, where $\tilde{\Omega}_{F,l,S,m}^{(q)}$ is defined using local augmented PDD approximations of $\tilde{y}_{l,S,m}^{(q)}$ of y_l; and $d_{k,0}^{(q)} - \beta_k^{(q)}(d_{k,U} - d_{k,L})/2$, $d_{k,0}^{(q)} + \beta_k^{(q)}(d_{k,U} - d_{k,L})/2$,

$s_{p,0}^{(q)} - \beta_{s,p}^{(q)}(s_{p,U} - s_{p,L})/2$, and $s_{p,0}^{(q)} + \beta_{s,p}^{(q)}(s_{p,U} - s_{p,L})/2$, also known as the move limits, are the lower and upper bounds, respectively, of the associated coordinate of subregion $\mathcal{D}^{(q)}$. Hence, the original objective and constraint functions are replaced with those derived locally from respective augmented PDD approximations. Since the augmented PDD approximations are mean-square convergent [97, 99], they also converge in probability and in distribution. Therefore, given a subregion $\mathcal{D}^{(q)}$, the solution of the associated RDO and RBDO subproblems also converges when $S \rightarrow N + M$, $m \rightarrow \infty$, and $m' \rightarrow \infty$.

6.5.2   Single-Step Procedure

The single-step procedure is motivated on solving each RDO or RBDO subproblem in Equation (6.78) or (6.79) from a single stochastic analysis by sidestepping the need to recalculate the PDD expansion coefficients at every design iteration. It subsumes two important assumptions: (1) an S-variate, mth-order augmented PDD approximation $\tilde{y}_{S,m}$ of y at the initial design is acceptable for all possible designs in the subregion; and (2) the expansion coefficients for one design, derived from those generated for another design, are accurate.

Consider a change of the probability measure of $(\mathbf{X}, \mathbf{D}, \mathbf{S})$ from $f_{\mathbf{X}}(\mathbf{x}; \mathbf{d})f_{\mathbf{D}}(\mathbf{d}; \boldsymbol{\mu}_{\mathbf{D}})f_{\mathbf{S}}(\mathbf{s}; \boldsymbol{\mu}_{\mathbf{S}})d\mathbf{x}d\mathbf{d}d\mathbf{s}$ to $f_{\mathbf{X}}(\mathbf{x}; \mathbf{d}')f_{\mathbf{D}}(\mathbf{d}; \boldsymbol{\mu}_{\mathbf{D}}')f_{\mathbf{S}}(\mathbf{s}; \boldsymbol{\mu}_{\mathbf{S}}')d\mathbf{x}d\mathbf{d}d\mathbf{s}$, where $(\mathbf{d}, \mathbf{s})$ and $(\mathbf{d}', \mathbf{s}')$ are two arbitrary design vectors corresponding to old and new designs, respectively, and $\boldsymbol{\mu}_{\mathbf{D}}'$ and $\boldsymbol{\mu}_{\mathbf{S}}'$ are new mean vectors for the corresponding affiliated random vectors. Let $\{\psi_{i_q j_q}(X_{i_q}; \mathbf{d}');\ j_q = 0, 1, \cdots\}$, $\{\phi_{k_r l_r}(D_{k_r}; \boldsymbol{\mu}_{\mathbf{D}}');\ l_r = 0, 1, \cdots\}$, and

$\{\varphi_{p_t n_t}(S_{p_t}; \boldsymbol{\mu}_{\mathbf{S}}^{'}); \ n_t = 0, 1, \cdots\}$ be three sets of new orthonormal polynomial basis functions consistent with the marginal probability measures $f_{X_{i_q}}(x_{i_q}; \mathbf{d}')dx_{i_q}$ of X_i, $f_{D_{k_r}}(d_{k_r}; \boldsymbol{\mu}_{\mathbf{D}}^{'})dd_{k_r}$ of D_{k_r}, and $f_{S_{p_t}}(s_{p_t}; \boldsymbol{\mu}_{\mathbf{S}}^{'})ds_{p_t}$ of S_{p_t}, respectively, producing new product polynomials

$$\psi_{u\mathbf{j}_{|u|}}(\mathbf{X}_u; \mathbf{d}')\phi_{v\mathbf{l}_{|v|}}(\mathbf{d}_v; \boldsymbol{\mu}_{\mathbf{D}}^{'})\varphi_{w\mathbf{n}_{|w|}}(\mathbf{s}_w; \boldsymbol{\mu}_{\mathbf{S}}^{'}) = \prod_{q=1}^{|u|}\psi_{i_q j_q}(X_{i_q}; \mathbf{d}')\prod_{r=1}^{|v|}\phi_{k_r l_r}(d_{k_r}; \boldsymbol{\mu}_{\mathbf{D}}^{'})$$
$$\times \prod_{t=1}^{|w|}\varphi_{p_t n_t}(s_{p_t}; \boldsymbol{\mu}_{\mathbf{S}}^{'}), \qquad (6.80)$$

where $\emptyset \neq u \subseteq \{1, \cdots, N\}$, $\emptyset \neq v \subseteq \{1, \cdots, M_d\}$ and $\emptyset \neq w \subseteq \{1, \cdots, M_s\}$. Assume that the expansion coefficients, $y_\emptyset(\mathbf{d}, \boldsymbol{\mu}_{\mathbf{D}}, \boldsymbol{\mu}_{\mathbf{S}})$ and $C_{u\mathbf{j}_{|u|}}(\mathbf{d}, \boldsymbol{\mu}_{\mathbf{D}}, \boldsymbol{\mu}_{\mathbf{S}})$, for the old design have been calculated already. Then, the expansion coefficients for the new design are determined from

$$y_\emptyset(\mathbf{d}^{'}, \boldsymbol{\mu}_{\mathbf{D}}^{'}, \boldsymbol{\mu}_{\mathbf{S}}^{'}) = \int_{\mathbb{R}^N}\left[\sum_{\substack{u\subseteq\{1,\cdots,N\},v\subseteq\{1,\cdots,M_d\}\\ w\subseteq\{1,\cdots,M_s\},|u|+|v|+|w|\geq 1}}\sum_{\substack{\mathbf{j}_{|u|}\in\mathbb{N}_0^{|u|},\mathbf{l}_{|v|}\in\mathbb{N}_0^{|v|},\mathbf{n}_{|w|}\in\mathbb{N}_0^{|w|}\\ j_1,\cdots,j_{|u|},l_1,\cdots,l_{|v|},n_1,\cdots,n_{|w|}\neq 0}}C_{uvw\mathbf{j}_{|u|}\mathbf{l}_{|v|}\mathbf{n}_{|w|}}(\mathbf{d}, \boldsymbol{\mu}_{\mathbf{D}}, \boldsymbol{\mu}_{\mathbf{S}})\right.$$
$$\times \psi_{u\mathbf{j}_{|u|}}(\mathbf{x}_u; \mathbf{d})\phi_{v\mathbf{l}_{|v|}}(\mathbf{d}_v; \boldsymbol{\mu}_{\mathbf{D}})\varphi_{w\mathbf{n}_{|w|}}(\mathbf{s}_w; \boldsymbol{\mu}_{\mathbf{S}}) + \left. y_\emptyset(\mathbf{d}, \boldsymbol{\mu}_{\mathbf{D}}, \boldsymbol{\mu}_{\mathbf{S}})\right]$$
$$\times f_{\mathbf{X}}(\mathbf{x}; \mathbf{d}^{'})f_{\mathbf{D}}(\mathbf{d}; \boldsymbol{\mu}_{\mathbf{D}}^{'})f_{\mathbf{S}}(\mathbf{s}; \boldsymbol{\mu}_{\mathbf{S}}^{'})d\mathbf{x}d\mathbf{d}d\mathbf{s} \qquad (6.81)$$

and

$$
\begin{aligned}
C_{uvw\mathbf{j}_{|u|}\mathbf{l}_{|v|}\mathbf{n}_{|w|}}(\mathbf{d}',\boldsymbol{\mu}_{\mathbf{D}}',\boldsymbol{\mu}_{\mathbf{S}}') &= \int_{\mathbb{R}^N}\Bigg[\sum_{\substack{u\subseteq\{1,\cdots,N\},v\subseteq\{1,\cdots,M_d\}\\ w\subseteq\{1,\cdots,M_s\},|u|+|v|+|w|\geq1}}\sum_{\substack{\mathbf{j}_{|u|}\in\mathbb{N}_0^{|u|},\mathbf{l}_{|v|}\in\mathbb{N}_0^{|v|},\mathbf{n}_{|w|}\in\mathbb{N}_0^{|w|}\\ j_1,\cdots,j_{|u|},l_1,\cdots,l_{|v|},n_1,\cdots,n_{|w|}\neq0}} \\
&\quad C_{uvw\mathbf{j}_{|u|}\mathbf{l}_{|v|}\mathbf{n}_{|w|}}(\mathbf{d},\boldsymbol{\mu}_{\mathbf{D}},\boldsymbol{\mu}_{\mathbf{S}})\psi_{u\mathbf{j}_{|u|}}(\mathbf{x}_u;\mathbf{d})\phi_{v\mathbf{l}_{|v|}}(\mathbf{d}_v;\boldsymbol{\mu}_{\mathbf{D}})\varphi_{w\mathbf{n}_{|w|}}(\mathbf{s}_w;\boldsymbol{\mu}_{\mathbf{S}}) \\
&\quad + y_\emptyset(\mathbf{d},\boldsymbol{\mu}_{\mathbf{D}},\boldsymbol{\mu}_{\mathbf{S}})\Bigg]\psi_{u\mathbf{j}_{|u|}}(\mathbf{x}_u;\mathbf{d}')\phi_{v\mathbf{n}_{|v|}}(\mathbf{d}_v;\boldsymbol{\mu}_{\mathbf{D}}')\varphi_{w\mathbf{n}_{|w|}}(\mathbf{s}_w;\boldsymbol{\mu}_{\mathbf{S}}') \\
&\quad \times f_{\mathbf{X}}(\mathbf{x};\mathbf{d}')f_{\mathbf{D}}(\mathbf{d};\boldsymbol{\mu}_{\mathbf{D}}')f_{\mathbf{S}}(\mathbf{s};\boldsymbol{\mu}_{\mathbf{S}}')d\mathbf{x}d\mathbf{d}d\mathbf{s} \qquad (6.82)
\end{aligned}
$$

by recycling the old expansion coefficients and using orthonormal polynomials associated with both designs. The relationship between the old and new coefficients, described by Equations (6.81) and (6.82), is exact and is obtained by replacing y in Equations (6.11) and (6.12) with the right side of Equation (6.10). However, in practice, when the S-variate, m-th order augmented PDD approximation (Equation (6.14)) is used to replace y in Equations (6.11) and (6.12), then the new expansion coefficients,

$$
\begin{aligned}
y_\emptyset(\mathbf{d}',\boldsymbol{\mu}_{\mathbf{D}}',\boldsymbol{\mu}_{\mathbf{S}}') &= \int_{\mathbb{R}^N}\Bigg[\sum_{\substack{u\subseteq\{1,\cdots,N\},v\subseteq\{1,\cdots,M_d\}\\ w\subseteq\{1,\cdots,M_s\},1\leq|u|+|v|+|w|\leq S}}\sum_{\substack{\mathbf{j}_{|u|}\in\mathbb{N}_0^{|u|},\mathbf{l}_{|v|}\in\mathbb{N}_0^{|v|},\mathbf{n}_{|w|}\in\mathbb{N}_0^{|w|}\\ \left\|\mathbf{j}_{|u|}\right\|_\infty,\left\|\mathbf{l}_{|v|}\right\|_\infty,\left\|\mathbf{n}_{|w|}\right\|_\infty\leq m\\ j_1,\cdots,j_{|u|},l_1,\cdots,l_{|v|},n_1,\cdots,n_{|w|}\neq0}} \\
&\quad C_{uvw\mathbf{j}_{|u|}\mathbf{l}_{|v|}\mathbf{n}_{|w|}}(\mathbf{d},\boldsymbol{\mu}_{\mathbf{D}},\boldsymbol{\mu}_{\mathbf{S}})\psi_{u\mathbf{j}_{|u|}}(\mathbf{x}_u;\mathbf{d})\phi_{v\mathbf{l}_{|v|}}(\mathbf{d}_v;\boldsymbol{\mu}_{\mathbf{D}})\varphi_{w\mathbf{n}_{|w|}}(\mathbf{s}_w;\boldsymbol{\mu}_{\mathbf{S}}) \\
&\quad + y_\emptyset(\mathbf{d},\boldsymbol{\mu}_{\mathbf{D}},\boldsymbol{\mu}_{\mathbf{S}})\Bigg]f_{\mathbf{X}}(\mathbf{x};\mathbf{d}')f_{\mathbf{D}}(\mathbf{d};\boldsymbol{\mu}_{\mathbf{D}}')f_{\mathbf{S}}(\mathbf{s};\boldsymbol{\mu}_{\mathbf{S}}')d\mathbf{x}d\mathbf{d}d\mathbf{s} \qquad (6.83)
\end{aligned}
$$

and

$$
\begin{aligned}
C_{uvw\mathbf{j}_{|u|}\mathbf{l}_{|v|}\mathbf{n}_{|w|}}(\mathbf{d}', \boldsymbol{\mu}'_{\mathbf{D}}, \boldsymbol{\mu}'_{\mathbf{S}}) &= \int_{\mathbb{R}^N} \Bigg[\sum_{\substack{u\subseteq\{1,\cdots,N\},v\subseteq\{1,\cdots,M_d\} \\ w\subseteq\{1,\cdots,M_s\},1\leq|u|+|v|+|w|\leq S}} \sum_{\substack{\mathbf{j}_{|u|}\in\mathbb{N}_0^{|u|},\mathbf{l}_{|v|}\in\mathbb{N}_0^{|v|},\mathbf{n}_{|w|}\in\mathbb{N}_0^{|w|} \\ \|\mathbf{j}_{|u|}\|_\infty,\|\mathbf{l}_{|v|}\|_\infty,\|\mathbf{n}_{|w|}\|_\infty\leq m \\ j_1,\cdots,j_{|u|},l_1,\cdots,l_{|v|},n_1,\cdots,n_{|w|}\neq 0}} \\
&\quad C_{uvw\mathbf{j}_{|u|}\mathbf{l}_{|v|}\mathbf{n}_{|w|}}(\mathbf{d},\mathbf{s})\psi_{u\mathbf{j}_{|u|}}(\mathbf{x}_u;\mathbf{d})\phi_{v\mathbf{l}_{|v|}}(\mathbf{d}_v;\boldsymbol{\mu}_{\mathbf{D}})\varphi_{w\mathbf{n}_{|w|}}(\mathbf{s}_w;\boldsymbol{\mu}_{\mathbf{S}}) \\
&\quad + y_\emptyset(\mathbf{d},\boldsymbol{\mu}_{\mathbf{D}},\boldsymbol{\mu}_{\mathbf{S}}) \Bigg] \psi_{u\mathbf{j}_{|u|}}(\mathbf{x}_u;\mathbf{d}')\phi_{v\mathbf{l}_{|v|}}(\mathbf{d}_v;\boldsymbol{\mu}'_{\mathbf{D}})\varphi_{w\mathbf{n}_{|w|}}(\mathbf{s}_w;\boldsymbol{\mu}'_{\mathbf{S}}) \\
&\quad \times f_{\mathbf{X}}(\mathbf{x};\mathbf{d}')f_{\mathbf{D}}(\mathbf{d};\boldsymbol{\mu}'_{\mathbf{D}})f_{\mathbf{S}}(\mathbf{s};\boldsymbol{\mu}'_{\mathbf{S}})d\mathbf{x}d\mathbf{d}d\mathbf{s},
\end{aligned} \tag{6.84}
$$

which are applicable for $u \subseteq \{1,\cdots,N\}$, $v \subseteq \{1,\cdots,M_d\}$, $w \subseteq \{1,\cdots,M_s\}$, and $1 \leq |u|+|v|+|w| \leq S$, become approximate, although convergent. Simply replacing $\boldsymbol{\mu}'_{\mathbf{D}}$ and $\boldsymbol{\mu}'_{\mathbf{S}}$ with $\mathbf{d}'$ and $\mathbf{s}'$, respectively, in Equations (6.83) and (6.84) leads to the PDD coefficients for the new design. Furthermore, the integrals in Equations (6.83) and (6.84) consist of finite-order polynomial functions of at most S variables and can be evaluated inexpensively without having to compute the original function y for the new design. Therefore, new stochastic analyses, all employing S-variate, mth-order augmented PDD approximation of y, are conducted with little additional cost during all design iterations, drastically curbing the computational effort of solving an RDO/RBDO subproblem.

6.5.3 Proposed Multipoint Single-Step Design Process

When the multipoint approximation is combined with the single-step procedure, the result is an accurate and efficient design process to solve the RDO and

RBDO problems defined by Equations (6.1) and (6.2). Using the single-step procedure, the design solution of an individual RDO/RBDO subproblem becomes the initial design for the next RDO/RBDO subproblem. Then, the move limits are updated, and the optimization is repeated iteratively until an optimal solution is attained. The method is schematically depicted in Figure 6.1. Given an initial design $(\mathbf{d}_0, \mathbf{s}_0)$, a sequence of design solutions, obtained successively for each subregion $\mathcal{D}^{(q)}$ and using the S-variate, mth-order augmented PDD approximation, leads to an approximate optimal solution $(\tilde{\mathbf{d}}^*, \tilde{\mathbf{s}}^*)$ of the RDO/RBDO problem. In contrast, an augmented PDD approximation constructed for the entire design space $\mathcal{D}$, if it commits large approximation errors, may possibly lead to a premature or erroneous design solution. The multipoint approximation in the proposed methods overcomes this quandary by adopting smaller subregions and local augmented PDD approximations, whereas the single-step procedure diminishes the computational requirement as much as possible by recycling the PDD expansion coefficients.

When $S \to N + M$, $m \to \infty$, $m' \to \infty$, and $q \to \infty$, the moments, reliability, and their design sensitivities by the augmented PDD approximations converge to their exactness, yielding coincident solutions of the original RDO/RBDO problems (Equations (6.1) and (6.2)) and RDO/RBDO subproblems (Equations (6.78) and (6.79)). However, if the subregions are sufficiently small, then for finite and possibly low values of S and m, Equation (6.78) or (6.79) is expected to generate an accurate solution of Equation (6.1) or (6.2), the principal motivation for developing the augmented PDD methods.
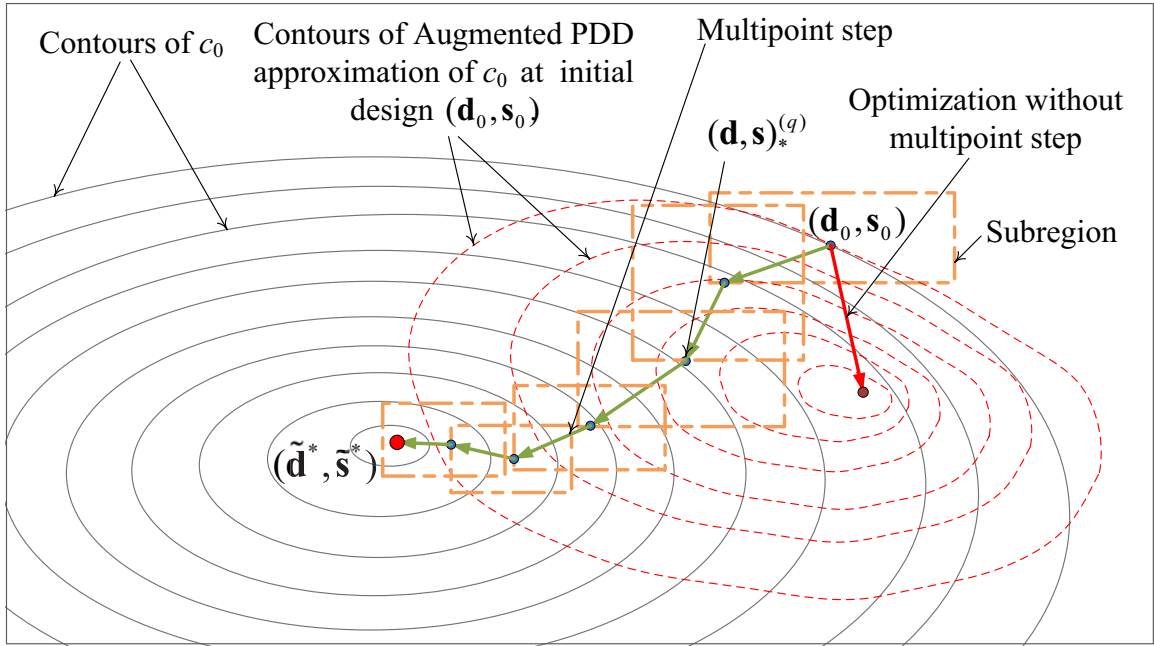
Figure 6.1: A schematic description of the multi-point, single-step design process

The augmented PDD methods in conjunction with the combined multi-point, single-step design process is outlined by the following steps. The flow chart of this method is shown in Figure 6.2.

Step 1: Select an initial design vector $(\mathbf{d}_0, \mathbf{s}_0)$. Define tolerances $\epsilon_1 > 0$, $\epsilon_2 > 0$, and $\epsilon_3 > 0$. Set the iteration $q = 1$, $(\mathbf{d}, \mathbf{s})_0^{(q)} = (\mathbf{d}_0, \mathbf{s}_0)$. Define the subregion size parameters $0 < \beta_{d,k}^{(q)} \le 1$, $k = 1, \cdots, M_d$, and $0 < \beta_{s,p}^{(q)} \le 1$, $p = 1, \cdots, M_s$, describing the qth subregion defined in Equation (6.77). Denote the subregion's increasing history by a set $H^{(0)}$ and set it to empty. Set two designs $(\mathbf{d}, \mathbf{s})_f = (\mathbf{d}_0, \mathbf{s}_0)$ and $(\mathbf{d}_0, \mathbf{s}_0)_{f,last} \ne (\mathbf{d}_0, \mathbf{s}_0)$ such that $||(\mathbf{d}_0, \mathbf{s}_0)_f - (\mathbf{d}_0, \mathbf{s}_0)_{f,last}||_2 > \epsilon_1$. Set $(\mathbf{d}, \mathbf{s})_*^{(0)} = (\mathbf{d}_0, \mathbf{s}_0)$, $q_{f,last} = 1$, and $q_f = 1$. Usually, a feasible design should be selected to be the initial design $(\mathbf{d}_0, \mathbf{s}_0)$. However,

when an infeasible initial design is chosen, a new feasible design can be obtained during the iteration if the initial subregion size parameters are large enough.

Step 2: Select ($q = 1$) or use ($q > 1$) the PDD truncation parameters S and m. At $(\mathbf{d}, \mathbf{s}) = (\mathbf{d}, \mathbf{s})_0^{(q)}$, generate the augmented PDD expansion coefficients, $y_\emptyset(\mathbf{d}, \boldsymbol{\mu}_\mathbf{D}, \boldsymbol{\mu}_\mathbf{S})$ and $C_{uvw\mathbf{j}_{|u|}\mathbf{l}_{|v|}\mathbf{n}_{|w|}}(\mathbf{d}, \boldsymbol{\mu}_\mathbf{D}, \boldsymbol{\mu}_\mathbf{S})$, where $\emptyset \neq u \subseteq \{1, \cdots, N\}$, $\emptyset \neq v \subseteq \{1, \cdots, M_d\}$, $\emptyset \neq w \subseteq \{1, \cdots, M_s\}$, $1 \leq |u| + |v| + |w| \leq S$, $\left\|\mathbf{j}_{|u|}\right\|_\infty, \left\|\mathbf{l}_{|v|}\right\|_\infty, \left\|\mathbf{n}_{|w|}\right\|_\infty \leq m$, using dimension-reduction integration with $R = S$, $n = m + 1$, leading to S-variate, mth-order augmented PDD approximations $\tilde{y}_{l,S,m}^{(q)}(\mathbf{X}; \mathbf{d}, \mathbf{s})$ of $y_l(\mathbf{X}; \mathbf{d}, \mathbf{s})$ and $\tilde{c}_{l,S,m}^{(q)}(\mathbf{d}, \mathbf{s})$ of $c_l(\mathbf{d}, \mathbf{s})$, $l = 0, 1, \cdots, K$, in Equation (6.78) or (6.79). For RDO, calculate the expansion coefficients of score functions, $s_{k,\emptyset}(\mathbf{d})$ and $D_{i_k,j}(\mathbf{d})$, where $k = 1, \cdots, M$ and $j = 1, \cdots, m'$, analytically, if possible, or numerically, resulting in m'th-order Fourier-polynomial approximations of $s_k(X_{i_k}; \mathbf{d})$, $k = 1, \cdots, M$.

Step 3: If $q = 1$ and $\tilde{c}_{l,S,m}^{(q)}((\mathbf{d}, \mathbf{s})_0^{(q)}) < 0$ for $l = 1, \cdots, K$, then go to Step 4. If $q > 1$ and $\tilde{c}_{l,S,m}^{(q)}((\mathbf{d}, \mathbf{s})_0^{(q)}) < 0$ for $l = 1, \cdots, K$, then set $(\mathbf{d}, \mathbf{s})_{f,last} = (\mathbf{d}, \mathbf{s})_f$, $(\mathbf{d}, \mathbf{s})_f = (\mathbf{d}, \mathbf{s})_0^{(q)}$, $q_{f,last} = q_f$, $q_f = q$ and go to Step 4. Otherwise, go to Step 5.

Step 4: If $||(\mathbf{d}, \mathbf{s})_f - (\mathbf{d}, \mathbf{s})_{f,last}||_2 < \epsilon_1$ or $\left| \left[\tilde{c}_{0,S,m}^{(q)}((\mathbf{d}, \mathbf{s})_f) - \tilde{c}_{0,S,m}^{(q_{f,last})}((\mathbf{d}, \mathbf{s})_{f,last}) \right] / \tilde{c}_{0,S,m}^{(q)} ((\mathbf{d}, \mathbf{s})_f)\right| < \epsilon_3$, then stop and denote the final optimal solution as $(\tilde{\mathbf{d}}^*, \tilde{\mathbf{s}}^*) = (\mathbf{d}, \mathbf{s})_f$. Otherwise, go to Step 6.

Step 5: Compare the infeasible design $(\mathbf{d}, \mathbf{s})_0^{(q)}$ with the feasible design $(\mathbf{d}, \mathbf{s})_f$ and

interpolate between $(\mathbf{d}, \mathbf{s})_0^{(q)}$ and $(\mathbf{d}, \mathbf{s})_f$ to obtain a new feasible design and set it as $(\mathbf{d}, \mathbf{s})_0^{(q+1)}$. For dimensions with large differences between $(\mathbf{d}, \mathbf{s})_0^{(q)}$ and $(\mathbf{d}, \mathbf{s})_f$, interpolate aggressively. Reduce the size of the subregion $\mathcal{D}^{(q)}$ to obtain new subregion $\mathcal{D}^{(q+1)}$. For dimensions with large differences between $(\mathbf{d}, \mathbf{s})_0^{(q)}$ and $(\mathbf{d}, \mathbf{s})_f$, reduce aggressively. Also, for dimensions with large differences between the sensitivities of $\tilde{c}_{l,Sm}^{(q)}((\mathbf{d}, \mathbf{s})_0^{(q)})$ and $\tilde{c}_{l,Sm}^{(q-1)}((\mathbf{d}, \mathbf{s})_0^{(q)})$, reduce aggressively. Update $q = q + 1$ and go to Step 2.

Step 6: If the subregion size is small, that is, $\beta_{d,k}^{(q)}(d_{k,U} - d_{k,L}) < \epsilon_2$, or $\beta_{s,p}^{(q)}(s_{p,U} - s_{p,L}) < \epsilon_2$, and $(\mathbf{d}, \mathbf{s})_*^{(q-1)}$ is located on the boundary of the subregion, then go to Step 7. Otherwise, go to Step 9.

Step 7: If the subregion centered at $(\mathbf{d}, \mathbf{s})_0^{(q)}$ has been enlarged before, that is, $(\mathbf{d}, \mathbf{s})_0^{(q)} \in H^{(q-1)}$, then set $H^{(q)} = H^{(q-1)}$ and go to Step 9. Otherwise, set $H^{(q)} = H^{(q-1)} \bigcup \{(\mathbf{d}, \mathbf{s})_0^{(q)}\}$ and go to Step 8.

Step 8: For coordinates of $(\mathbf{d}, \mathbf{s})_0^{(q)}$ located on the boundary of the subregionand $\beta_{d,k}^{(q)}(d_{k,U} - d_{k,L}) < \epsilon_2$, or $\beta_{s,p}^{(q)}(s_{p,U} - s_{p,L}) < \epsilon_2$, increase the sizes of corresponding components of $\mathcal{D}^{(q)}$; for other coordinates, keep them as they are. Set the new subregion as $\mathcal{D}^{(q+1)}$.

Step 9: Solve the design problem in Equation (6.78) or (6.79) employing the single-step PDD procedure. In so doing, recycle the PDD expansion coefficients obtained from Step 2 in Equations (6.83) and (6.84), producing approximations of the objective and constraint functions that stem from single calculation of these coefficients. To evaluate the gradients, recalculate the

Fourier expansion coefficients of score functions as needed. Denote the op-
timal solution by $(\mathbf{d}, \mathbf{s})_*^{(q)}$ and set $(\mathbf{d}, \mathbf{s})_0^{(q+1)} = (\mathbf{d}, \mathbf{s})_*^{(q)}$. Update $q = q + 1$
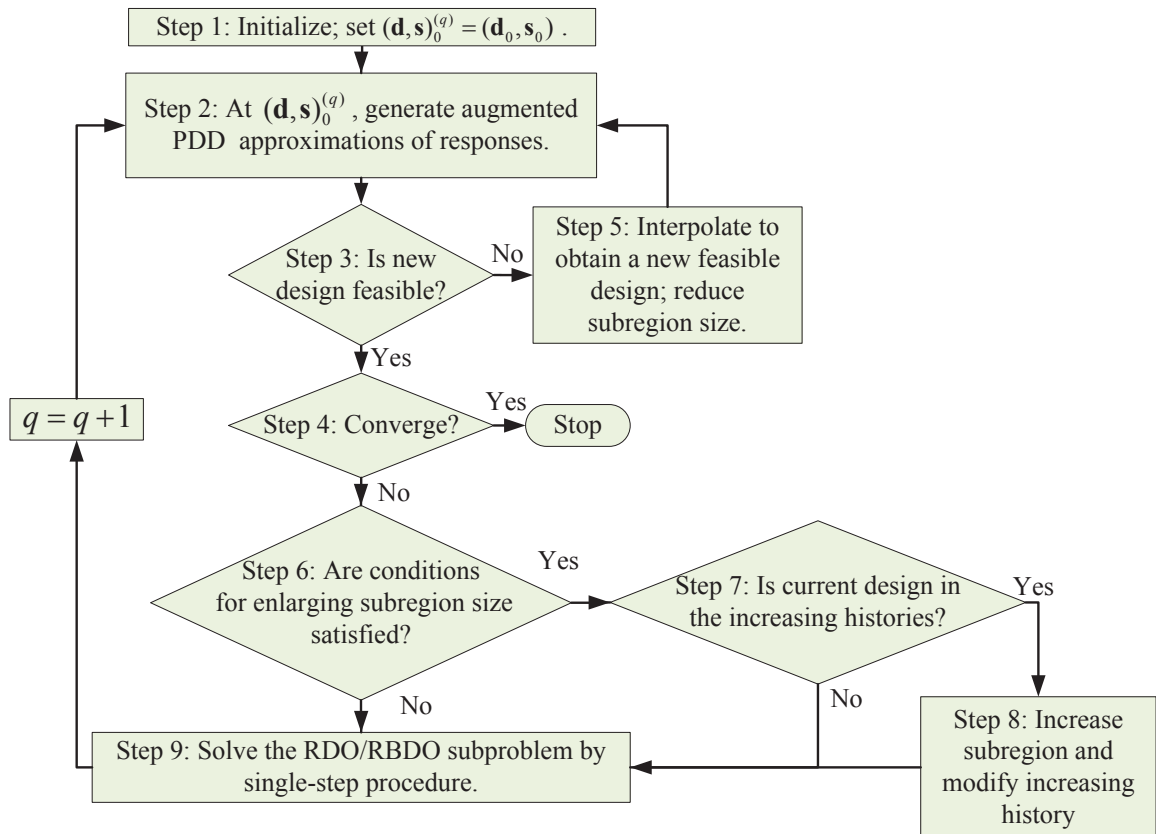and go to Step 2.

Figure 6.2: A flow chart of the proposed multi-point, single-step design process

6.6 Numerical Examples

Four examples are presented to illustrate the proposed methods developed in
estimating design sensitivities and solving various RDO/RBDO problems involving
mixed design variables. The objective and constraint functions are either elementary

mathematical functions or relate to engineering problems, ranging from simple structures to complex FEA-aided mechanical designs. Both size and shape design problems are included. The PDD expansion coefficients were estimated by dimension-reduction integration with the mean input as the reference point, $R = S$, and the number of integration points $n = m + 1$, where S and m vary depending on the problem. Since the distributional design variables describe both means and standard deviations of Gaussian random variables, the order m' used for Fourier expansion coefficients of score functions in Example 1 is two. However, in Example 4, where the distributional design variables are the means of truncated Gaussian random variables, m' is one. In Examples 1 through 4, orthonormal polynomials, consistent with the probability distributions of input random variables, were used as bases. For the Gaussian distribution, the Hermite polynomials were used. For random variables following non-Gaussian probability distributions, such as the Lognormal distribution in Example 3 and truncated Gaussian distribution in Example 4, the orthonormal polynomials were obtained either analytically when possible or numerically, exploiting the Stieltjes procedure [98]. The sample size for the embedded MCS is 10^6 in all examples. The multi-point, single-step design procedure was used in Examples 3 and 4 for solving RDO and RBDO problems. The tolerances, initial subregion size, and threshold parameters for the multi-point, single-step procedure are as follows: (1) $\epsilon_1 = 0.01$, $\epsilon_2 = 2$, $\epsilon_3 = 0.005$ (Example 3); $\epsilon_1 = 0.01$, $\epsilon_2 = 2$, $\epsilon_3 = 0.05$ (Example 4); (2) $\beta_{d,1}^{(1)} = \cdots = \beta_{d,M_d}^{(1)} = \beta_{s,1}^{(1)} = \cdots = \beta_{s,M_s}^{(1)} = 0.5$. The optimization algorithm selected is sequential quadratic programming [106] in Examples 3 and 4.

6.6.1 Example 1: Sensitivities of Moments

The first example involves calculating sensitivities of the first two moments of a polynomial function

$$
\begin{aligned}
y(\mathbf{X}; \mathbf{d}, \boldsymbol{s}) \;=\; & 13.2(X_1 + X_2 + \mu + \sigma + s_1 + s_2) + 0.18(X_1 + X_2)^3 \\
& + 0.31 X_1^2 X_2 s_1 + 0.25 X_2^2 s_1 \mu + 0.11 X_1 s_2 \sigma + 0.4 s_1^2 s_2 \mu^2, \quad (6.85)
\end{aligned}
$$

where X_1 and X_2 are two independent and identically distributed Gaussian random variables, each with the same mean μ and standard deviation σ. The distributional and structural design vectors are $\mathbf{d} = (\mu, \sigma)^T$ and $\mathbf{s} = (s_1, s_2)^T$, respectively. The affiliated random vector $\mathbf{D} = (D_1, D_2)^T$ is selected to be Gaussian, where the components D_1, D_2 are independent with the same standard deviation of 1 but different mean values $\mathbb{E}_1[D_1] = d_1 = \mu$ and $\mathbb{E}_1[D_2] = d_2 = \sigma$. The affiliated random vector $\mathbf{S} = (S_1, S_2)^T$ is also normally distributed with the independent components S_1, S_2, which have the same standard deviation of 1 but different mean values $\mathbb{E}_2[S_1] = s_1$ and $\mathbb{E}_2[S_2] = s_2$.

Table 6.1 presents the approximate sensitivities of the first two moments $\mathbb{E}_{\mathbf{d}}[y(\mathbf{X}; \mathbf{d}, \boldsymbol{s})]$ and $\mathbb{E}_{\mathbf{d}}[y^2(\mathbf{X}; \mathbf{d}, \boldsymbol{s})]$ at $\mathbf{d} = \mathbf{d}_0 = (0.4, 1)^T$ and $\mathbf{s} = \mathbf{s}_0 = (0.55, 0.48)^T$, obtained by the proposed augmented PDD methods (Equations (6.47),(6.48),(6.63), and (6.64)). Three sets of estimates stemming from univariate ($S = 1$), bivariate ($S = 2$), and trivariate ($S = 3$) third-order PDD approximations of y are included. The exact solution, which exists for this problem, is also included in Table 6.1. The univariate PDD, listed in the second column, provides satisfactory estimates for all sensitivities, requiring only 26 function evaluations. Although the bivariate approx-

imation is more expensive than the univariate approximation, the former generates highly accurate solutions, as expected. The function y, being both trivariate and a cubic polynomial, is exactly reproduced by the trivariate ($S = 3$), third-order ($m = 3$) augmented PDD approximation when orthonormal polynomials consistent with Gaussian probability measures are used. Therefore, the trivariate, third-order augmented PDD approximation, along with the proposed sensitivity analysis method, reproduces the exact solution. Although the third-order, bivariate augmented PDD approximation is unable to reproduce the original function exactly, it provides highly accurate sensitivity results for most cases, which are the same as the exact or trivariate results providing four significant digits, except for the sensitivity with respect to s_1, which has about one percent error. Comparing the computational efforts, 1546 function evaluations were required by trivariate PDD to produce the exact results, whereas 26 and 266 function evaluations were incurred by the univariate and bivariate approximations, respectively. Therefore, the univariate augmented PDD method furnishes very accurate and highly efficient estimates of the first two moment sensitivities.

Table 6.1: Sensitivities of the first two moments at $\mathbf{d}_0 = (0.4, 1)^T$ and $\mathbf{s}_0 = (0.55, 0.48)^T$

	Augmented PDD			Exact
	Univariate $(m = 3)$	Bivariate $(m = 3)$	Trivariate $(m = 3)$	
$\partial m^{(1)}(\mathbf{d}_0, \boldsymbol{s}_0) / \partial \mu$	41.6183	43.0063	43.0063	43.0063
$\partial m^{(1)}(\mathbf{d}_0, \boldsymbol{s}_0) / \partial \sigma$	15.1955	15.1955	15.1955	15.1955
$\partial m^{(1)}(\mathbf{d}_0, \boldsymbol{s}_0) / \partial s_1$	13.2696	13.4936	13.4936	13.4936
$\partial m^{(1)}(\mathbf{d}_0, \boldsymbol{s}_0) / \partial s_2$	13.2634	13.2634	13.2634	13.2634
$\partial m^{(2)}(\mathbf{d}_0, \boldsymbol{s}_0) / \partial \mu$	3700.9977	3895.1957	3895.1957	3895.1957
$\partial m^{(2)}(\mathbf{d}_0, \boldsymbol{s}_0) / \partial \sigma$	2201.2607	2365.6375	2365.6375	2365.6375
$\partial m^{(2)}(\mathbf{d}_0, \boldsymbol{s}_0) / \partial s_1$	1161.5037	1188.3302	1198.9252	1198.9252
$\partial m^{(2)}(\mathbf{d}_0, \boldsymbol{s}_0) / \partial s_2$	1160.9547	1164.1960	1164.1960	1164.1960
No. of Func. Eval.	26	266	1546	−

6.6.2 Example 2: Sensitivities of Failure Probability

For the second example, consider two performance functions

$$y_1(\mathbf{X}; s) = -s + 1 + \frac{X_1^2 X_2^2}{5s^2} \qquad (6.86)$$

and

$$y_2(\mathbf{X}; s) = -1 + \frac{5s^4}{X_1^2 + 8X_2 + 5}, \qquad (6.87)$$

where the random vector $\mathbf{X}$ comprises two independent Gaussian random variables, X_1 and X_2, with the same standard deviation of 0.3 but different mean values

$\mathbb{E}_{\mathbf{d}}[X_1] = 7.5$ and $\mathbb{E}_{\mathbf{d}}[X_2] = 1$. The structural design variable is s. The corresponding affiliated random variable S is selected to be Gaussian with mean $\mathbb{E}_2[S] = s$ and standard deviation σ_s. The objective of this example is to evaluate the accuracy of the proposed augmented PDD methods (Equation (6.75)) in calculating sensitivities of the failure probabilities $P_{F,1}(s) := P[y_1(\mathbf{X}; s) < 0]$ and $P_{F,2}(s) := P[y_2(\mathbf{X}; s) < 0]$. The perturbation size for finite-difference approximation is taken as $\Delta s = 0.001$.

Table 6.2: Sensitivities of probability of failure at $s_0 = 2$

			$\dfrac{\partial P_{F,1}(s_0)}{\partial s}$	$\dfrac{\partial P_{F,2}(s_0)}{\partial s}$	No. of Func. Eval. of y_1 and y_2
Augmented PDD ($m = 3$)	$\sigma_s = 1$	Univariate	0.1850	-3.8760	26
		Bivariate	9.0×10^{-3}	-8.3340	122
		Trivariate	0.0	-9.0910	250
	$\sigma_s = 0.3$	Univariate	0.6220	-2.5560	26
		Bivariate	0.3410	-1.5780	122
		Trivariate	0.3370	-1.5560	250
	$\sigma_s = 0.0005$	Univariate	0.5920	-1.8720	26
		Bivariate	0.3160	-1.4700	122
		Trivariate	0.3190	-1.4760	250
Exact			0.3228	-1.4100	–

Table 6.2 exhibits the sensitivities of the failure probabilities $P_{F,1}(s)$ and

$P_{F,2}(s)$ with respect to the structural design variable s calculated at $s = s_0 = 2$. It contains the estimates of the sensitivities by the univariate ($S = 1$), bivariate ($S = 2$), and trivariate ($S = 3$) third-order augmented PDD approximations of y_1 and y_2. Combined with the different values of σ_s, which are $\sigma_s = 1$, $\sigma_s = 0.3$, and $\sigma_s = 0.0005$, a total of nine cases were examined to study the convergence with respect to σ_s and the truncation S. The exact solution, also existing for this particular problem, is also listed in the last row to verify the approximate solutions. For $\sigma_s = 1.0$, all results of univariate, bivariate, and trivariate augmented PDD approximation deviate from the exact solution. However, when the value of σ_s decreases, the error is reduced significantly, especially for the bivariate and trivariate cases. When $\sigma_s = 0.0005$, reasonably accurate results are obtained by the bivariate and trivariate augmented PDD approximations, incurring 122 and 255 function evaluations, respectively. In addition, the univariate augmented PDD for $\sigma_s = 0.0005$ provides improved estimates of sensitivities of failure probabilities with only 26 function evaluations. It is important to note that the orders of σ_s and Δs have to be similar to achieve satisfactory estimates of sensitivities, as found, at least, in this particular example.

6.6.3 Example 3: Size and Configuration Design of a Six-bay, Twenty-one-bar Truss

The third example demonstrates how RBDO problems with constraints limiting the system reliability can be efficiently solved by the proposed method. A linear-elastic, six-bay, twenty-one-bar truss structure, with geometric properties shown in

Figure 6.3, is simply supported at nodes 1 and 12 and is subjected to a concentrated load of 56,000 lb (249,100 N) at node 7. The truss material is made of an aluminum alloy with the Young's modulus $E = 10^7$ psi (68.94 GPa). Considering the symmetry of the structure, the random input is selected as $\mathbf{X} = (X_1, \cdots, X_{11})^T \in \mathbb{R}^{11}$, where $X_i, \ i = 1, \cdots, 11$, represents the cross-sectional area of the ith truss member. The random variables are independent and lognormally distributed with means μ_i in^2 and standard deviations $\sigma_i = 0.1$ in^2, $i = 1, \cdots, 11$. As depicted in Figure 6.3, the structural design vector $\mathbf{s} = (s_1, s_2)^T$ describes the node locations, where s_1 represents the horizontal location of nodes 2, 3, 10, and 11, and s_2 represents the horizontal location of nodes 4, 5, 8, and 9. Let $v_{\max}(\mathbf{X}; \mathbf{s})$ and $\sigma_{\max}(\mathbf{X}; \mathbf{s})$ denote the maximum vertical displacement of all nodes and maximum axial stress in all truss members, respectively, determined from linear-elastic FEA. The permissible displacement and stress are limited to $d_{\mathrm{allow}} = 0.266$ in (6.76 mm) and $\sigma_{\mathrm{allow}} = 37,680$ psi (259.8 MPa), respectively. The system-level failure set is defined as $\Omega_F := \{\mathbf{x} : \{y_1(\mathbf{x}; \mathbf{s}) < 0\} \cup \{y_2(\mathbf{x}; \mathbf{s}) < 0\}\}$, where the performance functions

$$y_1(\mathbf{X}; \mathbf{s}) = 1 - \frac{|v_{\max}(\mathbf{X}; \mathbf{s})|}{d_{\mathrm{allow}}}, \ y_2(\mathbf{X}) = 1 - \frac{|\sigma_{\max}(\mathbf{X}; \mathbf{s})|}{\sigma_{\mathrm{allow}}}. \tag{6.88}$$

Due to the symmetry of the structure and loads, the distributional design vector is $\mathbf{d} = (\mu_1, \cdots, \mu_{11})^T \in \mathcal{D} \subset \mathbb{R}^{11}$. The objective is to minimize the volume of the truss structure subject to a system reliability constraint, limiting the maximum vertical displacement and the maximum axial stress. Therefore, the RBDO problem is

formulated to

$$\min_{(\mathbf{d},\mathbf{s})\in\mathcal{D}} \quad c_0(\mathbf{d},\mathbf{s}) = V(\mathbf{d},\mathbf{s}),$$

$$\text{subject to} \quad c_1(\mathbf{d},\mathbf{s}) = P_{\mathbf{d}}\left[\{y_1(\mathbf{X};\mathbf{s}) < 0\} \cup \{y_2(\mathbf{X};\mathbf{s}) < 0\}\right] - \Phi(-3) \leq 0,$$

$$1 \leq d_k \leq 30, \quad k = 1,\cdots,11,$$

$$8 \leq s_1 \leq 12, \quad 18 \leq s_2 \leq 22, \tag{6.89}$$

where $V(\mathbf{d},\mathbf{s})$ is the total volume of the truss. The initial value of the distributional design vector is $\mathbf{d}_0 = (15, 15, 15, 15, 15, 15, 15, 15, 15, 15, 15)^T$ in^2 ($\times 2.54^2$ cm^2), and the initial value of the structural design vector is $\mathbf{s}_0 = (10, 10)^T$ in ($\times 2.54$ cm). The approximate optimal solution is denoted by $(\tilde{\mathbf{d}}^*; \tilde{\mathbf{s}}^*) = (\tilde{d}_1^*, \tilde{d}_2^*, \cdots, \tilde{d}_{11}^*; \tilde{s}_1^*, \tilde{s}_2^*)^T$. The affiliated random vectors $\mathbf{D}$ and $\mathbf{S}$ are selected to be Gaussian, and their components are independent with the same standard deviation of 0.0005 but different mean vectors $\mathbb{E}_1[\mathbf{D}] = \mathbf{d}$ and $\mathbb{E}_2[\mathbf{S}] = \mathbf{s}$. The small perturbation size of d_k and s_p for finite-difference approximation of sensitivities of failure probabilities are taken as $\Delta d_k = 0.001$ and $\Delta s_p = 0.001$, respectively, for $k = 1,\cdots,11$ and $p = 1,2$.
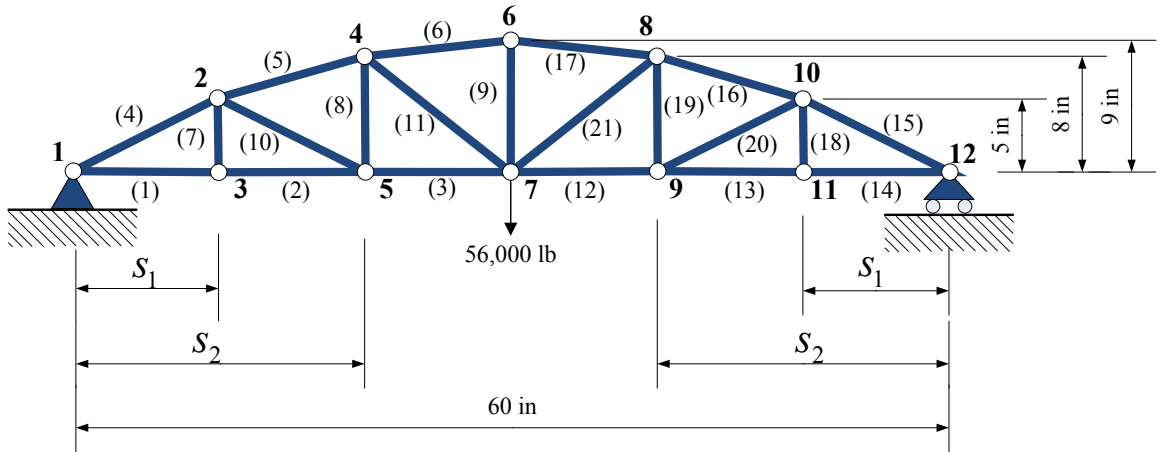
Figure 6.3: A six-bay, twenty-one-bar truss structure (Example 3)

The proposed multi-point, single-step design procedure was applied to solve this problem, employing bivariate, second-order augmented PDD approximations for the underlying stochastic and design sensitivity analysis. The first column of Table 6.3 summarizes the values of design variables, objective function, and constraint function for the optimal design, all generated by the augmented PDD method. The objective function c_0 is reduced from 3044.47 in^3 at initial design to 1049.02 in^3 at optimal design — an almost 66 percent change. At optimum, the constraint function c_1 is -0.21×10^{-3} and is, therefore, close to being active. Most of the design variables have undergone moderate to significant changes from their initial values, prompting substantial modifications of sizes and configurations of the truss structures. For further scrutinizing the optimum, the results by the crude MCS method, adapting the optimum solution by the proposed augmented PDD method as the initial design, are listed in the last column. The negligible difference between the results of the proposed

PDD method and the results of the corresponding crude MCS method demonstrates the accuracy of the proposed method. Comparing the computational efforts, only 7420 FEA were required to produce the results of the proposed method in Table 6.3, whereas 846 million FEA (samples) were incurred by crude MCS. Therefore, the proposed augmented PDD methods provide not only highly accurate, but also vastly efficient, solutions for this mixed RBDO problem.

Table 6.3: Optimization results for the six-bay, twenty-one-bar truss problem

	Augmented PDD $S = 2,\ m = 2$	Crude MCS[b]
$\tilde{d}_1^*$, in^2	7.6858	7.6665
$\tilde{d}_2^*$, in^2	7.7138	7.7005
$\tilde{d}_3^*$, in^2	4.3102	4.3101
$\tilde{d}_4^*$, in^2	4.7163	4.7162
$\tilde{d}_5^*$, in^2	4.9026	4.9025
$\tilde{d}_6^*$, in^2	4.2936	4.2935
$\tilde{d}_7^*$, in^2	6.0545	6.0544
$\tilde{d}_8^*$, in^2	5.0385	5.0384
$\tilde{d}_9^*$, in^2	6.2239	6.2239
$\tilde{d}_{10}^*$, in^2	4.5967	4.5967
$\tilde{d}_{11}^*$, in^2	3.3725	3.3723
$\tilde{s}_1^*$, in	12.0000	12.0000
$\tilde{s}_2^*$, in	19.1703	19.1702
c_0, in^3	1049.02	1048.35
c_1 [a]	-0.2100×10^{-3}	-0.5300×10^{-4}
No. of FEA	7,420	846,000,000

[a] The constraint values are calculated by MCS with 10^6 sample size.
[b] Crude MCS: initial design is set to the optimal solution of augmented PDD, i.e., the optimal solution in the second column.

6.6.4 Example 4: Shape Design of a Three-Hole Bracket

The final example involves shape design optimization of a two-dimensional, three-hole bracket, where five random shape parameters, $X_i,\ i = 1, \cdots, 5$, describe its inner and outer boundaries, while maintaining symmetry about the central verti-

cal axis. The distributional design variables, $d_k = \mathbb{E}_\mathbf{d}[X_k]$, $i = 1, \cdots 5$, are the means of these five independent random variables, with Figure 6.4(a) depicting the initial design of the bracket geometry at the mean values of the shape parameters. The structural design variables, s_p, $p = 1, \cdots 4$, are four deterministic shape parameters shown in Figure 6.4(a), along with the random shape parameters defining the geometry of the three-hole bracket. The bottom two holes are fixed, and a deterministic horizontal force $F = 15,000$ N is applied at the center of the top hole. The bracket material has a deterministic mass density $\rho = 7810$ kg/m^3, deterministic elastic modulus $E = 207.4$ GPa, deterministic Poisson's ratio $\nu = 0.3$, and deterministic uniaxial yield strength $S_y = 800$ MPa. The objective is to minimize the second-moment properties of the mass of the bracket by changing the shape of the geometry such that the maximum von Mises stress $\sigma_{e,\max}(\mathbf{X}; \mathbf{s})$ does not exceed the yield strength S_y of the material with 99.875% probability if y_1 is Gaussian. Mathematically, the RDO for this problem is defined to

$$
\begin{aligned}
\min_{(\mathbf{d},\mathbf{s})\in\mathcal{D}} \quad & c_0(\mathbf{d},\mathbf{s}) = 0.5 \frac{\mathbb{E}_\mathbf{d}\left[y_0(\mathbf{X};\mathbf{s})\right]}{\mathbb{E}_{\mathbf{d}_0}\left[y_0(\mathbf{X};\mathbf{s})\right]} + 0.5 \frac{\sqrt{\mathrm{var}_\mathbf{d}\left[y_0(\mathbf{X};\mathbf{s})\right]}}{\sqrt{\mathrm{var}_{\mathbf{d}_0}\left[y_0(\mathbf{X};\mathbf{s})\right]}}, \\
\text{subject to} \quad & c_1(\mathbf{d},\mathbf{s}) = 3\sqrt{\mathrm{var}_\mathbf{d}\left[y_1(\mathbf{X};\mathbf{s})\right]} - \mathbb{E}_\mathbf{d}\left[y_1(\mathbf{X};\mathbf{s})\right] \leq 0, \\
& 10 \text{ mm} \leq d_1 \leq 30 \text{ mm}, \ 12 \text{ mm} \leq d_2 \leq 30 \text{ mm}, \\
& 12 \text{ mm} \leq d_3 \leq 30 \text{ mm}, \ -15 \text{ mm} \leq d_4 \leq 10 \text{ mm}, \\
& -8 \text{ mm} \leq d_5 \leq 15 \text{ mm}, \ 0 \text{ mm} \leq s_1 \leq 14 \text{ mm}, \\
& 17 \text{ mm} \leq s_2 \leq 35 \text{ mm}, \ 30 \text{ mm} \leq s_3 \leq 40 \text{ mm}, \\
& 50 \text{ mm} \leq s_4 \leq 140 \text{ mm},
\end{aligned}
\tag{6.90}
$$

where

$$y_0(\mathbf{X}; \mathbf{s}) = \rho \int_{\mathcal{D}'(\mathbf{X}; \mathbf{s})} d\mathcal{D}' \tag{6.91}$$

and

$$y_1(\mathbf{X}; \mathbf{s}) = S_y - \sigma_{e,\max}(\mathbf{X}; \mathbf{s}) \tag{6.92}$$

are two random response functions, and $\mathbb{E}_{\mathbf{d}_0}[y_0(\mathbf{X}; \mathbf{s})]$ and $\mathrm{var}_{\mathbf{d}_0}[y_0(\mathbf{X}; \mathbf{s})]$ are the mean and variance, respectively, of y_0 at the initial design $(\mathbf{d}_0, \mathbf{s}_0) = (0, 30, 10, 40, 20, 20, 75, 0, 0)^T$ mm of the design vector $(\mathbf{d}, \mathbf{s}) = (d_1, \cdots, d_5, s_1, \ldots, s_4)^T \in \mathcal{D} \subset \mathbb{R}^9$. The corresponding mean and standard deviation of y_0 of the original design, calculated by the bivariate, first-order augmented PDD method, are 0.3415 kg and 0.00136 kg, respectively. Figure 6.4(b) portrays the contours of the von Mises stress calculated by FEA of the initial bracket design, which comprises 11,908 nodes and 3914 eight-noded quadrilateral elements. A plane stress condition was assumed. The approximate optimal solution is denoted by $(\tilde{\mathbf{d}}^*, \tilde{\mathbf{s}}) = (\tilde{d}_1^*, \cdots, \tilde{d}_5^*, \tilde{s}_1^*, \ldots, \tilde{s}_4^*)^T$. The corresponding affiliated random vectors $\mathbf{D}$ and $\mathbf{S}$ are selected to be Gaussian, and their components are independent with the same standard deviation of 0.2 but different mean vectors $\mathbb{E}_1[\mathbf{D}] = \mathbf{d}$ and $\mathbb{E}_2[\mathbf{S}] = \mathbf{s}$.
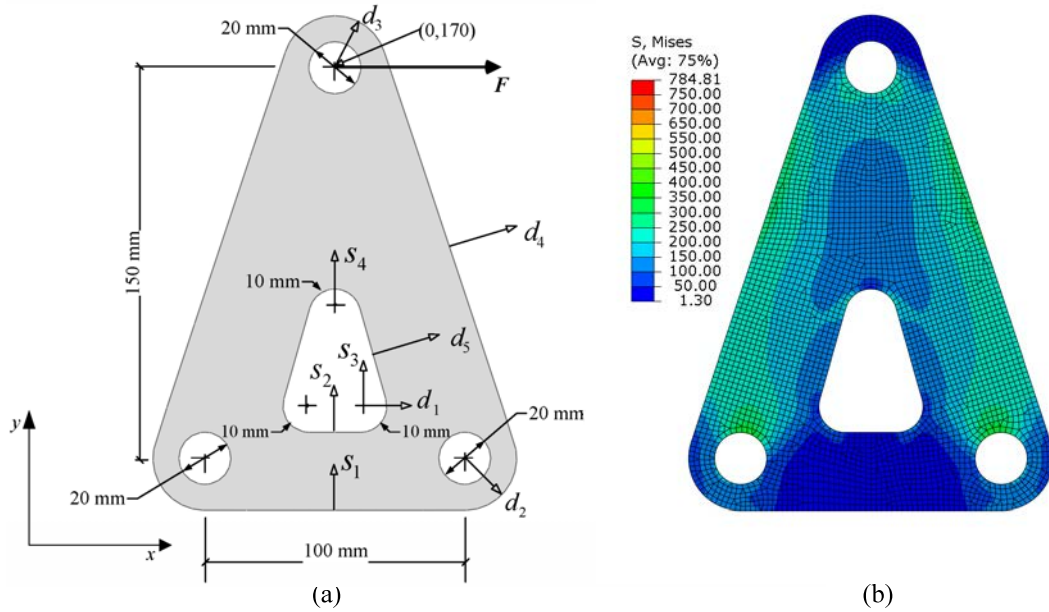
Figure 6.4: A three-hole bracket; (a) design parametrization; (b) von Mises stress at initial design

Due to their finite bounds, the random variables X_i, $i = 1, \cdots, 5$, were assumed to follow truncated Gaussian distributions with densities

$$f_{X_i}(x_i) = \frac{\phi\left(\dfrac{x_i - d_i}{\sigma_i}\right)}{\Phi\left(\dfrac{D_i}{\sigma_i}\right) - \Phi\left(-\dfrac{D_i}{\sigma_i}\right)} \tag{6.93}$$

when $a_i \leq x_i \leq b_i$ and *zero* otherwise, where $\Phi(\cdot)$ and $\phi(\cdot)$ are the cumulative distribution and probability density functions, respectively, of a standard Gaussian variable; $\sigma_i = 0.2$; and $a_i = d_i - D_i$ and $b_i = d_i + D_i$ are the lower and upper bounds, respectively, of X_i. To avoid unrealistic designs, the bounds were chosen with $D_i = 2$, which is consistent with the bound constraints of design variables stated in Equation (6.90).

The proposed multi-point, single-step PDD design procedure was applied to solve this problem, employing three univariate and one bivariate augmented PDD approximation for the underlying stochastic analysis: (1) $S = 1$, $m = 1$; (2) $S = 1$, $m = 2$; (3) $S = 1$, $m = 3$; and (4) $S = 2$, $m = 1$. Table 6.4 summarizes the optimization results by all four choices of the truncation parameters. The optimal design solutions rapidly converge as S or m increases. The univariate, first-order ($S = 1$, $m = 1$) PDD method, which is the most economical method, produces an optimal solution reasonably close to those obtained from higher-order univariate or bivariate PDD methods. For instance, the largest deviation from the average values of the objective function at four optimum points is only 3.8 percent. It is important to note that the coupling between the single-step procedure and multi-point approximation is essential to find optimal solutions of this practical problem using low-variate, low-order augmented PDD approximations.

Table 6.4: Optimization results for the three-hole bracket

Results	Augmented PDD Method			
	Univariate $(S = 1, m = 1)$	Univariate $(S = 1, m = 2)$	Univariate $(S = 1, m = 3)$	Bivariate $(S = 2, m = 1)$
$\tilde{d}_1^*$, mm	27.7537	28.0521	28.5815	26.8853
$\tilde{d}_2^*$, mm	12.0030	12.0000	12.0000	12.0000
$\tilde{d}_3^*$, mm	12.0003	12.0000	12.0000	12.0000
$\tilde{d}_4^*$, mm	-13.7431	-13.9282	-13.9025	-14.3121
$\tilde{d}_5^*$, mm	14.7886	14.9982	15.0000	15.0000
$\tilde{s}_1^*$, mm	13.6741	13.9833	14.0000	13.6256
$\tilde{s}_2^*$, mm	17.0081	17.0096	17.0000	17.0000
$\tilde{s}_3^*$, mm	30.0606	30.0002	30.0000	30.0000
$\tilde{s}_4^*$, mm	118.1092	117.6801	117.5495	124.1864
$\tilde{c}_0(\tilde{\mathbf{d}}^*)^{(a)}$	0.6668	0.6638	0.6628	0.6895
$\tilde{c}_1(\tilde{\mathbf{d}}^*)^{(a)}$	-1.8819	-14.1435	-18.3799	-10.1967
$\mathbb{E}_{\tilde{\mathbf{d}}^*}[y_0(\mathbf{X}; \mathbf{s})]$ $^{(a)}$, kg	0.1204	0.1184	0.1178	0.1278
$\sqrt{\operatorname{var}_{\tilde{\mathbf{d}}^*}[y_0(\mathbf{X}; \mathbf{s})]}$ $^{(a)}$, kg	0.00138	0.00138	0.00138	0.00135
No. of iterations	35	21	37	19
No. of FEA	665	588	1369	3078

[a] The objective and constraint functions, $\mathbb{E}_{\tilde{\mathbf{d}}^*}[y_0(\mathbf{X}; \mathbf{s})]$, and $\sqrt{\operatorname{var}_{\tilde{\mathbf{d}}^*}[y_0(\mathbf{X}; \mathbf{s})]}$ at respective optima, were evaluated by respective approximations.
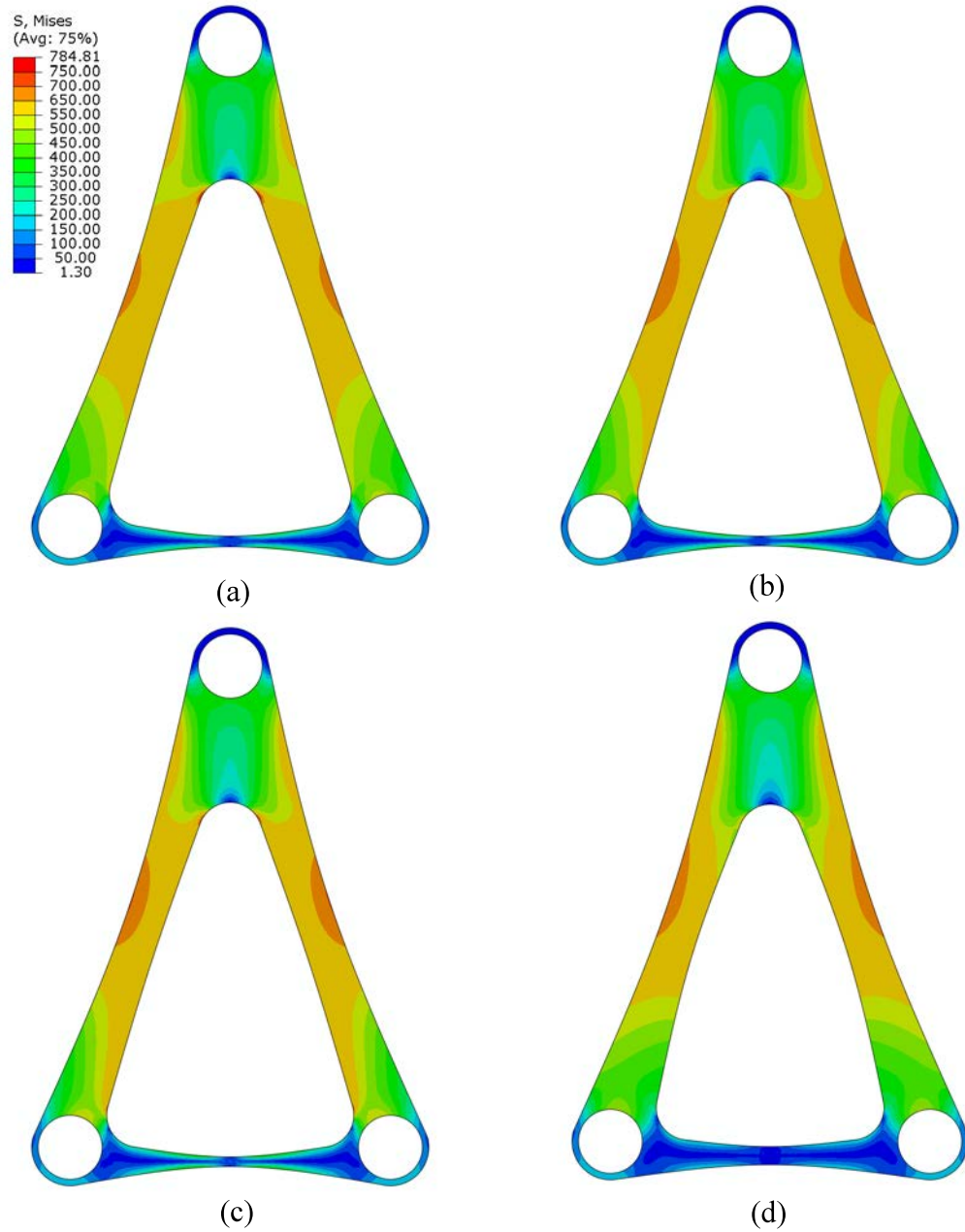
Figure 6.5: von Mises stress contours at mean values of optimal bracket designs by the multi-point, single-step PDD method; (a) univariate approximation ($S = 1$, $m = 1$); (b) univariate approximation ($S = 1$, $m = 2$); (c) univariate approximation ($S = 1$, $m = 3$); (d) bivariate approximation ($S = 2$, $m = 1$)

Figures 6.5(a) through 6.5(d) illustrate the contour plots of the von Mises stress for the four optimal designs at the mean values of random shape parameters. Regardless of S or m, the overall area of an optimal design has been substantially reduced, mainly due to significant alteration of the inner boundary and moderate alteration of the outer boundary of the bracket. All nine design variables have undergone moderate to significant changes from their initial values. The optimal masses of the bracket vary as 0.1204 kg, 0.1184 kg, 0.1178 kg, and 0.1278 kg − about a 63 percent reduction from the initial mass of 0.3415 kg. The second-moment statistics at optimal designs are averages of all PDD solutions described earlier. The largest reduction of the mean is 62.57 %, whereas the slight average drop, 0.99 %, in the standard deviations, is attributed to the objective function that combines both the mean and standard deviation of y_0. Compared with the conservative design in 6.4(b), larger stresses − for example, 800 MPa − are safely tolerated by the final designs in Figures 6.5(a) through 6.5(d).

6.7 Conclusion

A novel computational method, referred to as the augmented PDD method, is proposed for RDO and RBDO of complex engineering systems subject to mixed design variables comprising both distributional and structural design variables. The method involves a new augmented PDD of a high-dimensional stochastic response for statistical moment and reliability analyses; an integration of the augmented PDD, score functions; finite-difference approximation for calculating the sensitivities of the first

two moments and the failure probability with respect to distributional and structural design variables; and standard gradient-based optimization algorithms, encompassing a multi-point, single-step design process. For RDO sensitivity analysis, the method capitalizes on a novel integration of the augmented PDD and score functions, providing analytical expressions of mean-square convergent approximations of the design sensitivities of the first two moments. For RBDO sensitivity analysis, the method utilizes the embedded MCS of the augmented PDD approximation and a finite-difference approximation to estimate the design sensitivities of the failure probability. In each variant of design optimization, both the stochastic responses, whether the first two moments or the failure probability, and their design sensitivities are determined concurrently from a single stochastic analysis or simulation. Moreover, the multi-point, single-step design process embedded in the proposed method facilitates a solution of an RDO/RBDO problem entailing mixed design variables with a large design space. Numerical results, including a shape design optimization of a three-hole bracket, indicate that the proposed methods provide accurate and computationally efficient sensitivity estimates and optimal solutions for general RDO and RBDO problems.

CHAPTER 7
CONCLUSIONS AND FUTURE WORK

7.1   Conclusions

The major objective of this study was to develop novel computational methods for RDO and RBDO of high-dimensional, complex engineering systems. Four major tasks were completed to meet the objective of the study. They involved: (1) development of new sensitivity analysis methods for RDO and RBDO; (2) development of novel optimization methods for solving RDO problems; (3) development of novel optimization methods for solving RBDO problems; and (4) development of a novel scheme and formulation to solve stochastic design optimization problems with both distributional and structural design parameters. The major conclusions from these four tasks are summarized as follows:

1. **Development of new sensitivity analysis methods for RDO and RBDO**: Three new computational methods were developed for calculating design sensitivities of statistical moments and reliability of high-dimensional complex systems subject to random input. The first method represents a novel integration of PDD of a multivariate stochastic response function and score functions. Applied to the statistical moments, the method provides mean-square convergent analytical expressions of design sensitivities of the first two moments of a stochastic response. The second and third methods, relevant to probability distribution or reliability analysis, exploit two distinct combinations built on PDD:

the PDD-SPA method, entailing the SPA and score functions; and the PDD-MCS method, utilizing the embedded MCS of the PDD approximation and score functions. For all three methods developed, the statistical moments or failure probabilities and their design sensitivities are both determined concurrently from a single stochastic analysis or simulation. Numerical examples, including a 100-dimensional mathematical problem, indicate that the new methods developed provide not only theoretically convergent or accurate design sensitivities, but also computationally efficient solutions. A practical example involving robust design optimization of a three-hole bracket illustrates the usefulness of the proposed methods.

2. **Development of novel optimization methods for solving RDO problems**: Four new methods were developed for RDO of complex engineering systems. The methods involve PDD of a high-dimensional stochastic response for statistical moment analysis, a novel integration of PDD and score functions for calculating the second-moment sensitivities with respect to the design variables, and standard gradient-based optimization algorithms. New closed-form formulae were presented for the design sensitivities that are simultaneously determined along with the moments. The methods depend on how statistical moment and sensitivity analyses are dovetailed with an optimization algorithm, encompassing direct, single-step, sequential, and multi-point single-step design processes. Numerical results indicate that the proposed methods provide accurate and computationally efficient optimal solutions of RDO problems, including

an industrial-scale lever arm design.

3. **Development of novel optimization methods for solving RBDO problems**: Two new methods were developed for RBDO of complex engineering systems. The methods involve AS-PDD of a high-dimensional stochastic response for reliability analysis, a novel integration of AS-PDD and score functions for calculating the sensitivities of the failure probability with respect to design variables, and standard gradient-based optimization algorithms, encompassing a multi-point, single-step design process. The two methods, depending on how the failure probability and its design sensitivities are evaluated, exploit two distinct combinations built on AS-PDD: the AS-PDD-SPA method, entailing the SPA and score functions; and the AS-PDD-MCS method, utilizing the embedded MCS of the AS-PDD approximation and score functions. In both methods, the failure probability and its design sensitivities are determined concurrently from a single stochastic simulation or analysis. When applied in collaboration with the multi-point, single-step framework, the proposed methods afford the ability of solving industrial-scale design problems. Numerical results stemming from mathematical functions or elementary engineering problems indicate that the new methods provide more accurate and computationally efficient design solutions than existing methods. Furthermore, shape design of a 79-dimensional jet engine bracket was performed, demonstrating the power of the methods developed to tackle practical RBDO problems.

4. **Development of a novel scheme and formulation to solve stochastic**

design optimization problems with both distributional and structural design parameters: A new method, named as augmented PDD method, was developed for RDO and RBDO subject to mixed design variables comprising both distributional and structural design variables. The method comprises a new augmented PDD of a high-dimensional stochastic response for statistical moment and reliability analyses; an integration of the augmented PDD, score functions, and finite-difference approximation for calculating the sensitivities of the first two moments and the failure probability with respect to distributional and structural design variables; and standard gradient-based optimization algorithms, encompassing a multi-point, single-step design process. New closed-form formulae were presented for the design sensitivities of moments that are simultaneously determined along with the moments. A finite-difference approximation integrated with the embedded MCS of the augmented PDD was put forward for design sensitivities of the failure probability. In conjunction with the multi-point, single-step design process, the new method provides an efficient means to solve an RDO/RBDO problem entailing mixed design variables with a large design space. Numerical results, including a three-hole bracket design, indicate that the proposed methods provide accurate and computationally efficient sensitivity estimates and optimal solutions for general RDO and RBDO problems.

7.2 Recommendations for Future Work

Based on the research and development in this study, the following activities are recommended for future efforts:

1. The methods developed in this work are all based on the fundamental assumption that input random variables be independently distributed. Hence, further research is required for stochastic analysis and design optimization when the input random variables follow general dependent probability distributions.

2. The methods developed in this work are strictly valid for specified probability distributions of random input variables. Advances in sensor technology and high-performance computing allow scientists and engineers to generate and collect extremely large and high-dimensional data sets, referred to as big data, usually measured in terabytes and perabytes. Therefore, further developments of data-driven design optimization methods, avoiding the subjectivity of assigning parametric probability distributions, should be pursued.

APPENDIX A
ANALYTICAL SOLUTION OF SENSITIVITIES OF 1ST AND 2ND MOMENTS OF THE OAKLEY AND O'HAGAN FUNCTION

Consider the Oakley and O'Hagan function $y(\mathbf{X})$ in Equation 3.74. The analytical solutions for sensitivities of the first moment of $y(\mathbf{X})$ with respect to μ and σ are

$$\frac{\partial m^{(1)}(\mathbf{d})}{\partial \mu} = \sum_{i=1}^{15} a_{1i} + \mathrm{e}^{-\frac{\sigma^2}{2}} \cos \mu \sum_{i=1}^{15} a_{2i} - \mathrm{e}^{-\frac{\sigma^2}{2}} \sin \mu \sum_{i=1}^{15} a_{3i} + 2\mu \sum_{i,j=1;i\neq j}^{15} M_{ij} \quad \text{(A.1)}$$

and

$$\frac{\partial m^{(1)}(\mathbf{d})}{\partial \sigma} = -\sigma \mathrm{e}^{-\frac{\sigma^2}{2}} (\mathbf{a}_2^T \sin \boldsymbol{\mu} + \mathbf{a}_3^T \cos \boldsymbol{\mu}) + 2\sigma \mathrm{tr}(\mathbf{M}), \quad \text{(A.2)}$$

respectively, where $\mathbf{a}_l = \{a_{li}\} \in \mathbb{R}^{15}$, $l = 1, 2, 3$, and $\mathbf{M} = [M_{ij}] \in \mathbb{R}^{15\times15}$ are coefficient vectors and matrix, correspondingly, and tr is the trace operator. When $\mu = 0$ and $\sigma = 1$, they become

$$\left.\frac{\partial m^{(1)}(\mathbf{d})}{\partial \mu}\right|_{\mu=0,\sigma=1} = \sum_{i=1}^{15} a_{1i} + \mathrm{e}^{-\frac{1}{2}} \sum_{i=1}^{15} a_{2i} \quad \text{(A.3)}$$

and

$$\left.\frac{\partial m^{(1)}(\mathbf{d})}{\partial \sigma}\right|_{\mu=0,\sigma=1} = -\mathrm{e}^{-\frac{1}{2}} \sum_{i=1}^{15} a_{3i} + 2\mathrm{tr}(\mathbf{M}). \quad \text{(A.4)}$$

Similarly, the analytical solution for sensitivities of the second moment of $y(\mathbf{X})$ with respect to μ and σ at $\mu = 0$ and $\sigma = 1$ are

$$
\begin{aligned}
\left.\frac{\partial m^{(2)}(\mathbf{d})}{\partial \mu}\right|_{\mu=0,\sigma=1} = {} & 2 \times \left[\sum_{i,j=1;i\neq j}^{15} a_{1i}M_{jj} + \sum_{i,j=1;i\neq j}^{15} a_{1i}M_{ij} + \sum_{i,j=1;i\neq j}^{15} a_{1i}M_{ji} \right. \\
& {} + 3\sum_{i=1}^{15} a_{1i}M_{ii} + 2\mathrm{e}^{-\frac{1}{2}}\sum_{i=1}^{15} a_{2i}M_{ii} + \mathrm{e}^{-\frac{1}{2}}\sum_{i,j=1;i\neq j}^{15} a_{2i}M_{jj} \\
& {} + \mathrm{e}^{-\frac{1}{2}}\sum_{i,j=1;i\neq j}^{15} a_{2i}M_{ij} + \mathrm{e}^{-\frac{1}{2}}\sum_{i,j=1;i\neq j}^{15} a_{2i}M_{ji} + \mathrm{e}^{-\frac{1}{2}}\sum_{i,j=1;i\neq j}^{15} a_{1i}a_{3j} \\
& \left. {} + \mathrm{e}^{-1}\sum_{i,j=1;i\neq j}^{15} a_{2i}a_{3j} + \mathrm{e}^{-2}\sum_{i=1}^{15} a_{2i}a_{3i} \right] \tag{A.5}
\end{aligned}
$$

and

$$
\begin{aligned}
\left.\frac{\partial m^{(2)}(\mathbf{d})}{\partial \sigma}\right|_{\mu=0,\sigma=1} = {} & 2 \times \left[-2\mathrm{e}^{-\frac{1}{2}}\sum_{i=1}^{15} a_{3i}M_{ii} + \mathrm{e}^{-\frac{1}{2}}\sum_{i,j=1;i\neq j}^{15} a_{3i}M_{jj} + \mathrm{e}^{-\frac{1}{2}}\sum_{i=1}^{15} a_{1i}a_{2i} \right] \\
& {} + 2\sum_{i=1}^{15} a_{1i}^2 + 2\mathrm{e}^{-2}\sum_{i=1}^{15} a_{2i}^2 - 2\mathrm{e}^{-1}\sum_{i,j=1;i\neq j}^{15} a_{3i}a_{3j} - 2\mathrm{e}^{-2}\sum_{i=1}^{15} a_{3i}^2 \\
& {} + 4\sum_{i,j=1;i\neq j}^{15} M_{ii}M_{jj} + 4\sum_{i,j=1;i\neq j}^{15} \left(M_{ij}M_{ij} + M_{ij}M_{ji} \right) + 12\sum_{i=1}^{15} M_{ii}M_{ii},
\end{aligned}
\tag{A.6}
$$

respectively.

REFERENCES

[1] G. Taguchi. *Taguchi on robust technology development: bringing quality engineering upstream.* ASME Press series on international advances in design productivity. ASME Press, 1993.

[2] W. Chen, J. K. Allen, K. L. Tsui, and F. Mistree. Procedure for robust design: Minimizing variations caused by noise factors and control factors. *Journal of Mechanical Design, Transactions of the ASME*, 118(4):478–485, 1996.

[3] X. P. Du and W. Chen. Towards a better understanding of modeling feasibility robustness in engineering design. *Journal of Mechanical Design*, 122(4):385–394, 2000.

[4] Z. P. Mourelatos and J. Liang. A methodology for trading-off performance and robustness under uncertainty. *Journal of Mechanical Design*, 128(4):856–863, 2006.

[5] K. Zaman, M. McDonald, S. Mahadevan, and L. Green. Robustness-based design optimization under data uncertainty. *Structural and Multidisciplinary Optimization*, 44(2):183–197, 2011.

[6] G. J. Park, T. H. Lee, H. L. Kwon, and K. H. Hwang. Robust design: an overview. *AIAA Journal*, 44(1):181–191, 2006.

[7] C. Soize. A comprehensive overview of a non-parametric probabilistic approach of model uncertainties for predictive models in structural dynamics. *Journal of Sound and Vibration*, 288(3):623–652, 2005.

[8] X. P. Du, A. Sudjianto, and W. Chen. An integrated framework for optimization under uncertainty using inverse reliability strategy. *Journal of Mechanical Design*, 126(4):562–570, 2004.

[9] I. Lee, K. K. Choi, L. Du, and D. Gorsich. Dimension reduction method for reliability-based robust design optimization. *Computers & Structures*, 86(13):1550–1562, 2008.

[10] R. Durrett. *Probability: theory and examples.* Cambridge University Press, 2010.

[11] R. V. Hogg, J. W. McKean, and A. T. Craig. *Introduction to mathematical statistics.* Pearson Education, 2005.

[12] B. Huang and X. Du. Analytical robustness assessment for robust design. *Structural and Multidisciplinary Optimization*, 34(2):123–137, 2007.

[13] H. Wang and N. H. Kim. Robust design using stochastic response surface and sensitivities. In *11th AIAA/ISSMO Multidisciplinary Analysis and Optimization Conference*, 2006.

[14] S. H. Lee, W. Chen, and B. M. Kwak. Robust design with arbitrary distributions using gauss-type quadrature formula. *Structural and Multidisciplinary Optimization*, 39(3):227–243, 2009.

[15] E. Rosenblueth. Two-point estimates in probabilities. *Applied Mathematical Modelling*, 5(5):329–335, 1981.

[16] H. P. Hong. An efficient point estimate method for probabilistic analysis. *Reliability Engineering & System Safety*, 59(3):261–267, 1998.

[17] M. Kleiber and T. D. Hien. *The stochastic finite element method*. Wiley, 1992.

[18] S. Rahman and B. N. Rao. A perturbation method for stochastic meshless analysis in elastostatics. *International Journal for Numerical Methods in Engineering*, 50(8):1969–1991, 2001.

[19] D. H. Evans. An application of numerical integration techniclues to statistical toleraucing. *Technometrics*, 9(3):441–456, 1967.

[20] F. Yamazaki, M. Shinozuka, and G. Dasgupta. Neumann expansion for stochastic finite element analysis. *Journal of Engineering Mechanics*, 114(8):1335–1354, 1988.

[21] M. Grigoriu. Statistically equivalent solutions of stochastic mechanics problems. *Journal of Engineering Mechanics*, 117(8):1906–1918, 1991.

[22] H. Xu and S. Rahman. A generalized dimension-reduction method for multidimensional integration in stochastic mechanics. *International Journal for Numerical Methods in Engineering*, 61(12):1992–2019, 2004.

[23] H. Xu and S. Rahman. Decomposition methods for structural reliability analysis. *Probabilistic Engineering Mechanics*, 20(3):239–250, 2005.

[24] M. Grigoriu. *Stochastic calculus: applications in science and engineering*. Springer, 2002.

[25] E. Rosenblueth. Point estimates for probability moments. *Proceedings of the National Academy of Sciences*, 72(10):3812–3814, 1975.

[26] Y. G. Zhao and T. Ono. New point estimates for probability moments. *Journal of Engineering Mechanics*, 126(4):433–436, 2000.

[27] M. E. Harr. Probabilistic estimates for multivariate analyses. *Applied Mathematical Modelling*, 13(5):313–318, 1989.

[28] J. T. Christian and G. B. Baecher. Point-estimate method as numerical quadrature. *Journal of Geotechnical and Geoenvironmental Engineering*, 125(9):779–786, 1999.

[29] D. Ghosh, R. G. Ghanem, and J. Red-Horse. Analysis of eigenvalues and modal interaction of stochastic systems. *AIAA Journal*, 43(10):2196–2201, 2005.

[30] M. L. Lou and G. Chen. Modal perturbation method and its applications in structural systems. *Journal of Engineering Mechanics*, 129(8):935–943, 2003.

[31] G. B. Beacher and T. S. Ingra. Stochastic fem in settlement predictions. *Journal of the Geotechnical Engineering Division*, 107(4):449–463, 1981.

[32] K. K. Phoon, S. T. Quek, Y. K. Chow, and S. L. Lee. Reliability analysis of pile settlement. *Journal of Geotechnical Engineering*, 116(11):1717–1734, 1990.

[33] G. I. Schuëller and H. J. Pradlwarter. Uncertain linear systems in dynamics: retrospective and recent developments by stochastic approaches. *Engineering Structures*, 31(11):2507–2517, 2009.

[34] C. A. Cornell. A probability-based structural code*. In *ACI Journal Proceedings*, volume 66, pages 974–985. ACI, 1969.

[35] H. O. Madsen, S. Krenk, and N. C. Lind. *Methods of structural safety*. Prentice-Hall, Inc., 1986.

[36] A. M. Hasofer and N. C. Lind. Exact and invariant second-moment code format. *Journal of the Engineering Mechanics Division*, 100(1):111–121, 1974.

[37] B. Fiessler, R. Rackwitz, and H. J. Neumann. Quadratic limit states in structural reliability. *Journal of the Engineering Mechanics Division*, 105(4):661–676, 1979.

[38] M. Hohenbichler and R. Rackwitz. Non-normal dependent vectors in structural safety. *Journal of the Engineering Mechanics Division*, 107(6):1227–1238, 1981.

[39] K. Breitung. Asymptotic approximations for multinormal integrals. *Journal of Engineering Mechanics*, 110(3):357–366, 1984.

[40] A. Der Kiureghian, H. Z. Lin, and S. J. Hwang. Second-order reliability approximations. *Journal of Engineering Mechanics*, 113(8):1208–1225, 1987.

[41] Y. T. Wu, H. R. Millwater, and T. A. Cruse. Advanced probabilistic structural analysis method for implicit performance functions. *AIAA Journal*, 28(9):1663–1669, 1990.

[42] Y. T. Wu and P. H. Wirsching. New algorithm for structural reliability estimation. *Journal of Engineering Mechanics*, 113(9):1319–1336, 1987.

[43] P. L. Liu and A. Der Kiureghian. Optimization algorithms for structural reliability. *Structural Safety*, 9(3):161–177, 1991.

[44] M. Hohenbichler and R. Rackwitz. Improvement of second-order reliability estimates by importance sampling. *Journal of Engineering Mechanics*, 114(12):2195–2199, 1988.

[45] L. Tvedt. Distribution of quadratic forms in normal space-application to structural reliability. *Journal of Engineering Mechanics*, 116(6):1183–1197, 1990.

[46] S. Adhikari. Reliability analysis using parabolic failure surface approximation. *Journal of Engineering Mechanics*, 130(12):1407–1427, 2004.

[47] R. Y. Rubinstein and D. P. Kroese. *Simulation and the Monte Carlo method.* Wiley. com, 2011.

[48] G. I. Schuëller and R. Stix. A critical appraisal of methods to determine failure probabilities. *Structural Safety*, 4(4):293–309, 1987.

[49] S. Engelund and R. Rackwitz. A benchmark study on importance sampling techniques in structural reliability. *Structural Safety*, 12(4):255–276, 1993.

[50] M. D. McKay, R. J. Beckman, and W. J. Conover. Comparison of three methods for selecting values of input variables in the analysis of output from a computer code. *Technometrics*, 21(2):239–245, 1979.

[51] M. Stein. Large sample properties of simulations using latin hypercube sampling. *Technometrics*, 29(2):143–151, 1987.

[52] P. Bjerager. Probability integration by directional simulation. *Journal of Engineering Mechanics*, 114(8):1285–1302, 1988.

[53] O. Ditlevsen, R. E. Melchers, and H. Gluver. General multi-dimensional probability integration by directional simulation. *Computers & Structures*, 36(2):355–368, 1990.

[54] N. Metropolis, A. W. Rosenbluth, M. N. Rosenbluth, A. H. Teller, and E. Teller. Equation of state calculations by fast computing machines. *The Journal of Chemical Physics*, 21(6):1087–1092, 1953.

[55] S. K. Au and J. L. Beck. Estimation of small failure probabilities in high dimensions by subset simulation. *Probabilistic Engineering Mechanics*, 16(4):263–277, 2001.

[56] H. E. Daniels. Saddlepoint approximations in statistics. *The Annals of Mathematical Statistics*, 25(4):631–650, 1954.

[57] X. P. Du. Saddlepoint approximation for sequential optimization and reliability analysis. *Journal of Mechanical Design*, 130:1–11, 2008.

[58] B. Q. Huang and X. P. Du. Uncertainty analysis by dimension reduction integration and saddlepoint approximations. *Journal of Mechanical Design*, 128:26–33, 2006.

[59] L. P. Wang and R. V. Grandhi. Improved two-point function approximations for design optimization. *AIAA Journal*, 33(9):1720–1727, 1995.

[60] B. J. Bichon, M. S. Eldred, L. P. Swiler, S. Mahadevan, and J. M. Mc-Farland. Multimodal reliability assessment for complex engineering applications using efficient global optimization. In *Proceedings of the 48th AIAA/ASME/ASCE/AHS/ASC Structures, Structural Dynamics, and Materials Conference*, 2007.

[61] W. Hoeffding. A class of statistics with asymptotically normal distribution. *The Annals of Mathematical Statistics*, 19(3):293–325, 1948.

[62] B. Efron and C. Stein. The jackknife estimate of variance. *The Annals of Statistics*, 9(3):586–596, 1981.

[63] I. M. Sobol. Theorems and examples on high dimensional model representation. *Reliability Engineering & System Safety*, 79(2):187–193, 2003.

[64] S. Rahman. Approximation errors in truncated dimensional decompositions. *Mathematics of Computation*, 83(290):2799–2819, 2014.

[65] R. Bellman. *Dynamic Programming.* Princeton University Press: Princeton, NJ, 1957.

[66] R. Caflisch, W. Morokoff, and A. Owen. Valuation of mortgage backed securities using brownian bridges to reduce effective dimension. *Journal of Computational Finance*, 1:27–46, 1997.

[67] H. Rabitz and O. Alis. General foundations of high dimensional model representations. *Journal of Mathematical Chemistry*, 25(2):197–233, 1999.

[68] X. Q. Wang. On the approximation error in high dimensional model representation. In *Proceedings of 40th Conference on Winter Simulation*, pages 453–462. IEEE, 2008.

[69] F. Y. Kuo, I. H. Sloan, G. W. Wasilkowski, and H. Wozniakowski. On decompositions of multivariate functions. *Mathematics of Computation*, 79(270):953–966, 2011.

[70] F. Hickernell, I. Sloan, and G. Wasilkowski. On tractability of weighted integration over bounded and unbounded regions in $\mathbb{R}^s$. *Mathematics of Computation*, 73(248):1885–1901, 2004.

[71] M. Griebel and M. Holtz. Dimension-wise integration of high-dimensional functions with applications to finance. *Journal of Complexity*, 26(5):455–489, 2010.

[72] G. Boole and J. F. Moulton. *A treatise on the calculus of finite differences.* Macmillan, 1880.

[73] G. D. Smith. *Numerical solution of partial differential equations: finite difference methods.* Oxford University Press, 1985.

[74] R. Y. Rubinstein and A. Shapiro. *Discrete event systems: sensitivity analysis and stochastic optimization by the score function method.* Wiley New York, 1993.

[75] S. Rahman. Stochastic sensitivity analysis by dimensional decomposition and score functions. *Probabilistic Engineering Mechanics*, 24(3):278–287, 2009.

[76] A. Browder. *Mathematical analysis: an introduction.* Springer New York, 1996.

[77] M. Hohenbichler and R. Rackwitz. Sensitivity and importance measures in structural reliability. *Civil Engineering Systems*, 3(4):203–209, 1986.

[78] M. Rosenblatt. Remarks on a multivariate transformation. *The Annals of Mathematical Statistics*, 23(3):470–472, 1952.

[79] X. Z. Huang and Y. M. Zhang. Reliability–sensitivity analysis using dimension reduction methods and saddlepoint approximations. *International Journal for Numerical Methods in Engineering*, 93(8):857–886, 2012.

[80] H. Millwater. Universal properties of kernel functions for probabilistic sensitivity analysis. *Probabilistic Engineering Mechanics*, 24(1):89–99, 2009.

[81] S. Rahman and H. Xu. A univariate dimension-reduction method for multidimensional integration in stochastic mechanics. *Probabilistic Engineering Mechanics*, 19(4):393–408, 2004.

[82] B. D. Youn, Z. Xi, and P. Wang. Eigenvector dimension reduction (EDR) method for sensitivity-free probability analysis. *Structural and Multidisciplinary Optimization*, 37(1):13–28, 2008.

[83] S. Rahman. Decomposition methods for structural reliability analysis revisited. *Probabilistic Engineering Mechanics*, 26(2):357–363, 2011.

[84] V. V. Toropov, A. A. Filatov, and A. A. Polynkin. Multiparameter structural optimization using FEM and multipoint explicit approximations. *Structural and Multidisciplinary Optimization*, 6(1):7–14, 1993.

[85] E. Nikolaidis and R. Burdisso. Reliability based optimization: a safety index approach. *Computers & Structures*, 28(6):781–788, 1988.

[86] J. Tu, K. K. Choi, and Y. H. Park. A new study on reliability-based design optimization. *Journal of Mechanical Design, Transactions of the ASME*, 121(4):557–564, 1999.

[87] B. D. Youn, K. K. Choi, and Y. H. Park. Hybrid analysis method for reliability-based design optimization. *Journal of Mechanical Design*, 125:221–231, 2003.

[88] J. Liang, Z. P. Mourelatos, and J. Tu. A single-loop method for reliability-based design optimization. In *Proceedings of ASME Design Engineering Technical Conferences*, 2004.

[89] J. H. Liang, Z. P. Mourelatos, and E. Nikolaidis. A single-loop approach for system reliability-based design optimization. *Journal of Mechanical Design*, 129(12):1215–1224, 2007.

[90] J. O. Royset, A. Der Kiureghian, and E. Polak. Reliability-based optimal structural design by the decoupling approach. *Reliability Engineering & System Safety*, 73(3):213–221, 2001.

[91] X. P. Du and W. Chen. Sequential optimization and reliability assessment method for efficient probabilistic design. *Journal of Mechanical Design*, 126(2):225–233, 2004.

[92] T. Zou and S. Mahadevan. A direct decoupling approach for efficient reliability-based design optimization. *Structural and Multidisciplinary Optimization*, 31(3):190–200, 2006.

[93] S. Rahman and D. Wei. Design sensitivity and reliability-based structural optimization by univariate decomposition. *Structural and Multidisciplinary Optimization*, 35(3):245–261, 2008.

[94] D. Wei and S. Rahman. A multi-point univariate decomposition method for structural reliability analysis. *International Journal of Pressure Vessels and Piping*, 87(5):220–229, 2010.

[95] J. O. Royset and E. Polak. Reliability-based optimal design using sample average approximations. *Probabilistic Engineering Mechanics*, 19(4):331–343, 2004.

[96] A. A. Taflanidis and J. L. Beck. Stochastic subset optimization for optimal reliability problems. *Probabilistic Engineering Mechanics*, 23(2):324–338, 2008.

[97] S. Rahman. Extended polynomial dimensional decomposition for arbitrary probability distributions. *Journal of Engineering Mechanics*, 135(12):1439–1451, 2009.

[98] W. Gautschi. *Orthogonal polynomials: computation and approximation*. Numerical mathematics and scientific computation. Oxford University Press, 2004.

[99] S. Rahman. A polynomial dimensional decomposition for stochastic computing. *International Journal for Numerical Methods in Engineering*, 76(13):2091–2116, 2008.

[100] S. Rahman. Statistical moments of polynomial dimensional decomposition. *Journal of Engineering Mechanics*, 136(7):923–927, 2010.

[101] R. Lugannani and S. Rice. Saddle point approximation for the distribution of the sum of independent random variables. *Advances in Applied Probability*, 12(2):475–490, 1980.

[102] K. V. Yuen, J. Wang, and S. K. Au. Application of saddlepoint approximation in reliability analysis of dynamic systems. *Earthquake Engineering and Engineering Vibration*, 6(4):391–400, 2007.

[103] I. W. Busbridge. Some integrals involving hermite polynomials. *Journal of the London Mathematical Society*, 23:135–141, 1948.

[104] H. Kleindienst and A. Lüchow. Multiplication theorems for orthogonal polynomials. *International Journal of Quantum Chemistry*, 48(4):239–247, 1993.

[105] J. E. Oakley and A. O'Hagan. Probabilistic sensitivity analysis of complex models: a bayesian approach. *Journal of the Royal Statistical Society: Series B (Statistical Methodology)*, 66(3):751–769, 2004.

[106] DOT. *DOT – Design Optimization Tools, User's Manual*. Vanderplaats Research and Development, Inc., Colorado Springs, CO, 2001.

[107] B. Ramakrishnan and S. S. Rao. A general loss function based optimization procedure for robust design. *Engineering Optimization*, 25(4):255–276, 1996.

[108] R. I. Stephens and H. O. Fuchs. *Metal fatigue in engineering*. Wiley-Interscience, 2001.

[109] V. Yadav and S. Rahman. Adaptive-sparse polynomial dimensional decomposition for high-dimensional stochastic computing. *Computer Methods in Applied Mechanics and Engineering*, 274:56–83, 2014.

[110] S. Rahman and X. C. Ren. Novel computational methods for high-dimensional stochastic sensitivity analysis. *International Journal for Numerical Methods in Engineering*, 98:881–916, 2014.

[111] S. Rahman. Probability distributions of natural frequencies of uncertain dynamic systems. *AIAA Journal*, 47(6):1579–1589, 2009.

[112] X. C. Ren and S. Rahman. Robust design optimization by polynomial dimensional decomposition. *Structural and Multidisciplinary Optimization*, 48(1):127–148, 2013.

[113] A. Genz. Fully symmetric interpolatory rules for multiple integrals. *SIAM Journal on Numerical Analysis*, 23(6):pp. 1273–1283, 1986.

[114] A. Genz and B. D. Keister. Fully symmetric interpolatory rules for multiple integrals over infinite regions with gaussian weight. *Journal of Computational and Applied Mathematics*, 71(2):299 – 309, 1996.

[115] J. J. Lee and B. C. Lee. Efficient evaluation of probabilistic constraints using an envelope function. *Engineering Optimization*, 37(2):185–200, 2005.

[116] J. Golinski. Optimal synthesis problems solved by means of nonlinear programming and random methods. *Journal of Mechanisms*, 5(3):287–309, 1970.

[117] I Enevoldsen and John Dalsgaard Sørensen. Reliability-based optimization in structural engineering. *Structural safety*, 15(3):169–196, 1994.

[118] Norbert Kuschel and Rüdiger Rackwitz. Two basic problems in reliability-based structural optimization. *Mathematical Methods of Operations Research*, 46(3):309–333, 1997.

[119] Anukal Chiralaksanakul and Sankaran Mahadevan. First-order approximation methods in reliability-based design optimization. *Journal of Mechanical Design*, 127(5):851–857, 2005.

[120] Harish Agarwal and John E Renaud. New decoupled framework for reliability-based design optimization. *AIAA journal*, 44(7):1524–1531, 2006.

[121] Ikjin Lee, KK Choi, Liu Du, and David Gorsich. Inverse analysis method using mpp-based dimension reduction for reliability-based design optimization of nonlinear and multi-dimensional systems. *Computer Methods in Applied Mechanics and Engineering*, 198(1):14–27, 2008.

[122] Byeng D Youn and Pingfeng Wang. Bayesian reliability-based design optimization using eigenvector dimension reduction (edr) method. *Structural and Multidisciplinary Optimization*, 36(2):107–123, 2008.

[123] Gabseong Lee, Sunmin Yook, Kibong Kang, and Dong-Hoon Choi. Reliability-based design optimization using an enhanced dimension reduction method with variable sampling points. *International Journal of Precision Engineering and Manufacturing*, 13(9):1609–1618, 2012.

[124] X. Ren, V. Yadav, and S. Rahman. Reliability-based design optimization by adaptive-sparse polynomial dimensional decomposition. *Structural and Multidisciplinary Optimization*, 2014 (submitted).